

**Stratigraphic Sedimentology, Microfacies and Diagenesis of
Middle Jurassic (Jhurio Formation) Succession of Kachchh
Mainland, Gujarat, Western India**

Thesis submitted to
GOA UNIVERSITY
For the Degree of

DOCTOR OF PHILOSOPHY

in

GEOLOGY

*Certified that all the
suggested corrections
have been made.*

*P. K. Saraswati
(P.K. Saraswati)
1.09.01*



By

M. RAJEEVAN

*M. Mahender
(M. Mahender)
Guide*

*551
F.P.S.*

~~*201*~~

J-212

Department of Earth Science
GOA UNIVERSITY, GOA

2001

~~*J-143*~~
~~*F-138*~~

CERTIFICATE

As required by the University Ordinance 0.19.8 (vi), this is to certify that the thesis entitled "**Stratigraphic Sedimentology, Microfacies and Diagenesis of Middle Jurassic (Jhurio Formation) Succession of Kachchh Mainland, Gujarat, Western India**" submitted by Mr. *M. Rajeevan* for the award of the degree of Doctorate of Philosophy in Geology is based on the original and independent work carried out by him during the period of study under my supervision.

The thesis or any part thereof has not been previously submitted for any other Degree or Diploma in any University or Institute. The material obtained from other sources has been duly acknowledged.

Place: Goa University

Date : 29.03.2001



Dr. K. Mahender
Research Supervisor
Dept. of Earth Science
Goa University,
Goa -403 206

T-212

STATEMENT

As required by the University Ordinance 0.19.8 (ii), I state that the present thesis entitled "***Stratigraphic Sedimentology, Microfacies and Diagenesis of Middle Jurassic (Jhurio Formation) Succession of Kachchh Mainland, Gujarat, Western India***" is my original contribution and same has not been submitted on any previous occasion for any other degree or Diploma of this University or any other University/Institute. To the best of my knowledge, the present study is the first comprehensive work of its kind from the area mentioned. The literature related to the problem investigated has been cited. Due acknowledgements have been made wherever facilities and suggestions have been availed of.

Place : Goa University

Date: 29.03.2001



(Rajeevan. M)

Candidate

ACKNOWLEDGEMENTS

The realization of this research endeavor is due to the co-operative and combined efforts of numerous individuals who have been instrumental in inspiring, motivating and assisting me throughout this journey.

I wish to express my sincere gratitude to my Research Guide Dr. K. Mahender, Reader, Department of Earth Science. His scientific experience and vast knowledge of the subject, innovative ideas and constructive criticism have contributed immensely to my research work.

I am grateful to the Head, Department of Earth Science as well as the other teaching staff for extending the laboratory facilities and for valuable help. I would like to thank to the Department of Science and Technology, Govt. of India, New Delhi, for giving me an opportunity to work as a Junior Research Fellow and the financial support during this research work.

I wish to thank Dr. S.K. Biswas, Consultant Geologist, KDM Institute of Petroleum Exploration (KDMIPE), Oil and Natural Gas Corporation Limited, Dehra Dun, for extending the facilities at Sedimentology Lab at KDMIPE, ONGC Dehradun and for his valuable suggestions and discussions. I also thank Mr. Jacob, Director, Mr. Mahanti, Geologist, Mr. Sharma, Senior Chemist, ONGC, Dehara Dun for extending the facilities for Petrographic, SEM and XRF analysis.

I would like to express my deep and sincere gratitude to Prof. M. E. Tucker, Head of Geological Sciences, University of Durham, Durham, UK for his valuable suggestions on Sequence Stratigraphy and for providing the research materials. I also thank the Association of Petroleum Geophysicists, KDMIPE, ONGC, Dehradun for giving me a chance to attend the Contact Programme on Sequence Stratigraphy, Sponsored by Department of Science and Technology. I also thank to Prof. F.T. Fursich, Institut fuer Palaontologie der Universitat, Wurzburg Germany for the suggestions and support.

I would like to extend my sincere thanks to Dr. P.C. Rao, Scientist, Geological Oceanography Division, National Institute of Oceanography (NIO) for extending the XRD facilities and research materials. I am highly indebted to Dr. M. Thamban, Mr.

Balakrishnan Nair , Saji P.K., Rajesh, Sudheesh, Dr. Sudheer Joseph, Sheeba and Prabhu of NIO for valuable helps during research work.

My sincere thanks are there to the Principal, Govt. College Sanquelim, Principal, Goa Engineering College, Ponda and Principal, DCT Dhempe college for the granting the part-time teaching assistance for the last two years. I am deeply grateful for the encouragement and support that have given by my research colleague Mr.A.H.Osman and for the accompanying me during the field work.

I am deeply grateful to the constant encouragement given by my research colleagues and dear friends: Rajkumar, Madhan, Anthony, Neil, Janneth, Joanitha, Harsha, Shakuntala, Sebastian, Aftab, Mohan, Ratnakar, Sachin, Khelchandra, Naveen, Chandan, Mrigank, Rajesh, and Venugopal.

I am especially grateful to Mr.K.Raghurama Bhat, Dr. B. S. Choudri, Mr. Satish, Dr.K.Srinivas, Mr. Rajendra Prasad, Manu, Vinu Thomas, Varghese and Binu John for their constant encouragement, special concern and their skills at various stages^{of} my thesis.

I am very much thankful to Mr.P. L. Gauns, Mr. Prashant, Mr. Devidas and Mr. Ulhas for their time to time help in the successful completion of this work.

I express my deep gratitude to the people and friends of Bhuj, especially, Palanpur and Jhura village, for providing me generous hospitality and assistance for the successful completion of the field work. I pray God for the quick recovery of those innocent people from the after effects of last devastating earthquake.

Words can not express my deep and sincere gratitude to Shilpa who has been extending the valuable help at every stage of my research work and for her positive attitude and immense patience that lead to the creation of this manuscript.

I am deeply indebted to my mother, brother, sisters and brother-in-laws for their patiently bearing with me and for the valuable encouragement provided thorough out.

Last, but certainly not the least, I wish to express my sincere thanks to all my friends and well-wishers who have directly or indirectly extend their help and suggestions.

Rajeevan. M

Contents

	Page
Preface	
Acknowledgements	
Contents	
List of Figures	
List of Tables	
List of plates	
<hr/>	
CHAPTER 1 - INTRODUCTION	
1.1. General	1
1.2. Scope and Objectives	2
1.3. Study area	3
1.4. Materials and Methods	6
CHAPTER II - PREVIOUS WORK	
2.1 General	11
2.2. International status	11
2.3. National Status	14
2.3.1. Stratigraphic Studies	15
2.3.1. Palaeontologic studies	18
2.3.2. Sedimentological and other investigations	22
CHAPTER III - GEOLOGY AND STRATIGRAPHY	
3.1. General	30
3.2. Structure and Tectonics and Geomorphology	31
3.3.1. General Geomorphology of Kachchh	32
3.3. Sedimentary Structures	34
3.4. Geology	37
3.5. Systematic Stratigraphy of Middle Jurassic of Kachchh	49
CHAPTER VI - CARBONATE PETROGRAPHY	
4.1. General	57
4.2. Carbonate Petrography	58
4.3. Carbonate Diagenesis	73
4.4. Classification	85
4.4.1. Carbonate Microfacies Types	87
4.5. Spatial Distribution of Carbonate Petrographic types	95

(Contd....)

CHAPTER V – CLASTIC SEDIMENTOLOGY	
5.1. General	109
5.2. Sandstone	109
5.2.1. Texture	109
5.2.2. Petrography	121
5.2.3. Diagenesis of sandstone	126
5.2.4. Classification and Provenance	126
5.3. Other clastic sedimentary rock	132
CHAPTER VI – MINERALOGY AND GEOCHEMISTRY	135
6.1. General	135
6.2. Mineralogy	135
6.3. Geochemistry	148
6.4. Rare Earth Elements	183
CHAPTER VII - SEDIMENTATION HISTORY AND PALAEOENVIRONMENT	
7.1. General	189
7.2. Depositional History: Sequence stratigraphic approach	190
7.3. Depositional Model of Middle Jurassic of Kachchh Mainland	208
7.4. Diagenetic Model: Parasequence and Sequence scale in the Middle Jurassic rocks of Kachchh Mainland.	214
SUMMARY AND CONCLUSIONS	219
BIBLIOGRAPHY	225

List of Figures

No.	Title	Page
Fig.1.1	Location map of the study area showing Middle Jurassic Outcrops	4
Fig.3.1	Geological map of the part of Kachchh Mainland (after Biswas and Deshpande, 1975)	38
Fig.3.2	Geological map of Jhura Dome (after Agarwal, 1957)	40
Fig.3.3	Lithostratigraphic column of Jhurio Formation(Jhura Dome).	41
Fig.3.4	Lithologic columns of Kachchh Mainland (3.3a, b & c)	42
Fig.4.1	Temporal distribution of framework elements in Jhurio Formation (Jhura Dome).	60
Fig.4.2	Temporal distribution of Microfacies in Jhurio Formation (Jhura Dome).	89
Fig.4.3a	Vertical variation of framework components of limestones, Habo Dome	97
Fig.4.3b	Vertical variation of framework components of limestones, Jhura Dome.	97
Fig.4.3c	Vertical variation of framework components of limestones, Jumara Dome.	97
Fig.5.1a	Vertical variation of clastic grain-textural parameters, Habo section	115
Fig.5.1b	Vertical variation of Clastic grain-textural parameters, Jhura section.	115
Fig.5.1c	Vertical variation of Clastic grain-textural parameters, Jumara section.	115
Fig.5.2	Bivariate Textural Plots	117
Fig.5.3	CM Diagram for Middle Jurassic sandstone samples.	118
Fig.5.4	Multivariate Discriminant Plot for Middle Jurassic sandstone samples.	118
Fig.5.5a	Vertical variation of framework components of sandstones, Habo Dome.	128
Fig. 5.5b	Vertical variation of framework components of sandstones, Jhura Dome.	128
Fig. 5.5c	Vertical variation of framework components of sandstones, Jumara Dome.	128
Fig. 5.6	Tectonic provenance diagram (Dickinson et al., 1983) of Middle Jurassic sandstones of Kachchh	129

List of Figures (contd...)

No.	Title	Page
Fig. 6.1	X-ray Diffractograms of shale samples of Middle Jurassic succession.	137
Fig.6.2	Temporal distribution of Clay minerals in the insoluble residue of carbonates of Jhurio Formation.	139
Fig.6.3	X-ray diffractograms of representative samples of Insoluble residue of carbonates of Jhurio Formation, Kachchh Mainland.	140
Fig.6.4	X-ray diffractograms of representative samples of Insoluble residue of carbonates of Jhurio Formation.	141
Fig.6.5	X-ray diffractograms of representative samples of Oolitic grainstones of Jhurio Formation.	142
Fig.6.6	X-ray diffractograms of representative samples of Oolitic grainstones of Jhurio Formation.	145
Fig. 6.7	Temporal Member-wise distribution of major elements in the Jhurio Formation.	155
Fig. 6.8	Temporal Member-wise distribution of trace elements in the Jhurio Formation.	156
Fig. 6.9.	Temporal variation of selected elements Jhura Dome.	157
Fig. 6.10.	Relationship between $1000 \cdot \text{Sr}/\text{Ca}-\text{Mn}$ (ppm) in Jhurio Formation.	172
Fig. 6.11.	Relationship between $1000 \cdot \text{Sr}/\text{Ca}-\text{Mn}$ (ppm) in Jhurio Formation.	173
Fig. 6.12a	Vertical variation of chemical parameters, Habo section.	180
Fig. 6.12b	Vertical variation of chemical parameters, Jhura section.	180
Fig. 6.12c	Vertical variation of chemical parameters, Jumara dome	181
Fig. 6. 13.	Scatter plots of chemical data for Middle Jurassic samples.	180
Fig.6.14	Chondrite Normalised REE plot for the Jurassic samples.	186
Fig. 6.15	Shale Normalised REE plot for Jurassic samples of Kachchh.	186
Fig. 7.1	Facies distribution and shallowing upward cycles stacked in a system tract model of Sequence -I (Jhurio Formation).	198
Fig. 7.2	Parasequence types in the Sequence I (Jhurio Formation).	199
Fig.7.3	Facies depositional model of Middle Jurassic Megasequence of Kachchh.	214

List of Tables

No.	Title	Page
Table 2.1	The biostratigraphic classification of Middle Jurassic to Late Jurassic succession of Kachchh	23
Table 2.2	The Lithostratigraphy of Mesozoic sequence of Kachchh Mainland (Biswas, 1981).	26
Table 3.1	Palaeocurrent Analysis of Kachchh (by Frequency Method).	36
Table 3.2	Lithostratigraphic succession of Jhurio Formation (Biswas, 1977)	44
Table 5.1	Clastic grain-textural parameters of Middle Jurassic succession.	114
Table 5.2	Framework composition of sandstones (fossiliferous).	122
Table 5.3	Modal composition of sandstones of Middle Jurassic succession.	123
Table 6.1	Temporal distribution of elements in the Jhurio Formation (Jhura Dome).	151
Table 6.2	Correlation matrix of the elements of Jhurio Formation (Jhura Dome).	153
Table 6.3	Temporal Member-wise distribution of elements in the Jhurio Formation (Jhura Dome).	154
Table 6.4	Factor analysis of elements of Jhurio Formation (Jhura Dome).	165
Table 6.5	Correlation matrix of Subtidal facies of Jhurio Formation	167
Table 6.6	Correlation matrix of Peritidal facies of Jhurio Formation	169
Table 6.7	Factor analysis of subtidal facies of Jhurio Formation,	170
Table.6.8a	Trace element distribution of Jurassic succession of Habo dome.	177
Table.6.8b	Trace element distribution of Jurassic succession of Jhura dome.	177
Table.6.8c	Trace element distribution of Jurassic succession of Jumara dome.	177
Table.6.9a	REE distribution of Jurassic succession of Habo dome.	185
Table.6.9b	REE distribution of Jurassic succession of Jhura dome.	185
Table.6.9c	REE distribution of Jurassic succession of Jumara dome.	185

List of Plates

No.	Title	Page
Plate 3.1	Field Photographs	54
Plate 3.2	Field Photographs	55
Plate 3.3	Field Photographs	56
Plate 4.1	Photomicrographs of Carbonate rocks	101
Plate 4.2	Photomicrographs of Carbonate rocks	102
Plate 4.3	Photomicrographs of Carbonate rocks	103
Plate 4.4	Photomicrographs of Carbonate rocks	104
Plate 4.5	Photomicrographs of Carbonate rocks	105
Plate 4.6	Photomicrographs of Carbonate rocks	106
Plate 4.7	SEM-micrographs of Carbonate rocks	107
Plate 4.8	SEM-micrographs of Carbonate rocks	108
Plate 5.1	Photomicrographs of Sandstones	132
Plate 5.2	Photomicrographs of Sandstones	133

CHAPTER - 1

INTRODUCTION

1.1. GENERAL

The Jurassic System first established in Jura Mountains of Western Europe by Brogniart in 1829 (in Arkell, 1956) forms an important rock succession. It is of exceptional importance in the study of stratigraphy and sedimentology because many of the basic principles and concepts were first enunciated after the study of its rocks and fossils. Jurassic was a period of world wide marine transgression and the deepening of the sea that began towards the close of the Early Jurassic is demonstrated by wide spread change in facies and appearance of new ammonite fauna. The most impressive of all the marine transgression of the Era took place during Middle Jurassic (Callovian). In many parts of the world, the Era began with a new phase of sedimentation.

As elsewhere in the world, the Jurassic period witnessed a widespread transgression of the sea in several coastal regions of India. The Kachchh sedimentary basin situated on the western margin of the Indian Peninsula has received enormous deposition of sediments and thus accommodated the wide range of condensed sections exposing from Bathonian to Pleistocene. During the Middle and Late Jurassic Period, almost the entire Kachchh and Rajasthan region of Western India covered by a gulf, which has evidently in direct connection with Tethys in the north. The Jurassic rocks of Kachchh and Rajasthan are noteworthy and form the first significant record of the marine fossiliferous deposits in the Peninsular India.

The sedimentary succession of Kachchh has attracted the attention of various geologists since long by its fabulous fossil content and the condensed horizons, which are unique to the Jurassic sediments. The Jurassic sediments, deposited in the pericratonic Kachchh Basin in response to the fluctuating sea levels, rest directly over the Precambrian syenetic basement and underlies the Cretaceous, Tertiary and Sub-Recent to Recent sediments. The complete absence of the Paleozoic and even Triassic exposures is quite interesting.

Although there have been many valuable works carried out on the Jurassic exposure of the world, very little emphasis is given to the Jurassic sequence of Kachchh as regards to its characteristic facies assemblage and their distribution and with respect to development of the various carbonate and clastic microfacies in response to the sea-level changes.

1.2. SCOPE AND OBJECTIVES

The classic Jurassic outcrops of Kachchh have been attracting the paleontologists and stratigraphers all over the world since the last hundred years. The excellent outcrops, weather, working conditions and accessibility (though very remote) offers a vast scope for work on various aspects of geology. The discovery of the oil fields in the nearby and neighbouring regions and the favourable geological set up of the Kachchh basin for hydrocarbon accumulation boosted the scope to receive greater attention in the recent past by the Oil and Natural Gas Commission to undertake intensive exploratory studies in the basin.

An attempt has been made in the present study to understand the transgressive-regressive tracts for the reconstruction of the palaeoenvironments

during Middle Jurassic Period. The present study focuses attention on the Middle Jurassic (Middle Bathonian to Callovian) succession (with special reference to Jhurio Formation in the type section) of Kachchh with the following objectives :

- a) to identify and describe the lithofacies distribution,
- b) to study the detailed textural and petrographic characters and the diagenetic nature of the clastic and carbonate microfacies types,
- c) to understand the temporal and spatial variation in the mineralogical and geochemical characteristics, and
- d) finally, to establish depositional sedimentation model and to interpret palaeoenvironments and palaeogeography of the Kachchh basin during the Middle Jurassic Period.

1.3. STUDY AREA

The present study area forms an important part of the Pericratonic Kachchh Basin situated on the western margin of the Indian Peninsula covering the entire Kachchh District and part of the Banas Kantha district of Gujarat State and is bounded between Latitudes $23^{\circ} 10' 00''$ N & $23^{\circ} 50' 00''$ N and Longitudes $69^{\circ} 05' 00''$ E & $70^{\circ} 0' 00''$ E (Fig.1.1). The peculiar characteristic of the Kachchh district is the Great Rann of Kachchh, which is entirely covered with thick salt layer mixed with fine sand and clay devoid of vegetation and habitation. Out of the total area of 45612 Sq. km. the area under desert is 23881 Sq. km. An extensive low-lying track of about 2144 Sq. km. is known as "BANNI" (means "GRASSLANDS"). The main outcropping area distributed among the various island belts (Kachchh Mainland, Pachham Island, Khadir Island, Bela Island, Chorar Hill and Wagad Highland) is

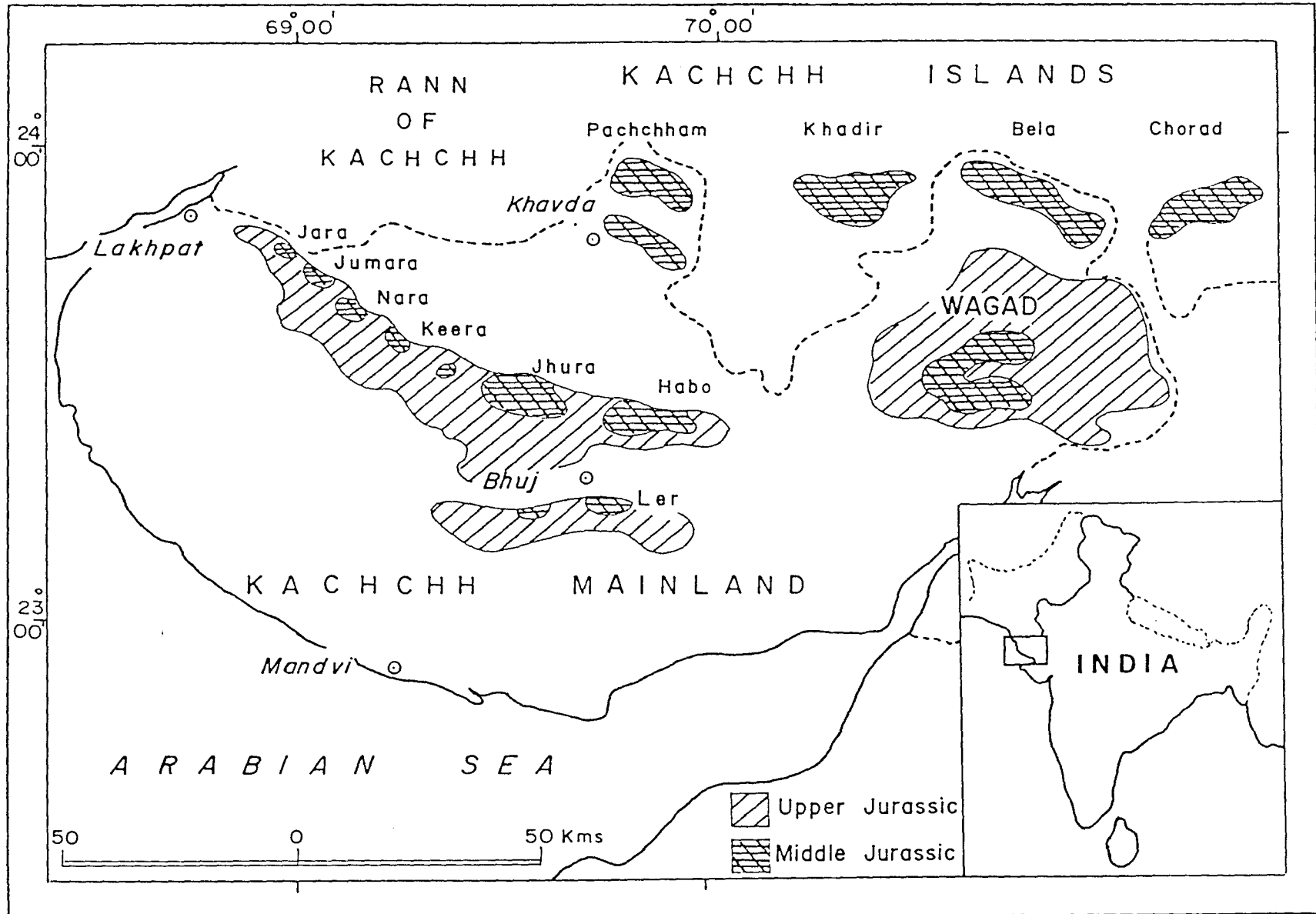


Fig. 1.1 Location Map of Kachchh

approximately 8000 sq. km. The present study is restricted mainly on the exposed Jhurio Formation of Kachchh Mainland with special reference to Jhura dome lying 30kms to the NNW of Bhuj, falling within the sheet Nos. 41 E/11 and E/15 on the topographical map of Survey of India. The other localities selected for the present study for a comparative purpose are Jumara and Habo Domes situated on the west and east of the Jhura Dome respectively (Fig.1.1).

The study area can be accessed by road, rail or air up to Bhuj, the administrative headquarter of Kachchh District. From Bhuj all the localities are accessible by metallic and semi-metallic road. The nearest semi-metropolitan city is Ahmedabad situated 411km. due east. Bhuj is connected with Ahmedabad and Mumbai with daily air service from the domestic airport located 5 Km. North of town. A number of daily private and state run transport buses ply to various other important places of Gujarat (viz., Ahmedabad, Rajkot, Jamnagar and Bhavnagar). A meter-gauge railway line connects Delhi with Bhuj. The Broad-gauge railway line connects Ahmedabad and Mumbai.

The climate of the area is comparatively dry. Monsoon is of very short duration and the average rainfall is around 322mm. Due to poor rainfall, there are no perennial rivers in the study area. The mean daily temperatures vary from 10° - 27° in winter to 27° – 40° in summer seasons. The vegetation is scanty and belongs to a mixed flora characteristic of coastal and desert conditions.

1.4. MATERIALS AND METHODS

The various methods employed in the present study on the sedimentary deposits of Kachchh basin includes the geological fieldwork and laboratory processing of the samples for detailed investigation.

1.4.1. Field work

The geological fieldwork has been conducted for sampling and collection of field data from the Middle Jurassic Formations of Jhura, Jumara and Habo Domes following the standard methods of sampling. Spot samples have been collected from various other localities. The different structural and stratigraphic features of each bed such as the thickness, colour of the sediments, grain-size, shape, mineralogy, structures such graded bedding, cross-bedding, lenses, etc. are noted. The boundaries of strata whether sharp, gradational, hardgrounds, subaerial exposure surfaces etc. are also recorded. The data on the sedimentary depositional structures has been used in the palaeocurrent analysis. The various lithological information collected from the field has been used in order to construct a composite stratigraphical column for the interpretation of temporal and spatial variations in different parameters.

1.4.2. Laboratory work

The following laboratory methods have been applied in the present study :

1.4.2.1. Thin-section petrography

The qualitative and the quantitative petrographic studies of more than 100 thin-sections of carbonates and sandstones were carried out using standard petrographic techniques. The thin-sections used for petrographic study were

prepared without cover slips to carry out etching and staining of the sections for observation under the microscope. The classification of microfacies is carried out on the basis of broad textural criteria (grain-supported, matrix supported and bioclastic or non-skeletal). Standard reference guides (Carozzi, 1961; Milliman, 1974; Scholle, 1978; Flugel, 1982; and Adams, et al.,1984) have been used for visual comparison for understanding the various textural, petrographic and diagenetic signatures.

1.4.2.2. Acid etching and Staining

Standard techniques of acid etching and staining methods as given in Friedman(1959) have been adopted in the present study to distinguish between various carbonate minerals under the microscope. The method of staining permits differentiation of dolomite, calcite, aragonite, Mg-calcite, gypsum and anhydrite. The observations of mineralogy of carbonates and sandstones under the microscope have been used for the identification and classification of the petrographic facies types.

1.4.2.3. SEM-studies

Scanning Electron Microscopy has been considered as a valuable method in order to identify the particles, morphology of cements and used as an important tool in diagenetic studies of sedimentary rocks. In the present study the samples have been prepared using methods given in Tucker (1988) and examined under SEM at higher magnification. The SEM photographs of the carbonate rock samples have been interpreted by comparing with the standard SEM photographs given in Bathurst (1975) and Scholle (1978). In the present study, the SEM observations

have been made at the Sedimentological Laboratory of the KDM Institute of Petroleum Exploration, ONGC, Dehradun.

1.4.2.4. Textural analysis of clastic sediments:

The textural analysis of clastic sediments was carried out by thin section petrography and grain projection methods. The various textural parameters viz. grain-size, roundness, shape, surface features, etc. have been measured using the standard methods of calculation. The various size parameters viz. mean, standard deviation, skewness and kurtosis were calculated by graphical method using Folk and Ward (1957) formulae. The textural data of sandstones have been utilized for plotting on various standard univariate and multivariate discriminant plots for environmental interpretation.

1.4.2.5. XRD-Studies :

X-ray diffraction (XRD) is an indispensable tool in the mineralogical analysis of sediments in general and fine-grained sediments in particular. It is the most widely used techniques for the identification, characterization and qualitative and quantitative estimation of clay and carbonate minerals.

In the present study, the shale, carbonate sample powders (-200 mesh size) and the insoluble residues collected after the carbonate sample is treated with the dilute HCl (10% v/v). have been made in to paste to spread over one half of the glass slide. The air-dried sample slides have been analyzed using Philips X-ray diffractometer at the Geological Oceanography Division, National Institute of Oceanography, Goa. The insoluble residue (IR) of some of the selected samples is carried out based on glycolation method along with raw analysis. The

specifications used in the X-ray analysis are : Target - Cu K α at 40 kV; scanning speed – 2cm/min and scanning range (2θ) – variable (5-80 degrees for Insoluble residues and clays and 20-35 for carbonate samples). The 2θ values of various characteristic peaks identified have been converted to respective d-spacing values using the conversion tables given in Carver(1971). The peak heights have been measured and relative intensities of peaks are calculated by taking the strongest peak as 100%. The d-spacing values along with the corresponding relative intensities have been compared with the JCPDC powder data files for identification of different mineral phases.

1.4.2.6. Geochemical Analysis

(a) Ca-Mg Determination : The selected samples were powdered and 0.5 mg of samples is treated with 10% v/v HCl for few hours and insoluble residue is filtered off and the solution is made up to 50ml. with distilled water. The major elements such as Ca and Mg were determined by EDTA titration procedure by digesting the sample in 1N HCl and titrating against 0.2 M EDTA solution in the presence of NaOH with Murexide as indicator for Ca and in the presence of Buffer solution with Eriochrome Black T as indicator for Mg.

(b) Whole rock analysis : The major, minor and trace elements have determined for selected samples using the XRF (ONGC, Dehradun) and AAS (NIO, Goa) . Selected rock samples were also analyzed for Rare Earth Elements (REE) using ICP-MS at the National Geophysical Research Institute, Hyderabad, following the procedures outlined in Balaram et al., (1996). Statistical methods have been used for data analysis to know the behavior of these elements with respect to each other.

The spatial and temporal distribution of the chemical elements is used for the interpretation of the depositional and diagenetic environments of the succession.

1.4.2.7. Data Presentation and Analysis

The composite lithostratigraphic column and the other logs have been prepared using the *LogPlot* (Rockware) software. The quantitative analysis of the textural, mineralogical, petrographic and geochemical data has been carried out using the *SPSS* softwares.

CHAPTER - II

REVIEW OF LITERATURE

2.1 GENERAL

The establishment of Jurassic System in the Jura Mountains of Western Europe is an important milestone in the study of stratigraphy because many of the basic principles and concepts first enunciated after the study of its rocks and fossils in Europe. These classic works have been amply reviewed by Arkell (1933) and Holder (1964). Arkell's (1956) "Jurassic Geology of the World" is a measure of the proliferation of knowledge on the Jurassic sequence of various parts of the world. Jurassic was a period of marine transgression and forms an important system of the Mesozoic Era. In many parts of the world the Era began with a new phase of sedimentation.

2.2. INTERNATIONAL STATUS

The type sections of various stages of the Jurassic are situated in England , France, West Germany and Russia. The Jurassic succession of rocks from various parts of the world has received greater attention especially for their varied depositional facies and fossil content. The literature available on stratigraphy, palaeontology, sedimentology and other applied aspects of these rocks is exhaustive and it is beyond the scope of presentation in this work. However, some of the important contributions on the Jurassic rocks related to the proposed study have been listed below.

The sedimentologic character and provenance of the arenaceous, argillaceous and ferruginous facies of Jurassic of the Northern Europe have been investigated by Allen (1969). The work of Smithson (1942) on the Middle Jurassic sandstone of northern England illustrates the complicating effects of diagenesis. Hudson (1964), in his thorough

study of the petrology of Middle Jurassic Great Estuarine Sandstone Series of W.Scotland, found it profitable to use quantitative methods and the sedimentological study on the same was made by Hudson and Harries (1979). The great value of petrography and sedimentology in elucidating Jurassic depositional environments has been brought out by Hantzschel and Reineck (1968), Davies (1969), Sellwood (1972a), Knox (1973), etc. The Jurassic 'shales' of Northern Europe have been studied for their mineralogy and environmental interpretations by Hallam and Sellwood (1968) and Sellwood (1972b). The different types of pyritisation of fossils in the Oxford Clay have been dealt in detail by Hudson and Palframan (1969) and the geochemistry of the Jurassic Jet rocks and shales is discussed in Gad et al., (1969). Palaeontological aspects of clastic facies of northern Europe are discussed in Sellwood (1971) and Hallam(1972). Regional environmental analyses have been made by Hemingway (1974), Sellwood (1972b), Knox (1973), Wilson (1975), etc. The limestones and marls occurring widely to the north of Circum-Mediterranean Province, extending far into England Bajocian-Bathonian and Late Oxfordian have been investigated for their petrography, composition and depositional environments by Pugh (1968), Purser (1969), etc. By relating his observations on hardgrounds in the Middle Jurassic limestones in the eastern Paris Basin to the broader stratigraphic context and to recent discoveries in the Persian Gulf, Purser (1969) has made significant contribution to our understanding of Jurassic limestone sequences.

Palaeontological aspects of the calcareous-argillaceous sequence have been given in Hallam (1972), Sellwood (1972b), etc. The first systematic attempt to compare the British Middle Jurassic limestones with the deposits in the Bahama has been undertaken for the Great Oolite Group of the Bath area of Somerset by Green and Donovan (1969),

who have subdivided the succession into four formations and the environments of deposition of which have been interpreted by Sellwood and McKerrow (1974). Talbot (1973) has also attempted an environmental interpretation of the relationship of the limestone horizons within the Corallian to the interbedded terrigenous clastic sediments. Interesting work has also been done on the diagenesis of the corallian limestones by Talbot (1971) and Davies (1971). Bosellini and Broglio-Lorgia (1971) have undertaken the facies analysis of the Lower Jurassic sequence of the Venetian Alps. Sellwood (1970) in his comprehensive study of part of the Lower Jurassic Britain, recognized three types of minor sedimentary and faunal cycles developed in clastic and calcareous sequences.

The Jurassic of United States Western Interior has been more researched than other parts of the world. The present knowledge of Jurassic of United States is due primarily to the extensive work which were carried out on stratigraphical and palaeontological aspects by Imlay (1967). Palaeontological reconstructions of the Jurassic sequences have been presented in Smith and Hallam (1970), and Smith et al., (1973). The Jurassic sea level changes have been illustrated in Hallam (1969). The palaeoclimatic studies of Jurassic Period have been made by Barnard (1973), Moore et al., (1992), Hallam (1993), etc. Veizer (1978, 1983) Morrow and Mayers (1978), Marshal and Ashton (1980), Brand and Veizer (1980), and Banner (1995) have worked on diagenesis and geochemical aspects of carbonate rocks of Phanerozoic. The other important studies on the Jurassic sequence of rocks from various parts of the world include those of Steikien et al., (1958), Powers (1962), Brown (1964), Wilson (1974), Hallam (1969), Davies (1972), Abbate et al., (1974), De Wet (1987), Emery et al., (1989), Sellwood et al., (1989), etc. A comprehensive

list of references on Jurassic work can be found in Arkell (1956), Hallam (1975) and the recent proceedings of symposia on Jurassic Geology.

The sequence stratigraphic techniques and its applications are given in many recent textbooks and research papers. The important valuable references are Sloss (1963), Mitchum et al., (1977), Heckel (1981), Tucker (1990), Mitchum and Van Wagoner (1990), Van Wagoner et al., (1990), Wilson (1992), and Embry (1992). The sequence stratigraphic techniques on carbonate rocks are well explained in Sarg (1988). The various recent approaches of sequence stratigraphic methods adopted by many researchers are given in Wright (1995), Muto and Steel (1997), Soreghan (1997), De Wet (1998), Carter (1998), Geel (1999), and Spence and Tucker (1999).

2.3. NATIONAL STATUS

The classic outcrops of Jurassic sediments of Kachchh basin have attracted geologists since the pioneering work of Wynne and Fedden in 1868-72. The abundance of fossil faunas and the wide range of condensed sections exposing Bathonian to Pleistocene, have attracted both palaeontologists as well as stratigraphers. Latter studies brought out that it is a discrete basin formed during Gondwanaland rifting in Late Triassic. The Tertiary and Mesozoic successions which filled the basin were studied by the geologists of GSI and ONGC.

The Mesozoic successions of Kachchh Basin attain enormous thickness of about 2400 m., the thickness of marine pile being incompatible with coastal deposits. Arkell (1956) quoted this classic area probably the most favoured locality in the world for Upper Jurassic Ammonites. He also pointed out that the lower part of Callovian is probably more fully developed in Kachchh than elsewhere in the world. There has been wide variety of

work carried out on Jurassic of Kachchh on stratigraphical, palaeontological and sedimentological aspects.

2.3.1. Stratigraphic studies

The effects of devastating earthquake in 1819 in Kachchh had been discussed by earliest geological work. Sykes(1834) has prepared the first document of Kachchh geology in the field of stratigraphy of lithosomes. Attempt has also been made to write a comprehensive account of the geology of Kachchh accompanied by a map and plates, it does not add much to the knowledge of geology of that area. W.T.Blandford (1865) recorded the first satisfactory account of the geology of Kachchh after a cursory examination of a small portion of Kachchh.

Wynne and Fedden (1868-72) were the first to prepare a detailed account of the geology of Kachchh along with a map in 1 inch = 4 miles scale, which is quite accurate and has been the only published map providing the basis and reference for all subsequent work. They divided the Jurassic rocks (the Cretaceous rocks also included) in to lower marine and an upper non-marine units which he termed respectively as Lower and Upper Jurassic. Their pioneering work has published by A.B.Wynne, in the Memoir (vol. IX, 1872) of the Geological Survey of India. However, the use of the terms "Lower" and "Upper" had been erroneous in as much as they had not been used to denote the two subdivisions of the Jurassic System. Wynne's memoir on Kachchh does not give an concise description of the structures and tectonics of the region. The two units of th earliest lithostratigraphic classification are useful in regional mapping on the basis Stoliczka's field notes. Based on "mineralogical and palaeontological" characters Waa (1875) introduced a four-fold division of Kachchh Jura into "Putchum", "Char

“Katrol”, and “Umia” Groups in ascending order. Waagen’s classification in which the Upper part of the succession was modified by Rajnath (1933, 1942). He utilized the aforesaid divisions but with chronostratigraphic terminology, that is, called them “Series” and introduced new unit - Bhuj “Series”/ “Stage” for Upper Umia Group of Waagen introducing Zamia beds (Upper Series of Wynne).

A detailed account of the stratigraphy of the Kachchh is given in Rajnath (1934, 1942). Many researchers have been following Rajnath’s classification for the Mainland. Though the map (1”= 16 miles) produced by him is not free from ambiguity it is the first and the only map which showed the stratigraphic subdivisions originally produced by Stoliczka. Among the earlier workers Cox (1940, 1952) was the first to doubt the validity of the stratigraphic names and remarked “there would appear to be little object in continuing to use such terms as “Pachham Group”, “Chari Group”, “Katrol Group”, when the more familiar European Stage names are available.

Agarwal (1957) while mapping the Jhura Dome for biostratigraphic work renamed the terms such as “Chari Series” and its topmost constituent Dhosa Oolite used by earlier researchers as Habo Series and Mebha Oolite respectively (Table – 2.1). According to him neither Mebha Oolite nor the beds of Upper Habo series lying below it can be assigned a precise age and consequently the Upper Habo Series of Jhura dome, Mebha Oolite included there in, has been considered the Callovo-Oxfordian. Pascoe (1959) from all the available data compiled a classification in which he described each unit giving the lithological and palaeontological characteristics. The Golden Oolite Stage described by him at the base of the Chari Series is a local development in Keera dome and in Jhura dome only. Poddar (1964) adopted Rajnath’s classification, but considered that th

two rank terms of "Series" and "Formation" are interchangeable. But this modification is not acceptable. Poddar's (1959) paper gives a summary of the geology of Kachchh in the context of the oil prospects of the region. His paper is not accompanied by any map.

The basement of Kachchh sediments according to Wynne (1872) is of metamorphic crystalline rocks. Wynne (1875) and Mathur and Evans (1964) also have referred it. Biswas and Deshpande (1968) reported the occurrence of similar (syenetic) rocks in Meruda Thakker Hill (24° 7' 30" N, 70° 18' 00" E) within the limits of Kachchh Basin. Jaitly and Singh (1978) discovered another occurrence of igneous complex at Nir Wandh (23° 35' 20" N, 69° 56' 00" E) in the Eastern Kaladongar (Pachham Island) where a conglomerate bed has been found directly over it, and which in turn, is overlain by sandstones and shales of Jurassic succession. This complex is described to consist of pyroxenite/hornblende, gabbro, lamprophyres and basalts (Jaitly et al., 1980).

The exposures of Jurassic of Kachchh are excellent and tracing and mapping of beds can be done with ease. They occur in six highland areas, Kachchh Mainland, Wagad and Island belt comprising Pachham, Khadir, Bela and Chorad Islands. Biswas (1981) grouped these exposures into three lithostratigraphic provinces viz., Kachchh Mainland, Pachham Island and Eastern Kachchh (Wagad, Khadir, Bela and Chorad). Biswas (1971; Biswas and Deshpande, 1968) rejects the old classification because of "..... lack of precise definition of units with respect to designated type sections, mappability and regional applicability and improper use of stratigraphic terminology". He has proposed a scheme such with a different set of names such as Jhurio, Jumara, Jhuran and Bhuj Formations in ascending order with Dhosa Oolite Member between Jumara and Jhuran and Ukra Member as intertonguing in Bhuj Formation, for Kachchh Mainland. For

Pachham Island Biswas subdivided the Pachham Series into Lower Kaladongar and Upper Goradongar Formations, but the top of Goradongar and the base of Kaladongar is not exposed. In Eastern Kachchh three mappable rock units have been recognized which are formally named as the Khadir Formation, Washtawa Formation and Wagad Sandstone (Biswas, 1977).

Kanjilal (1978) described the detailed geology and stratigraphy of the Jurassic rocks of Habo dome and proposed the name "Habo Formation" for the rocks exposed there, but not as an alternate term for the Habo Series. These proposed five divisions are (i) Black limestone Member, (ii) Dhrang Member, (iii) Jhikadi Member, (iv) Rudra Mata Member and (v) Lodai Member in ascending order. The Dhosian Stage introduced recently by Pandey and Dave (1993) constitutes marine sediments of Dhosa Shale and Dhosa Oolite, in Kachchh, is homotaxial with Oxfordian Stage (Dave, 1996). The Oxfordian in Kachchh is represented by a thick succession (48m) of Transgressive Dhosa Oolite included in Dhosian Stage of Pandey and Dave (1996) corresponding stage Malm Series concluded that the Dhosian stage representing the Oxfordian in Kachchh is more than 48m (and not 1-3m, Singh, 1989) and top and bottom bounded by unconformity. Though Bhalla (1977), Bardan and Datta (1987) and Cariou and Jai Krishna (1988) stressed the retention of Stolicza's terminology with suffix formation as done first by Poddar (1964) become the focus of subsequent studies.

2.3.2. Palaeontological Studies

The palaeontologists all over the world were particularly attracted by the rich invertebrate fossil fauna and fossil flora, since the beginning of the nineteenth century.

Palaeontological work started since the time of Sykes (1834) as he prepared the first document of the taxonomy of fossil biota, with the fossils he collected from Captain W. Smeeth. On the study of cephalopods Grant (1837) published lists of fossils along with his paper. On the basis of the study of cephalopods from the Jurassic of Kachchh and on the basis of other palaeontological evidences Waagen (1875) introduced a four-fold division of Kachchh Jura into "Putchum", "Charee", "Katrol" and "Umia" Groups in ascending order. Waagen adopted the classification and defined the units by "ammonite assemblage zones", which were correlated with European Zones to fix their ages. Subsequently Gregory (1893, 1900) studied the echinoids and corals of the lower part of the Upper Pachham Series, which are in corals (in Jumara Dome) and correlated the same with Bathonian and Callovian of Europe. Vredenberg (1910) evaluated the fossil record from the Jurassic of Kachchh and made some modifications in the age assignment to different groups of Waagen. A comprehensive account on the Middle to Upper Jurassic cephalopod megafossil fauna with description of nearly 600 species, belonging to 114 genera has been given in the form of massive monograph by Spath (1924, 1927-33). Spath (1933) revised the work of Waagen on ammonites and working on the collections of Smeeth, Blake and Wynne, Rajnath further subdivided the units by ammonitic zones which he referred as Macrocephalous "Beds", Rehmani "Beds", Anceps "Beds", etc. Waagen's classification in which the Upper part of the succession was modified by Rajnath (1933, 1942). Spath (1933) has the earlier palaeontologic works and for the first time he has elaborated the tie-up of the stratigraphic units with the European ammonite zones and stages.

The correlation of *Trigonia* with those from Europe, Somalia and South Africa has an attempt of Cox (1952) to understand the palaeogeography of Kachchh megafauna. Shukla (1953) recorded rich molluscs, brachiopods, and echinoid assemblages from Kayia Hill, northwest of Bhuj and divided the sedimentary strata into 20 beds. Agarwal (1957) studied Jhura dome for biostratigraphic work. He carried out the studies on ammonites, brachiopods, gastropods, echinoids, corals and plant fossils mainly from Jhura-Habo Dome area and recorded essentially Callovian mega-fauna. Pascoe (1959) described each unit giving the palaeontological characteristics. Mitra and Ghosh (1964) carried out purely biostratigraphic map. They were the first to realize the significance of environment and facies change in the shallow-marine shelf deposits of Kachchh.

Pratap Singh (1975) reported seven species of nannoplankton from the Jurassic succession in the subsurface of Banni. The subsurface rocks may be referred to Oxfordian based on the presence of nannoplankton and were deposited in inner neritic environment. The biostratigraphy of Bathonian-Callovian Beds of Mouwana dome, eastern Bela Island has described by Agarwal and Kacker (1978). They proposed 28 beds in to Mouwana Formation and correlation is done based on the available fauna. According to them the Mouwana Formation appears to have been laid down under shallow marine to brackish water conditions, the depth perhaps ranging from wave base to upper neritic.

Jaikrishna and Westermann (1987) have recorded faunal associations of Middle Jurassic ammonite genus *Macrocephalites* in Kachchh. They distinguished six successive new larger and stratigraphically controlled *Macrocephalites*, which are collected from Jumara. The macrocephalid succession probably starts in the uppermost Bathonian, certainly the basal Callovian and terminates below the top of Lower Callovian. Pandey and

Dave (1990) based on the changes in the foraminiferal assemblage, defined the Jurassic/Cretaceous (J/K) boundary at the top of the green oolite bed in Mundhan Anticline. In this paper the authors described the important benthic foraminifera of Tithonian and Neocomian. The major changes at this (J/K) boundary include (a) regression and elimination of calcareous benthic foraminifera followed by an arenaceous foraminifera in a new termination, (b) evolutionary development in some arenaceous foraminifera, (c) termination of older ammonites in the upper Trigonia bed of Umia, and (d) less significant change in the spore pollen assemblage.

Fursich and Oschman (1991) revealed the faunal response to transgressive-regressive cycles in Jurassic of Kachchh. The transgressive phases are represented by thin layers of reworked and bored concretions, sometimes in association with skeletal concretions, the regressive phases are documented by much thicker units of largely fine-grained sediments. The authors also found that the benthic fauna of transgressive and regressive phases differs markedly and thus mirrors the sedimentary cycles.

The microfossils of Kachchh Mesozoic were studied very little. Subbotina et al., (1960) described a rich assemblage of Jurassic foraminifera referable to the Chari Series from southeast of village of Lodai, on the eastern flank of Habo dome and from shales of Khavda. The faunal assemblage was assigned a Callovian to Oxfordian Age following the views of Poddar (1959). Smaller benthic foraminiferal fauna from the Habo dome was reported by Agarwal and Singh (1961). Rao (1964) on the evolution of faunal evidences suggested a Callovian age for Pachham Series, Callovian to Early Oxfordian for the overlying Chari Series, Upper Argovian (Oxfordian) for Katrol Series and Late Tithonian to Post-Aptian for the top most Umia Series. Tewari (1957) reported the

occurrence of *Autotortus* and few other foraminiferal genera from the Habo dome. Bhalla and Abbas (1978) and Shringarpore (1975) studied on foraminifers.

Pandey and Wurzburg (1994) described the ammonite *Parapatoceras tuberculatum* (Baugier and Sauze, 1843) from the Early Callovian "Macrocephalus Beds" of Pachham Island of Kachchh also. Shukla and Singh(1993) recorded marine macroinvertebrate from Bhuj sandstone for the first time. These are shell impressions (external moulds) of *Indotrignonia* and a marine bivalve. Highly porous nature of Bhuj sandstones caused dissolution of shells during diagenesis, destroying the body fossils but preserving the fossils.

The Jurassic foraminifera from the Pachham-Chari Formations of Jhurio Hill were described by Niti Mandal and Singh (1996). The description of Middle Jurassic ammonites from Jumara Dome is given in Sreepat Jain (1997). Recent finding of fossil remains of dinosaurs from the Middle Jurassic sediments of Kachchh (Sathyanarayana et al., 1999) is also an important milestone in the palaeontological studies. The biostratigraphic classification of Middle Jurassic to late Jurassic succession of Kachchh is given in the Table 2.1.

2.3.3. Sedimentological and Other Investigations

Though detailed stratigraphy and palaeontology of Mesozoic succession has been worked out, little information is available on the detailed sedimentology of the Jurassic rocks of Kachchh. Important contributions on the sedimentology of the Jurassic rocks of Kachchh include those of Balagopal and Srivastava (1973), Balagopal (1977), Biswas (1977, 1981, 1982, 1987), Singh (1989), Fursich et al (1992), Bhalla (1996) and Nandi and Dessai (1997), Dubey and Chatterjee(1997) and Osman and Mahender(1997).

Table-2.1 Biostratigraphic Classification of Middel to Late Jurassic Sediments of Kachchh, Gujarat

Stages	Waagen 1933	Spath 1937	Agarwal 1957	Kanjilal 1974	Mitra et.al 1979	Bardhan 1987	Krishna 1987	Prasad 1988	S.Prasad 1998
Oxfordian	Dhosa Oolite	Upper Dhosa Oolite Lower Dhosa Oolite				Biozone 6	Discontinuity unnamed Semirugose	Perisphintes Maya Semirugose	Helena Maya
Callovian	Athleta Beds	Upper Athleta Beds Lower Athleta Beds	Reinekeia	Hect.Lirens-Hubert Omphales-Orionoides	Peltoceras	Biozone 5	Unnamed Athleta	Laladeanum Athleta	Atleta
	Anceps Beds	Upper Anceps Beds Lower Anceps Beds		Sub-kossmatia Indiocyclo-ceras	Obtusicosites	Biozone 4 Biozone 3	Coronatum Anceps Opis	Anceps Opis	Anceps
	Macrocephalum Beds	Upper Macrocephalus Beds Middle Macrocephalus Beds Lower Macrocephalus Beds	Macrocephalite	Macro-cephalites	Macrocephalite	Biozone 2 Biozone 1	M.semioevis M.formosus M.chrysolithicus M.medagaskerenis M.triangularis	Formosus	Formosus
Bathonian									Triangularis

Balagopal (1972) has classified the Pachham and Chari limestones of Jhura and Habo domes, on the basis of their modal classification following Folk's classification of carbonate rocks. He divided the Chari Series into four subdivisions (Ci to Civ). Of which, Ci and Civ are predominantly calcareous, while Cii and Ciii are overwhelmingly arenaceous and include several bands of conglomerates. Also the petrography of Chari arenites were studied by Balagopal and Srivastava (1973) and they proposed a classification to these arenites and included it as a part of the orthoquartzite-carbonate facies. Desai et al., (1975) discussed the depositional environment of Western Wagad Mesozoic sediments and suggested a warm and moderate environment of deposition. Deshpande (1978) has stratigraphically divided the Wagad rocks into three formations, namely Washtawa Formation, Kantkote Formation and Wagad Sandstone in ascending order. The Mesozoic sediments of western Wagad and their depositional environments has been described by Desai and Shringarpore (1975). They proposed a sedimentation model of the western Wagad depositional cycle. Deshpande and Merh (1980) proposed a sedimentary model of Wagad Hills, which is comprising environments of deposition, basin geometry, lithic fill, lithic arrangement, directional structures and tectonic setting. According to Biswas (1977) the environment of deposition of the units indicates that Bathonian to Oxfordian (represented by the Kaladongar, Goradongar, Khadir, Washtawa, Jhurio and Jumara Formations) was a period of transgression when the environment changed from littoral to neritic and post Oxfordian to Lower Cretaceous (represented by the Wagad Sandstone, Jhuran and Bhuj Formations) was the period shifting the environment from neritic to fluvio-deltaic as the depocentre moved westward. It is clear from the stratigraphic description and the trend of facies variation that

the sea transgressed from west to east and receded westward after attaining the peak of transgression framework is also indicated by the facies pattern.

The basin framework, palaeoenvironment and depositional history of Mesozoic sediments of Kachchh basin have been described by Biswas (1981) in detail. The lithostratigraphy of Mesozoic Kachchh Mainland proposed by Biswas (1981) is given in the Table-2.2. According to him the two distinct sedimentary parts within the basin are a lower marine carbonate-shale section and an upper clastic section, which represents a major transgressive-regressive cycle. Biswas (1981) proposed the environment of deposition as sub-littoral. He also recorded intertonguing facies tracts and their distribution shows spatial arrangement of environment during a time period. According to Biswas (1981) the upper clastic section represented by the deltaic Jhuran and Bhuj Formations and Wagad Sandstone is diachronous. The delta build up took place in a time span from Oxfordian to Kimmeridgian (when it started to prograde from the eastern margin of the basin) to Lower Cretaceous (when reached the depocentre).

Jaikrishna et al., (1983) found numerous wave-built sedimentary structures, abundant marine fossils and highly bioturbated and glauconite-rich beds. Based on this, authors propose a marine origin for the entire Kachchh succession. Singh (1989) described the genesis, fossil content, sedimentological characteristics and stratigraphic significance of Dhosa Oolite. He suggested that the Dhosa oolite is a transgressive condensation horizon representing the time-span, related to the worldwide sea-level rise. According to him the mixing of ammonite fauna of various ammonite zones is probably a result of the combination of processes, slow rate of sedimentation, burrowing activity of organisms and storm events causing sediment reworking. Biswas (1981) considers Dhosa

Table : 2.2 MESOZOIC LITHOSTRATIGRAPHY OF KUTCH MAINLAND (After Biswas, 1981)

AGE	Formation	Member	Lithological charactersitics	Depositional environment
Neocomian to Albian (Lower Cretaceous)	BHUI FORMATION (350-900mt +) (Thickening Westwards)	Upper	Light coloured sandstone, kaolinitic claystone and sandy iron-stone bands. Sandstones, medium to fine grained feldspathic wackes, coarse arenites in channel fills; Crossbedded-planar & tabular, cut and fill. Occasional plant fossils, fossil wood common.	Upper deltaic plain to fluvial
		Middle	Green glauconitic sandstones and shales, thin fossiliferous limestones and red ironstone bands containing pelecypods, gastropods and ammonites. Large chunks of fossil wood in random orientation. Interfingers with Upper and Lower members towards the east.	Restricted Bay or lagoon
		Lower	Deeply coloured, red and yellows andstones: ferruginous, feldspathic wacke, fine grained. moderately sorted; coarse to fine grained arenites in channel fills showing fining up. Rhythmites of sandstones shales ironstone bands; Cross-bedded (planar) ripple marked; abundant leaf impressions. Occasional coal beds.	Lower deltaic plain
Kimmerdgian to Neocomian	JHURAN (420 – 850 M+) (Thickening westwards)	Kaesar	Greenish yellow sandstone: calcareous and ferruginous feldspathic wacke, very fine to medium grained; moderately to well sorted; Cross-bedded (planar, trough & festoon); (contain Trigonina sp. & Astarte sp.)	Delta front (distributory complex)
		Upper	Mainly sandstones with subordinate shale. Sandstones: fine to medium grained, moderately well sorted feldspathic wacke; Current bedded (tabular, festoons, & herring-bones), ripple marked; convolute bedding, load casts, cut & fills common. Local bands of pelecypods and also plant beds.	Delta fringe
		Middle	Mainly grey shales with fine grained, fissile sandstone bands. Highly fossiliferous in the west but sparsely so in the east, mainly ammonites, pelecypods, belemnites, gastropods, cut & fill structure common.	Prodelta
		Lower	Shale/sandstone alternation. Sandstones: fine grained, moderately sorted feld-spathic wacke; Cross-bedded, ripple marked; fossiliferous in the west, less so in the east.	Sub-littoral
Callovian to Oxfordian	JUMARA (280 m)	Upper	Greenish grey, gypseous glauconitic shales well laminated with thin limestone alternations. Characteristic oolitic bands near the top. Highly fossiliferous. diverse (mainly cephalopods, brachiopods, pelecypods and corals).	Upper Infra-littoral Lower shales Circa-littoral
		Middle	Base biomicrite, middle yellow calcareous sandstone, top conglomerate. Fossiliferous with pelecypods. Represented in the west by fossiliferous limestones with golden oolites (oolitic intrasparrudite).	Littoral
		Lower	Olive and grey shales with thin limestone bands, containing rich crop of fossils: ammonites, corals, brachiopods, pelecypods, belemnites etc.	Circa-littoral
Bathonian to Callovian	JHURIO (300 m)	Upper	Interbedded micritic (biopelmicrite) and sparitic (biopelsparite, oosparite) limestones with "golden oolite" (oolitic intasparite and intrasparrudite), with iron-oxide coated pseudo-oolitic bands in the lower part. Fossiliferous: cephalopods, brachiopods, pelecypods etc.	Littoral Wave zone- Intertidal
		Middle	Thickly interbedded shales and limestones (mainly "golden oolites"- Oolitic intrasparrudite). Fossiliferous: brachiopods, pelecypods, cephalopods etc.	Littoral (Peritidal) to Sub-littoral
		Lower	Interbedded shales and limestones, with lenticular "golden oolites". Fossiliferous as above.	Littoral to Sub-littoral

Oolite to mark the maximum transgression related to the deposition of regressive coastal deposits of Katrol and Umia Formations.

The depositional environment of Bhuj sandstone was traditionally considered fluvial or deltaic though recently it has been argued that the Bhuj sandstone represents Coastal marine sand (Jaikrishna et al., 1983; Howard and Singh, 1985). Shukla and Singh (1990) distinguished five distinct lithofacies in Bhuj sandstone. Lithofacies 1 to 4 represent deposition in a prograding estuarine, tide-dominated coastline, while lithofacies 5 represents deposition on shallow shelf below wave base during the events of sea-level rise (transgression). The authors suggested that the Bhuj sandstone is made up of repeated complete or incomplete facies cycles punctuated by short lived transgressive events in dominated estuarine coastal line. Fursich and Oschmann (1992) made an attempt to document the features such as hardgrounds, reworked concretion levels and condensed horizons in the Jurassic rocks, to unravel the sequence of events that led to their formation and discussed their significance for the depositional history of Kachchh basin.

Phansalkar and Kadkikar (1992) revealed the sedimentary characters of the Jhuran Formation (Late Jurassic) – Bhuj Formation (Early Cretaceous) clastics exposed near Bhuj and have thrown light on their depositional environment. The interlayered sandstone-shale succession of Jhuran Formation shows shallow marine environment of deposition, and the essentially sandstone of Bhuj Formation with a polymict conglomerate at its base, shows a change from a shelf to an estuarine environment. Shukla and Singh (1991) described the significance of Bhuj sandstone. According to the authors, these bioturbated sandstone horizons show complex superimposition of dense networks of

various burrow systems, and thus represent submarine non-depositional events related to sea-level rise or short-term transgressions.

Khadkikar (1996) suggested that the beginning of break-up of Gondwanaland recorded in the ironstones of Jurassic rocks of Kachchh basin system. According to him the older ironstone known as Golden Oolite documents the formation of a mid-oceanic ridge after a period of rifting the Greater India as a discrete continental land mass, from the Gondwanaland. He suggested that the iron content in the ironstones is on account of hydrothermal plumes.

The stratigraphic and sedimentologic account of the Middle Jurassic (Callovian) succession of Habo dome is given in Osman and Mahender (1997). The stratigraphic variation of field observations made by them and also the texture and mineralogical characters suggest an early regressive latter transgressive phase of depositional environment. On the basis of lithologic characters and depositional textures and their inferred relationships, five lithofacies associations have been identified. Dubey and Chatterjee (1997) has given a detailed study on the provenance and basin evolution of Kachchh basin during Mesozoic based on the quantitative and qualitative analyses of mineralogical composition of sandstone. According to them the Mesozoic sedimentation in Kachchh basin commenced with the deposition of retrogradational and aggradational successions (RS & PS) in the lower part followed by the progradational succession (PS) in the upper part. The petrographic and geochemical characters and comparative account of diagenesis and stable isotope geochemistry of the Middle Jurassic carbonates is given in Nandi and Dessai (1997). The importance of Kachchh basin as regards to the geology, stratigraphy, tectonics and mineral resources has been discussed at the recently held

National Seminar on Kachchh Basin at the Department of Geology, Banaras Hindu University, Varanasi from 21-23rd Dec 2000. Recently, due to the devastating earthquake on January 26, 2001, the Kachchh area has once again attracted the attention of scientists world over.

From the review of literature it is very clear that there has been a very little emphasis made in the past to understand the lithofacies distribution, microfacies variation, depositional and diagenetic history of the basin during the initial sedimentation in Jurassic Period resulting in the deposition of Middle Jurassic sediments in a transgressive Tethys Sea over the Kachchh basin. Therefore, the present work is an attempt to study the above parameters.

CHAPTER - III

GEOLOGY AND STRATIGRAPHY

3.1 GENERAL

The pericratonic sedimentary basin of Kachchh is developed in an east west aligned (between 68° 00' 00" E to 71° 30' 00" E) embayment deepening to the west into Arabian Sea (Biswas, 1982). Kachchh Basin came in to existence in Late Triassic- Early Jurassic at the time of rifting of Africa and India exposes a well developed Mid-Jurassic to Early Cretaceous succession. Kachchh Basin is unique in its rugged high lands standing amidst vast plains of the Great and Little Ranns of Kachchh (Plate: 3.1-1). The basin is delimited in the northeast and east by the Precambrian inliers of Pakistan (Nagar Parkar), South Rajasthan, Aravalli and North Gujarat. Kathiawar (Saurashtra) peninsula marks its southern limit. The basin experienced periodic carbonate sedimentation from Middle Jurassic to Neogene times. The total thickness of the Mesozoic sediments in Kachchh ranges from 1525 to 3050 m deposited on crystalline basement composed of Archean and Proterozoic Rocks (Biswas and Deshpande, 1968).

The successions were developed due to repeated marine incursions during the Middle Jurassic to lower Cretaceous period followed by major tectonic movements and Deccan Trap volcanism in the Late Cretaceous time. The Mesozoic rocks are exposed in six highland areas of Kachchh Mainland, Wagad, Pachham, Khadir, Bela and Chorar; whereas the Tertiary strata are exposed only in the bordering plain lands. Regional structural elements of Kachchh Mainland consists of two parallel fault flexures along the NW-SE striking master faults (Biswas, 1982). The Jurassic rocks are best developed in the northern

flexure. A string of culminations observed along this flexure with depressions between them. These zones of culminations stand out in domal forms at Jara, Jumara, Nara, Keera, Jhura and Habo hills where inliers of relatively older Jurassic rocks, the Jhurio and Jumara formations occur in the core of domes. The dried-up nalas, cliff sections and road cuts provide good exposures of Jurassic outcrops for sample collection.

The procedures of sample collection include: (a) systematic sampling along selected traverses, (b) samples from cliff sections and (c) spot sampling from specific localities. In all, more than 300 samples have been collected for the detailed field description and laboratory analyses and the results of which are given in subsequent chapters.

3.2. STRUCTURE , TECTONICS and GEOMORPHIOLOGY

The basin frame work consists of an embayment closed by Radhanpur –Barmer Arch in the east, a sloping platform featured by parallel east-west fault ridges and a Median High across them. The Median High, a synchronous one (Scholten, 1959), occurs along the hinge-zone of the basin west of which the sediments thicken considerably with accompanying change of facies. The northern margin of the Basin is faulted along Nagar Parker fault. The structural axis of the basin plunges southwest, trending parallel and close to the south-eastern margin. The margin of the basin is surrounded by Precambrian terrain of Pakistan (Nagar Parker), Meruda Hill of Great Rann, Rajasthan, Aravalli Range and North Gujarat.

The structure of the Kachchh Basin (Biswas, 1980) includes six major uplifts which have given rise to highland areas of Kachchh Mainland, Wagad and Pachham, Khadir, Bela and Chorar ‘Islands’. The sub-basins between them in which Tertiary sediments have been deposited, are parts of the ‘residual depressions’ (Belousov, 1962). These structural lows form the great plains of the Ranns of Kachchh and Banni covered by Recent marine sediments. The Gulf of Kachchh sub-basins separates the Kachchh Mainland and Kathiawar

uplifts. The uplifts are tilted fault blocks and sub-basins are half-grabens between them. The uplifts have been produced by a series of parallel east to west, quasivertical, marginal faults which follow the major tectonic trends of the Precambrian basement. These marginal or master faults are up-thrusts (Prucha et al., 1965) with associated "fault flexures" or "bruchfaltens". The repetitive movements along the faults were essentially vertical and unidirectional. The marginal bruchfaltens are asymmetric in cross-section and broken up by higher order idiomorphic folds like domes, brachy-anticlines, and narrow doubly plunging anticlines of varying shapes, sizes and orientations. Thus, a chain of such folds are seen along the marginal faults which separate the uplifts and the covered sub-basins. Similar folds are developed also along the important longitudinal faults within the uplifts.

Besides the major uplifts, several small uplifts also occur close to the major ones, e.g. Kuar Bet, Cheriya Bet, Gangta Bet, etc. Secondary high angle tensional and shear faults of low magnitude occur across the uplifts. The tensional faults are generally accompanied by intrusions of basic dyke. Numerous basic dykes, sills, and plugs have intruded the Mesozoic rocks. Laccoliths associated with domes are seen in the Mainland. Most of the intrusions are syntectonic but episodic. Deccan trap flows followed the main Upper Cretaceous diastrophism (Biswas and Deshpande, 1973) when the highlands were uplifted exposing the Mesozoic rocks.

3.2.1. GEOMORPHOLOGY

The general, shape, size, elevation and orientation of the hill ranges in Kachchh Basin appear to be controlled by the structural geometry of rocks. The islands and the highlands are the zones of principal uplifts of second order within them. The hills composing them are the anticlinal and domal uplifts of the subsequent orders within the zones of parent uplifts. The structure of Kachchh is controlled by block faulting. The

highlands representing principal uplifts are the tilted fault blocks and the low lying plains are the residual depressions.

The domal hills of Northern Range of the Mainland present interesting geomorphological features. They are in various stages of erosion due to different uplift during the range which are at structurally lower level, are maturely dissected. Among the western domes, Jara and Jumara, Jara is characterised by annular valleys and Jumara is markedly dissected and is in its late youth stage. Jhurio Dome in the middle of the Northern Range is a huge dome hill in its early youth stage. The Jurassic limestones form the protective roof above the dome and the older rocks are only exposed in deeply cut fault valleys. Drainage is centrifugal and the radial consequents have already started cutting down the protective roof of the dome by active headward erosion. The Habo Dome is the biggest dome in Kachchh. It is in mature stage of erosion. The older competent limestone beds have just started to crop out at the core and the shales above have been removed by erosion to produce a central depression. The landforms of Pachham Island are also very youth with two fault block hill ranges and a central valley between them. Whereas, Khadir and Bela islands show matured topography. Chorar Hills topography approaches the old age.

The drainage pattern is greatly influenced by the structural morphology. The marginal hill ranges are the principal water-sheds. The consequent rivers and streams flow down their back-slopes while the younger obsequent streams flow down the scarp faces. The regional drainage pattern is therefore, parallel.

3.3. SEDIMENTARY STRUCTURES

The sedimentary structures observed in the study area include cross-bedding of various types, ripple marks, laminated bedding, mudcracks, trace fossils, hardgrounds, concretions, nodules, soft sediment deformation, jointing etc.,.

3.3.1. Cross-Bedding

Cross-bedding is perhaps the most important sedimentary structure seen at many localities(Plate: 3.3-1 & 2) of the exposed middle Jurassic succession of Kachchh. It is better seen in sandstone and sandy limestones. In most cases the cosets are few centimeters thick and the individual lamina is less than one centimeter thick.. The strike and dip of the cross-bedding unit varies abruptly from place to place, usually inclined at an angle of 5-10 to the horizontal plane. The cross-bedding is mostly of high angle wedge type cross-stratification. Large scale planar and herringbone cross-stratification types are also observed in this rock succession. The dip of the foreset varies from gentle ($<10^{\circ}$) at a few places to quite steep ($>20^{\circ}$) at several localities. Abrupt reversals of the direction of dips are observed frequently. The thickness of the individual cross-laminae vary between $<5\text{mm}$. to few centimeters. Skeletal composition and grain-size changes and their weathered surfaces define the cross-strata. The individual cross-bedding units commonly range from 4-15m. in length and with a variable thickness of 1 to 5m.

3.3.1.1. Palaeocurrent analysis :

More than 130 readings of azimuth and dip of the cross-bedding strata of Middle Jurassic sequence of Kachchh are recorded from various localities (Jumara, Jhurio and Habo domes) in order to calculate the vector mean direction. The vector means of the cross-bedding dip azimuths were calculated trigonometrically by following the procedures of Curray (1956). The locality wise distribution of dip azimuth and calculated vector mean

data and composite rose diagrams are given in Table – 3.1. The vector mean of the cross-strata in all the localities in general indicates a palaeocurrent direction towards west and southwest.

3.3.2. Ripple Marks

Varying scales of ripple bedding is observed (Plate: 3.3-3). in sandstones and sandy limestones of Jumara Formation indicating the shallow nature of the depositional environment. Large interference ripples observed in Jhikhidi area of Habo domes is shown Plate: 3.

3.3.3. Laminated Bedding

Laminated bedding with alternating fine and coarse laminae has been observed in the sequence at various localities especially from cliff sections, where it can be clearly seen. Grain-size and weathered surfaces define the laminations (Plate: 3.1-4).

3.3.4. Trace Fossils

Several types of trace fossils have been observed in Middle Jurassic sequence of Kachchh from shaly units. Although the preservation of trace fossils is better seen in argillaceous units, sandy-carbonate units also exhibit poorly preserved trace fossils such as *Rhizocorallium*, *Thalssinoides* etc. (Plate: 3.2-3). The various burrow patterns observed in the succession include vertical burrows, sand-filled burrows and bioturbated horizons.

3.3.5. Jointing

Jointing is prominently developed in ferruginous and calcareous sandstones and sandy limestones. Two sets of joints are clearly seen giving rise to the well shaped blocks (Plate: 3.3-5) of the litho units. At places columnar jointing is prominently developed in

Table – 3. 1 Palaeocurrent Analysis data of Middle Jurassic of Kachchh (Frequency method)

	Bhuj (around)	Jhura	Habo	Composite
Class Interval (degrees)	30	30	30	30
Population	42	42	52	136
Maximun %	23.80	33.30	25.00	23.50
Mean %	8.30	11.10	9.10	8.30
Standard Deviation	6.05	10.24	7.79	7.03
Vector Mean (degrees)	240.52	245.89	239.59	242.35
Confidence Interval (degrees)	44.62	17.45	20.85	13.90
R-mag	0.27	0.62	0.49	0.46
Current Rose Diagrams				

sandstones belonging to Late Jurassic to Early Cretaceous. The pattern (Plate: 3.3-4) is very similar to the columnar structures commonly observed in Basalts. Best exposures of columnar sandstone occur in and around Bhuj. Regular hexagonal columns developed perpendicular to bedding are with four to five sides are common. Each column is about 1 to 1.2 m. height and about 20-30 cm. in diameter.

3.3.6. Stromatolitic mineral crusts or hard grounds

Iron crusts, usually exhibiting a stromatolitic texture (Plate: 3.2-5) are commonly seen on the top of oolitic sandy beds at some localities are associated with large iron oncoids. The crusts are 2-4 cm. thick.

3.3.7. Concretions, nodules and other miscellaneous Structures

Concretion layers are very common with in the argillaceous limestone interbeds of Kachchh Jurassic. These beds consists of elongate, cylindrical and irregular shaped nodules of conspicuous origin are seen in limestone at a few localities (Plate:3.2-6). These concretions show evidences of reworking.

Miscellaneous structures noticed in the study area include the typical weathering pattern of calcareous sandstone (Plate: 3.2-4) and soft sediment deformation (Plate : 3.3-6) etc.

3.4. GEOLOGY

The Middle Jurassic sequence exposed in Jumara, Jhura and Habo domes (Fig.3.1) has been studied for understanding the geology, sedimentology and palaeoenvironments of Kachchh Mainland. Jurassic rocks exposed as inliers in these hills are belong to Jhurio

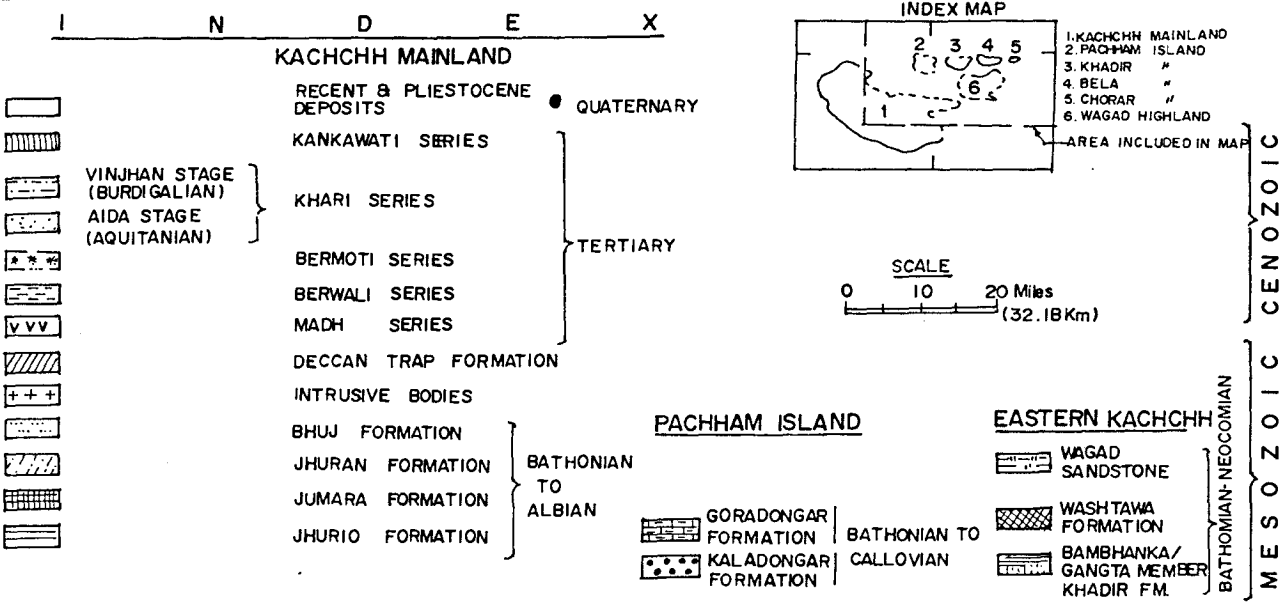
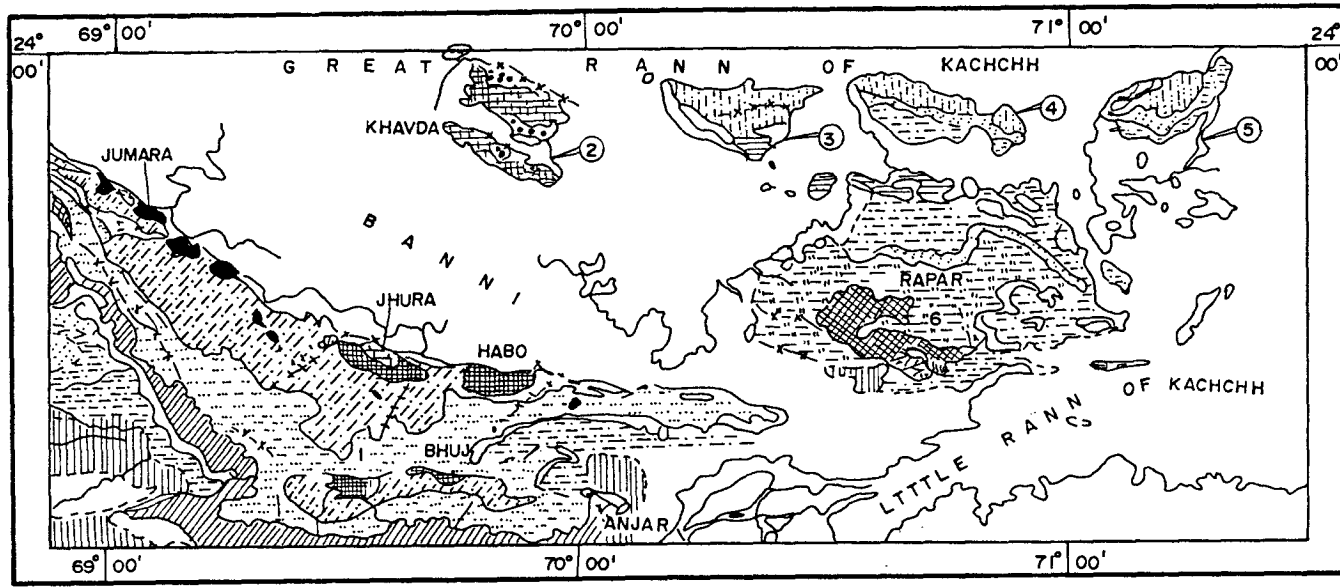


Fig. 3.1 Geological map of Kachchh

(Pachham) Formation and Jumara (Chari) Formations. The geology and stratigraphy as observed in these areas has been discussed below.

3.4.1. Jhura Dome

The Jhura Dome lying 38km. NNW of Bhuj covers approximately 140 sq.km. is composed of numerous small hills and valleys. The maximum altitude of this area is about 320 m. The topography is apparently related to dome structure. More or less concentric and parallel ridges (Plate: 3.1-2) of different beds characterize the relief of the hills. The beds dip at high angles towards the north, whilst towards the south the dip values are quite low. The geological map of the Jhura Dome is given in the Fig. 3.2. The nala section west of the Badi village offers an excellent area for the study of the complete Middle Jurassic succession of Kachchh Mainland. A thick succession of Jhurio Formation exposed in these hills comprises dominantly of calcareous shale/siltstone, golden oolite and limestones. The overlying Jumara (Chari) Formation is represented by dominant argillaceous with varying arenaceous and calcareous units. The top of this formation is marked with prominent Dhosa Oolite which is overlain by a hard and compact ridge forming sandstone. Limestones are sandy oolitic and conglomeratic with varying amount of fossils including trace fossils (Plate: 3.2-3). The sandstones are hard, compact and ferruginous. Shales display varying shades of colours are gypsiferous (Plate: 3.2-1) in the upper part. The composite lithostratigraphic column of Jhurio Formation is shown in the Fig. 3.3. The entire lithostratigraphic column as observed in the study area (Jhura dome) is presented in Fig. 3.4b.

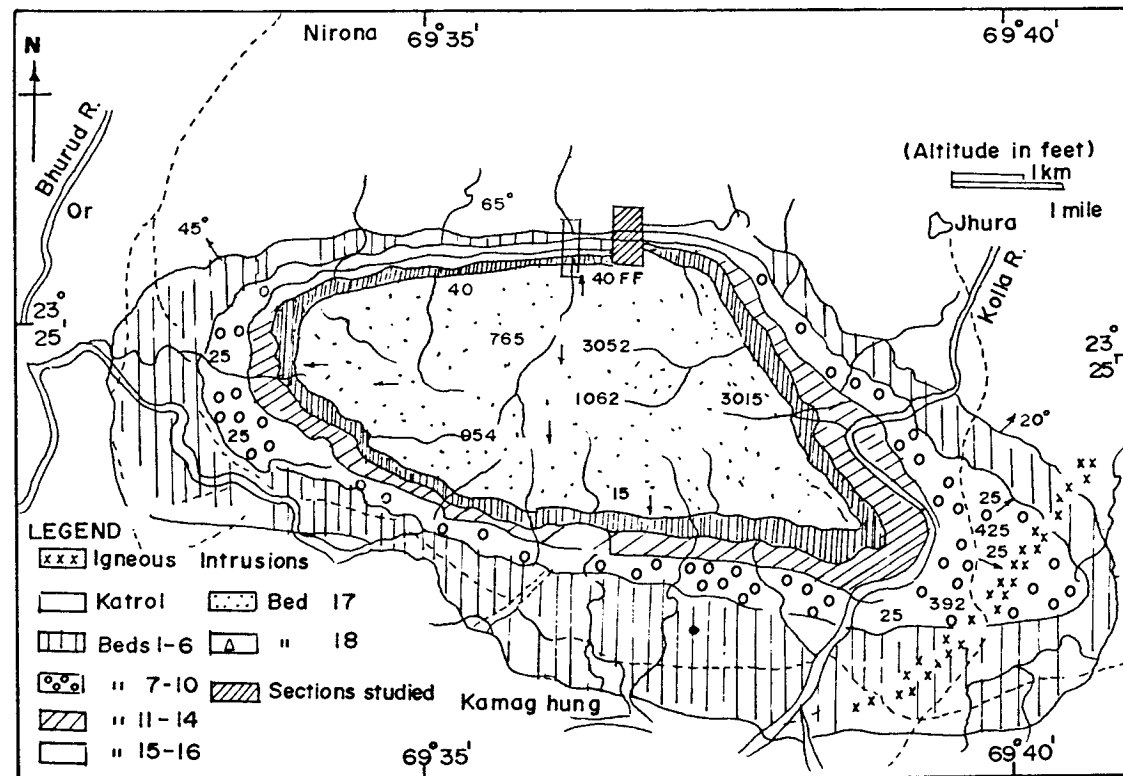


Fig.3.2 Geological map of the Jhura Dome (After Agarwal, 1957)

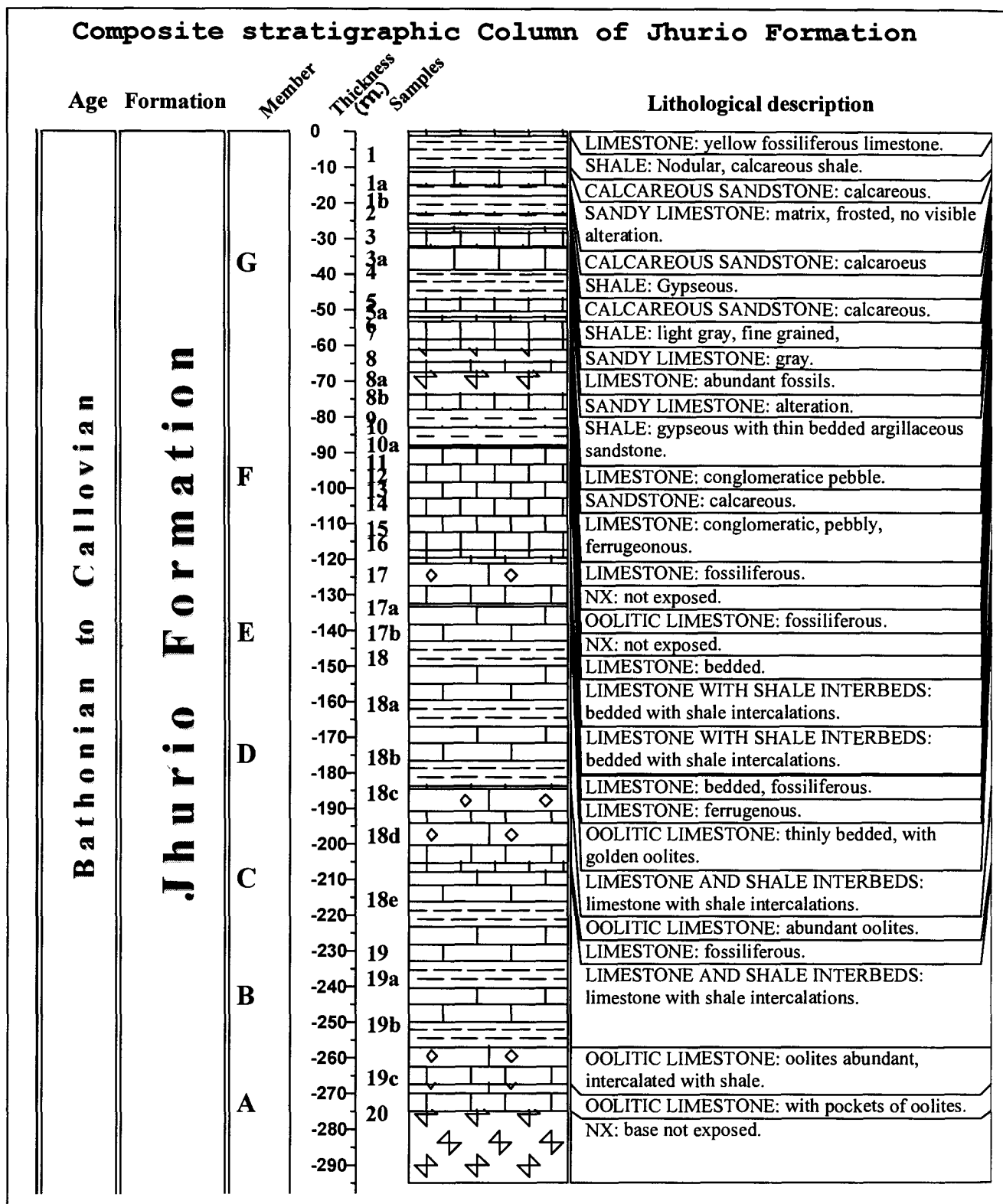


Fig.3.3 Composite Lithostratigraphic Column of Jhurio Formation, Jhura Dome, Kachchh Mainland

3.1

Fig. 3. ~~3a~~ Lithostratigraphic Column of Jurassic of Habo Hills

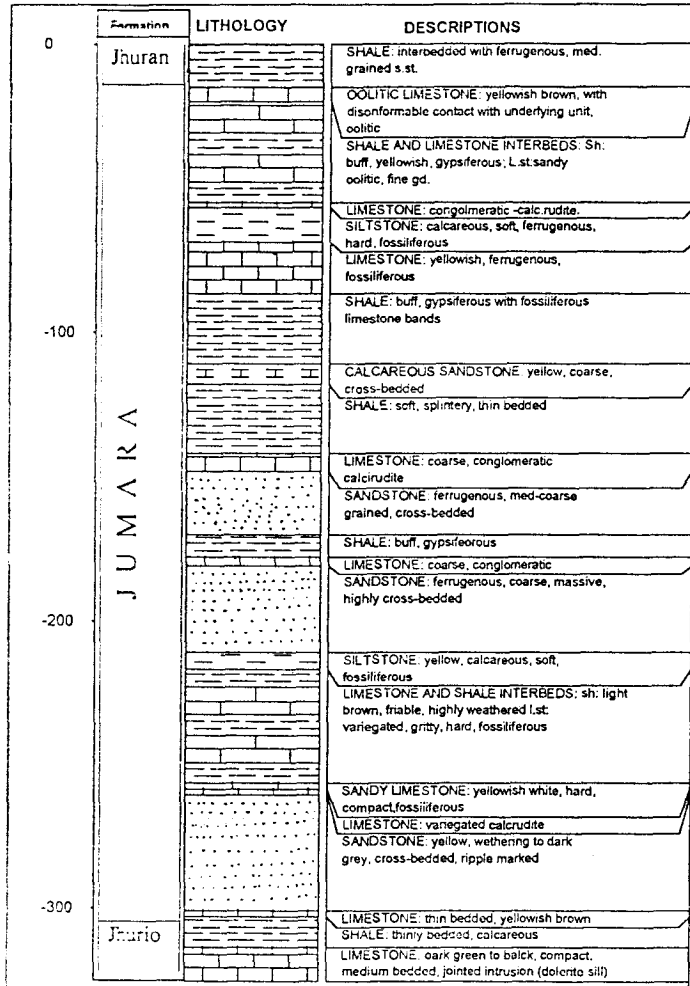


Fig. 3. ~~3b~~ Lithostratigraphic Column of Jurassic of Jhura Hills Fig. 3. ~~3c~~ Lithostratigraphic Column of Jurassic of Jumara Dome

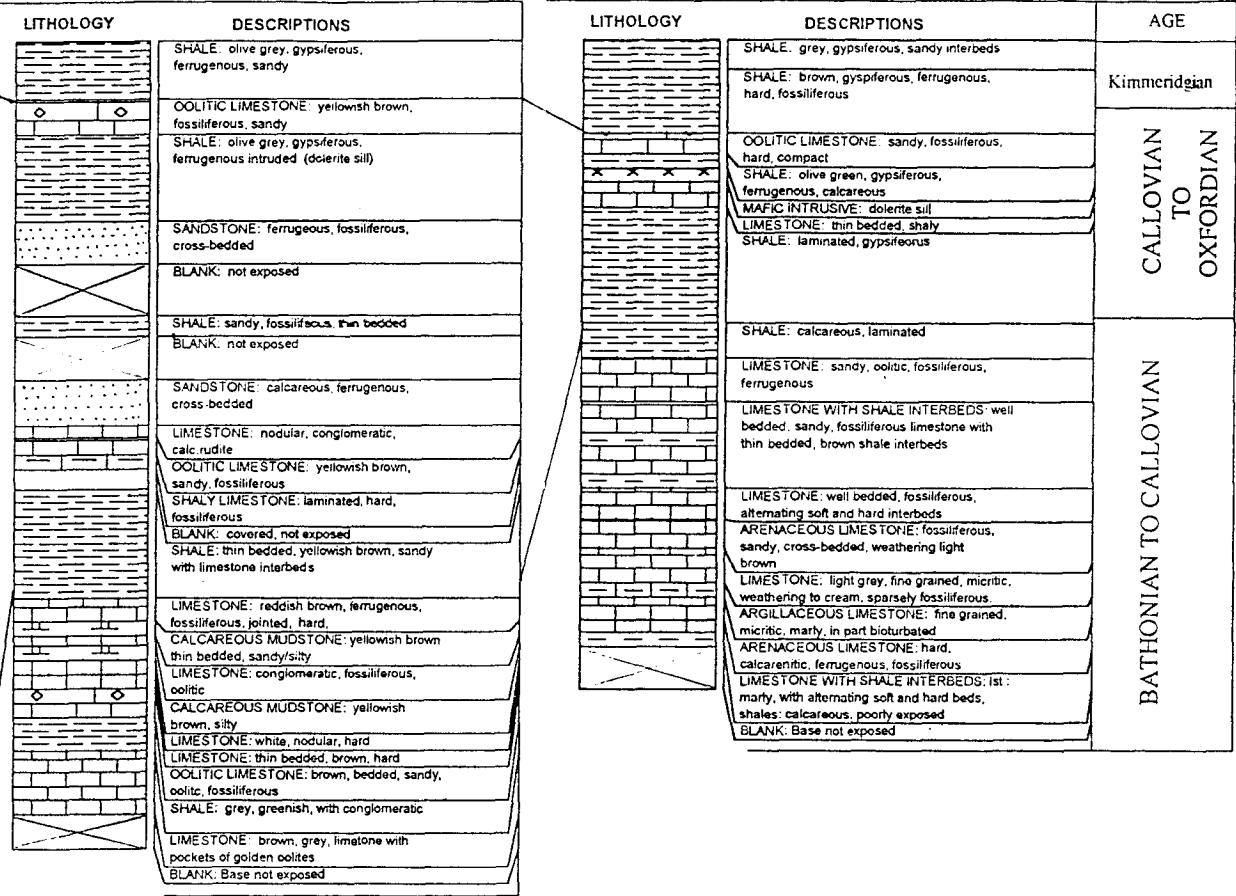


Fig. 3. ~~3d~~ Lithostratigraphic Columns of Kachchh Mainland

3.4.1.1. Lithofacies Associations :

The rock types present in the area can be grouped in to three broad lithofacies associations (LFA 1 to 3) representing the earlier classified seven members (Member A to G in ascending order) of Biswas (1977)(Table - 3.2).

(a) Golden oolitic limestone – Grey limestone lithofacies Association (LFA – 1)

The associated rock types are fossiliferous golden oolitic limestone interbedded with greenish grey to dark grey fossiliferous limestone with patches and some bands of golden oolites. The golden oolitic rocks are deposited with intercalations of shale which are quartzose in texture. The limestones are pale brown and dark grey, fine to medium textured silty sparite. The megafossils of golden oolitic rock include brachiopods, bivalves, molluscs, etc.

The fossils are of benthic type in majority in the golden oolitic rocks. Where as the fossil types in the grey limestones indicate an environment of subtidal and shallow shelf to deep lagoonal in character. This lithofacies corresponds to the Member A, C, and E in the vertical stratigraphic column (Fig.3.3). The Member A and C have the similar petrological characters, while the Member E is characterised by rhythmic cyclic sedimentation in which the thickness of the beds decrease towards up. In this member the golden oolitic rock are deposited interbedded with fossiliferous yellowish brown limestone with mud intraclasts and mud pellets. The fossils are mainly thin shells of pelagic bivalves and planktic fossils. This lithofacies could be peritidal type which were deposited during the repeated rise and fall of shore line in a transgressing sea.

Table- 3.2 Lithostratigraphic succession of Jhurio Formation (Biswas, 1977)

AGE	Formation	Member		Lithological Description	Environment
Callovo-Oxfordian Jumara Fm					
Bathonian to Callovian	JHURIO (300 m)	Upper (80 m)	G	Thinly bedded, yellowish-brown & white limestone interbedded with white calcareous shales	Littoral Wave zone-Intertidal
			F	Thin bedded yellowish limestone with thin bands of limestone pebble conglomerate & Golden oolite limestone	
		Middle (140 m)	E	Brownish gray thin bedded limestone interbedded with Golden oolitic limestone beds	Littoral (Peritidal) to Sub-littoral
			D	Gray calcareous shale	
			C	Golden Oolitic limestone weathering into brick red	
		Lower (80 m)	B	Gray calcareous shale	Littoral to Sub-littoral
			A	Interbedded, yellowish brown & gray limestone with local golden oolites and shales	
		Base not exposed			

(b) Pelagic limestone – hemipelagic mudstone lithofacies (LFA – 2)

The lithofacies characterised by rhythmically bedded pelagic limestone with alternating thin hemipelagic mudstone beds. The lithofacies varies slightly in character from pelagic lime-mudstone through calcareous siltstone to bedded limestone, from the Member-B through Member-D to Member-F. The thickness of the limestone bed is increasing upward. The calcareous mudstone is nodular in Member-B and is massively bedded in Member-D. The Member-F is characterised by the thin interbeds of ferruginous shale with pebbles in the middle part of the member. The most characteristic feature of the Member-F is the repeated thin (5-15 cms.) interbedded crystalline fossiliferous limestone laminated with clay. The megafossil content could be thin-shells of bivalves and other characteristic fossil types are absent.

No well preserved depositional structures are present in the pelagic limestone lithofacies. The rock appear to have undergone early diagenetic lithification and compaction. The Member-F starts with a basal thin-bedded ferruginous pebbly conglomeritic limestone. The characteristic fossil faunas in this basal conglomeritic limestone includes mainly large shells of brachiopods, oysters, bivalves and gastropods. The fossils and ferruginous cherty flat pebbles are embedded in a massive ferruginous micritic mud. The fossils are highly bored, corroded and some are partly silicified. The Member-B and D are deposited in a slope to basinal open shelf area during the transgressive period of the Tethys sea. Where as the Member-F may be formed in a slope to basin floor or deep lagoonal environment.

(c) The limestone - calcareous sandstone – gypseous shale lithofacies (LFA – 3)

The lithofacies association is characterised by thick bedded ferruginous pebbly conglomeritic micritic limestone at the base and overlain mainly by calcareous sandstone, sandy limestone with alternate thick beds of gypseous shale. The thick bedded gypseous shale is characterised by the presence of thin-beds of evaporites (gypsum and anhydrite). This is overlain by the thick calcareous shale with yellowish white nodular limestone bodies and thin lenses of black limestones and the top most thin-bed of yellow limestone. This facies corresponds to the Member – G.

The member is influenced by the abundant terrigenous input which indicates a nearshore environment which was active through out the deposition of the member. The sandy limestones and calcareous fossiliferous sandstones are deposited in a nearshore-beach environment characterised by the sorting of the grains, roundness of the quartz grains and the cement types. These rocks are also characterised the abundant fossil shells of bivalves, molluscs and brachiopods at the top of the beds with abundant ferruginous cement. The borings of the fossil shells are also indicative of the environment. These beds are interbedded with thick gypseous shales with thin bedded argillaceous sandstone which may be of deep marine or sabkha environment.

The calcareous shale is interbedded with the thin fossiliferous yellow limestone bed observed in the outcrops of the north-eastern, eastern and southern parts of the Jhura Dome which is due to cyclic sedimentation in the shelf area. The top calcareous shale and limestone bed indicates again a shallow marine shelf environment. The thickness of the beds are decreasing towards the top indicating a deepening upward trend. The yellow limestone beds are characterised by very abundant fossil content. The fossils are of benthic in

character. The belemnites preserved are observed to be oriented with its apex showing north. This could be the indication of the palaeo-shoreline in the north. The bivalves are observed to be deposited with most of its shell valves showing concave upward and few in reverse position. This indicates the energy conditions of the depositional medium.

3.4.2. Habo Dome

The Habo Dome located approximately 20km NE of Bhuj, is roughly elliptical in outline (15km. Long and 6km wide) with its longer axis trending approximately E-W. The southern slopes are relatively gentler whereas the northern ones are steep. The Jurassic succession exposed in these hills comprises mainly the Jumara Formation (also known as Habo Formation). The area has been investigated along selected traverses to cover all the Middle Jurassic out crops. The lower contact of the Jumara Formation is exposed in the Kalajar Nala section south of Dhrang village and whereas the upper contact is observable along the Lodai nala section. The generalized stratigraphic column of the Habo dome is presented in Fig 3.4a. In all about 15 units have been identified belonging to the Middle Jurassic Formations. The lower part of the section belonging to the top of Jhurio Formation is well exposed in the scarp section facing Kalajar nala (Plate: 3.1-3), south of Dhrang village. The lithology of this part comprises mainly the black to grayish black, hard and compact thick-bedded to thin bedded limestone and alternating calcareous shales. Nala sections south of Dhrang village exposes the limestone, calcareous sandstone and shale units which form the basal part of the Jumara Formation. Limestones are fossiliferous and sandstone is fine to medium grained and moderately sorted. The shales are calcareous. The thick arenaceous unit forming the middle part of the Jumara Formation is better exposed in the hill section around village Jhikhidi. This section comprises mainly of sandstones with

subordinate silty shale. The sandstone is ferruginous with few calcareous variations. The sandstone exhibits cross-bedding and ripple mark structures. The upper part of the Jumara formation is well exposed in the hill sections around Rudramata Dam and nala section around Lodai village (Plate: 3.1-5). Grayish to yellowish shale and limestone and subordinate sandstone constitute the main lithology of the Rudramata section (Rudramata Member) and alternate shale and limestone intergradations constitute the lithology of Lodai nala section which forms the top of the Jumara Formation. An oolitic sandy limestone (equivalent to Dhosa Oolite) marks the top of the formation. The overlying shale-sand lithology exposed on the slopes of Habo hills belong to the Upper Jurassic Jhuran Formation. The stratigraphic column observed at the Habo dome is shown in the Fig.3.4a.

3.4.3. Jumara Dome

The Jumara Dome (23°40'00";69°04'00") named after the village Jumara, is about 120 kms northwest of Bhuj, Kachchh. This Dome provides an important Jurassic locality for their abundant mega-fauna and good exposures of Middle Jurassic (Jhurio and Jumara) formations. The Jumara Dome form a dome which is a doubly plunging anticline and the major axis of which is aligned in E-W direction and comprise all the three Jurassic formations. Although the contact between the two lower formations (Jhurio and Jumara) is not clearly seen the upper contact of Jumara Formation with the overlying Jhuran Formation is marked by prominent Dhosa oolite beds. The stratigraphic column observed at the Jumara dome is given Fig.3.4c.

3.5. SYSTEMATIC STRATIGRAPHY OF MIDDLE JURASSIC OF KACHCHH.

The stratigraphy of Kachchh Basin comprises strata ranging in age from Middle Jurassic (Bathonian) to Recent (Holocene). Exposed Mesozoic rocks as seen in Kachchh Mainland were divided into four formations viz., Jhurio, Jumara, Jhuran, and Bhuj in ascending order. The first two formations (Jhurio and Jumara) belong to Middle Jurassic, the Jhuran Formation is Late Jurassic and the topmost Bhuj Formation belongs to an Early Cretaceous age. Mesozoic rocks overlies Archean basement and disconformably underlies the Late Cretaceous basic flows of the Deccan Trap Formation (Biswas, et al., 1973) in the southern and western parts and Tertiary sediments in the eastern part of the basin. The Tertiary sediments lie over the Trap and over the Mesozoic sediments wherever the Trap is absent.

3.5.1. Jhurio Formation (Author: Biswas, 1977). (earlier known as Patcham Formation)

A thick sequence of dominant limestone with interbedded shale and occasional bands of "golden oolite" and sandstone has been named as Jhurio Formation. The formation shows a facies change from carbonate in the west to clastics in the east.

Type Section : Jhurio Dome, 38 km. North of Bhuj.

Geographical Extension : This formation has a very wide extent. It is present in Kachchh Mainland and has been recognized in subsurface also. The formation is exposed as small inliers in three domes (Habo, Jhurio and Jumara, from east to west) along the northern margin of the Mainland. Maximum development (exposed) of the formation can be seen in Jhura Dome. The major part of the dome is composed of this formation and numerous good sections are seen in radial streams. In Habo and Jumara domes only the upper part of the

formation is exposed. In Habo it crops out only at three places in the northern flank of the dome, south of Dhrang and Fulae. North of Jumara it is exposed in the hill adjacent to the Rann. The steeply dipping hard limestone beds form whitish country of high relief featured by cuestas and annular valleys.

Lithology : The lower part comprises thin beds of yellow and grey limestones occasionally containing golden oolites, in grey shales. The middle part is composed of thick beds of grey, yellow weathering shales alternated with thick beds of golden oolitic limestones and the upper part of the formation is made up of thinly bedded white to cream coloured limestones with thin bands of golden-oolites. The formation has been formally subdivided into seven informal members marked A to G by Biswas(1977) on the basis of the occurrences of the limestone, golden oolite, and shale. In Habo dome only the topmost part of the formation is exposed. In Jumara section top member is underlain by olive-grey gypseous shale(Plate: 3.2-1) with thin bands of coral bioliths equivalent to Member-F (Fig. 3.3).

Boundaries: The lower boundary is not exposed in the type section. The upper contact with the overlying Jumara Formation is conformable and well marked by the contrast of its white limestones and the green shales of the Jumara Formation. The geomorphic expression of the limestones forming high relief against the low areas of shales help to pick up the boundary easily.

Thickness: In the type section the thickness of the formation is 287 m. In Jumara and Habo Domes the exposed thickness is only 70 m. (+) and 16 m. (+) respectively.

Palaeontology: Common Fossils include Rhynchonella, Terebratula, Kachchhithyris, Allectryonia, Ostrea, Astarte, Trigonia, Belemnites and ammonites (Macrocephalites). This

formation is particularly rich in fossils in Jumara dome where the shales and biostromes are packed with corals, brachiopods, pelecypods and ammonites.

Age : The presence of benthic foraminifera referable to *Epistomina regularis* - *E.ghoshi* Assemblage zone, *Lenticulina dilectaformis* Partial-Range-Zone, *Tewaria Kachchhensis* partial-Range-Zone in stratotype indicate Bathonian-Callovian age (Pandey and Dave, 1993). The formation was deposited in a littoral to infra-littoral environment, neritic transgressive environment

3.5.2. Jumara Formation (Author: Biswas, 1971;. earlier known as Chari Series)

Monotonous grey to dark grey, laminated, rarely silty and often calcareous shale sequence overlying the Jhurio Formation was named after its type section of Jumara Dome in the western Kachchh. The formation shows gradual increase in thickness from east to west.

Type Section: Jumara Dome, Western Kachchh. The Jhurio and Habo dome sections to the east of the type section are important reference section.

Geographic extent : The formation is exposed as inliers at the center of the domal and anticlinal hills along the northern edge of the Mainland and in central Charwar Range in more or less circular and elliptical outcrops. Being soft formation, it usually gives rise to a grey undulating topography. Jumara Formation is very widespread extending from Banni graben (subsurface) to Kachchh Mainland. It has also been recognized in the shelf part of the offshore and the wells.

Lithology: In the type Section the formation is characterized by monotonous olive-grey, gypseous, laminated shales with thin, red ferruginous bands, alternating beds of limestone and occasional sandstone inter-beds. It has been sub-divided into four informal members

numbered I to IV on the basis of the limestone or sandstone inter-beds dividing the continuous shale succession (Biswas, 1977). Thin fossiliferous oolitic limestone bands occur in the shales near the top of the member IV the popular "Dhosa Oolite beds" or "Stage". It is a very characteristic horizon and used as the main key-bed in the Mainland stratigraphy. In these sections and Chorar Range outcrops, more sandstone beds appear in the lower part. East of the type section, in Manjal dome, the lowest exposed bed is a limestone developed locally embracing the lower and upper parts of the members I and II respectively.

The Jhurio and Habo dome sections to the east of the type section are important reference sections. In these sections and in Charwar Range outcrops, more sandstone beds appear in the lower part. East of the type section, in Manjal dome, the lowest exposed bed is a limestone developed locally embracing the lower and upper parts of the members III and II respectively. Further east in Keera dome, a major portion of the Member I has been replaced by a golden-oolite-shale lithosome. This lithosome resembles the middle part of the Jhurio Formation.

Boundaries: The top and basal part of the formation is exposed only in Jhura, Habo and Jumara domes. The lower boundary is defined by conformable limestone shale contact and the upper boundary is marked by Dhosa Oolite Member. The contact is marked by the topmost oolitic band which is conglomeratic and separates the unfossiliferous grey shales (of Jhuran Formation) and the green fossiliferous shales with oolite bands.

Thickness: The thickness of the formation (273.5 m as observed in type section) is more or less uniform throughout the study area.

Palaontology : This formation is the richest of all in fossil content. Varieties of ammonites, belemnites, brachiopods, pelecypods, corals and gastropods are found throughout the formation. Besides, megafossils, the formation is rich in foraminifera.

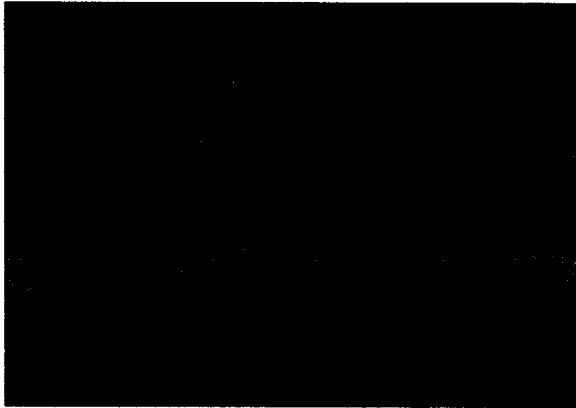
Age : The benthic foraminifera recorded from the type area are referred to *Tewaria kachchhensis* Partial Range-Zone, *Protonina difflugiformis* - *Astacolus anceps* Assemblage-Zone and *Epistomina majungaensis* Range-Zone (Pandey and Dave, 1993). The fossil assemblage gives an age of Callovian- Oxfordian to the formation.

Environment : A littoral to shallow marine circa-littoral (below the wave base) environment of deposition is inferred for the formation.

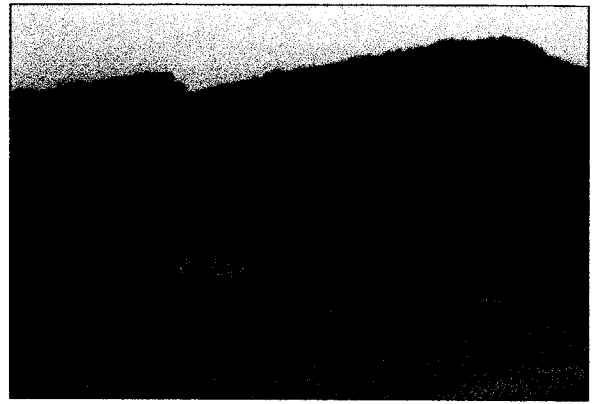
3.5.3. Jhuran Formation (Author : Biswas, 1977)

The upper Jurassic Jhuran Formation consists of thick sequence of alternating sandstone and shale interbeds. The formation is richly fossiliferous in the western part and less fossiliferous in the eastern part.

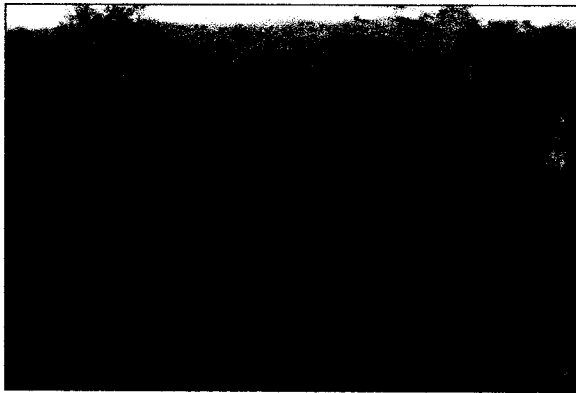
PLATE – 3.1
Field Photographs



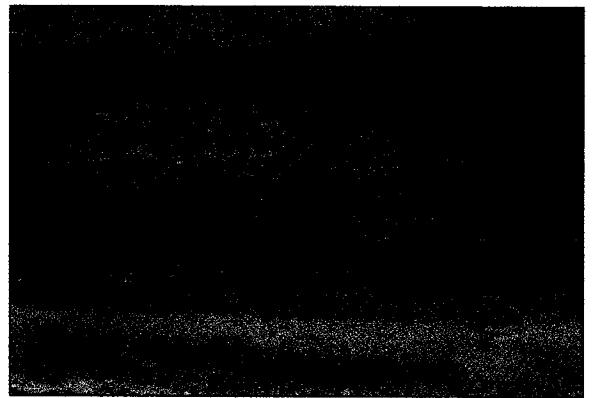
1. A panoramic view of Great Rann of Kachchh



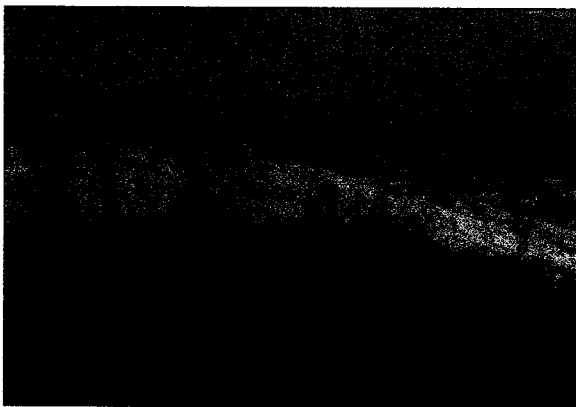
2. Southerly sloping (gentle) cuesta of Jhura Dome capped by Ridge Sandstone & view of Khimod talab, Jhura, Kachchh.



3. Regularly interbedded pelletal limestone and shale. Basic sill /limestone (Jhurio Fm.) contact in the Kalajar Nala, Core of Habo Dome, Kachchh.



4. Flat pebble Intraformational conglomerate (Jumara Fm.) at Kamaguna section, Kachchh.

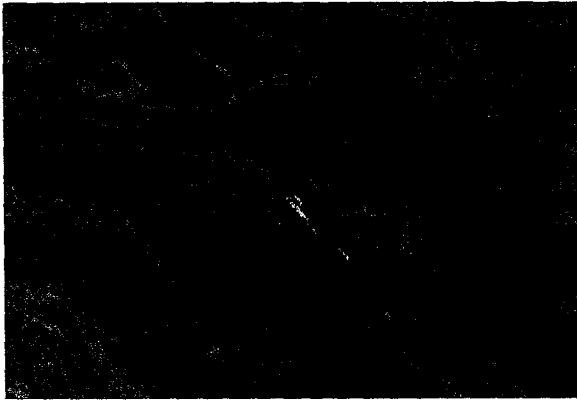


5. Disconformable top contact of Jumara Formation capped with oolitic limestone.



6. Uniform, rhythmically bedded sandy oolitic limestone (light) and shale (dark), Ler, Kachchh

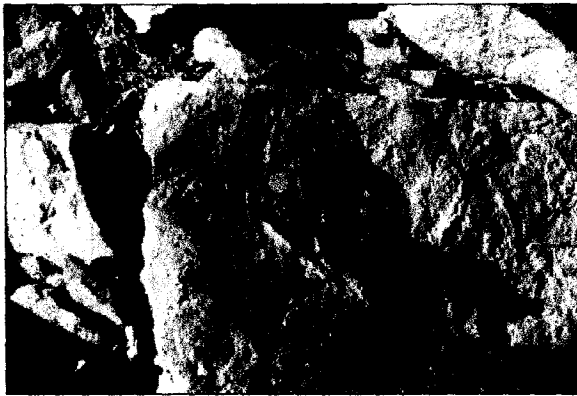
PLATE – 3.2
Field Photographs



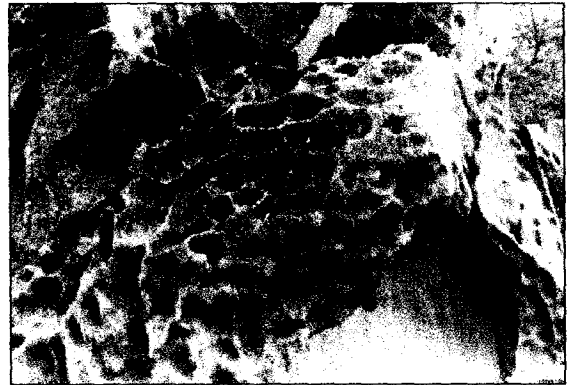
1. Gypsiferous clays of lower part of Jumara Formation, Jumara Dome, Kachchh



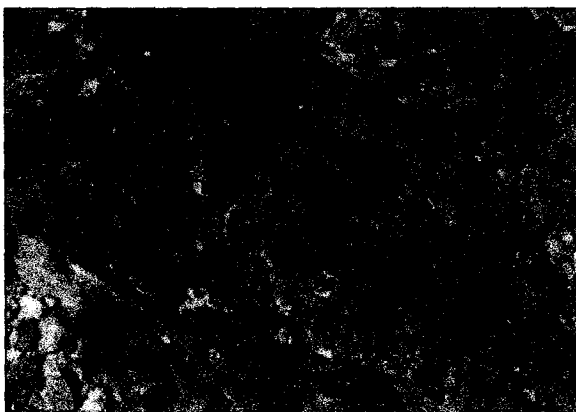
2. A View of large ammonite embedded in the sandy ferruginous limestone, Jhura, Kachchh



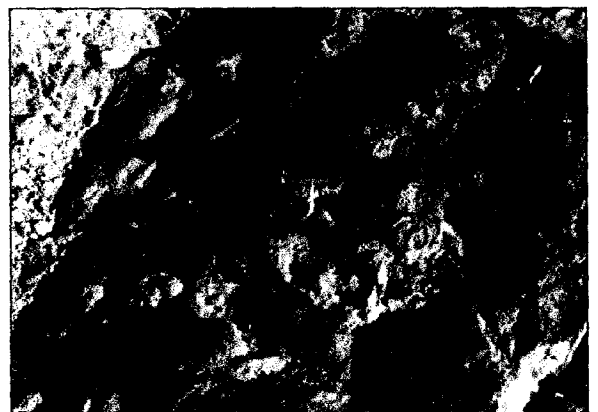
3. Fine grained shaly limestone displaying burrowing and trace fossils, Jhura, Kachchh.



4. Typical weathering of sandy coralline limestone bed, Habo Dome, Kachchh.

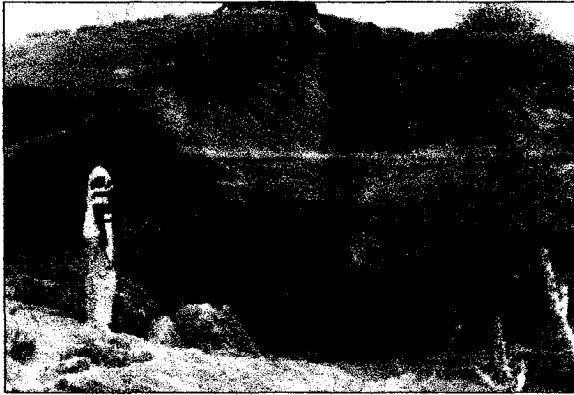


5. Ferruginous, stromatilitic? mineral crust at the top of sandy oolitic limestone, Jumara Fm, Kachchh.



6. Nodular bedding of limestone pebble conglomerate, Jhura, Kachchh

PLATE – 3.3
Field Photographs



1. Large scale, composite cross-bedding structure of ferruginous sandstone, Habo Dome, Kachchh.



2. Well developed tabular cross-bedding. Note the uniformity of inclination, Jhikidi, Kachchh.



3. Large straight crested, slightly sinuous wave ripples shown by sandstone, Habo, Kachchh.



4. Columnar jointing displayed by Late-Jurassic to Early Cretaceous Bhuj Sandstone.



5. Jointing pattern characteristic of fossiliferous, ferruginous sandstone of Jumara Fm. Kachchh.



6. Synsedimentary? Deformation exhibited by sandstone, Habo Dome.

CHAPTER -IV

CARBONATE PETROGRAPHY

4.1. GENERAL

Since the pioneering work of Henry Clifton Sorby (1851, 1858) the sections of rock ground thin enough to transmit light have been the stable material for sedimentary petrography. The main aim of petrography is to identify the framework components and their interrelationships in the rocks to understand the mode of life (endo- or epibiota), boring organisms, existence of predators, mechanical breakdown of the skeletons in a high energy environment, transportation and isolation of the hard parts and dissolution in the case of carbonate rocks. Carbonate sediments and rocks preserve valuable information regarding the physical, chemical and the biological conditions that have prevailed during the deposition and post-depositional conditions that have passed through it. The texture and composition of limestones in the recent period and their progressive development in to characteristic forms are very important and thus the study of carbonate rocks are interesting compared to that of clastic rocks. Carbonate rocks in the present study are characterized by various frame work elements such as bioclasts which give the idea about the palaeoecology and palaeoenvironment, together with other elements such as ooids, peloids, intraclasts, etc., whose mineralogical composition give idea about the energy condition prevailed during the marine depositional environment and the conditions of diagenetic realm.

The lower and middle part of the Jhurio Formation (type section) is characterised by bedded limestones, oolitic limestones and calcareous shales and the upper part of the succession is characterised by various rock types such as sandstone, shale, limestone and evaporites. The limestones are hard compact and often nodular in character.

More than 85 thin-sections of carbonate rock samples were studied using petrologic microscope to know the framework elements, texture, depositional facies and nature of diagenetic modifications. All the carbonate samples were stained with 2 % dilute HCl solution of Alizarine red-S to distinguish calcite from dolomite. The staining test has revealed that the presence of calcite in most of the rock samples and dolomite in few samples at some stratigraphic levels. The framework composition has been identified in thin sections under the petrologic microscope with the help of a number of standard reference guides (Carozzi, 1961; Scholle, 1978; Milliman, 1974; Flugel, 1982 and Adams et al., 1984,) to understand the petrographic characteristics.

4.2. CARBONATE PETROGRAPHY

The carbonate rocks of Jhurio Formation in Jhura Dome of Kachchh Mainland have been critically examined under the microscope and are described in detail with respect their microfacies classification, depositional and diagenetic properties. Since this is the only section where carbonate rocks form the continuous succession, the study has been concentrated in depth on this particular succession. The petrography of carbonate rocks from the other localities (Habo and Jumara Domes) where Middle Jurassic exposures present also has been carried out to know the spatial/lateral variations in the depositional and diagenetic conditions during the Middle Jurassic Period.

Carbonate rocks are basically composed of two elements, which include the allochem and the orthochemical particles. Allochem particles are the main framework elements that are deposited in any marine basin. These elements are bounded together to form carbonate rock by the syndepositional or postdepositional material called cements and matrix which are the orthochemical particles. Both these particle textures are modified

greatly by diagenesis resulting changes in their composition and texture with varying environmental setup.

4.2.1. Allochem Carbonate particles

In carbonate rocks these grains are produced chemically or biochemically within the basin of accumulation and hence most of them are intrabasinal in origin. Limestones, whether current deposited or formed in situ, are made up of large complex grains. To these grains Folk (1959, 1969) has applied the term allochems. Thus there are four principal types of allochems viz., skeletal grains, oolites, intraclasts and pellets. The Petrographic study of the carbonate rocks of Jhurio Formation has revealed finer details on the mineralogy, types of texture, nature of frame work elements, microfacies types and its constituents and diagenetic characteristics. The temporal variation in allochem particles of Jhurio Formation is shown in Fig. 4.1.

4.2.1.1. Skeletal Particles

Because of their different rates of evolution and various diversities, organisms appearing in the thin-sections of limestones have varying abundance in individual systems (Flügel, 1982). The destruction of organic tissue, types of microstructures and the primary porosity of the skeletons control the fragmentation of hard parts. The basis of microscopic work is the determination of the shape, size and orientation of crystals and crystal groups and the spatial relationships between them - in a nutshell the study of mineralogy and fabric (Bathurst, 1975). Carbonate rocks are of primary deposition: consequently, an understanding of skeletal structure allied to mineralogy is indispensable as a basis for the varied investigations. The skeletal components of limestone relate to distribution of carbonate secreting organisms through space and time. The main skeletal

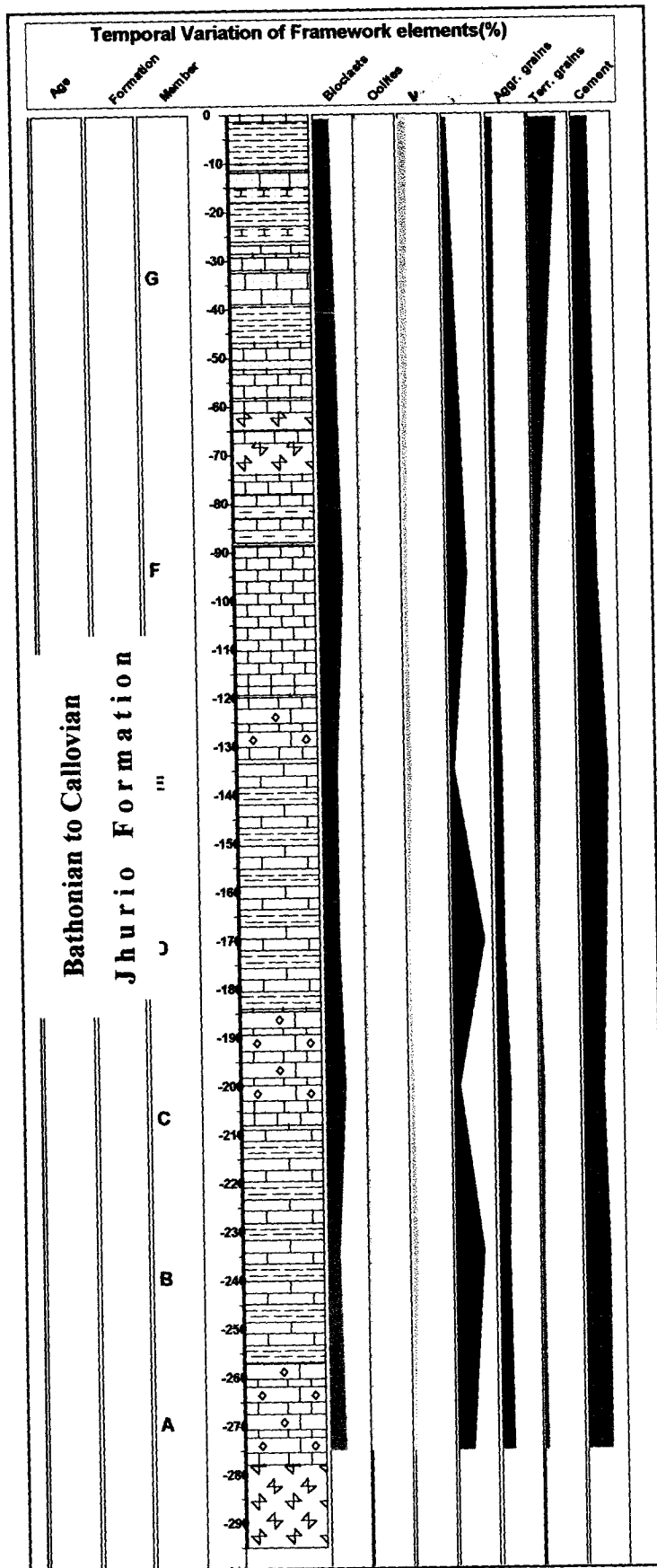


Fig.4.1 Temporal variation of Framework elements

elements in the Kachchh Jurassic sequence includes the fragments of calcareous algae, molluscs, echinoids and brachiopods followed by other such as sponges, corals, bryozoa and foraminifers. These are the important carbonate particles displaying varying stages of abrasion and rounding. In the present samples all stages of transformation of shell fragments to peloids is observed which can be attributable to the process of abrasion and increasing micritization by the boring action of algae.

4.2.1.1.1. Molluscs

Molluscan shells are constructed for the most part of organized aggregates of micron sized crystals disposed in layers. These layers differ from one another in structure, orientation of structure and mineralogy. In any one unaltered species the layers are either all aragonite or interlayered aragonite and calcite: both high magnesian and low-magnesian calcite occur (P.D.Blackmon *in* Cloud, 1962). Bivalves, gastropods, belemnites and ammonites are the important molluscan skeletal structures that have been identified in these carbonate rocks thin-sections. Bivalves are the most commonly and frequently found molluscan grains in the thin-sections of carbonate rocks of Middle Jurassic succession of Kachchh Mainland. They are abundant in the oolitic grainstone of lower and middle parts and in the bioclastic grainstones of middle and upper parts of the Jhurio Formation.

The original aragonitic mineralogy of these bivalves is replaced by the low magnesian calcite as evidenced by the characteristic coarse mosaic texture of calcite (Plate.4.2 – 1 & 2) . The replacement has been occurred by the dissolution-reprecipitation process and the incomplete filling of the intragranular porosity by the coarse calcite mosaic is an example of the original aragonite mineralogy (Plate.4.2 – 4). Molluscan shells are

chiefly aragonitic and hence appear as a mosaic of calcite in the older rocks. Some pelecypod shells have an outer layer of calcite. In some genera (notably *Ostrea* and *Pecten*) in two layers. The outer and principal layer has a prismatic structure in which the prisms, unlike those of brachiopods, are perpendicular to the shell surface. The inner pearly layer has a fine lamellar structure. Similarly most gastropods have an aragonitic shell, but a few exhibit a two-layer structure consisting of an inner aragonitic layer covered by an outer calcitic layer. The guard of belemnite is calcite, with the calcite fibers set radially about an axis (Plate.4.4 – 5). However, the radiating crystals show the ghosts of original aragonite mineralogy with square tips.

4.2.1.1.2. Brachiopods

Brachiopods and molluscan shell fragments can normally be differentiated on the basis of differences of shell structures in addition to their shell mineralogy and shell layering. The skeletal elements are normally well preserved because of their shell mineralogy. The low-Mg calcite skeleton of brachiopods undergoes relatively little observable structural change during diagenesis, hence are well preserved. Brachiopods skeletal elements in the present samples are chiefly calcitic. Their shells are built up of bundles of prisms, the prisms of each bundle being parallel and having a quadrangular cross-section. The brachiopod valve reveals a two-layered wall of low magnesian calcite in thin-sections. The brachiopods shells are disarticulated and the important varieties seen are endopunctate and impunctate. The most brachiopods are seen associated with oolitic grainstones in the lower and middle and in the bioclastic grainstones and lithoclastic-bioclastic rudstones in the middle and upper part of the Jhurio Formation.

4.2.1.1.3. Echinoderms

Crinoids and echinoids are abundant in the peloidal packstone-grainstones of the lower and middle part of the Jhurio Formation. Spines and other skeletal parts of echinoids are present; crinoidal and echinoidal fragments can be identified by their characteristic structure delineating a regular lattice; the sterom. The hard parts of echinoderms are most singular in that each plate or skeletal element is a single crystal of calcite. Larger ones clearly show the calcite cleavage to the unaided eye, and the limestone composed primarily of such remains accordingly has a marked "crystalline limestone". In most cases the oscicles and plates have been cemented with clear calcite in crystallographic and optical continuity with crinoid fragments. The original fragment is distinguished by a dusty area showing the usual circular or elliptical (in oblique section) outline with internal canals (Plate: 4.1-4; Plate: 4.3-1). The original fragment, however, is traversed by cleavage cracks that pass uninterrupted into a secondary cement. Usually the echinoderms disarticulate rapidly so that one sees only scattered debris whose shapes are highly variable because of original growth or the plane sectioned. Their crystallographic unity is their diagnostic feature (Pettijohn 1962). Crinoids are also seen in the bedded limestones and as nuclei for the ooids in the oolitic grainstones. The crinoidal oscicles and echinoidal spines display syntaxial rim cementation (Plate: 4.1 - 4; Plate: 4.3 - 1 & 6).

4.2.1.1.4. Foraminifers & Ostracods

Smaller foraminifers (protoglobigerinids) and larger benthic foraminifers such as miliolids, textularids and fusulinids are abundant. The miliolids and smaller foraminifers (protoglobigerinids) are abundant in the peloidal limestones of the lower and middle part of the Jhurio Formation (Plate: 4.3 - 5 & 6; Plate: 4.4 - 2 & 3). The benthic foraminifers are

present in moderate amounts in the middle and upper part of the Jhurio Formation. Ostracod carapaces are seen in the oolitic limestones and in the bioclastic limestones (Plate: 4.5 – 1) and in the bioclastic wackestone (Plate: 4.8 - 2). They present in moderate amounts in the lower, middle and upper part of the formation.

4.2.1.1.5. Bryozoans

Bryozoans along with calcareous algae are abundant in the peloidal limestones (Plate: 4.7 – 4 ; Plate: 4.8 - 1) and in the lower and middle part of the formation (Plate: 4.5 – 3 & 4).

4.2.1.1.6. Corals

Coral fragments occur in Kachchh Jurassic sediments in minor quantities. Some times these are confused with echinoid plates. Exact identification of corals can be made only in oriented sections (transverse and longitudinal sections). Due to their rapid diagenetic alterations and recrystallization, the identification of corals becomes somewhat difficult. In some thin sections, longitudinal and oblique sections often exhibit a net-like porous structure of the septal filaments. The coral elements can be identified by their characteristic patterns in transmitted light.

4.2.1.1.7. Sponges

In a few instances, the limestones of Kachchh Jurassic (mainly wackestones) show the presence of hollow or calcite filled external molds of siliceous sponge spicules. The presence of cherty dolomite in some beds is indicative of the original presence of sponges.

4.2.1.1.7. Calcareous Algae

The calcareous algae are seen abundant in the algal foraminiferal peloidal fenestra laminated wackestone, peloidal packstone-grainstones (in both foraminiferal and crinoida

and in oolitic intraclastic bioclastic grainstones.

4.2.1.2. Non-skeletal grains

Non-skeletal grains are those not obviously derived from the skeletal material of micro-organisms or invertebrates or thalli of calcareous plants (Tucker and Wright, 1990). Four main types are recognized (Folk, 1959): coated grains (oids mainly), peloids, intraclasts and aggregate grains.

4.2.1.2.1. Ooids :

A remarkable variety of coated grains occurs and many classifications including Peryt's(1983), have distinguished two broad categories of coated grains; chemically formed (especially ooid) and biogenically formed (oncoids). According to them an ooid (or oolith) is a coated grain with a calcareous cortex and a nucleus which is variable in composition. The cortex is smoothly and evenly laminated especially in its outer parts, but individual lamina may be thinner on points ^{of} stronger curvature on the nucleus. The shape is typically spherical or ellipsoidal with sphericity increasing outwards. In the Jhurio Formation the main coated gains present are ooids and there are some oncoids present. The ooids rarely grade in to pisoids. Such pisoids are seen with in the oolitic packstone-graistone towards the top of the bioclastic peloidal wackestone/oolitic packstone-grainstone shallowing upward cycle.

The ooids are tight packed and are abundant in oolitic packstone-grainstone microfacies. Basically there are two types of ooids, one is with peloidal nucleus and concentric layers of calcite and the other type with radiating calcite crystals (Plate: 4.1-1; Plate: 4.3 – 2 & 4). These are the true ooids with many concentric layers. These ooids have perfect spherical to ovoid shape. There are considerable amount of superficial ooids which

have variable shapes. The nuclei of such superficial ooids are bioclasts, including ostracod carapaces, foraminiferal and algal grains and crinoidal and echinoidal spines. The vast amount of superficial ooids indicate that the energy conditions of the depositional medium was very high which led to the coating of almost all the grains available within the area. Both types of ooids are coated with iron oxide matter which in many samples imparting golden yellow to yellowish brown and brownish black colour to the ooids. Thus in all the types of ooids mentioned above the nuclei include micritised bioclasts such as the crinoidal and echinoidal spines, foraminiferal, algal and molluscan shell fragments. Also seen are the quartz grains as nuclei of the ooids which are in considerable amounts towards the top of the shallowing upward cycle where the ooids generally have the larger size and sometimes grade in to pisoids.

The size of the ooids vary from 0.2 mm to 1 mm. The maximum size sometimes reaches to 2mm. The size is almost almost homogenous in individual thin-section. The colour varies from golden yellow to yellowish brown and sometimes brownish black when fresh. These characters strongly suggest a dynamic deposition and reject a strictly in situ intrasedimentary genesis of ooids (see Odin,1988). Ooids with larger nuclei are characterised by thin layers in concentric to random pattern. Where as those with small one are characterised by the presence of many concentric layers. Some are composite ooids, which show two or more ooids bounded by cement. The percentage of ooids ranges from 25-40 % in oolitic packstone-grainstones and in oolitic intraclastic bioclastic grainstones it ranges from 10 - 15 %.

Mineralogy of ooids influence not only their subsequent diagenesis but also their microfabric (Tucker and Wright, 1990). Shearman et al., (1970) observed an anomalous

fact that in many ancient ooids, detrital nucleus presumably once aragonite has been replaced by calcite cement, yet the oolitic coat, which has been superimposed a pattern of radial-fibrous calcite crystals. This is true in the case of ooids of Jhurio Formation, where the original aragonitic mineralogy has been evidenced from the XRD-studies of ooids. The XRD-studies (given Chapter-V) indicate that the present mineralogy is low-magnesian calcite. The coating of the ooids are mainly goethite in composition. This goethite coating upon oxidation gives a golden colour to the ooids. Shearman et al., (1970) suggested that, during diagenesis, the original aragonite was dissolved but the organic matter remained as a template on which tiny crystals of calcite cement grew with the typical preferred orientation that accompanies competitive growth.

That could be the reason for the preservation of radial calcitic structures in the most perfect ooids of Jhurio Formation. The re-use of pieces of broken ooids, is also noticed. This indicates that already hard ooids were present and were used again as nuclei for the growth of new ooids. In other words, favourable conditions for growing iron coated ooids are also compatible with an in situ reworking of previously deposited hard ooids of similar composition. Therefore, the genesis can be inferred as to the site of formation of original aragonitic ooids, iron is introduced probably from the submarine source (see Khadkikar, 1996) or from the land. The oolitic structure itself indicates the sea-water movements, and sea-water roughness also indicated by the figure drawn on sediments and underlain by the ooids. Finally the movements must have sometimes been very strong in order to break already indurated ground mass or ooids found today as nuclei in other ooids. Therefore, ooids appear to have formed in a very stirred environment usually regarded as necessarily linked with high oxidising conditions in sea water (see Odin, 1988).

The ooids also shows dissolution of the nuclei and the original aragonitic concentric layers in fresh water phreatic conditions and reprecipitation as calcite, whereas the outer goethite coating has remained as such. This is an example of oomouldic porosity preservation and cementation (Plate: 4.3 - 1; Plate: 4.6 - 1)

4.2.1.2.2. Peloids

McKee has coined the term peloid to embrace all grains that are constructed of an aggregate of cryptocrystalline carbonate, irrespective of origin (McKee and Gutschick, 1969). A peloid is a sandsized grain with an average size of 100-500 μm , composed of microcrystalline carbonate. The peloids are abundant in the lower and middle part of the Jhurio Formation. These grains are observed with the bedded lime mudstones (peloidal packstone-grainstone and bioclastic mudstone-wackestone microfacies types) (Plate: 4.1-4; Plate: 4.2 - 4; Plate: 4.3 - 5 & 6; Plate: 4.4 - 2 & 3; Plate: 4.5 -2). The percentage ranges from 20-45 % in the bedded lime-mudstones. Size increases from lower to middle in the section in a shallowing upward cycle. The shape is usually rounded or subrounded, spherical, ellipsoidal to irregular and are internally structureless. The colour is usually greenish black to brownish black. The peloids are important constituent of shallow water marine carbonate sediments. They indicate a particular facies along with the particular fossil abundance which indicate a quite water depositional conditions.

It is widely felt that, in both recent and ancient carbonate sediments, elongated peloids, ellipsoids of revolution, are faecal pellets. Similarly the experience of Purdy(1963a, 1963b) and Barthust(1966) in the Bahamas suggests that the many of the irregular grains, at least, are skeletal particles that have been replaced by micrite as a result of processes associated with endolithic algae. This is true in the case of peloids present

in the crinoidal peloidal packstone-grainstones (MF-23) of Jhurio Formation. Here many peloids are micritised skeletal particles (Plate: 4.3-5 & 6). Some peloids are clubbed together to give a grapestone to lump structure (Plate: 4.1 - 4). It could be due to bioturbation. It may also be due to the fact that, it has long been known that in some peloidal grainstones the peloids tend to merge (Beales, 1958). The apparent blurring of the outline of peloidal to form grumeleuse structure, is not much evident from the peloidal packstone-grainstones of the lower and middle part of the section of the Jhurio Formation. Where as this kind of tendency is seen in few rock types especially pure peloidal grainstones where peloids are formed by the micritisation of skeletal fragments.

The peloids are polygenetic group of grains and identifying their exact origin is often impossible in limestones. The peloids present in the sediments of Jhurio Formation are mainly micritized skeletal grains and some are faecal pellets. Faecal pellets are soft and significant compaction can occur during even very shallow burial (Ginsburg, 1957; Shinn and Robin, 1983). Many ancient, finely mottled lime mudstones, wackestones and packstones probably owe their origin to the compaction of soft faecal pellets (Tucker and Wright, 1990). Peloids are probably the most abundant ubiquitous of the allochems (McLane, 1995). Most faecal pellets are initially quite soft and under overburden pressures are readily mashed into what commonly comes to be labeled as matrix (Shinn and Robin, 1983; McLane, 1995). Some of the peloids are very minute as seen in foraminiferal peloidal packstone-grainstones (Plate: 4.3 - 1; Plate: 4.5 - 2). Marshal (1983a) suggested that such small spherical peloids formed by chemical precipitation. Criteria for their recognition in limestones have been discussed by Flugel (1982) and concentrations of well-sorted peloids especially in burrow structures are often used as evidence of a

faecal origin (Tucker and Wright, 1990). The preservation of recognizable pellets in limestones is clear evidence of early lithification. The peloids of foraminiferal as well as crinoidal peloidal packstone-grainstones mostly represent micritised grains such as abraded shell fragments or ooids (Plate: 4.1-4; Plate: 4.3-5). The original grain has been completely micritized by endolithic microorganisms (Barthust, 1975).

4.2.1.2.3. Intraclasts

The fourth category of non-skeletal grains are limestone clasts (Tucker and Wright, 1990) or intraclasts (Folk, 1959). They are reworked sediments of at least partly consolidated carbonate sediments. Intraclasts are fragments of typically weakly consolidated sediment reworked from within the area of deposition. Intraclasts present in moderate amounts in the oolitic packstone-grainstones, oolitic intraclastic bioclastic grainstones and in peloidal grainstones (as mud intraclasts). Minor amounts of intraclasts are seen in the lithoclastic bioclastic rudstones and in peloidal grainstones. In oolitic packstone-grainstones the presence of mud intraclasts are noticed. The percentage of intraclasts in oolitic intraclastic bioclastic grainstones ranges from 15 - 20 %. In lithoclastic bioclastic rudstones also the percentage is approximately same.

4.2.1.2.4. Aggregate grains

Grain aggregates are found when several carbonate particles become bound and cemented together (Tucker and Wright, 1990). Such aggregate grains are seen in lithoclastic bioclastic rudstones, oolitic intraclastic-bioclastic grainstones and in bioclastic wackestone-grainstones (Plate: 4.1-3; Plate: 4.3-6). The size usually range from 0.5 mm to 3mm and have irregular shapes. In some peloidal grainstones especially in crinoidal peloidal packstone-grainstones the peloidal gains are cemented together to form a grapestone to

lump structure (Plate: 4.1-4). These aggregates are an important environmental indicator of its depositional energy conditions. The percentage of aggregate grains is 10-15% in the peloidal grainstone-packstones and in the oolitic intraclastic bioclastic grainstone and 5-10% in the bioclastic wackestone-grainstones.

4.2.2. Orthochemical Constituents

The orthochemical particles are matrix or cement precipitated from the sea water and the interstitial solutions. These orthochemical particles are generally aragonite or high Mg-calcite in the carbonate sediments and then these particles are modified in to different morphologies and have characteristic textural patterns. Accordingly early diagenetic and late diagenetic cements have different textures and mineralogy. Usually orthochemical particles show low Mg-calcite mineralogy in the ancient carbonate sediments since ~~the~~ both aragonite and high Mg-calcite are metastable. The characteristic orthochemical particles and their textural types are micrite and sparite and their different morphological varieties such as microsparite, columnar fringe cement, coarse blocky sparite and syntaxial rim cement. These cement textures are described in the discussion on diagenesis.

4.2.3. Visual Porosity

The visual porosity types are identified as different pore spaces under low porosity magnification in carbonate and in mixed carbonate-siliciclastic-evaporite microfacies types. Different types of porosities are observed under the microscope in the rock sections of Jhurio Formation. These are the following types:

4.2.3.1. Intergranular porosity

The pore spaces available between the frame work elements are usually considered as intergranular porosity. It is usually abundant in recent carbonate types and which are

buried at shallow depths. Where as during the post depositional changes including the deep burial, much of the primary porosities are lost. Thus in ancient limestones the primary porosities are rarely preserved. This occurs due to the cementation by carbonate cement. Thus intergranular porosity dependent on particle shape, sorting and alteration during diagenesis. The intergranular porosities in Jhurio Formation is present in bioclastic grainstones, oolitic grainstones and in calcareous sandstones (Plate: 4.1-1; Plate: 4.2-3; Plate: 4.4 -4; Plate: 4.7-3 & 4; Plate: 4.8-2). The peloidal mudstones which form more than fifty percent of the Jhurio Formation are almost devoid of intergranular porosities.

4.2.3.2. Intragranular porosity

This is the most abundant types of porosities available in ancient carbonate rocks. It is basically formed simultaneous with the deposition, but mostly during the post depositional changes. The porosity is developed due to the dissolution within the bioclasts and pore-spaces are usually partially or completely left unfilled by the secondary calcite cement. Such intragranular porosities are observed in considerable percentage in bioclastic grainstones, oolitic grainstones, oolitic intraclastic bioclastic grainstones and in peloidal group of microfacies (Plate: 4.2-4; Plate: 4.3-3 & 4; Plate: 4.7-1 & 3; Plate: 4.8-1).

4.2.3.3. Secondary void porosity

The secondary void porosity is exhibited by the various allochem particles such as oolites, intraclasts, etc. Oomoldic porosity is well exhibited by oolitic grainstones (Plate: 4.1-2; Plate: 4.6-1). The voids are produced by undersaturated fresh water reaction with the calcareous ooids. The nucleus which are usually of peloidal bioclasts are dissolved and thus leaves voids which are latter produced by the reprecipitation processes. Some of the intraclasts also exhibit the same type of secondary void porosity especially in the oolitic

intraclastic bioclastic grainstones.

4.2.3.4. Disrupted porosity

Different types of porosity are formed with irregular shapes during the postdepositional changes in carbonate rocks. The bioclastic grainstones exhibit peculiar types of disrupted porosities which are associated with the stylolites and are similar to the stylolites but are very short and small (Plate: 4.2-3; Plate: 4.4 -4). The main causes of formation of disrupted porosities are activity of burrowing organisms, slumping and pressure dissolution under burial diagenesis.

4.3 CARBONATE DIAGENESIS

Because diagenetic structures related to lithification can be confused with primary depositional structures and textures, knowing the possible diagenetic processes is extremely important for the interpretation of microfacies characteristics (Flügel, 1982). The diagenesis of carbonate sediments and rocks encompasses all the processes that affect the sediments due to physical, chemical and biochemical changes immediately after the deposition until realms of incipient metamorphism at elevated temperatures and pressures. Diagenetic changes can begin on the sea floor, as the grains are still being washed around or as a reef is still growing, or it may hold off until burial when overburden pressure has increased or pore-fluid chemistry has changed so that reactions are induced within the sediments (Bathurst, 1975).

A variety of factors influence the diagenesis of carbonates, which according to Chilingar et al., (1967) include : i) Geographic factors, ii) Geotectonism, iii) Geomorphic position, iv) Geochemical factors in regional sense, v) Rate of sediment accumulation, vi) Initial compaction of the sediments, vii) Purity of sediments, viii) Grain size, ix)

Accessibility of limestone framework to surface, x) Interstitial fluids, xi) Physiographic conditions and xii) Previous diagenetic history of the sediment materials. The processes of diagenesis includes six major processes: cementation, microbial micritization, neomorphism, dissolution, compaction (including pressure dissolution) and dolomitisation. Thus in summary the major controls on the diagenesis are the composition and flow rates, geological history of the sediment in terms of burial/uplift/sea-level changes, influx of different pore-fluids and prevailing climate (Tucker and Wright, 1990).

4.3.1. Diagenesis of Jhurio Formation (Jhura Dome), Kachchh Mainland

Cementation, Micritisation, dissolution-reprecipitation, neomorphism, compaction, dolomitisation are the important processes of diagenesis with small scale processes of silicification and stylolitisation.

4.3.1.1. Cement Textures

The petrographic study of carbonate rocks of Jhurio Formation has revealed the three different types of cements such as the carbonate, iron oxide and smectite that have developed during the successive stages of diagenetic environments. Also there are seven types of cement textures which are the products of diagenesis developed during the four diagenetic environments. The four diagenetic environments are in the order as marine phreatic, fresh water phreatic, burial and fresh water vadose diagenetic.

4.3.1.1.1. Micrite

Micrite cement is abundant in the peloidal packstones and bioclastic wackestone-grainstone microfacies types(MF-20, 21, 22 23 & 40). The microfacies numbers (MF- 21, 40,etc.) are explained in the classification of microfacies. The micritisation must have occurred in a stagnant marine phreatic environment where by abundant micritic mud has

been produced by ^{the} disintegration of skeletal material by endolithic bacteria. The micritic matrix later neomorphosed to form microspar at places in bioclastic wackestone (MF-40) which grade in to grainstone at places (Plate: 4.5-1) The micritisation is the main diagenetic process that have predominant in this microfacies. The peloidal packstone-grainstones (MF-20, 21, 22 & 23) in the lower and middle part of the Jhurio Formation is also predominantly originally micritic cement which later neomorphosed in to microspar to pseudospar (Plate: 4.1-4; Plate: 4.3-1, 5 & 6). In bioclastic peloidal mudstone-wackestone microfacies(MF-21) micritic mud is predominant nearly about 50% which later neomorphosed in to microspars and pseudospars. Thus neomorphism is the dominant process that occurred in the peloidal group of microfacies. Where as in the case of peloidal packstones the micritic cement binding the peloids comes about 20 - 35 %. This variation can be inferred from the percentage of peloids. The bioclastic mudstone-wackestones are cyclically deposited with the oolitic packstone-grainstone. In peloidal packstones and bioclastic mudstone-wackestones the micrite shows the tendency to form clots. In oolitic intraclastic bioclastic packstones and bioclastic grainstones the micritisation is evidenced by presence of micrite envelopes(Plate: 4.2-1 & 2). Micritisation is also evidenced in the SEM-analysis as observed in the Plate: 4.7- 3, 4 & Plate: 4.8 - 6. These micrographs shows the micritised algal, foraminiferal, bryozoan and ostracodal skeletons. In Plate: 4.2 - 1 & 2, the micrite envelope is composed of micritic calcite. As is noticed by Bathurst(1975), the outer surface of the coat has gentle smooth contours and the inner surface is irregular. The envelope apparently formed centripetally in carbonate grains by precipitation of micrite in vacated algal bores is initially composed of micritic aragonite or high magnesian calcite, with some impurity depending on the amount of

residual primary carbonate. Where as in ancient limestones it is low magnesian calcite micrite and if it should have formed around an aragonite grain while on the sea-floor, then that aragonite core has normally been replaced by calcite spar (Plate: 4.2-1 & 2). So the micritic envelope has a great role in repeating diagenetic history of a carbonate sediment. Thus micritisation and micrite cement are the product of stagnant phreatic marine environment. Subsequent burial at shallow depth brings the microsparite patches in some microfacies types (e.g. bioclastic wackestone-grainstone).

4.3.1.1.2. Equant calcite cement

The equant calcite cement of first generation marine phreatic diagenetic environment is noticed over the ooids and bioclasts in the oolitic intraclastic bioclastic grainstones (MF-11) and oolitic packstone-grainstone (MF-10) microfacies types . Here the earlier marine phreatic equant cement is partly covered by late diagenetic micrite matrix at places (Plate: 4.1 - 1 & 2). In Plate: 4.1-1, the central portion shows the early cemented oolites. In the microfacies, oolitic packstone-grainstone, the early equant cement over the oolite grains is an evidence of the active marine phreatic environment where true calcareous oolites have been formed which later replaced by low magnesian calcite. During the formation of this first generation cement the water depth was very shallow and active waves and shallow agitating water was strong enough to form oolites with almost all the material available in the area.

4.3.1.1.3. Columnar fringe sparite

The columnar fringe sparite with scalenohedral habit which is of earlier generation is seen over the bioclasts in oolitic intraclastic bioclastic grainstone microfacies (MF-11). This sparite cement has grown over the molluscan bioclasts (Plate: 4.2-1 & 2).

The length and width varies from 0.05 to 0.5 m. and 0.02 to 0.06 mm. respectively. The scalenohedral fringe cement is not bright and clear compared to the rhombohedral sparite cement formed after the fringe cement. The cementation of this fringe type must have formed in a marine phreatic environment. Because it resembles columnar fibrous cement and is seen as isopachous fringes over the grains (over molluscan bioclasts in Plate: 4.2 -1 & 2). Finally it is followed by rhombohedral sparry cement (Tucker and Wright, 1990).

4.3.1.1.4. Blocky mosaic calcite

The blocky mosaic calcite sparite is very coarse clear and bright compared to that of first generation marine phreatic cements. This cement occupies both intragranular and intergranular porosities (Plate: 4.1-1 & 3; Plate: 4.2-1 & 2; Plate: 4.3-3). The approximate diameter of the crystals vary from 0.1 to 0.5 mm. This cement type is observed in oolitic intraclastic bioclastic grainstones(MF-11), oolitic packstone-grainstone (MF-10) and bioclastic packstone-grainstone(MF-41). It has been originated usually by the dissolution of original aragonitic or high magnesian calcite mineralogy and reprecipitation into low magnesian calcite by inversion or recrystallisation in a fresh water phreatic diagenetic environment. The Plate-4.7-1 & 4 and Plate: 4.8-1 show the coarse sparite cement formation from the algal grains due to the dissolution reprecipitation process. During the precipitation process some of the porosities are still left unfilled as micropores.

4.3.1.1.5. Syntaxial replacement rim

Syntaxial replacement rim cements are seen in peloidal packstone-grainstones (MF-23 and in bioclastic mudstone-wackestones (MF-21). The host is usually crinoid ossicles and echinoid spines. The Plate: 4.3-1 shows the rim cement over the crinoid ossicles at the center and in the central lower portion. The syntaxial overgrowth is seen

over the foraminiferal and other few bioclasts. In the Plate-4.1, Photomicrograph-4, the rim cement embay the surface of pellets. The nuceii that underwent syntaxial enlarge usually seen floating in the spar. In both the microfacies the main primary cement is micrite cement. This is an indication of stagnant marine phreatic cement. The quite water conditions of the depositional medium were evidenced by the peloids mainly the faecal pellets. The syntaxial replacement rim cement is formed due to the shallow burial diagenesis. Plate-4.7, SEM-micrograph-4 shows the syntaxial rim cementation in peloidal grainstone, showing the cementation over the micritised crinoidal and algal grains.

4.3.1.1.6. Ferruginous micritic cement

The ferruginous micritic mud is observed as main binding material in the lithoclastic bioclastic rudstone microfacies (Microfacies 30). This carbonate mud is red to reddish black in colour and is iron oxide in composition. The micritic mud is filled both the intergranular and intragranular primary porosities and gives a compact form for the microfacies. The micritic mud is dark colour under the microscope. The mud has been filled within the borings of many bioclasts (Plate-4.4 -6). The bioclasts which are bored on the subaerial exposure in the intertidal area and were reworked during the flooding due to transgression of the sea and the bioclasts were carried to the place of red micritic mud. The ferruginous micritic mud has been lithified during the early diagenetic processes.

4.3.1.1.7. Smectite rim cement

The algal foraminiferal peloidal fenestral laminated wackestone microfacies (MF-22) is characterised by the thin smectite rim cement lining the fenestral laminations (Plate-4.5 - 3 & 4). This microfacies is very thin bedded (5-15cms. thick) and is cyclically deposited with crinoidal peloidal packstone-grainstone. The smectite abundance

in insoluble residues of the above microfacies is evidenced by the XRD-studies. The glycolation studies of insoluble residue revealed the dominance of smectite over quartz in this microfacies. The laminations of fenestral cement are parallel to the bedding and at intervals. The smectite must be of authigenic in character.

4.3.1.2. Compaction

Compaction refers to any processes that reduces the bulk volume of the rocks. This includes mechanical processes that decrease the bulk volume of single grains (grain deformation) or that cause closer packing of grains (re-orientation) and pressure solution which decrease the volume of grains and cementing materials. Important evidences of compaction observed in Kachchh Jurassic rocks are (i) some oolites show pressure solution effects in which some grains have been pressed into others, and (ii) fecal pellets, presumably soft at the time of deposition, commonly show effects of squeezing and bending due to compaction (Plate: 4.1-4). Over packing of pelecypod shells in bioclastic grainstones (Plate: 4.2-3; Plate: 4.4 -4) is also indicative of compaction.

4.3.1.3. Dissolution

Dissolution produces pore space by dissolving pre-existing minerals. This process is particularly important in carbonate rocks because it often creates additional porosity that might serve as a hydrocarbon trap. Dissolution can leave a variety of distinctive and interesting textures in the limestone rocks. Selective dissolution of aragonitic or high-Mg calcitic fossils and ooids are seen selectively dissolved producing voids (Plate: 4.3-2). Such dissolution produces *secondary porosity* (Plate: 4.2-4).

4.3.1.4. Neomorphism

The term neomorphism was introduced by Folk (1965) to cover processes of replacement and recrystallization where there may have been change of mineralogy. Recrystallization, strictly, refers to changes in crystal size without any change of mineralogy. Since many carbonate sediments originally consist of mixtures of calcite and aragonite, the term recrystallization cannot properly be applied to replacement textures and neomorphism is used instead. Neomorphic processes takes place in the presence of water through dissolution-reprecipitation; that is, they are wet processes. Most neomorphism in limestones is of the aggrading type, that is leading to general increase in crystal size, and this occurs chiefly in fine grained limestones, resulting in microsparitic patches, lenses, laminae and beds. The opposite, degrading neomorphism, is not most common. Calcitisation is another process of neomorphism, wherein aragonitic skeletal grains and cements are replaced by calcite. Dolomite and evaporitic minerals can also be replaced by calcite. The calcitization process involves gradual dissolution of the original mineral and precipitation of calcite, so that usually some minute relics of the original shell or cements are retained in the neomorphic calcite (Plate: 4.4 -5). In the present samples it can be clearly observed in some carbonate particles especially bioclasts wherein the original metastable minerals probably aragonite and high-Mg calcite have been selectively replaced by the neomorphic calcite (Plate: 4.2-1 & 2; Plate: 4.4 -5). However, under the light microscope there is no change is observed in the original shell structure.

4.3.1.5. Micritisation

Micritisation is a process whereby bioclasts are altered while on the sea floor or just below by endolithic algae, fungi and bacteria. The skeletal grains are bored around the margins and the holes filled with fine grained sediment or cement. Micrite envelopes are produced in this way and if the activity of the endolithic microbes is intense, completely micritized grains are formed. The Middle Jurassic Limestones of Kachchh Mainland exhibit in many samples, the process of micritisation wherein some bioclasts are in the process of the micritisation and other are completely micritised with the continuous and boring activity of algae. Evidences of micritisation is left as micrite envelopes on some bioclats (Plate: 4.2 - 1 & 2).

4.3.1.6. Replacement

Simultaneous dissolution of original material and precipitation of a new mineral while preserving the original form is known as replacement. In the present samples many evidences of replacement have been observed. Many carbonate particles such as fossils or ooids, have been replaced with all the fine details still intact suggesting slow, step-by-step dissolution and immediate cementation (Plate: 4.2-4). In some samples the dolomite is seen replacing the original calcite grains indicating a replacement origin of dolomite (Plate: 4.2-3; Plate: 4.4 -4). At some levels some samples show replacement of calcite by chert.

4.3.2. Diagenetic environments

The three kinds of cements and seven types of cement textures are basically formed during the four different types of diagenetic environments, such as marine phreatic, meteoric phreatic burial and fresh water vadose diagenetic in the order. By identifying the different cement textures from the petrographic evidences and integrating the

environments of diagenesis, it is understood that the carbonate microfacies together with the mixed carbonate-siliciclastic-evaporite facies belonging to Jhurio Formation have undergone alternative episodes of marine and freshwater influence during early diagenetic processes and subsequently been subjected to burial diagenesis and after the upliftment it has again undergone the fresh water vadose diagenetic condition. During this mesogenetic regime mineralogical and textural changes preserved the magnitude of diagenesis in these ancient carbonates. Marine diagenesis of carbonates of Jhurio Formation is characterized by the presence of kinds of cements such as calcitic micrite and isopachous smectite rim cement. The cement textures such as micrite, equant calcite cement and columnar fringe cement are also a development of marine diagenesis (Plate-4.1-1; Plate-4.2 - 1 & 2). The main change in porosity during marine diagenesis is one of porosity loss through cementation (Tucker in Wright, 1993). The cements are mostly precipitated directly from sea water and many thousands of volumes of water must pass through a pore to occlude the porosity. The marine phreatic diagenetic environment is characterised by a stagnant and active condition prevailed during marine diagenetic processes. During the formation of oolites and their early diagenesis, active marine phreatic environment prevailed which caused the formation of equant calcite cementation over the oolites. While during the stagnant marine conditions the early diagenesis took place in the bedded limestone and calcareous mudstone which have undergone diagenetic bedding.

Fresh water phreatic diagenetic environment is then followed the marine diagenetic conditions. During the meteoric phreatic environment the blocky sparite and bladed calcite sparite are formed. Since the fresh water is having low ionic concentrations cements were precipitated slowly and thus exhibits coarse, clear and bright calcite crystals

under the microscope. In the near surface fresh water diagenetic environment, porosity can be gained or lost. Porosity reduction mostly occurs through cementation (plus internal sedimentation) and this may take place in vadose and/or phreatic zone. During meteoric diagenesis porosity is created in these carbonate sediments through leaching of grains by carbonate undersaturated waters. The main controls on meteoric diagenesis are climate, amplitude and duration of sea-level fluctuations causing subaerial exposure and original sediment mineralogy. Climate is the fundamental control on meteoric diagenesis, since the quantity and frequency of meteoric water passing through the sediments control the degree of leaching and cementation. The magnitude of relative sea-level fall is important in controlling the depth to which the meteoric processes operate. The original sediment mineralogy is important in terms of the degree of leaching and cementation that can take place, that is, the sediment diagenetic potential. Modern shallow water carbonate sediments are composed of a mixture of aragonite, high-Mg calcite and low-Mg calcite grains. Aragonite is the least stable in meteoric waters and is readily dissolved. The evidences of fresh water phreatic diagenesis is recorded in the oolitic grainstones, bioclastic grainstones, and peloidal mudstone-packstone-grainstone exhibiting micrite through microsparite to pseudosparite cement textures and drying and dewatering through the cracks. The oomoldic porosity preserved in the oolitic grainstones are due to the activity of freshwater due to which dissolution or leaching of original aragonite occurred in the shallow burial conditions. Since the mineralogy of the sediments and as well as limestone forming organisms of Jurassic/Cretaceous Period was dominantly calcitic, the amount of meteoric leaching is less in the sediments of Middle Jurassic of Kachchh. During the transition period between the marine diagenesis and the fresh water diagenesis the carbonate

sediments and rocks are buried at shallow depth in mixed marine-fresh water diagenetic conditions for short period if the regression is soon followed by the next transgression. During this condition the rocks undergoes dolomitisation. The evidences of such dolomitisation and partial dolomitisation processes are seen in some of the microfacies types (Plate: 4.2-4; Plate: 4.2-3; Plate: 4.3-5; Plate4.4-4; Plate: 4.6-4).

Burial diagenetic processes lead to almost complete destruction of the porosity. Cementation in burial environment is by calcite spar, and in many limestones this has completely occluded the porosity. In many carbonate reservoirs, it appears that oil entry took place early, before burial spar cementation in adjacent rocks. The intensity of burial is also an important factor in the development of typical cement textures and complete occlusion of porosity. The burial diagenetic features are characterized by shallow burial and deep burial cement textures. In the case of bedded limestones of Jhurio Formation, the syntaxial rim cement over the crinoids and echinoids are characteristic of shallow burial diagenetic processes. The burial diagenetic condition has also brought changes in the cement textures of oolites. The oolitic textures are also seen with neomorphosed textures. The compaction of sediments, especially both the shallow marine deposits of oolitic grainstones and deep shelf deposits of bedded limestone/calcareous mudstone exhibit evidences of burial diagenesis. The fragmentation of bioclasts in oolitic grainstones and oolitic intraclastic grainstones and neomorphosed microsars of bedded limestone and the presence of syntaxial rim cement over peloids are the result of diagenetic processes that has taken place under the burial diagenetic conditions. The dolomitisation processes are also initiated during the burial diagenesis in some of the microfacies. The stylolitisation is the another important process that have occurred to microfacies types such are bioclastic

grainstones and peloidal group of microfacies types (Plate-4.2-3; Plate-4.4-4; Plate-4.8-2). The stylolites are produced due to the chemical diagenesis and pressure dissolution during the compaction due to deep burial pressure conditions. In the final the carbonate rocks of Jhurio Formation in its type section have undergone fresh water vadose diagenetic condition. During this period the oolites have developed oomoldic porosity and cemented later (Plate: 4.3-2; Plate: 4.6-1). The other important properties are the geopetal structures in some of the microfacies types (Plate: 4.5-1) and the fenestral cements in the algal foraminiferal peloidal fenestral laminated microfacies (Plate: 4.5-3 & 4). These cement textural types developed during the fresh water vadose diagenetic environment.

4.4. CLASSIFICATION

The classificatory schemes of both Dunham (1962) and Folk (1959, 1962) distinguishes allochems, matrix or micrite, and sparry calcite cement, and both emphasize texture. In the Folk's classification, sparry allochemical limestones (sparites) and micritic allochemical limestones (micrites) are subdivided on the basis of the kind and proportion of allochems and given composite names. Micritic limestone contains less than 10% allochems; specific varieties are named based on the predominant allochem. The recrystallized, bioturbated micrite is called *dismicrite*. Biolithites are limestones that were crystallized directly from the activity of reef-building corals or algae. Folk (1962) introduced the concept of limestone textural maturity, which is determined by measuring the grain-to-matrix ratio (GMR). Textural maturity adds precision to limestone description and allows energy conditions at the depositional site to be implied. Stronger or more frequent currents (contingent in most instances on shallower depth) abrade away micrite; allochems become better sorted and, with continued abrasion, better rounded. One major aspect of limestones not reflected in Folk's classification is whether the sparry calcite is primary

cement or a secondary recrystallization of micrite. In other words, any limestone with a sparry calcite cement is a *sparite* even if it started out as a *micrite*. Since this determination is often hard to make, Folk's classification is much more descriptive and objective.

The Dunham's (1962) classification emphasizes limestone texture, especially grain (allochem) packing and the ratio of grains to matrix. Allochem type is ignored. In his scheme five types of limestones are identified : *mudstone*, *wackestone*, *packstone*, *grainstone*, and *boundstone*. All except boundstone accumulate as clastic carbonates; individual components are not bound together during deposition. Mudstone, wackestone, and packstone contain mud (any silt- or clay-size grains, regardless of composition). Mudstone and wackestone are mud-supported in which allochems are scattered through the micritic rock. Packstone contains less mud and is grain-supported. Grain-supported limestones typically have their allochems in tangential contact. Grainstone contains no mud, and allochem grains support one another. Limestones in which the components have been bound together from origin (such as reef rocks) are called boundstones (equivalent to Folk's biolithites). A sixth category, crystalline carbonate, refers to any limestone in which the original depositional texture is unrecognisable. Embry and Klovan (1972) further modified the original Dunham classification to provide niches for limestones that contain allochems coarser than 2 mm. Those with a matrix-supported texture are called *floatstone*. Those with a grain-supported texture coarser than 2 mm are called *rudstone*. Boundstones are further subdivided into *framestone*, *bindstone*, and *bafflestone*.

For the present work, the classification of carbonate rocks proposed by Dunham (1962) has been largely followed. Dunham's (op.cit.) classification is considered useful for its simplicity and direct utility in interpreting the depositional environment. Though

Dunham's original terminology has been retained a few prefixes have been added to the types present in the area with an aim to distinguish the petrographic sub-types which are important for environmental reconstruction. The wackestone and packstone with variable amount of allochems are dominant types followed by grainstones and mudstones. The petrographic types identified in the present study have close resemblance to the standard microfacies assemblages (SMF-9, 11, 14, 15 and 16 etc.,) characteristic of facies belts 6, 7, 8 & 9 of Wilson (1986). The various petrographic types of Kachchh Jurassic carbonates are described as follows.

4.4.1. Carbonate Microfacies Types

Carbonate facies are the product of complex, interwoven processes. The microfacies classification of carbonate rocks of Jhurio Formation is carried out based on the petrographic properties and the criteria used are the types of dominant biota, non-skeletal grains, texture of the microfacies, proportion of sparite to micrite, etc. The quantitative microfacies classification is based on the modal analysis of different elements in the section. The concept of depositional interpretation of microfacies may be credited to French micropalaeontologist J. Cuivillier (1952) of the Sorbonne in Paris. An early review of the importance of the concept was given by Fairbridge (1954). Many of the basic types have been categorized by Flugel (1972) who added sedimentological criteria to the basic palaeontological approach used by Horowitz and Potter (1971). Using the general category of Folk (1962), Dunham (1965) and Flugel (1972), Wilson (1975) proposed a classification of Standard Microfacies Types (SMF) which has been utilized in the present study. The microfacies are named as 10, 20, 30, 40, 50 and 60 representing different textural groups. The use of numerical series is standard practise in microfacies studies, it associates

genetically related microfacies, provides an opportunity to accommodate new data (Dawson and Carozzi, 1986; Feiznia & Carozzi, 1987), since the present study included only on the microfacies of Middle Jurassic of Kachchh Mainland. Further microfacies studies on the Upper Jurassic rocks in future can be added to the genetically related microfacies types of the present study. From the studies of different vertical stratigraphic sections of Jhurio Formation about 9 microfacies types which belongs to four microfacies groups have been identified and described, which occupy almost the lower and middle part and also at the topmost portion of the upper part of the Jhurio Formation. The four microfacies groups fall in to two facies belts such subtidal facies and peritidal facies. Subtidal facies includes the peloidal group. Where as the peritidal facies includes oolitic, bioclastic and lithoclastic groups. Fig.4.2 shows the temporal distribution of microfacies types of Jhurio Formation.

4.4.1.1. Oolite Group

4.4.1.1.1. Microfacies 10: Oolitic grainstone (Plate: 4.3-2; Plate: 4.6-1).

The oolitic grainstone microfacies is constituted by the ooids, superficial ooids and few bioclasts, especially of brachiopods and molluscan shells and ostracod carapaces. The nuclei of ooids are both peloids and fine quartz grains. The ooids cemented by first generation marine phreatic cement and followed by the second generation coarse blocky sparite of the meteoritic phreatic diagenetic environment (Plate-4.3-2; Plate-4.6-1). The intragranular porosities filled with the reprecipitated sparry calcite and the original aragonitic concentric layerings of the ooids are neomorphosed into low magnesian calcite. The grainstones grade into well sorted packstone. The ooids constitute approximately 30-40% of the rock volume. The size of the ooids in the microfacies increases towards the

Temporal Variation of Microfacies Types

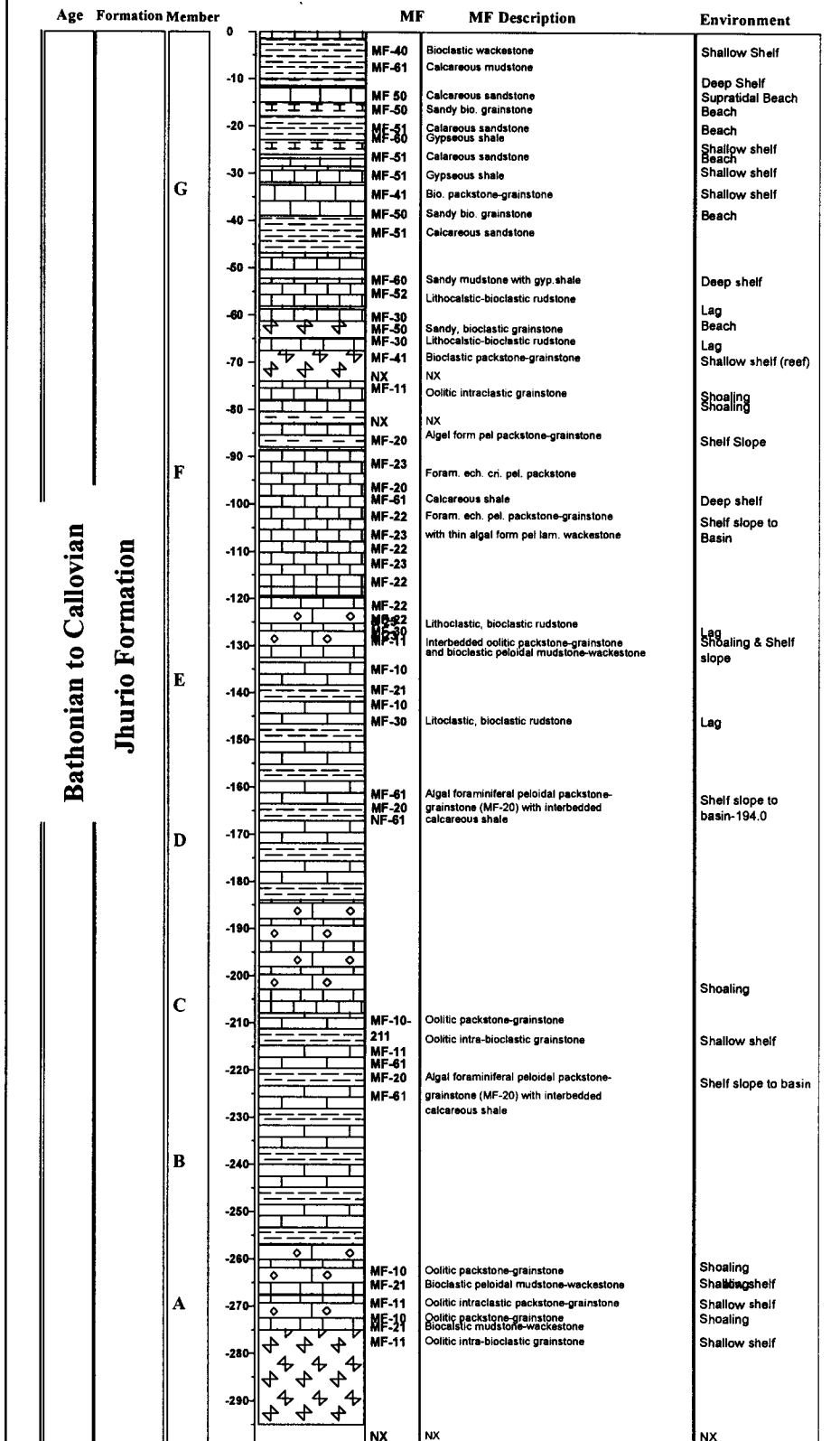


Fig.4.2 Temporal distribution of Carbonate Microfacies of Jhurio Formation.

top within the bed and the average grain size of the ooids increases in the top of the ooid grainstone cycle. The microfacies is further characterised by the coating of goethite over the calcareous ooids and gives a yellowish to brownish golden colour to the ooids. Most of the ooids are seen with only one or few concentric layerings. Such are superficial ooids. Most of the larger bioclasts and other grains can be thus included under superficial ooids. This indicates high energy conditions in a shallow marine shoaling environment. Thus the microfacies is mineralogically and compositionally matured. The oomoldic porosity shown by the ooids of oolitic grainstone microfacies (Plate: 4.3-2; Plate-4.6-1) is indication of fresh water phreatic diagenesis.

4.4.1.1.2. Microfacies 11 : Oolitic intraclastic bioclastic grainstone (Plate: 4.1-1; Plate: 4.2-1 & 2).

The oolitic intraclastic bioclastic grainstone comprises oolitic patches and bands and bioclasts of bivalves and brachiopods, echinoids, crinoids and ostracods. The microfacies differs in colour from dark grey to greenish brown. The ooid grains show first generation of cement (Plate: 4.1-1). The bioclasts show the neomorphic changes mainly inversion through dissolution of original aragentic mineralogy of molluscan bioclasts to coarse granular mosaic calcite (Plate: 4.2-1 & 2). The ooids comprise 10-15%. Intraclasts also constitute the approximate volume. The bioclasts comprise 30-35% of the volume.

4.4.1.2. Peloidal Group

4.4.1.2.1. Microfacies 20 : Algal foraminiferal peloidal packstone-grainstone (Plate: 4.2- 3 & 4).

The foraminifers are mainly smaller ones (protoglobigerinids) and larger ones

(benthic) such as miliolids, and fusulinids forms the main biota along with algal grains and few crinoid and echinoid spines. The peloids are small and the size increases upward in a shallowing upward cycle. The peloids include both faecal pellets and small micritised bioclasts. The sparite cement is the microspar produced by the porphyroid neomorphism. Syneresis cracks filled with coarse blocky sparite reveals the tectonic upliftment from the basin and consequent dessication and dewatering of fresh water.

4.4.1.2.2. Microfacies 21 : Bioclastic peloidal mudstone-wackestone (Plate: 4.3-1).

The bioclasts are thin-walled bivalves, spicules and few smaller foraminifera. The micrite mud is the main cement which is sparitised at places due to porphyroid neomorphism. The microfacies has a yellowish brown colour. The peloids are mainly faecal pellets and some are fine micritised bioclasts probably of smaller foraminiferal tests. The peloids are seen with blurred boundaries in some.

4.4.1.2.3. Microfacies 22 : Algal foraminiferal peloidal fenestral laminated mudstone-wackestone (Plate: 4.5-3 & 4).

The foraminifers are smaller and the encrusting fine algal mats are cemented with micritic cement. The microfacies is characterised by the fine laminations of fenestral sparite cement. This fenestral laminations are lined with smectite. Thus thin bedded microfacies (5-15 cms. thick.) is characterised by the dominance of smectite over quartz. The microfacies is seen cyclically deposited with the crinoidal peloidal packstone microfacies. The microfacies is mineralogically and compositionally poorly matured. The environment of deposition might have been quite water conditions in a deep shelf slope to basinal environment.

4.4.1.2.4. Microfacies 23: Foraminiferal echinoidal crinoidal peloidal packstone-grainstone. (Plate: 4.2- 4; Plate: 4.3-1 &6).

The echinoidal spines and crinoidal oscicles are abundant along with minor amounts of benthic foraminifera such as miliolids and fusulinids and smaller foraminifers. The crinoid oscicles and the echinoid spines are centred with syntaxial replacement rim cement. The peloids are larger and in some they club together which appears to form grapestone to lump structure. This indicates a quite water depositional conditions. Partial dolomitisation is observed which is due to the fresh phreatic, burial diagenetic conditions and the final fresh water vadose diagenetic processes during the upliftment of the basin deposits.

4.4.1.3. Lithoclastic Group

4.4.1.3.1. Microfacies 30 : Lithoclastic bioclastic rudstone (Plate: 4.3-4; Plate: 4.4 – 6)

The bioclasts include large bivalves, brachiopods and oysters. The bioclasts are extensively bored and embedded in ferruginous micritic mud along with large pebbly lithoclasts. In some rudstone types the place of ferruginous mud is occupied by the micritic mud in which reworked ooids and aggregate grains are seen along with large bioclasts. Both types can be considered under the same microfacies headings since both appear as a lag deposit with its thin bedded form at the base of a shallowing upward cycle.

4.4.1.4. Bioclastic Group

4.4.1.4.1. Microfacies 40 : Bioclastic wackestone-grainstone (Plate: 4.5-1).

The bioclasts include brachiopods, bivalves, belemnites, algal and coral grains. The microfacies contains abundant matrix and is neomorphosed in to microsparite cement. The microfacies grade in to packstone. The characteristic feature of this microfacies is the

abundant belemnites compared to the other microfacies types. The belemnite rostrum shows the evidence of original aragonitic mineralogy seen concentric and is later inverted to sparry calcite. The tabular pointed crystals of sparry calcite is the clear evidence of original aragonitic mineralogy. The umbrella effects and geopetal structures are seen in the microfacies types. This microfacies type is seen at the top of the Jhurio Formation in the central northern portion of the Jhura Dome. Whereas in the north-eastern part, the microfacies is seen deposited cyclically with the Microfacies-61, indicating a deep lagoonal environment.

4.4.1.4.2. Microfacies 41 : Bioclastic grainstone (Plate: 4.2-3; Plate-4.4 - 4)

Mainly bivalves and subordinate brachiopods, and very few algal remains, foraminifers and peloids. The bivalves are packed and pressure welded due to pressure solution by the over packing due to shallow burial. Thus the chemical diagenesis during the burial conditions has produced abundant irregular stylolites. The bivalves are aligned parallel to the bedding plane. The original aragonitic mineralogy has been inverted to coarse blocky sparite due to fresh water dissolution and reprecipitation. The micritic matrix is very little, about 5-8%. The dolomitisation of the bioclasts is initiated in the microfacies.

4.4.1.5. Mixed Siliciclastic-carbonate-evaporite Microfacies Types

The mixed siliciclastic-carbonate-evaporite microfacies belt is seen at the upper part of the Jhurio Formation (Member G) comprised of terrigenous materials which ranges from 35-70%. The siliciclastic microfacies belt is thus very important in the prediction of sea-level change during the deposition of the formation. The absence of any siliciclastic belt in the lower and middle portion of the Jhurio Formation and its presence in the upper part

is the indication of nearshore proxy and the migration of microfacies towards land from the shallow marine environment.

4.4.1.4.1. Microfacies 50 : Sandy bioclastic grainstone (Plate: 4.4-1; Plate: 4.6-3)

The main bioclasts are bivalves, brachiopods, foraminifers, algal grains (Dascycladacean ?) and ostracods. The fibrous calcite cement forms the major cement. The terrigenous grains including quartz (mainly) and feldspars are about 30-35%. Few mica flakes are seen. Ferruginous bands are characterised by the abundant bioclasts. Microfossils are coated and their intragranular porosities are thus filled with ferruginous matter. Thus ferruginous matter replaced the carbonate skeletons in many bioclasts. The presence of characteristic algal grains (Dascycladacean ?) in the similar microfacies types forms the microfacies of that type (Sandy dascycladacean grainstone?).

4.4.1.4.2. Microfacies 51 : Calcareous sandstone (Plate: 4.5-5 & 6; Plate: 4.6-2 & 4)

The dominant mineral is quartz about 50% and few feldspars and mica flakes. The calcareous cement is fibrous and meniscus at places indicating a beach environment. The quartz grains are replaced marginally by the calcareous cement. The microfacies is characterised by the few bioclasts such as molluscan shell fragments and few algal grains. Dolomitisation is well documented in this microfacies due to the burial in the mixed marine-fresh water phreatic environment (Plate-4.6-4).

4.4.1.4.3. Microfacies 52 : Sandy mudstone

The thin beds of sandy mudstone microfacies is seen with in the gypseous mudstone beds. The thickness of this microfacies increases towards up with in the shale bed. The sand content of the microfacies also increases towards up. The gypseous laminations separate the sandy mudstone microfacies from the gypseous mudstone beds

and also between the individual microfacies of the sandy mudstone. The sandy mudstone microfacies thin out laterally.

4.4.1.4.4. Microfacies 60 : Gypseous mudstone

The microfacies is observed at the upper part of the Jhurio Formation. The mudstone is greenish, yellowish brownish and reddish in colour with gypsum crystals and gypsum laminations. The evidence of precipitation of gypsum crystals from the mudstone is observed. This probably due to the evaporation and desiccation of shale beds which were under the shallow lagoonal environment.

4.4.1.4.5. Microfacies 61 : Calcareous mudstone

This microfacies is observed in the lower and middle part and thick bedded in the upper part of the Jhurio Formation. The top portion of the formation is characterised by the limestone nodules in this microfacies. The microfacies is nodular to lenticular. Fossils include brachiopods (*Rhynchonella* and *Terebratula* mainly), foraminifera (planktonic and benthic), algal remains and ostracods. This microfacies is deposited cyclically with the Microfacies - 40, in the north-eastern part of the Jhura Dome indicating a deep lagoonal depositional conditions on that part behind the barrier ridges situated near the present Badi section.

4.5. SPATIAL DISTRIBUTION OF CARBONATE PETROGRAPHIC TYPES

The carbonate sedimentology and diagenesis of Jhurio Formation is well explained so far. The Jhurio Formation exposed at Jhura Dome is the only continuous section and it provides a complete variety of carbonate microfacies developed during the early transgression of the Tethys sea across the Kachchh Basin. The carbonate rocks of Jhurio Formation exposed at Jumara are very thin bedded and are not continuous and are

mainly interbedded with thick shale beds. While at Habo, being situated towards the shore, only very thin-bedded section of Jhurio Formation is exposed. Thus an attempt is made to understand the carbonate sedimentology of Middle Jurassic of Kachchh Mainland. In order to understand the sedimentology of carbonate rocks deposited during the Middle Jurassic, the sections exposed at these three domes Jumara(near the depocentre), Jhura (middle) and Habo (near the shore) are studied. The Middle Jurassic sections in these areas comprises two formations the lower Jhurio and the upper Jumara which are deposited during a major transgressive-regressive phase. The carbonate rocks of these sections studied under the microscope and depositional and diagenetic properties are being described.

4.5.1. Jumara Dome Section

The temporal distribution of framework elements in the carbonate rocks of Jumara Dome section is given in the Fig. 4.3a The intraclasts ranges from 12-51%. The Jhurio Formation is characterised by the presence of less intraclasts compared the Jumara Formation carbonates. The oolites ranges from 6-42%. The amount of oolitisation was more during the deposition of Jumara Formation especially during the deposition of Dhosa Oolite Member on the top of Jumara Formation. The Dhosa Oolite Member is a marker horizon and is continuous through out the Kachchh Mainland. The peloids are less abundant compared to both the intraclasts and oolites in the carbonates of Jumara Dome section. Fossils makes up 27-57%. The main bioclasts include brachiopods, molluscs, algae, foraminifers, bryozoans, corals and ostracods. The important microfacies types grainstones grading to packstones (bioclastic packstone-grainstones, algal grainstones, oolitic grainstones, and coralline bioclastic grainstone), wackestones (bioclastic

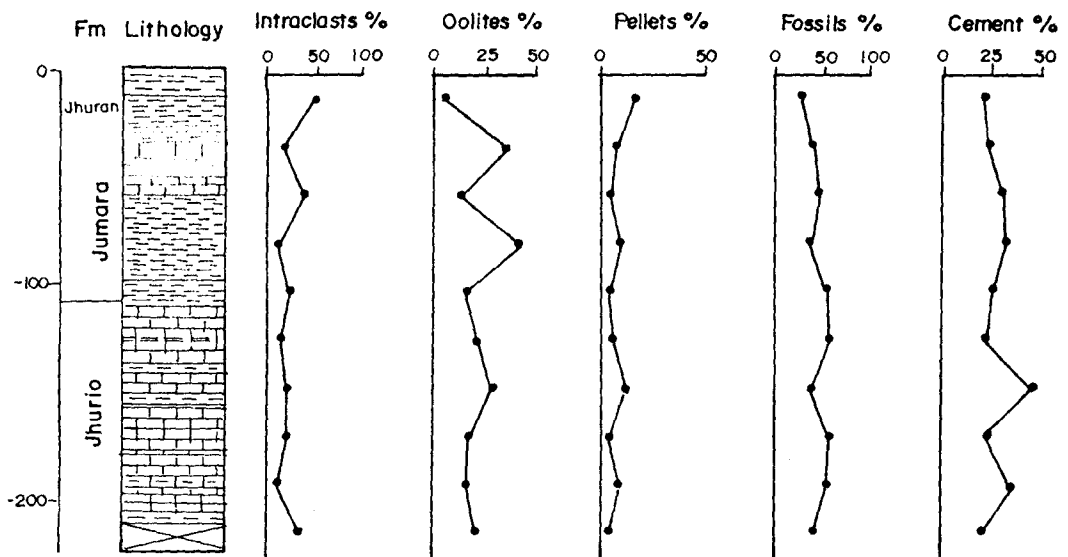


Fig.4.3a. Vertical variation of framework components of limestones, Jumara H

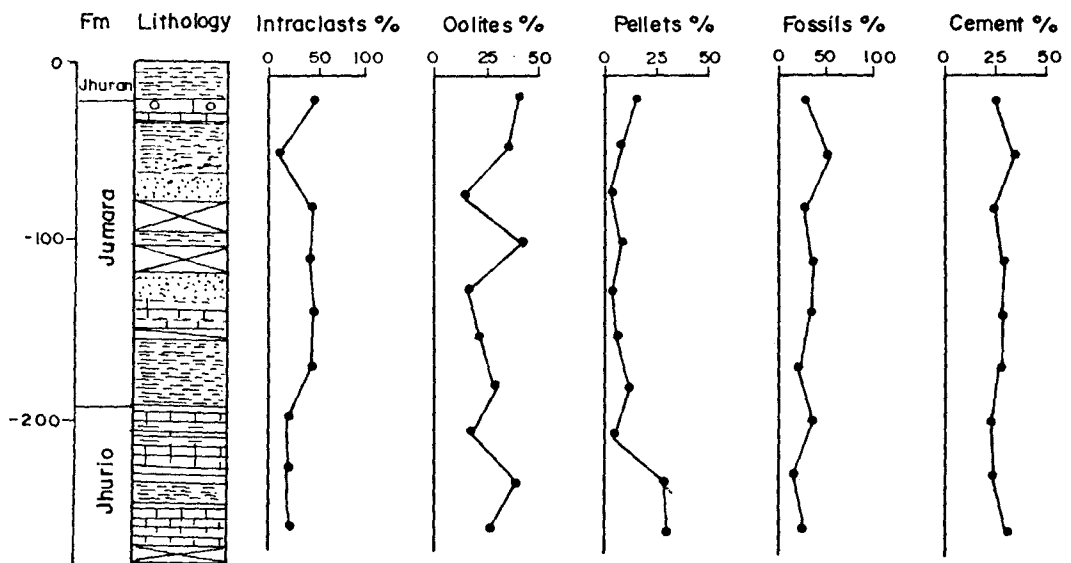


Fig.4.3b. Vertical variation of framework components of limestones, Jhura Hi

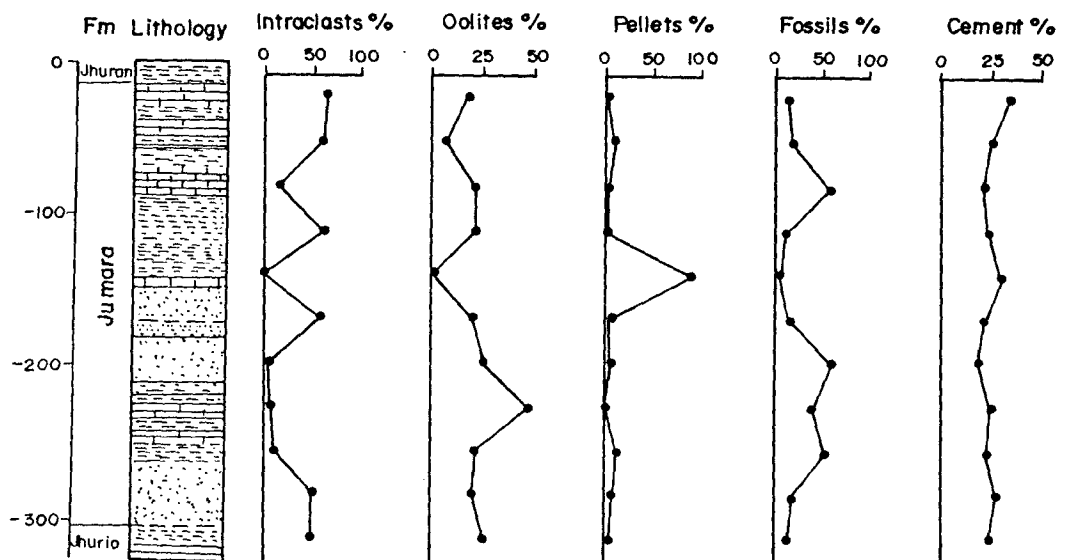


Fig.4.3c. Vertical variation of framework components of limestones, Habo

wackestones, algal wackestones, etc.), few rudstones (lithoclastic bioclastic floatstones grading in to rudstones) and few mudstones.

The depositional environment of carbonate rocks of Jhurio Formation is characterised by the deep marine environment during the deposition of coralline bioclastic grainstone microfacies to shallow marine shelf environment with the deposition of algal grainstone microfacies. The environment became very shallow and shoaling increased in the bottom causing the deposition of oolitic grainstones. The diagenesis of carbonate rocks of Jumara Dome section is characterised by the four diagenetic environments such as marine phreatic, fresh water phreatic, burial and fresh water vadose. These environments followed in the same manner from one to other. Thus each diagenetic environment has produced its peculiar textural types. The main type of cements are micrite, coarse blocky sparite, syntaxial rim cement, and ferruginous cement.

4.5.2. Jhura Dome Section

The Jhura Dome section is characterised by the lower Jhurio Formation (278m. thick) and upper Jumara Formation (272m.). The carbonate rocks of Jhurio Formation is already explained. The temporal distribution of various framework elements in the temporal scale of Jhurio Formation (Fig.4.1) indicates the abundance and diversity of bioclats in the upper part of the formation, that is in the Member-G. The distribution of non-skeletal materials show relative abundance which are evidently environmentally controlled. For example, in the case of ooids the percentage abundance is characterized in the Member-C and E and also in the Member-A. The Member-C and E are characterized minor regressive phases of transgressing sea across the basin, during which the high energy prevailed has lead to the formation of calcareous oolites. Where as the peloids

which are characteristic of quite water environments are seen very minor percent in the oolitic limestones or sometimes absent. Instead peloids make the dominant constituent in the bedded limestones (Member-B, D and F) deposited during the transgressive phases of the Tethys sea. The intraclasts also makes significant presence in the lower and middle part of the formation indicating a submarine erosion and deposition during the deposition of sediments in the active carbonate realm.

Compared to the carbonates of Jhurio Formation, the frame work elements of carbonates of Jumara Formation (Fig. 4.3b) shows characteristic abundance of intraclasts and oolites while peloids are very small in percentage. Oolites are abundant in the middle and upper part of the Jumara Formation in the Jhura Dome. The main microfacies types present in the carbonate rocks of Jumara Formation are grainstones (oolitic packstone-grainstone, molluscan bioclastic grainstone and foraminiferal algal grainstone), wackestone-mudstone (bioclastic wackestone-mudstone) and few rudstones (lithoclastic bioclastic rudstones) which sometimes appear as floatstones. The depositional environment of carbonate rocks of Jumara Formation is characterised by deep to shallow shelf marine to shoaling environment towards the top. The diagenetic textures include the micrite, microspar, coarse blocky sparite, syntaxial rim and ferruginous cement. The diagenetic environment are marine phreatic, fresh water phreatic, burial and fresh water vadose. Dolomitisation and silicification is evidenced from the microfacies types. While stylolites are not so evident as seen in the carbonates of Jhurio Formation.

4.5.3. Habo Dome section

The Habo Dome section is characterised by the lower Jhurio Formation (50m thick) and upper Jumara Formation (290m thick). The Jhurio formation in Habo dome is

mainly thin-bedded yellow limestones with shale interbeds. The Jumara Formation is characterised by the thin-bedded limestones with interbedded thick shales and thick sandstone beds. The framework elements of carbonates of Habo Dome section (Fig.4.3b) shows the abundance of intraclasts and oolites in the Jumara Formation than in the Jhurio Formation. Peloids are abundant in the middle part of the Habo section. Fossil content varies from bottom to the top with the abundance in the lower and upper part of the Habo section. The main types of microfacies include grainstone (bioclastic grainstone, oolitigrainstone and algal grainstone) wackestone-packstone (algal packstone-wackestone, peloidal packstone) and mudstone (peloidal mudstone) and few rudstones and boundstones. The diagenetic textures include micrite, acicular fringe, coarse blocky sparite, syntaxial rim and minor dolomitic cements. These textural types are developed in marine phreatic, mixed marine-fresh water phreatic, fresh water phreatic, burial and fresh water vadose diagenetic environment.

Plate – 4.1

PHOTOMICROGRAPHS

(Magnification 24X, otherwise stated)

1. Microfacies showing calcareous ooids with equant calcite cement at the centre. Also seen sparitised bioclast with coarse blocky sparite cement.
2. Coarse blocky sparite showing ghosts of original mineralogy is a fresh water diagenetic cement. The algal, foraminiferal and ostracodal bioclasts are the sparitised grains [40X]
3. Large intraclast coated with iron oxide matter and encloses various carbonate grains which are seen with first generation marine cement. Calcitic veins formed due to desiccation and dewatering.
4. Microfacies showing peloids (including faecal pellets) showing micritised crinoids, foraminifers and algal grains. The crinoidal peloids show syntaxial rim cement. Peloids showing grapestone to lump structure. Partial dolomitisation and stylolitisiation are evidenced due to burial diagenesis.

Plate - 4.1

Photomicrographs
(Magnification: 24X. Otherwise stated)

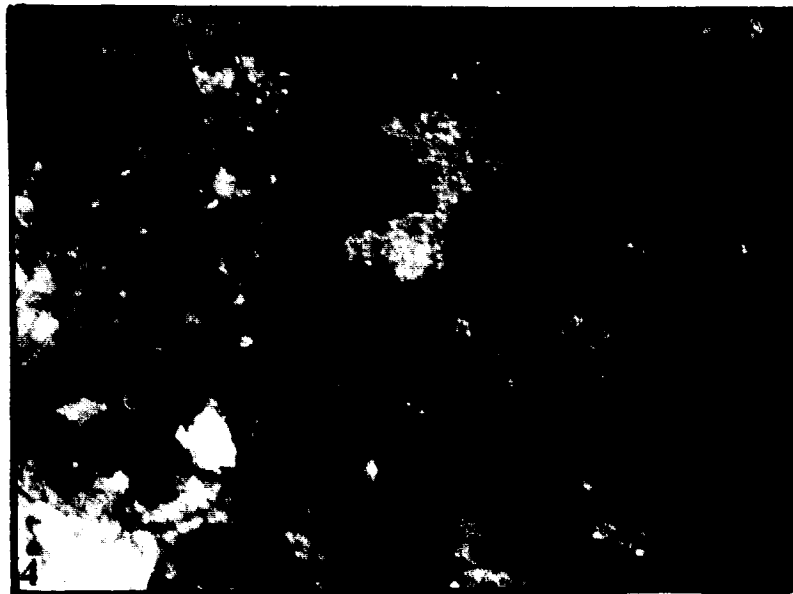
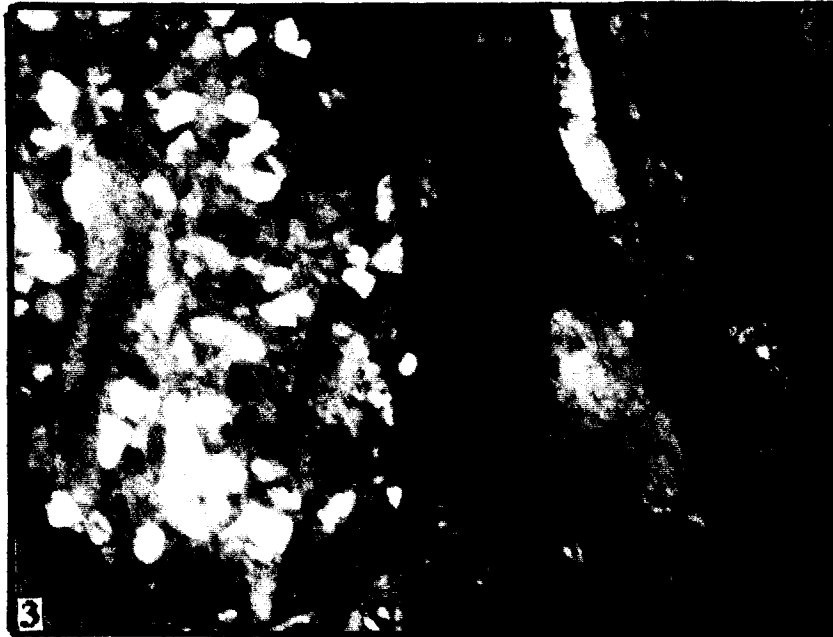
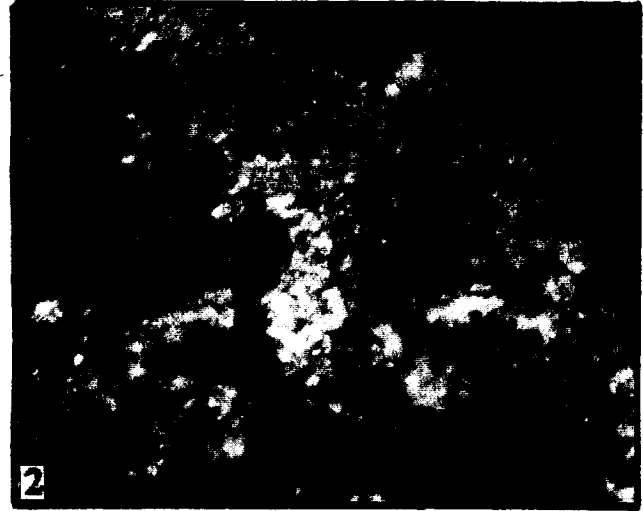
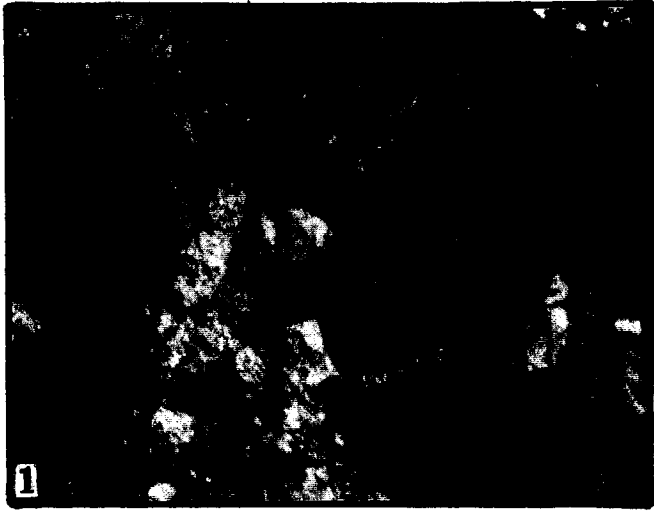


Plate – 4.2

PHOTOMICROGRAPHS

(Magnification 40X, otherwise stated)

1. Sparitised (Blocky sparite in extinct position) bioclasts (bivalves) in oolitic intraclastic bioclastic grainstone. The original aragonitic mineralogy is evident from the ghosts. Sparitised bioclasts is cemented with first generation columnar fringe cement. This is followed by the second-generation coarse cement (2.5/0.08 – Xn- 10x).
2. Blocky sparite in bright position (same of Photomicrograph-5).
3. Packed bioclastic grains in bioclastic grainstone microfacies. The bioclasts include bivalves and foraminifers (benthic). The microfacies shows sparitisation and partial dolomitisation. Stylolites are abundant which are more or less parallel to the bedding plane.
4. Crinoidal peloidal packstone microfacies showing dissolution-reprecipitation in a bivalve bioclast. The intragranular porosity is preserved due to the incomplete filling by the secondary diagenetic cement.

Plate – 4.2

Photomicrographs
(Magnification: 40X. Otherwise stated)

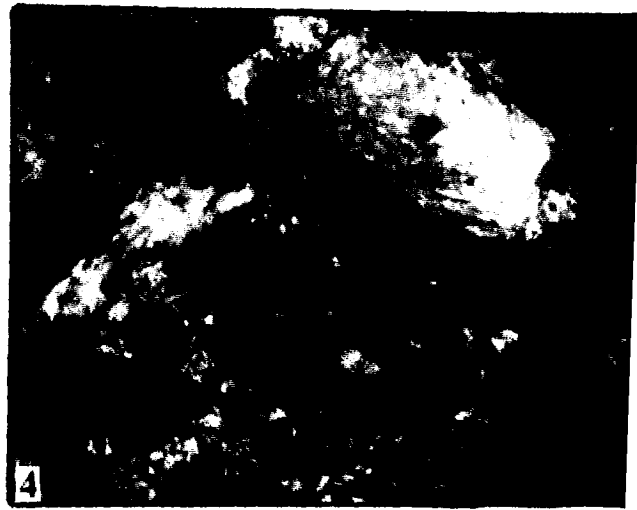
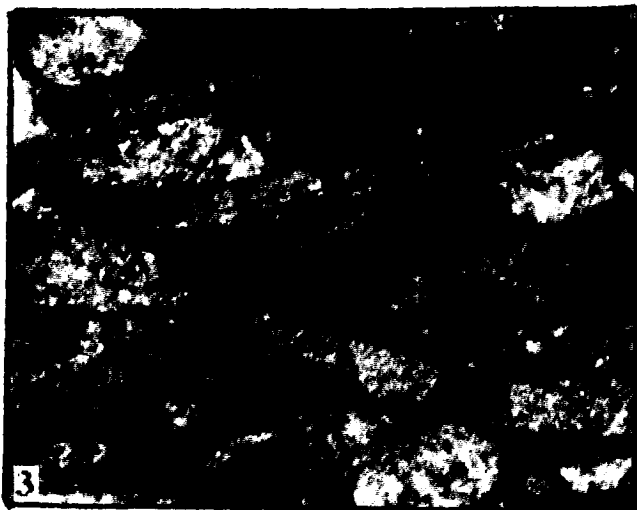
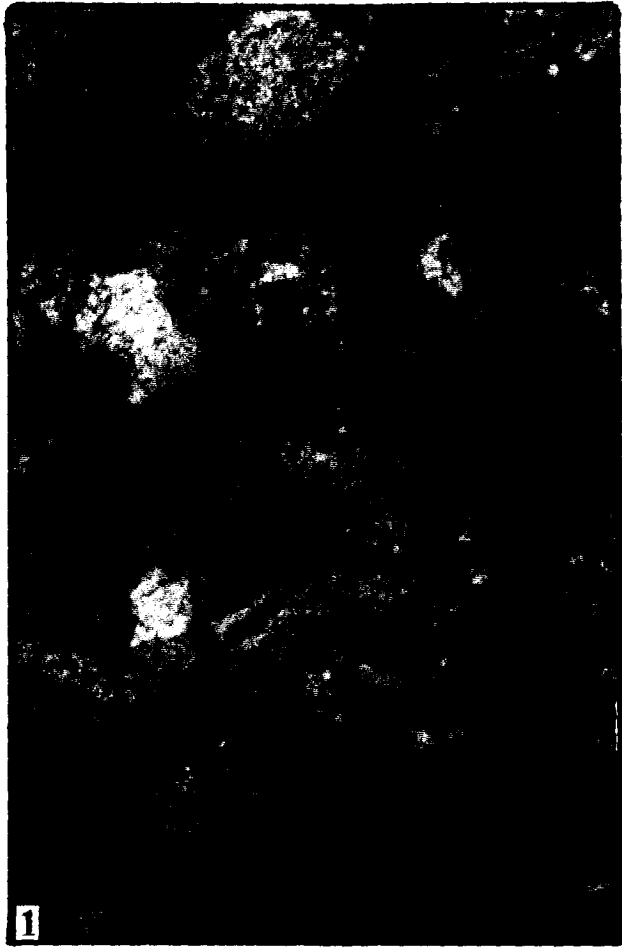


Plate – 4.3

PHOTOMICROGRAPHS

(Magnification 24X, otherwise stated)

1. Peloidal microfacies characterized by crinoids, foraminifers (planktonic and benthic). Syntaxial rim cement is characteristic of burial diagenetic cement. Micrite to microsparite cement showing evidences of ~~aggrading~~ neomorphism in peloidal microfacies.
2. Normally packed oolitic grainstone microfacies with calcareous ooids coated with iron oxide matter shows first generation cement as micritic rinds. True ooids with spheroidal shape with radiating calcite crystals also seen. Coarse granular mosaic cement formed due to meteoric diagenesis and also evidences of oomoldic porosity indicating the original aragonitic mineralogy.
3. Sandy bioclastic grainstone showing molluscan bioclasts with coarse blocky mosaic calcite. Micritic envelopes are collapsed in the bioclast. Quartz crystals are pressure welded due to compaction under burial diagenesis.
4. Lithoclastic bioclastic rudstone with micrite to sparite cement over the reworked oolites and aggregate lithoclasts. Ooids are with radiating calcite crystals and might ^{be} redeposited in the site of deposition.
5. Microfacies showing foraminifers (benthic) and crinoids in the packstone-grainstone microfacies with microsparite to pseudosparite cement. Syntaxial rim cement over foraminifers and crinoids is seen with compromise planes. [40X, X_n]
6. Packed peloids in foraminiferal crinoidal peloidal packstone-grainstone. Crinoidal oscicles, foraminiferal tests and algal grains are common. Syntaxial rim cement is developed under burial diagenetic environment.

Plate - 4.3

Photomicrographs
(Magnification: 24X. Otherwise stated)

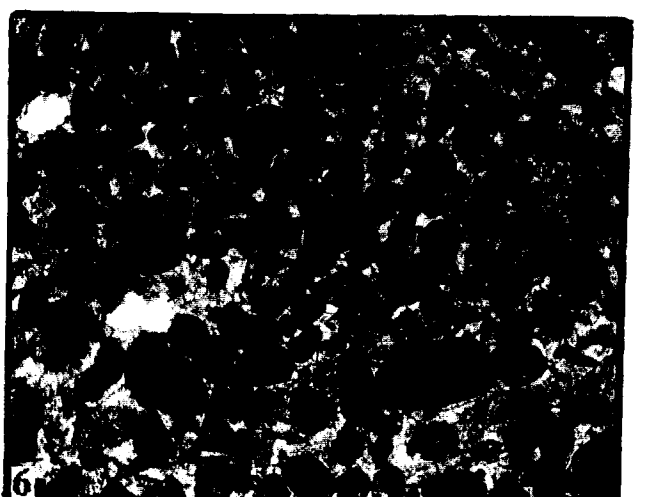
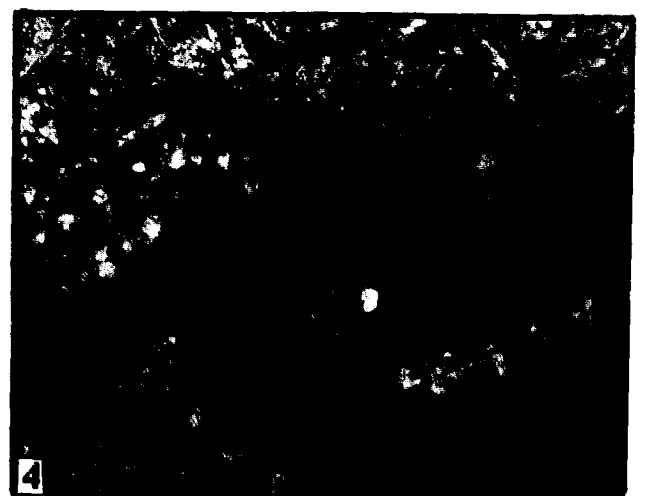
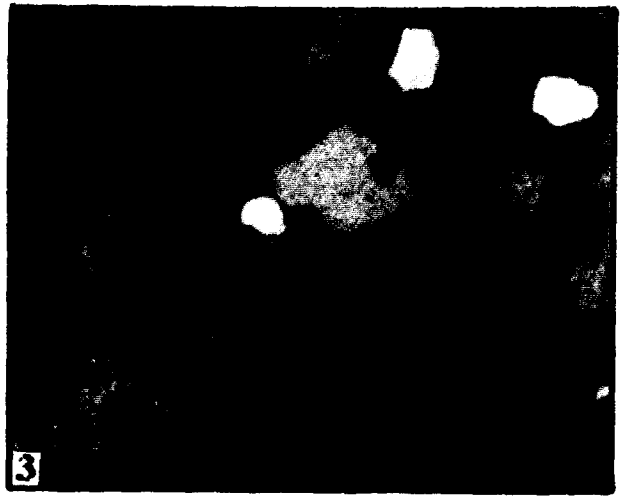


Plate – 4.4

PHOTOMICROGRAPHS

(Magnification 24X, otherwise stated)

1. Calcareous sandstone with ferruginous bands. The bioclasts are abundant in the ferruginous layer, which are coated and corroded iron oxide matrix. Algae, bivalves and brachiopod fragments are the main bioclastic grains.
2. Foraminiferal peloidal packstone-grainstone with abundant smaller (protoglobigerinids) and few benthic foraminifers and algal grains. Syneresis cracks are filled with coarse sparite cement, which are evidence of desiccation upon subaerial exposure. (Plain light).
3. Same as above with Xn position)
4. Packed bioclastic grainstone microfacies. Bivalves and brachiopods are abundant with few benthic foraminifera and ostracods. Partial dolomitisation is seen and stylolites are developed due to compaction and pressure solution under burial diagenesis (40X , Xn).
5. Belemenite rostrum in bioclastic wackestone microfacies. The original aragonitic mineralogy of the rostrum is neomorphosed in to low Mg-calcite. The evidences of the same are seen as ghosts of original minerals as square tips[40X, Xn]
6. Corroded and bored large bioclasts in lithoclastic rudstone microfacies. The microfacies was formed as a lag deposit forming hardground. The dark cement portion is ferruginous micritic matrix.

Plate – 4.4

Photomicrographs
(Magnification: 24X. Otherwise stated)

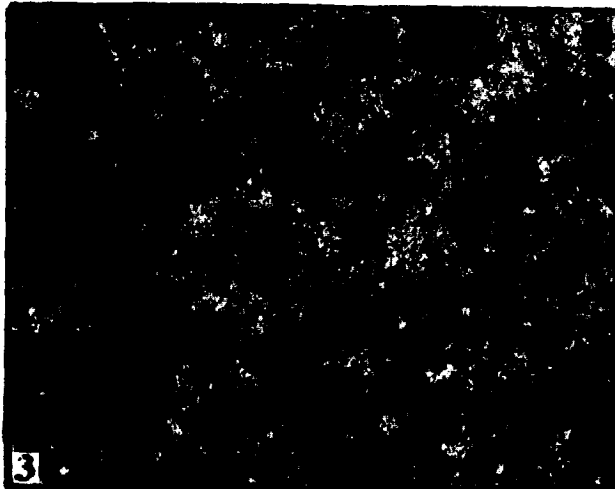
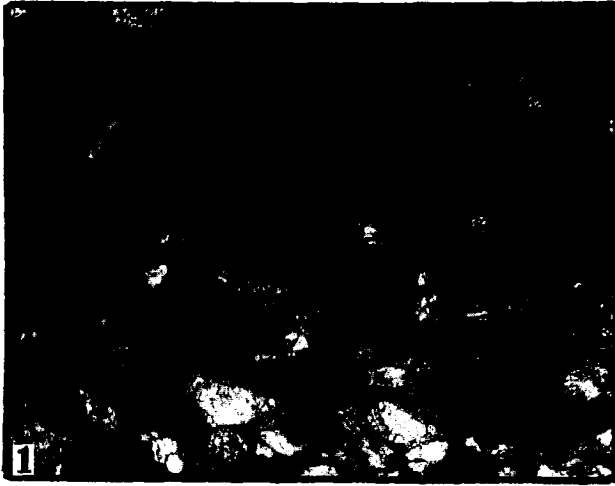


Plate – 4.5

PHOTOMICROGRAPHS

(Magnification 24X, otherwise stated)

1. Bioclastic wackestone microfacies with micrite to microsparite cement. Umbrella effects are seen at the centre. Yellow colour of the microfacies is due to the iron content. The main bioclasts include bivalves, brachiopods, belemnites, echinoids, ostracods and algae.
2. Peloidal packstone-grainstone showing abundant faecal pellets, peloids, bioclasts of pelagic bivalves, smaller foraminifera (protoglobigerinids). The microfacies shows a cross laminations.
3. Fenestral laminated wackestone microfacies with abundant algae, foraminifera and faecal pellets and peloids. The bioclasts are seen with smectite rim cement and the fenestral cement lined with smectite cement are seen as parallel bands of laminations.
4. Calcareous sandstone microfacies with medium grained subangular quartz grains seen intensively corroded. Few bioclasts are also seen
5. Calcareous sandstone microfacies showing abundant angular quartz grains, which are seen, corroded with the carbonate cement.
6. Sandy bioclastic grainstone showing the evidence of sparitisation of the original mineralogy of the molluscan bioclast. The evidences of compaction is also seen with fractured bioclast. The yellow colour is due to the iron content.

Plate - 4.5

Photomicrographs
(Magnification: 24X. Otherwise stated)

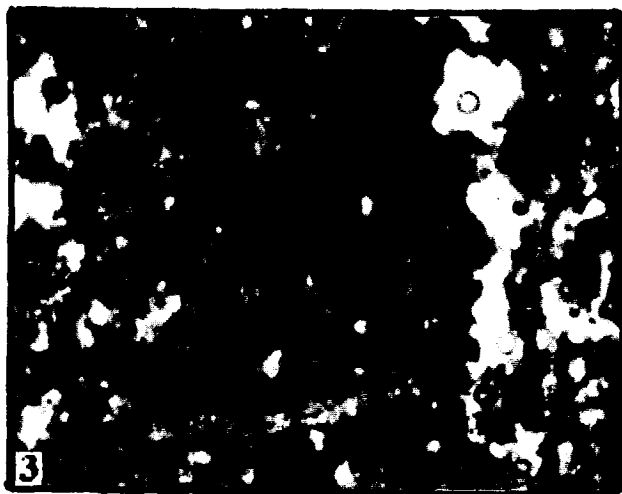
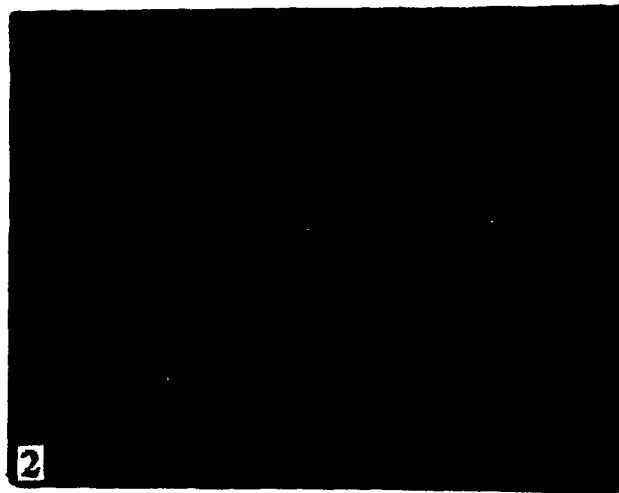


Plate – 4.6

PHOTOMICROGRAPHS

(Magnification 40X, otherwise stated)

1. The oolitic grainstone showing the regressive features of the microfacies. The ooids are seen with microsparite to sparite cement and the oomoldic porosity development due to diagenetic stabilization of the allochems with meteoric water during the regressive phase.
2. Corroded grains in a sandy bioclastic grainstone microfacies evidences the regressive phase. The corrosion is intensified with the activity of ferruginous matter. Pseudomorphs of calcite after gypsum (?) are seen.
3. The sandy bioclastic grainstone showing evidences of dolomitisation the dolomitic crystals are formed from the intergranular cement spar and the solution. During mixed marine-fresh water phreatic or burial diagenesis.
4. Photomicrograph displaying dolomitization of calcareous sandstone.

Plate – 4.6

Photomicrographs
(Magnification: 40X. Otherwise stated)

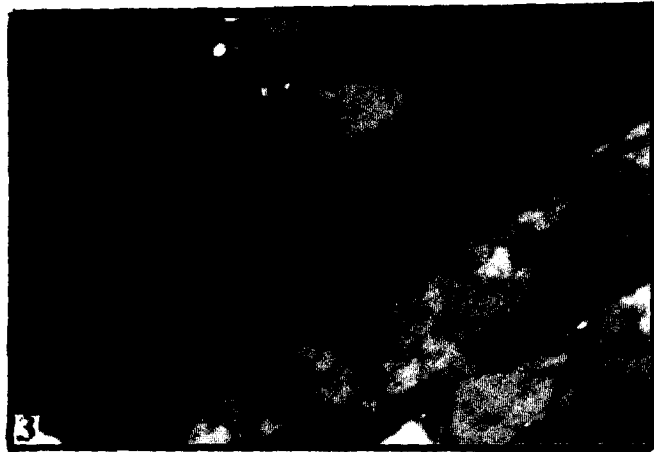


Plate – 4.7

SEM-MICROGRAPHS

1. Dissolution and reprecipitation in an algal grain. The coarse sparite cement is formed with in the algal porosity. Also seen is the disrupted porosity in the algal grain.
2. The replacement of bioclasts, coarse calcite cement and precipitation of granular sparite over the grains. Much intragranular porosity is preserved in the microfacies.
3. The micritised bioclasts of algae, crinoids, etc. in peloidal packstone-grainstone microfacies. The intergranular cement is sparite showing syntaxial rim over the crinoids and algal grains.
4. The formation of secondary coarse sparite in the intergranular spaces of the peloidal packstone-grainstone. The first generation fringe cement is observed over the algal, crinoidal and bryozoan grains.

Plate - 4.7

SEM-micrographs

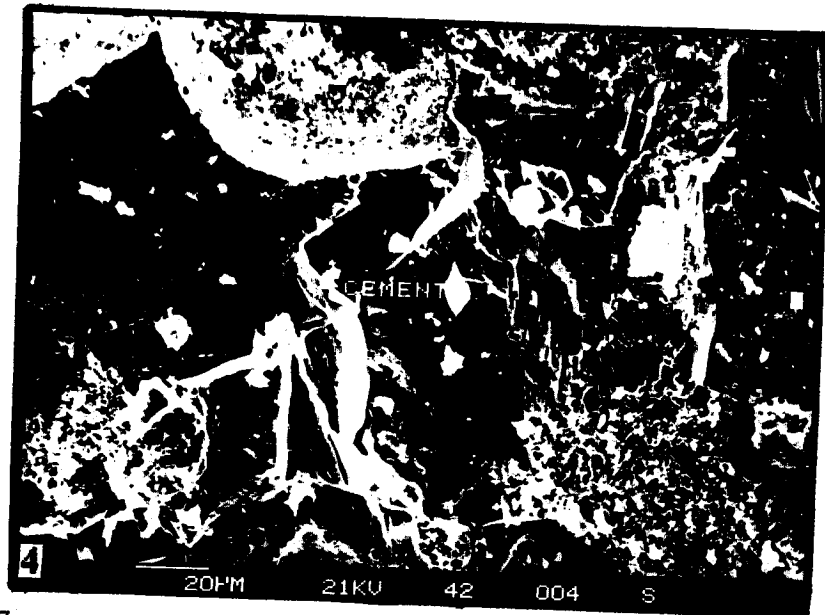
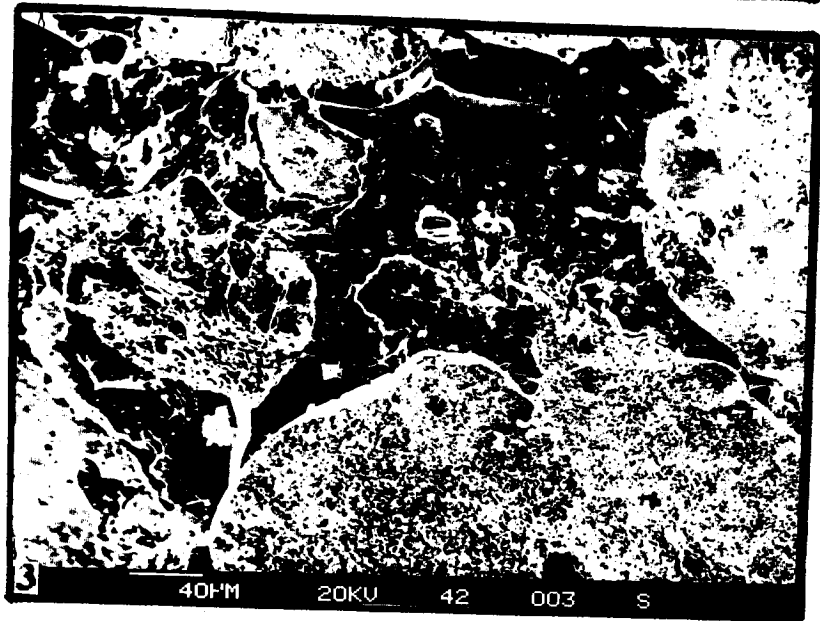
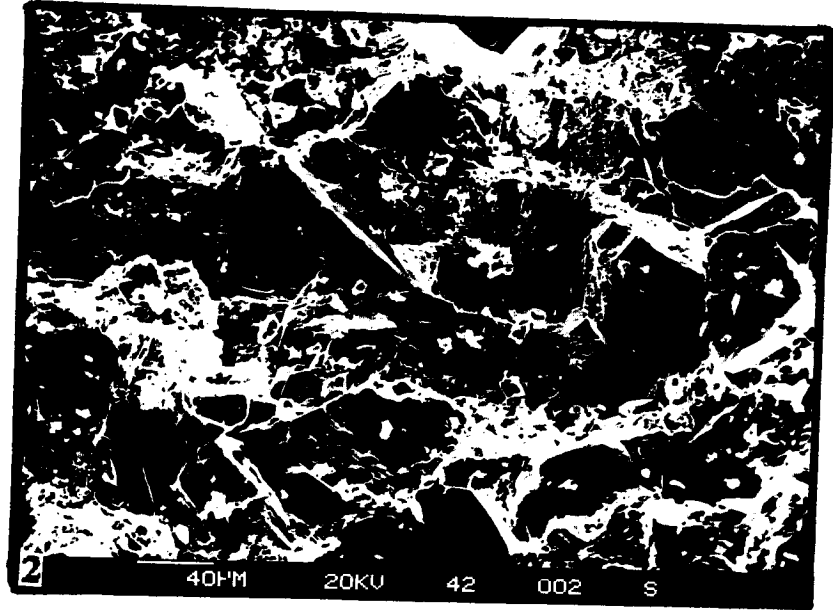
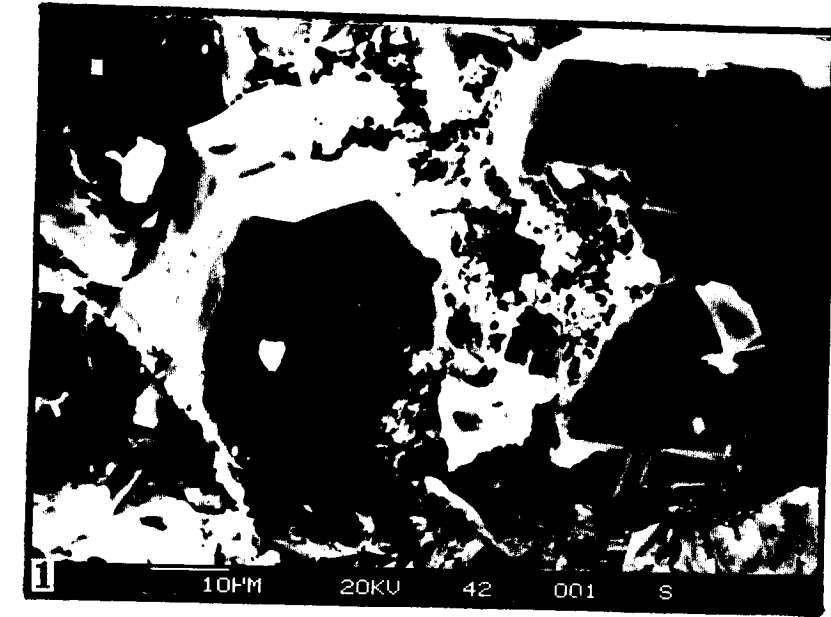


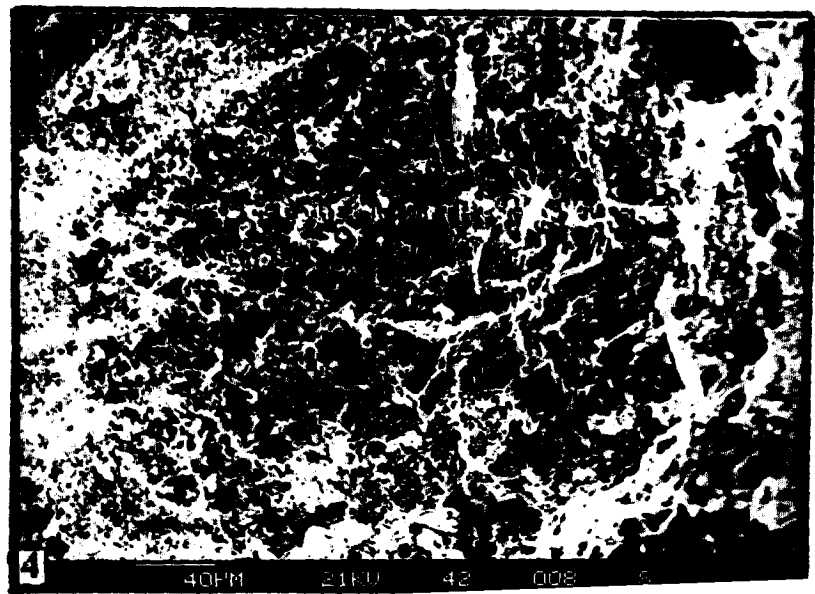
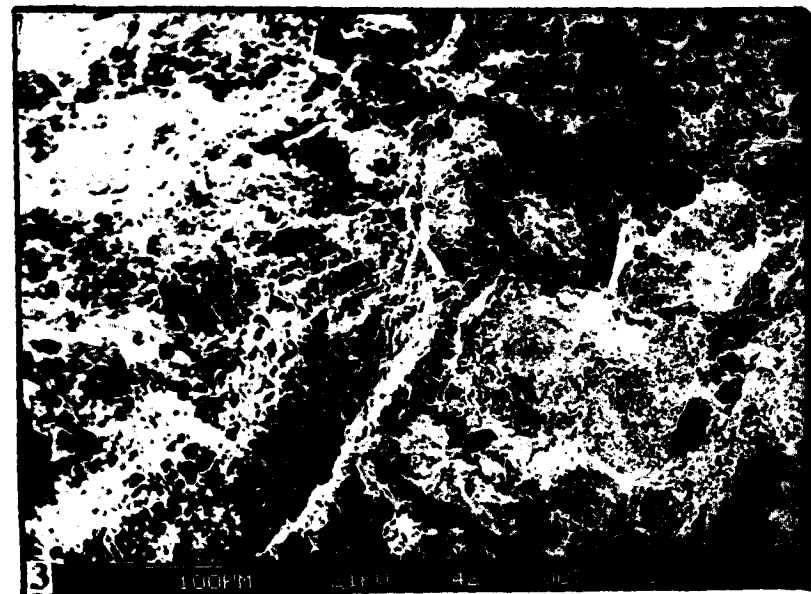
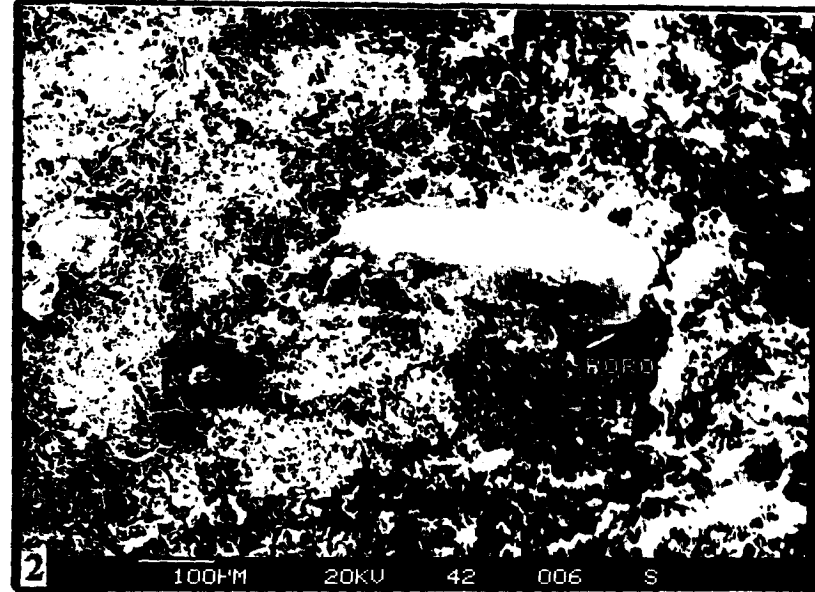
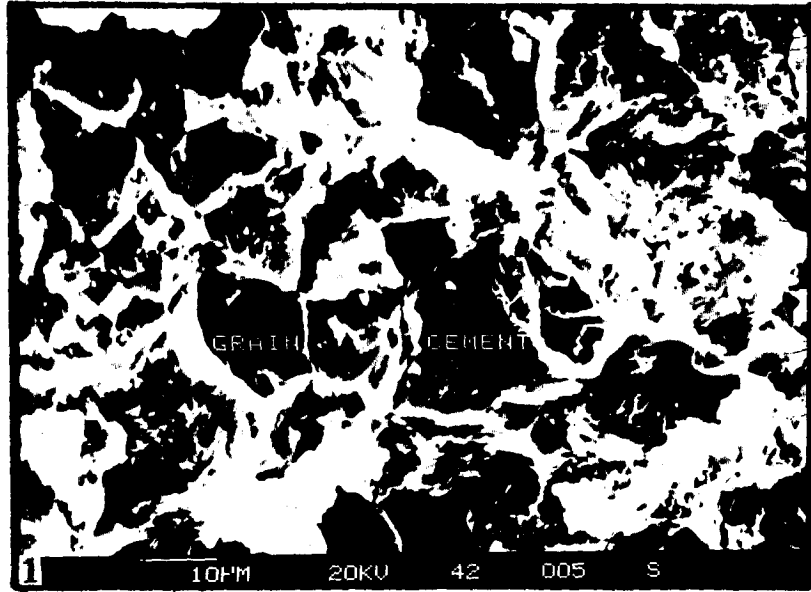
Plate – 4.8

SEM-MICROGRAPHS

1. Tightly cemented fabric in a bioclastic wackestone microfacies. The dissolution and precipitation of sparite from the algal and bryozoan grains. The zoaria of bryozoans are visible.
2. The ostracod carapace embeded in a micrite to microsparite cement. The porosity is of both intragranular and intergranular types. The stylolites are observed on the top left part of the microfacies.
3. The sparitised oolitic grainstone microfacies with tightly cemented,packed with ooids.
4. Sparitised bioclasts with coarse sparite cement in the oolitic packstone-grainstone microfacies

Plate - 4.8

SEM-micrographs



CHAPTER - V

CLASTIC SEDIMENTOLOGY

5.1. GENERAL

Terrigenous clastic sediments are a diverse group of rocks, ranging from fine-grained mudrocks, through coarser grained sandstones to conglomerates and breccias. The sedimentary rocks are largely composed of fragments or clasts of pre-existing rocks and minerals. They are also referred to as detrital or epiclastic. Three types of clastic sedimentary rocks recognized in the Middle Jurassic sequence of Kachchh which include sandstone, mudrocks(shales) and conglomerates in the order of abundance. The textural, mineralogic and petrographic study of more than 100 samples from different horizons and localities were carried out to know the clastic textures and framework composition which is very useful for classification and for understanding the provenance.

5.2. SANDSTONE

Sandstone textures and sedimentary structures reveal depositional setting, dispersal, and transporting mechanism. Because of their resistance weathering and erosion, they have the dominant control on topography and mainly seen in ridges capping the hills. The Middle Jurassic sequence of Kachchh Mainland comprises a major lithology consisting of predominant sandstone, limestone and subordinate shales.

5.2.1. Texture

The texture of terrigenous clastic rock is largely a reflection of depositional process and so many sediments/sedimentary rocks have been studied to determine their textural characteristics. The texture of a sandstone includes grain size, size variation, roundness

shape, surface features, and overall. Texture is analyzed for many reasons, in addition to simple description. Often, stratigraphic units can be differentiated on the basis of mean grain size alone. Sandstone porosity (the ratio of the volume of empty space to that of solid material) and permeability (the degree to which pores are interconnected) are of practical importance in petroleum geology, hydrology, and waste disposal. Regional variations in texture allow inferences to be made about sediment dispersal. These reasons aside, the principal motivation behind present study of sandstone texture is ^{to} understand the transporting agent and depositional setting.

Although there have been several attempts made in the past to determine the origin and depositional environment of these rocks based on field and laboratory observations, a detailed textural account of the rocks was not included in their work. The present study undertakes a detailed textural investigation of the Middle Jurassic sandstones of Kachchh for providing additional information on the depositional environment of these rocks.

5.2.1.1. Grain-size

Grain size distribution measures serve to describe, classify and genetically interpret sediments and sedimentary rocks and have been widely employed for interpreting depositional environments of ancient and modern sediments (eg. Folk, 1966; Klovan, 1966; Friedman, 1961, 67; Moiola and Weiser, 1968). Initially grain-size analysis were made primarily on siliceous clastic rocks, but in the recent years, repeated attempts have been made to apply these analyses to carbonate sediments and carbonate rocks as well (Ginsburg, 1956; Folk, 1962, 66; Pilkey et al, 1967;; Davis and Conley, 1977).

5.2.1.1.1. Grain size Analysis

Grain-size can be measured by various methods viz., sieving for loose unconsolidated sediments and thin sections for well-indurated lithified rocks. Present study utilizes the method of grain-size determination using thin sections. In all about 30 thin sections of representative samples were taken for the analysis of size, shape and roundness. The thin sections have been projected using a grain projector and the individual grain boundaries have been traced. The grain boundaries of about 300 grains in each sample were traced and the magnification was noted. The smallest circumscribing and largest inscribing diameters have been measured along with the diameters of the individual corners for determining the size, shape and roundness parameters.

$$\text{Size} = P = \text{SQRT}(d_i \times d_c)/m$$

where d_i = diameter of the largest inscribing circle; d_c = diameter of the smallest circumscribing circle; and m = magnification.

After obtaining the size for each grain, the various size parameters viz. mean, standard deviation, skewness and kurtosis were calculated by graphical method using Folk and Ward (1957) formulae. The one percentile (C) and fifty percentile (M) values are also been recorded from the cumulative curves for plotting on C-M diagram.

Since most interpretations of grain size distribution are based on the evaluation of unconsolidated sediments (sieve data) the necessary statistical corrections have been made before the interpretation of the observed data. Since the plane of the thin section does not pass through the centers of all the grains, the observed diameters will not be accurate indication of the grain diameters themselves. Generally the average size of the thin

section will be less than the average size of the actual grain (in 3-D). Grain size diameter measured in thin section, corresponds to the maximum diameter visible. Because the plane of a thin section cuts randomly through grains, data obtained from thin sections must be corrected arithmetically (Friedman, 1961). To eliminate the effect of random sectioning the correction procedures for the observed arithmetic moments for number and weight frequency moments have been proposed by Krumbein(1934) and Sahu (1983). In the present study the observed parameters have been corrected using the procedure laid in Krumbein (1938) to eliminate the random sectioning effect.

5.2.1.1.2. Grain-size Parameters

The grain size distribution patterns of the samples exhibit in general a marked Unimodal to bimodal nature of the rocks. The various grain-size parameters have been interpreted in order to understand the transportational and depositional conditions. Standard statistical measures of grain size are mean size, standard deviation, skewness, and kurtosis. These statistical measures are used because the fundamental purpose of sandstone grain size studies is to identify the transporting agent and depositional setting. These measures of averageness are supposed to record potentially distinctive characteristics of the depositional agent, presumably its kinetic energy and competence (which vary with velocity and viscosity). Some transporting agents do produce distinctive textural imprints. Mean, median, and modal sizes of sediment carried by the wind (high velocity, low viscosity) are much finer than those of grains transported by ice (low velocity, high viscosity). Sand deposited by fast-moving (steep-gradient) rivers typically exhibits a coarser mean than sand deposited by rivers flowing down lower gradients. Waves and longshore currents repeatedly winnow Beach sandstones; they are typically Unimodal with a single modal size. Conversely,

sandstones deposited by density currents are bimodal. The spatial distribution of grain-size parameters of the samples is presented in Table - 5.1 and the vertical variation is shown in Fig. 5.1.

5.2.1.1.2.1. Mean grain-size (M_z)

Mean grain-size indicates the central tendency of the size of the sediments. Translated in terms of available energy it indicates the average kinetic energy (velocity) of the depositional medium. However the average size of the sediments is also dependent upon the source material. A marked unimodality in grain-size exists within all the samples. The overall mean grain-size vary from 0.3627 to 2.9282 with a mean of 1.8037, and standard deviation of 0.7383 and can be used to classify the samples into fine to medium grained category. The locality wise variation of the same is shown in Table-5.1.

5.2.1.1.2.2. Standard Deviation (σ)

Standard Deviation measures the sorting of the sediments and indicates the fluctuations in the kinetic energy (velocity) conditions of the depositing agent in terms of its average velocity. Sorting has an inverse relation with standard deviation. Variation in grain size or sorting expresses the number of significant size classes in a population. The implied significance of sorting is that transporting agents differ in their ability to entrain, transport, and deposit grains of different sizes. Sorting may reflect variations in velocity and the ability of a particular process to transport and deposit certain sizes preferentially. Wave-related currents in the surf zone and blowing wind sort sand better than do turbidity currents and rivers. The standard deviation values of the samples fall in the range 0.2516 to 1.2801 (Mean : 0.6928; σ : 0.2335), which according to the nomenclature of Friedman (1962) fit into the Well sorted to moderately well sorted category.

Table-5.1 Clastic grain textural parameters of Middle Jurassic Sequence of Kachchh Mainland.

		Habo						Jhura						Jumara					
		Mz	σ	Sk	KG	C	M	Mz	σ	Sk	KG	C	M	Mz	σ	Sk	KG	C	M
Upper	\bar{X}	1.7728	0.6257	0.0805	1.1925	0.3075	1.7325	1.5018	0.6182	0.0786	1.1316	-0.3449	2.0810	1.2758	0.7640	0.2162	1.0837	0.3993	1.7844
	σ	0.8658	0.2857	0.1964	0.3746	1.1266	0.8762	0.5051	0.1687	0.3249	0.1535	0.4402	0.2242	0.1716	0.1380	0.0773	0.2960	0.1483	0.6448
	Min.	0.7612	0.2542	-0.1700	0.9600	-1.2500	0.6500	0.9561	0.4286	-0.1355	0.9565	-0.8215	1.9423	1.0812	0.6199	0.1323	0.7421	0.2292	1.0905
	Max.	2.7800	0.9284	0.2800	1.7500	1.3500	2.6600	1.9530	0.7514	0.4524	1.2430	0.0463	2.3396	1.4054	0.8949	0.2847	1.2657	0.5009	2.3652
Middle	\bar{X}	1.4251	0.6482	0.0983	0.8667	0.0000	1.3767	2.7117	0.5281	0.3165	0.9347	0.4347	2.1476	1.6110	1.0120	-0.1819	1.2373	0.0159	1.6523
	σ	0.4762	0.1604	0.2076	0.1713	0.7043	0.3785	0.1892	0.2484	0.1801	0.3153	0.3816	0.2342	1.6133	0.3792	0.0413	0.0423	0.3193	0.2517
	Min.	0.5173	0.4551	-0.2790	0.6400	-1.3000	0.6500	2.5779	0.2516	0.1602	0.5738	0.0091	1.8997	0.4703	0.7438	-0.2111	1.2074	-0.2098	1.4743
	Max.	1.8000	0.9311	0.2780	1.1000	0.7500	1.7000	2.9282	0.7326	0.5135	1.1565	0.7465	2.3652	2.7518	1.2801	-0.1527	1.2672	0.2417	1.8303
Lower	\bar{X}	2.3661	0.7004	-0.2548	1.2075	0.4125	2.5125	1.5042	0.5858	0.1574	1.1089	0.2938	1.5235	2.4018	1.1133	-0.0058	1.0784	-0.3856	1.7027
	σ	0.1462	0.0914	0.0874	0.0954	0.3568	0.1652	1.0801	0.1404	0.1431	0.1428	1.0255	0.5470	0.1216	0.2147	0.3218	0.2894	1.1360	0.7752
	Min.	2.2603	0.5871	-0.3480	1.1100	0.0500	2.3000	0.3628	0.4664	0.0284	1.0242	-0.8624	0.9548	2.3159	0.9614	-0.2334	0.8737	-1.1889	1.1546
	Max.	2.5821	0.8103	-0.1370	1.3300	0.9000	2.7000	2.5102	0.7405	0.3113	1.2738	1.0933	2.0459	2.4878	1.2651	0.2217	1.2830	0.4176	2.2508

Mz--Mean grainsize; σ - Standard Deviation; Sk - Skewness; KG - Kurtosis; C - One percentile (Coarsest size); M - Median; \bar{X} - Mean; Min - Minimum; Max - Maximum

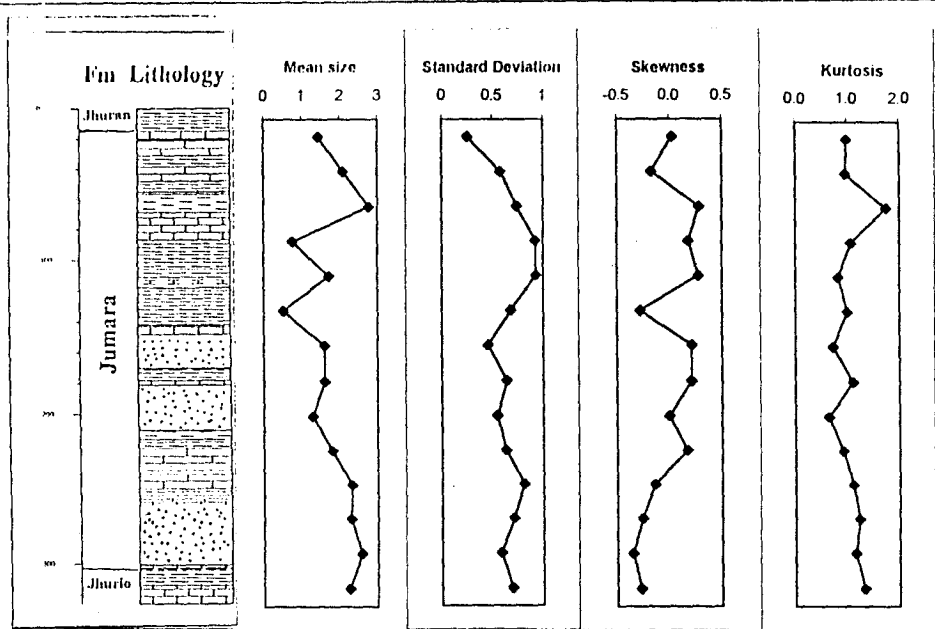


Fig. 5.1a Vertical variation of Clastic grain-textural parameters, Habo section.

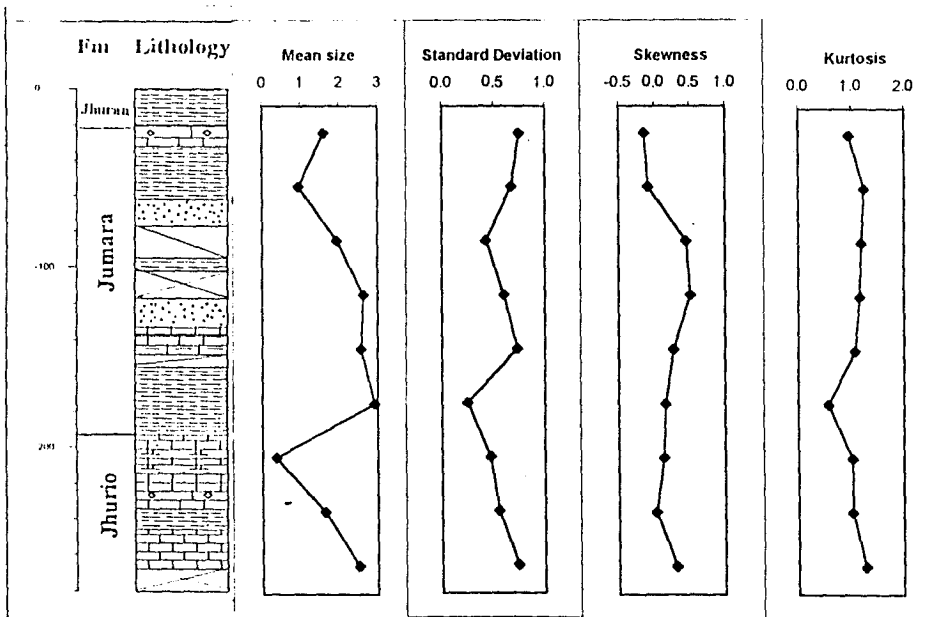


Fig. 5.1b Vertical variation of Clastic grain-textural parameters, Jhura section.

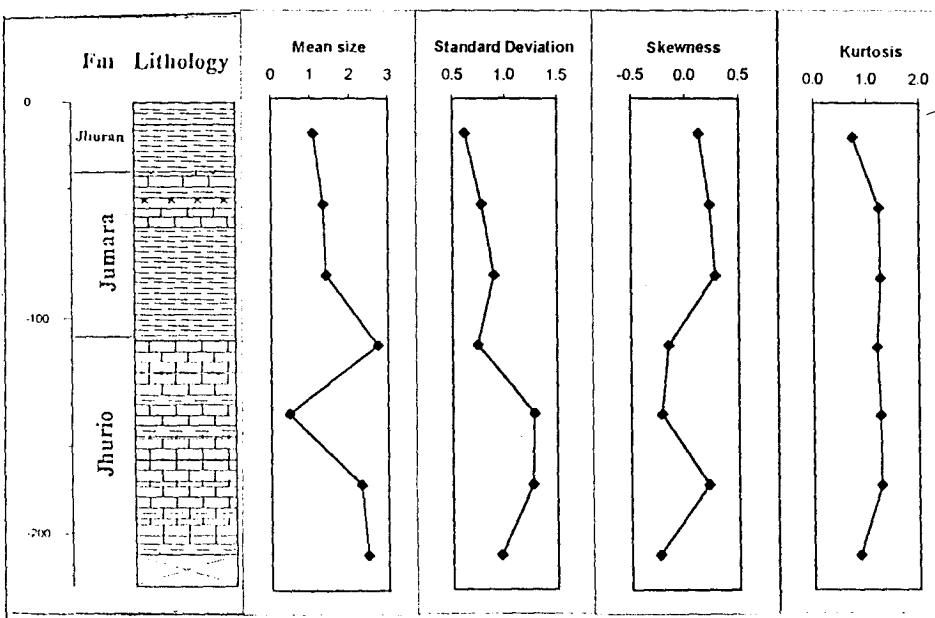


Fig. 5.1c Vertical variation of Clastic grain-textural parameters, Jumara section.

5.2.1.1.2.3. Skewness (sk)

Skewness is a statistical measure of the symmetry of a distribution and marks the position of the mean with respect to the median. In asymmetrical or skewed distributions, the median and mean shift from the mode (central peak) towards coarser or finer sizes. With negative skewness coarser grains are less well sorted than finer grains. This produces a long, more gently sloped coarse tail. With positive skewness, finer grains are more poorly sorted than coarser grains, producing a long, more gently sloped fine tail indicating excess of fine particles. Skewness is genetically significant because transporting agents differ in their ability to entrain, transport, and deposit coarse versus fine material. The Skewness variation can be readily explained by the presence of sand sized materials in the coarse and fine tails of the distribution. The skewness values fluctuate between -0.3480 and 0.5135 indicating the presence of both finer and coarser fractions. The skewness close to zero reflects the broader spectrum of populations present in these samples.

5.2.1.1.2.4. Kurtosis (KG)

Kurtosis or peakedness compares sorting in the central portion of a population with that in the two tails. Kurtosis, as used by most sedimentologists, measures the ratio of the sorting in the extremes of the distribution compared with the sorting in the central part i.e., ratio of sorting within the central 90 percent of the distribution to the sorting of the central 50 percent. Normally peaked distributions (for example, a bell-shaped distribution) are described as mesokurtic. Excessively peaked distributions (better sorting in the central portion of the population than in the tails) are leptokurtic; deficiently peaked (flattened) distributions are platykurtic. Kurtosis values fluctuate erratically around a central values of 1 with the dominant leptokurtic sands ranging 0.5738 to 1.7500 with a mean value of

1.0736. Friedman (1961) points out that most sands are leptokurtic, a fact interpreted by Mason and Folk(1958) as resulting from a mixing of predominant populations with very minor amount of finer gravel material. In general the present samples are mostly mesokurtic.

5.2.1.1.3. Textural plots

Several combinations of textural parameters have been suggested to differentiate sediments or rocks from various depositional environments (Friedman, 1961,67; Moiola and Weiser, 1968; Passega, 1957, 64; Folk,1968; Sahu, 1983), although the worldwide applicability and effectiveness of the resulting plots remains uncertain (eg. Solohub and Klovan, 1970; Omara et al, 1974).

In the present study the grain size data has been plotted on several standard bivariate plots (Friedman, 1961,67; Folk, 1968; Passega, 1957) and multivariate plots (Sahu, 1983) to discriminate depositional environments. The standard bivariate diagrams (Figs. 5.2a-d) of Moiola and Weiser (1968) Friedman (1967) and Passega (1957) diagram (Fig.5.3) have been used for plotting of textural data and to interpret the depositional processes and the multivariate discriminatory plot (Fig.5.4) of Sahu (1983) for determining the depositional environments.

The sinusoidal relationship described by Folk (1968) between M_z and sorting is partly evident, although for any particular grain-size the sorting is somewhat poorer than indicated by Folk (1968). The two vectors v_1 and v_2 for plotting on multivariate discriminant plot of Sahu (1983), have been calculated using the following formulae and data is plotted Fig.5.4.

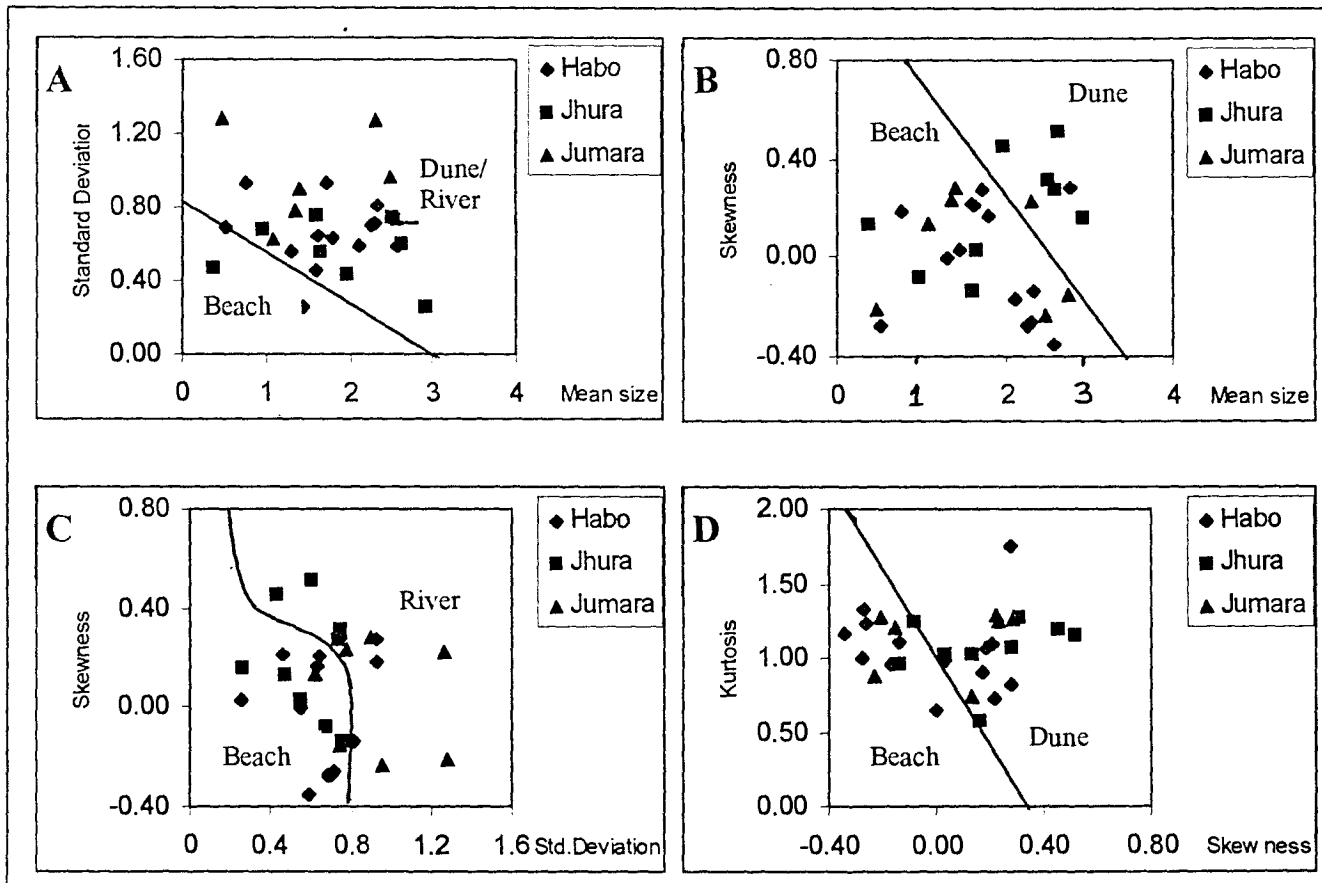


Fig. 5.2 Bivariate Textural Plots (Environment boundaries are shown)
 a) Mean size v/s Standard Deviation
 b) Mean size v/s Skewness
 c) Standard Deviation v/s Skewness
 d) Skewness v/s Kurtosis

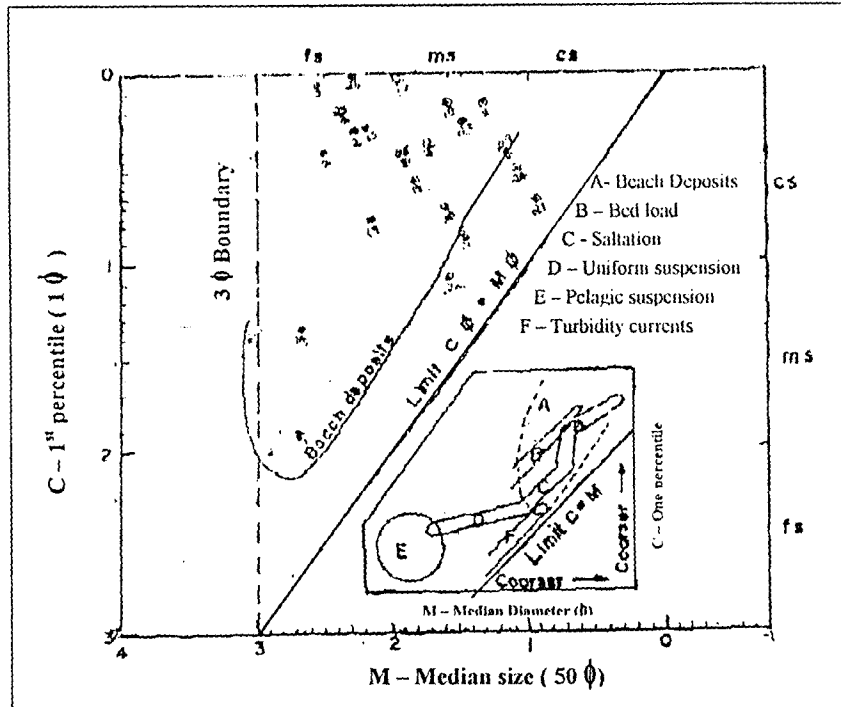


Fig. 5.3 CM Diagram for Middle Jurassic sandstone samples of Kachchh Mainland (Basic CM patterns of Passega(1957) shown in inset).

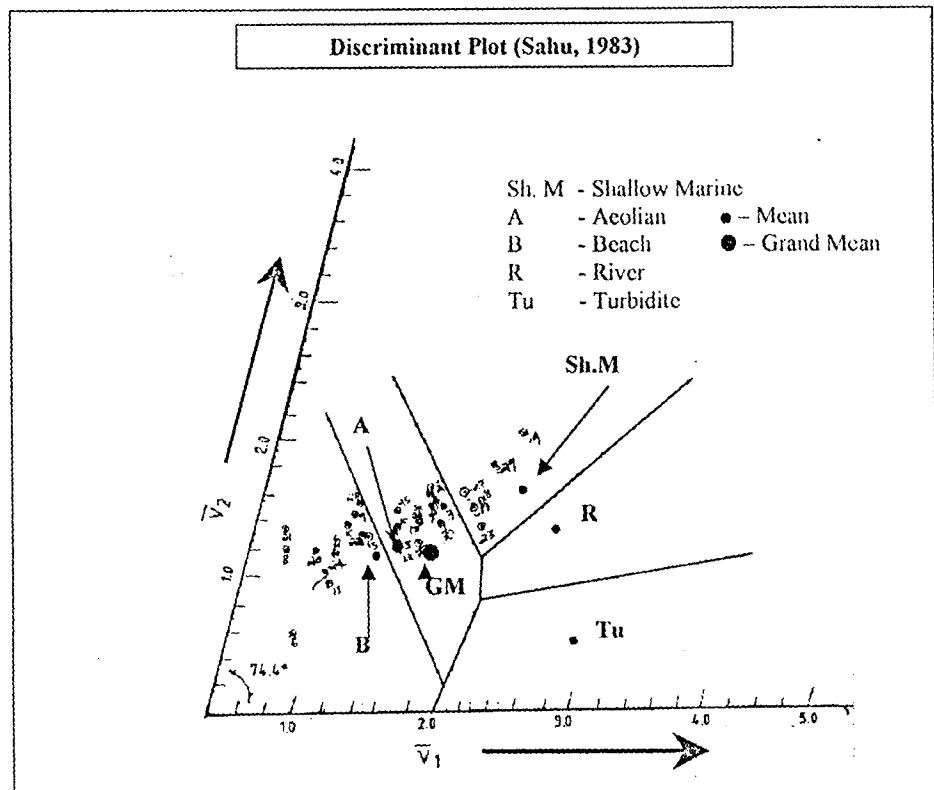


Fig. 5.4 Multivariate Discriminant Plot for Middle Jurassic sandstone samples of Kachchh Mainland.

$$v1 = 0.48048*X1 + 0.62301*X2 + 0.40602*X3 + 0.44413*X4 \quad (1)$$

$$v2 = 0.24523*X1 - 0.45905*X2 + 0.15715*X3 + 0.83931*X4 \quad (2)$$

The sample textural data points on bivariate plots fall in Beach and Dune/River fields (Fig.5.2 a - d). The C-M pattern (Fig.5.3) of the present samples clearly resembles the pattern of Passega (1957) given for beach sediments. The data points on multivariate discriminant plot (Fig.5.4) indicating a mixed shallow marine, beach to aeolian depositional setting of the samples.

5.2.1.2. Grain shape and roundness

The morphometric parameters of sediment/rock include the shape (sphericity), roundness and surface textures; which provide information about the kind and direction of sediment transport and also reflect the amount of transport and abrasion a grain has undergone. Sand grain shape (form) and roundness (angularity) are useful properties for describing and differentiating sandstone units. They are of limited value in identifying provenance, dispersal, and depositional mechanism. The rounding of sand grains is a slow process, usually requiring long-distance transport. Most well-rounded sand grains have probably experienced periods of intense abrasion that occurred during wind transport or during episodes in which they were repeatedly washed back and forth along shorelines.

The sphericity and roundness values of the present samples range from 0.5812 to 0.8710 and 0.3806 to 0.6820. These values suggests a near spherical, moderate to well rounded nature of the particles, indicating considerable abrasion/rounding during their transportation.

5.2.2. Petrography

Sandstone petrology is best studied in the laboratory. The most generally useful technique is thin section analysis. The sandstones are fine to medium/coarse grained, moderate to better sorted and cemented with calcite/hematite. These can be broadly grouped into the submature to mature quartz arenite and feldspathic arenite categories.

Matrix content in these sandstones is relatively less abundant and ranges from 2-20% or more with cement varying up to 40-50%. Matrix occurs as crushed lithic grains, small quartz grains and phyllosilicates (particularly sericite, pseudomatrix), and as epimatrix and orthomatrix. Poikilotopic, pore-filling and patchy carbonate (sparite, micrite) is abundant in some samples (range 0-25%). Cementation by hematite/ferruginous material also a common feature of the sandstones. Quartz cementation is less common. In some sandstones anhydrite is seen as an important cementing material. The framework grains in most of these sandstones are composed of detrital quartz and feldspar grains, lithic and fossil fragments and oolites and pellets. The relative abundance of framework grains of the sandstones is shown in Table- 5.2 and 5.3.

5.2.2.1. Quartz

Quartz forms the most prominent constituent of the rocks forming 52-73% by volume of the sandstone. Monocrystalline quartz (Qm) and poly-crystalline quartz (Qp) occur throughout the sequence. Monocrystalline quartz is commonly sub-rounded to sub-angular with no grains showing evidences of embayment. Undulose and non-undulose Qm is present. They do not show any common orientation, suggesting that strain occurred in the source area.

Table – 5.2 Framework composition of sandstones(fossiliferous) of Middle Jurassic sequence of Kachchh Mainland

		Habo					Jhura					Jumara				
		Qz	Fs	Rx	Bioclasts	Cement	Qz	Fs	Rx	Bioclasts	Cement	Qz	Fs	Rx	Bioclasts	Cement
Upper	\bar{X}	54.50	3.75	2.25	11.25	27.75	53.75	3.25	2.00	16.75	24.25	56.67	3.00	2.67	8.33	30.00
	σ	3.11	1.50	1.26	8.54	6.70	3.86	2.22	1.83	3.30	2.06	3.06	2.65	2.89	10.41	6.56
	Min.	52.00	2.00	1.00	4.00	19.00	50.00	1.00	0.00	13.00	22.00	54.00	1.00	1.00	0.00	24.00
	Max.	59.00	5.00	4.00	23.00	35.00	59.00	6.00	4.00	20.00	27.00	60.00	6.00	6.00	20.00	37.00
Middle	\bar{X}	61.25	2.25	1.25	6.00	29.25	61.00	3.00	1.33	8.33	26.33	58.00	4.00	3.33	6.33	28.33
	σ	2.99	1.71	1.89	7.35	2.87	3.61	1.73	1.53	5.86	4.16	4.36	2.65	1.53	3.21	4.62
	Min.	58.00	0.00	0.00	0.00	25.00	58.00	2.00	0.00	4.00	23.00	53.00	2.00	2.00	4.00	23.00
	Max.	65.00	4.00	4.00	15.00	31.00	65.00	5.00	3.00	15.00	31.00	61.00	7.00	5.00	10.00	31.00
Lower	\bar{X}	65.75	2.25	2.25	0.00	29.75	57.00	4.67	1.67	11.67	25.00	59.50	0.50	0.50	15.00	24.50
	σ	5.91	0.96	1.89	0.00	5.74	6.08	2.08	2.89	5.86	6.08	7.78	0.71	0.71	7.07	0.71
	Min.	60.00	1.00	1.00	0.00	23.00	50.00	3.00	0.00	5.00	21.00	54.00	0.00	0.00	10.00	24.00
	Max.	73.00	3.00	5.00	0.00	37.00	61.00	7.00	5.00	16.00	32.00	65.00	1.00	1.00	20.00	25.00

Qz – Quartz; Fs – Feldspar; Rx – Rock fragments; \bar{X} - Mean; σ – Standard Deviation; Min. - Minimum; Max. – Maximum; (values in %)

Table – 5.3 Modal composition of sandstones of Middle Jurassic Sequence of Kachchh Mainland

		Habo Hill					Jhura Hill					Jumara Hill				
		Qz	Fs	Rx	HM	Other	Qz	Fs	Rx	HM	Other	Qz	Fs	Rx	HM	Other
Upper	\bar{X}	88.74	2.40	1.50	1.38	5.96	86.43	3.86	3.30	2.51	3.91	75.55	3.81	4.41	2.18	14.06
	σ	4.11	1.34	1.72	1.12	3.05	2.03	1.55	0.70	0.50	0.73	11.98	0.58	2.10	0.88	13.78
	Min	79.86	0.58	0.00	0.00	2.95	85.00	2.76	2.80	2.15	3.40	67.07	3.40	2.92	1.56	4.31
	Max	91.78	4.01	4.73	2.87	12.21	87.87	4.95	3.79	2.86	4.42	84.02	4.22	5.89	2.80	23.81
Middle	\bar{X}	81.04	6.19	4.84	1.62	5.61	83.46	5.18	2.17	2.12	7.07	84.66	4.26	4.84	2.19	4.06
	σ	9.33	3.02	6.18	0.87	3.32	7.72	5.47	3.07	0.66	0.15	3.59	2.57	2.14	0.02	1.11
	Min	54.13	2.35	0.61	0.34	0.00	78.00	1.31	0.00	1.66	6.96	82.12	2.44	3.32	2.18	3.28
	Max	91.74	10.87	25.68	2.92	12.97	88.92	9.04	4.34	2.59	7.18	87.19	6.07	6.35	2.20	4.85
Lower	\bar{X}	76.33	4.63	5.70	2.18	12.71	77.71	5.58	3.39	1.79	11.54	85.68	4.85	1.34	2.22	5.91
	σ	8.67	2.76	7.70	0.57	7.78	6.70	3.09	3.30	0.52	7.43	8.04	5.27	1.12	0.92	2.96
	Min	65.78	2.60	1.55	1.38	2.25	72.98	3.40	1.05	1.42	6.28	80.00	1.12	0.55	1.57	3.81
	Max	89.12	9.78	21.30	2.97	24.56	82.45	7.76	5.72	2.15	16.79	91.37	8.57	2.13	2.87	8.01

Qz – Quartz; Fs – Feldspar; Rx – Rock fragments; HM – Heavy minerals; \bar{X} - Mean; σ - Standard Deviation

Poly crystalline quartz grains are usually coarser and consists of more than 3 crystals (Plate.5.2 - 3). The contact between the sub-grains are straight to sutured, the latter occurs more commonly. The sub-grain size is variable, even with in a single composite grain of polycrystalline quartz. Microcrystalline chert and chalcedony are also recognized.

Qm showing undulose extinction exhibit strain shadows indicating the metamorphic origin. Some of the quartz grains show large elongation ratio and acicular and needle like inclusions supporting the metamorphic origin. Monocrystalline quartz grains with sharp extinction contains inclusions of zircon, rutile and tourmaline suggesting their derivation from a possible igneous source. Secondary quartz overgrowths are identifiable due to thin clay rims and hematite coatings.

5.2.2.2. Feldspar

Feldspars rank next to quartz in all the sandstones comprising of 0 % to 11 % by volume and are represented by Microcline, orthoclase, perthite and plagioclase feldspars. Plagioclase grains range from small sub-angular grains to a few large euhedral, compositionally zoned crystals. Lamellar twinning is common. K-feldspar grains are typically small and show variable degrees of rounding and are less abundant than plagioclase. Microcline and orthoclase are the abundant feldspar types. Perthitic and microperthitic feldspars are rarer. Feldspars may be fresh and unaltered but, more commonly, they are replaced by carbonate or altered to sericite or clay minerals.

5.2.2.3. Lithic (Rock) fragments

These are the small fragments of the rocks from the provenance that have contributed to the sedimentation. Therefore, their study provides direct clues for understanding

provenance history. Rock fragments of sedimentary, metasedimentary and plutonic types are recognized. Lithic-sedimentary fragments are dominantly intrabasinal carbonate clasts, silicified oolites, fine-grained sandstones and mudstones. Lamination is some times noted in the fine-grained clasts. Lithic-metasedimentary fragments are largely polycrystalline quartzite clasts and occasionally microliths of muscovite and biotite are present. Clasts composed of quartz and muscovite, probably derived from schists and gneisses occur rarely. Lithic-plutonic fragments (clasts of quartz and feldspar) are less in abundance and are of granitic origin.

5.2.2.4. Biogenic constituents

Biogenic constituents in the fossiliferous sandstones include the fossil fragments ranging from about 0% to 23% by volume and oolites and pellets. Varying degrees of preservation of bioclasts is recognized. The abundant fossil fragments belong to mollusc and brachiopod phyla. Despite the variability in abundance, the composition of the fossil fragments, both as regards to quality and to relative abundance, remains almost uniform in all the samples.

5.2.2.5. Heavy Minerals

The heavy mineral content of the sandstones vary from 0.0 % to 2.97% . The dominant minerals present include the opaque and non-opaque minerals. Non-opaque heavy minerals include zircon, rutile, garnet, tourmaline, chlorite, apatite, epidote, andalucite, hornblende and pyroxenes. Opaque minerals include hematite, magnetite and ilmenite.

5.2.3. Diagenesis of Sandstones

Detrital composition of the sandstone has been altered by diagenesis leading, in particular, to reduction of the feldspar and unstable lithic fragments. Presence of matrix in these rocks is also supportive of the above (Plate.5.1 - 5 & 2). Poikilotopic (Plate.5.1 - 4), pore-filling and patchy carbonate (sparite and micrite) is abundant in many samples as an early diagenetic cement. Cementation by quartz (Plate.5.2 - 4) is less common. In many samples hematite cementation (Plate.5.1 - 1 & 2) is also recognized along with the carbonate cements. X-ray diffraction of the authigenic minerals present revealed the presence of calcite, dolomite, chlorite, anhydrite, gypsum, halite and hematite.

5.2.4. Classification and Provenance

Middle Jurassic Sandstones of Kachchh can be divided on the basis of framework mineralogy into various petrographic types. Type 1 sandstones (Quartz Arenites; Plate. 5.1 - 1, 2 and 3) are distinguished by abundant quartz, very little feldspars with complete absence of rock fragments. Mono crystalline quartz greatly predominate over poly crystalline quartz. Quartz grains are mostly sub rounded to sub-angular and many show sutured contacts. The heavy minerals include predominant tourmaline and rutile. Sandstones belonging to Type 2 (Feldspathic sandstones; Plate.5.2 - 2) are characterized by moderate quartz, and moderate amounts of plagioclase feldspars and rock fragments. Textural characteristics of the quartz are similar to Type 1 sandstones. Heavy minerals include tourmaline, epidote, andalucite and garnet etc. Type 3 (Sub-litharenites; Plate. 5.1 - 5) sandstones are characterized by relatively low quartz content, moderate feldspars and rock fragments with abundant sedimentary lithic fragments and are cemented with poikilotopic calcite cement (Plate. 5.1 - 4).

The vertical variation of the framework composition of the sandstones is presented in Fig.5.5. Although there is no regular vertical or spatial variation is observed, the mineralogical composition of the sandstones can be better used to understand the geology and climate of source area and the transportational history. Fine to medium grained hard, compact sandstones containing abundant undulose quartz, lithic fragments in excess of feldspars characterize a metamorphic source. The relatively coarse grained sandstones with abundant feldspars and non-undulose quartz suggest an igneous origin. The ternary diagrams (Fig.5.6a) of Dickinson(1985) have been used to plot the data . The Q-F-L plots (Fig.5.6 b-c) show the data to plot largely in the Recycled orogenic provenance field and craton interior fields of with all the sample from different horizons showing similar distribution pattern.

5.2.4.1. Quartz Arenites

Typically, quartz arenites are light coloured (white to light gray) sandstones, although they are often stained pink, brown, or red by iron oxide cement. They consist almost entirely of sand-sized monocrystalline quartz grains (many with abraded authigenic overgrowths). Resistant grains of chert, metaquartzite, and such "heavy minerals" as zircon, tourmaline, and rutile are present. Chemical composition reflects this restricted mineralogy: >85% SiO₂, 1.0%-3.0% Al₂O₃ (traces of matrix and detrital feldspar). Quartz arenites have a typical supermature texture and composition. They are usually well-bedded and exhibit ripple marks, lamination, cross-lamination, and, in some cases, large-scale cross-bedding. Body fossils of very shallow-water neritic or hyper-saline organisms are present. Such trace fossils as worm burrows are locally abundant. The thickness of individual sheets varies from a few meters to several tens of meters. Many quartz arenites are shallow marine (but above storm wave base) sands that accumulated along or near the shoreline as beach, shoreline dune,

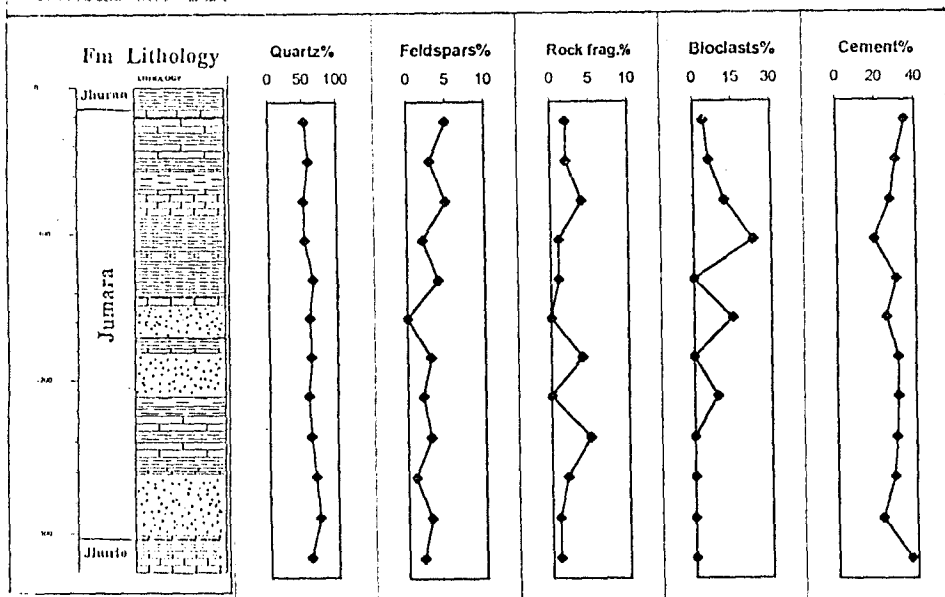


Fig. 5.5a Vertical variation of framework components of sandstones, Habo Hill.

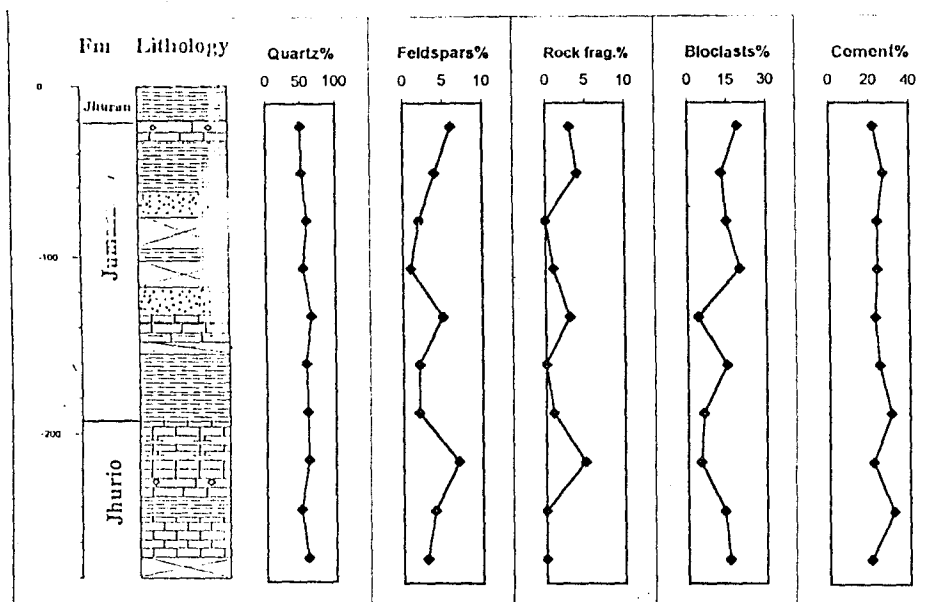


Fig. 5.5b Vertical variation of framework components of sandstones, Jhura Hill.

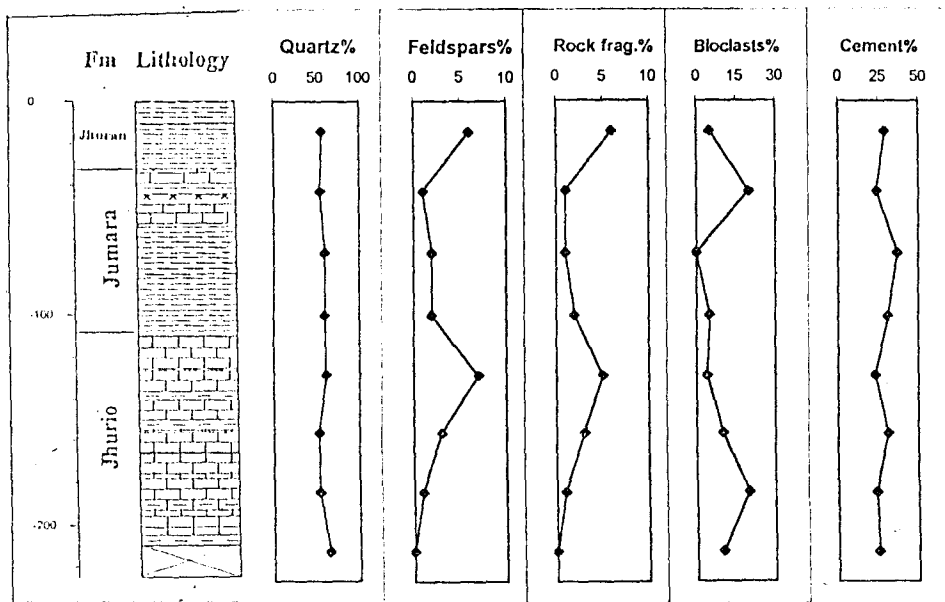


Fig. 5.5c Vertical variation of framework components of sandstones, Jumara Hill.

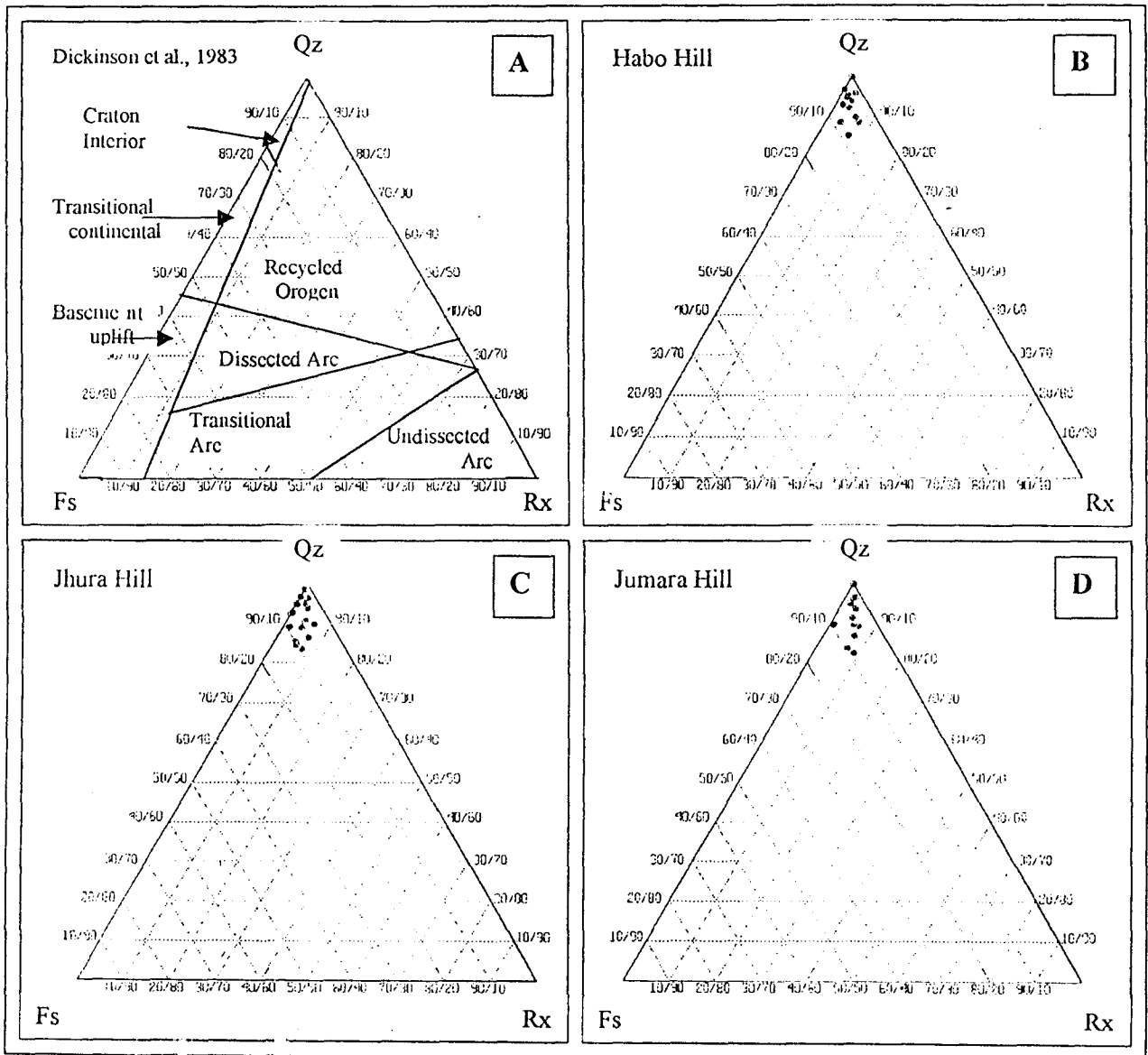


Fig. 5.6 Tectonic provenance diagram (Dickinson et al., 1983) of Middle Jurassic sandstones of Kachchh. (Qz- Total quartz; Fs – Total Feldspars; Rx – Unstable Lithic Fragments. Note that most of the sandstones derived from a recycled orogenic setting).

56

tidal flat, spit, barrier island, or longshore bar deposits. Repeated recycling of detritus weathered from stable, low-lying cratonic continental block sources probably played an important role in their genesis. The predominance of quartz arenites suggests a lengthy interval of tectonic stability that promoted intense weathering.

5.2.4.2. Feldspathic Arenites

The major framework grains found in this sandstone type are monocrystalline quartz and feldspar. Feldspar content typically reaches more than 10%. The white, gray, or pink color of feldspar imparts a similar tint to feldspathic arenites, further enhanced by ferruginous cement. Orthoclase and microcline exceed plagioclase when continental crust is the dominant source; where plagioclase predominates, a volcanic arc source is indicated. Other abundant framework grains are micas (muscovite and biotite) and rock fragments. High quartz and feldspar abundance produce an SiO₂ content ranging from 60% to 80% and a high percentage of Al₂O₃. The amount of K₂O (2%-4%) exceeds that of Na₂O when K-feldspar is more abundant than plagioclase. Feldspathic arenites are not as mature texturally or compositionally as quartz arenites. They are typically coarser, less well sorted and less well rounded. Bedding and internal organization are ordinarily less well developed than in quartz arenite and are typically unfossiliferous.

Survival of feldspar, with little decomposition to clay minerals signals a dry or arctic climate and/or a steep-sloped mountainous topography. Many classic feldspathic arenites coincide temporally and spatially with episodes of continental distension and the development of fault-bounded, rift-related grabens and half-grabens bordering steep-sloped basement rock. Feldspathic arenites (and wackes) are also deposited adjacent to active and/or dissected magmatic arcs.

5.2.4.3. Sublitharenites

Clasts of monocrystalline quartz (20%-50%) and rock fragments (5%-40%) are the most important constituents in this type. Sand flakes of detrital mica are common; feldspar content is low (a few percent). Broad compositional diversity due to wide variations in rock fragment content and type is a distinguishing character. The variation in mineral constituents generates a wide range in chemical composition. Rock fragments of limestone are common and show submature to mature textures. Lithic arenites that accumulate as alluvial deposits are well bedded and exhibit tabular and trough cross-bedding, ripple marks, internal lamination, current lineation, scour-and-fill structures and fining-upward cycles. Fossils are common, although deposits laid down in deltaic sequences that are interbedded with shallow marine shelf mudrock contain abundant fossils. These deposits exhibit internal lamination, oscillation ripple marks, and well-developed bedding.

Many lenticular sand bar deposits that interfinger with channel conglomerate and floodplain mudrock are lithic arenite, as are some sheetlike shallow marine shelf and deeper water abyssal plain deposits. Many orogenic clastic wedges consist largely of lithic arenite. This is not surprising, because physical disintegration of mountainous supracrustal rocks invariably generates detritus rich in rock fragments. Therefore, lithic arenites typically coincide temporally and spatially with subduction-related active magmatic arcs and collisional orogeny.

5.3. OTHER CLASTIC SEDIMENTARY ROCKS

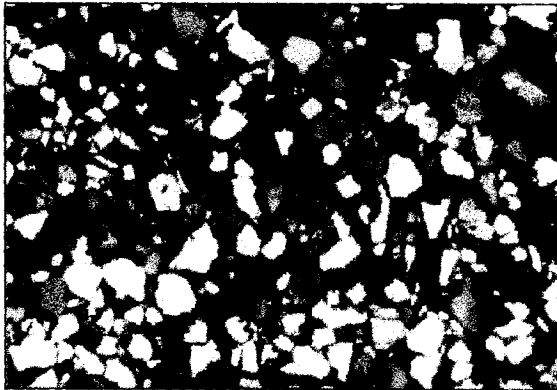
5.3.1. FINE CLASTIC SEDIMENTARY ROCKS

The fine-grained mudrocks (shales) of the Middle Jurassic Sequence of Kachchh consists of claystones, well laminated shales (Plate.1-3), silty shales and calcareous shales of various colours and shades. Since the study of mineralogy and texture of fine-grained rocks in thin sections is difficult a detailed X-ray diffraction analysis has been undertaken to describe the mineralogy of these rocks. The mineralogical studies of fine clastics are given in the Chapter-VI.

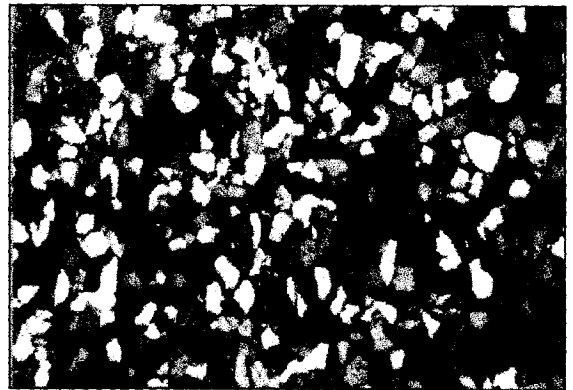
5.3.2. CONGLOMERATES

Very coarse clastic rocks are referred to as rudites or rudaceous sedimentary rocks. Conglomerates of various types have been identified from the Middle Jurassic succession of Kachchh Mainland which include quartz-pebble conglomerate, shale-pebble (Plate. 3.1 - 4) and limestone-pebble intraformational conglomerates. Framework clasts in all the above types are elliptical, flat, tabular-shaped disks with long axes aligned parallel or subparallel to stratification.

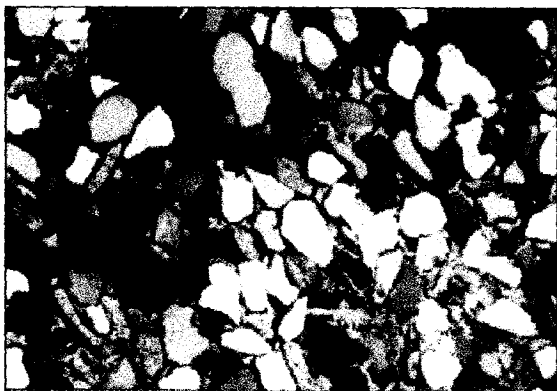
Plate – 5.1
Photomicrographs
(Magnification 24X, otherwise mentioned)



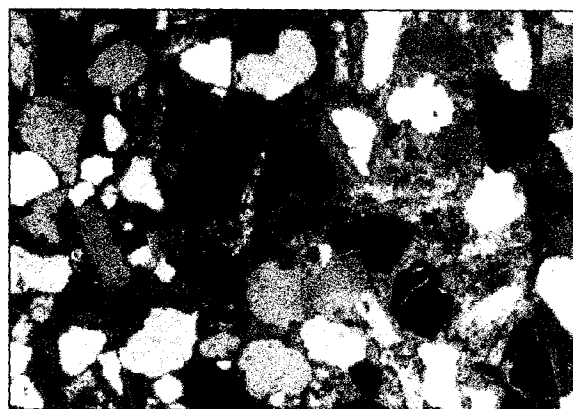
1. Ferruginous, fine-medium grained, poorly sorted sandstone.



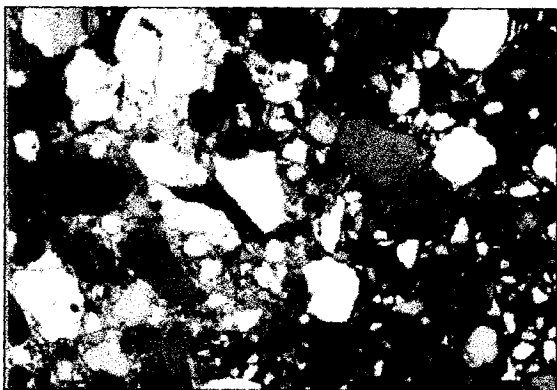
2. Stained thin section of a well sorted calcareous sandstone (calcite cement – red stained).



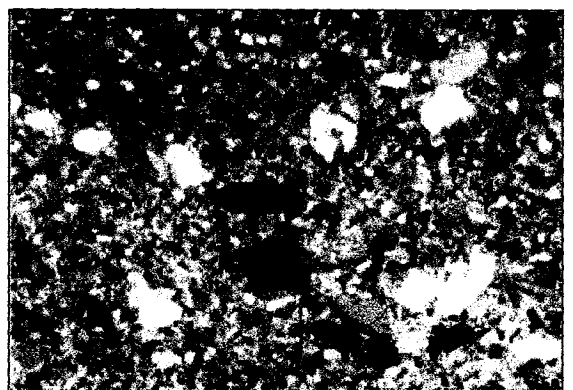
3. Subrounded to well rounded, well sorted calcite cemented quartz arenite. Matrix between the grains contain opaque iron oxide.



4. Sandstone cemented by large poikilotopic calcite crystals. Note the typical high order interference colours of calcite.

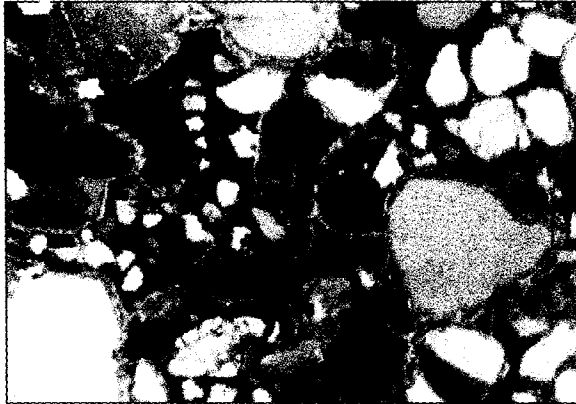


5. Subangular to sub rounded, poorly sorted quartz wacke showing lithic fragments of limestone and glauconite pellet (left center)

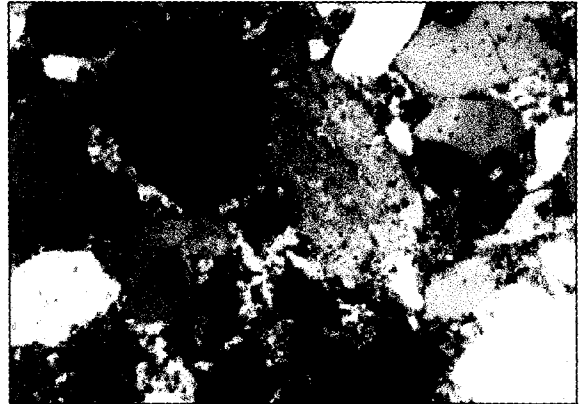


6. Photomicrograph showing rounded quartz and chert grains together with smaller subangular to subrounded quartz grains in a fine grained matrix.

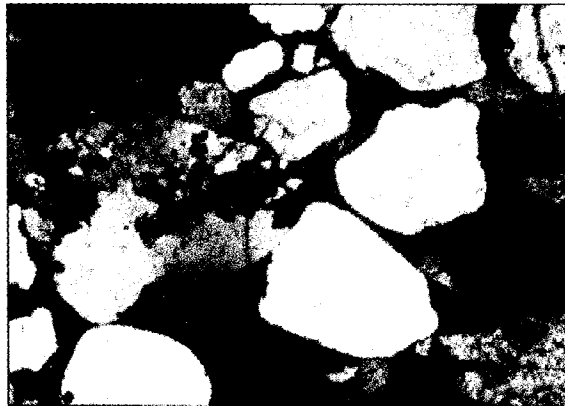
Plate – 5.2
Photomicrographs
(Magnification 24X, otherwise mentioned)



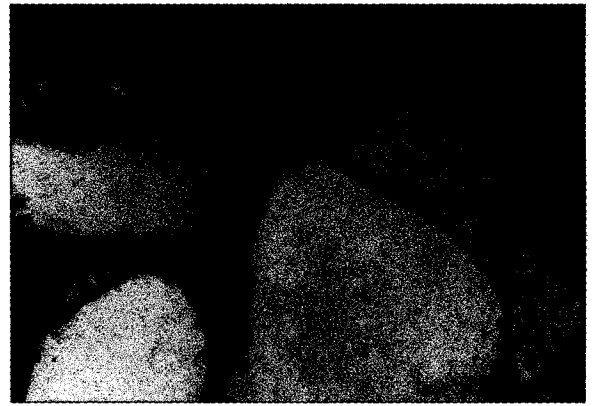
1. Poorly sorted, quartz arenite showing grains coated with kaolinitic cement and subsequent iron oxide impregnation.



2. Feldspathic sandstone showing dissolution and alteration of feldspars and subsequent calcite cementation.



3. Calcarenite showing polycrystalline (composite) quartz. The sutured boundaries between crystals clearly indicate metamorphic source.



4. Sandstone displaying pore filling silica cementation in the form of isopachous fringe around quartz grains.



5. Photomicrograph of basic dolerite sill displaying microporphyrific texture in a intergranular groundmass.



6. Photomicrograph of dyke rock exhibiting microporphyrific texture in a fine grained groundmass.

CHAPTER - VI

MINERALOGY AND GEOCHEMISTRY

6.1 GENERAL

It has been well established through the study of sedimentary rocks that distribution of mineralogical and chemical (major/minor/trace elements) composition is essentially controlled by the depositional facies (Veizer et al.,1978). In Phanerozoic rocks with abundant biota, such chemical criteria, although of supplementary importance, may be indispensable in the interpretation of diagenesis and origin. Furthermore, the knowledge of variation in mineralogy and chemical composition of particular facies is important in the reconstruction of various mineral and chemical components having varied depositional and diagenetic histories. The Middle Jurassic samples of Kachchh are composed of various mineral and chemical components which may have similarities and dissimilarities in their behaviour due to varying conditions at the time of their formation. In such cases it is most appropriate to discern the relationships and variability of these components in the rocks. In the present study the carbonate and fine clastic rocks have been subjected to detailed mineralogical and chemical study in order to understand the spatial and temporal variations for the interpretation of the depositional and diagenetic setup of the Middle Jurassic Sequence of Kachchh Mainland.

6.2. MINERALOGY

The various rock types of the Middle Jurassic succession of Kachchh Mainland subjected to mineralogical study using XRD include shale (normal marine and gypseous), limestone, golden oolitic limestones and the insoluble residues of limestones. XRD-analysis is one of the most commonly used mineralogical analysis of fine-grained sediments (carbonates and mudrocks) for both qualitative and

quantitative estimation of mineral phases. The theoretical details of XRD equipment and principles are given in Carver (1971) and Tucker (1988). The interpretation of modern X-ray diffractograms require several steps during which the nameless electronic peaks of the diffractograms are connected and interpreted in to significant geologic data.

The following are the important steps: (i) measurement of molecular plane repeat distances (d-spacings) which can be obtained or read from the conversion tables (2 θ to d-spacings) given in many books, (ii) identification of mineral species using ASTM / JCPDS powder data files, (iii) qualitative and semiquantitative and qualitative interpretation of mineral abundance and (v) measurements of average crystalline size of selected minerals.

6.2.1. Fine-grained clastic sediments

The fine grained clastics of Middle Jurassic of Kachchh Mainland are characterised by their different colours ranging from white, whitish grey greenish yellow, brown to reddish brown. The various colours are due to chemical composition of the impurities present in these sediments. The shale appear as few indurated beds but thick beds of noudular and friable sediments are abundant. The shales^a are mainly ferruginous, calcareous, carbonaceous and gypseous in compositions.

The samples from the Jumara, Jhura and Habo sections show a variable composition consisting of predominant Kaolinite, Illite, Chlorite and Montmorillonite. The Fig.6.1 shows the X-ray diffractograms of representative samples from the Middle Jurassic of Kachchh Mainland. The interlayering of chlorite with smectite in some samples indicates the degraded nature of these minerals. In others the sharp peaks indicating the absence of degradation. The distribution of clay minerals are uniform (Fig. 6.1) in the finer clastics indicating unifrom weathering in these outcropping areas.

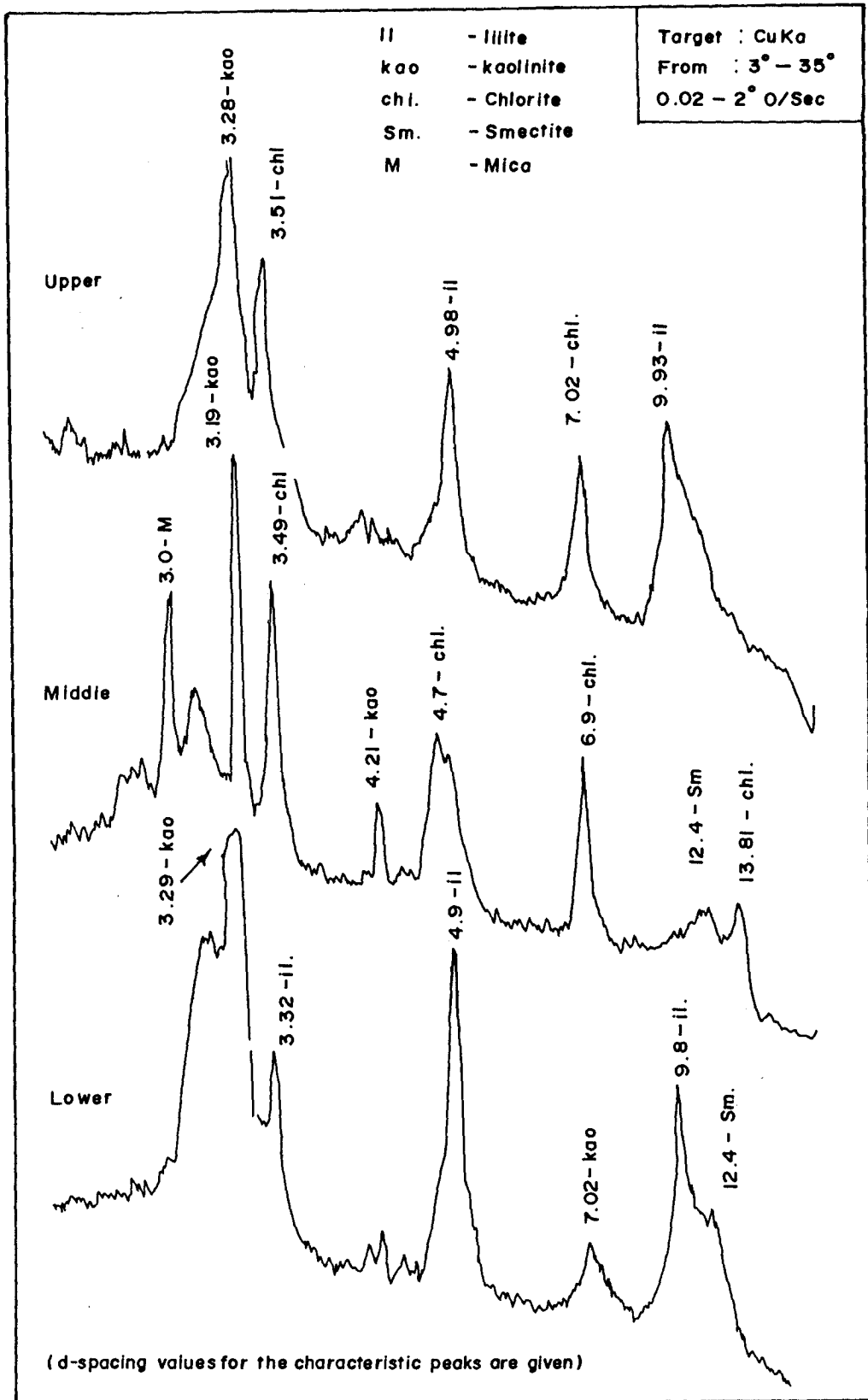


Fig.6.1 X-ray Diffractograms of representative samples from Jurassic of Kachchh Mainland

6.2.2. Limestones and insoluble residues

The carbonate rocks of Jhurio Formation (Jhura Dome), Middle Jurassic of Kachchh Mainland in bulk and their insoluble residues have been analysed systematically in the stratigraphic order to know the mineralogy of clay mineral fractions. The carbonate minerals are mainly low magnesian calcite. The insoluble residue mineralogy shows predominant quartz content in many samples, except in the fenestral laminated peloidal mudstone-wackestone microfacies (Microfacies-22). The quartz mainly occur as fine fragments and in some bioclasts the quartz mineralogy indicates a secondary origin, due to silicification of bioclasts. The distribution of clay minerals in the insoluble residue of carbonates of Jhurio Formation is given in the Fig. 6.2. The important clay minerals present in the analyzed rocks are illite, smectite, chlorite and kaolinite. Illite is dominant in most of the carbonates with almost equal percentage of smectite and chlorite. The dominance of kaolinite is seen in the upper part of the Jhurio Formation and in the Jumara Formation. The X-ray Diffractograms of representative samples (IR) of Jhurio Formation is given in the Fig. 6.3 and 6.4.

The Fig.6.3 represents the X-ray diffractograms^{of} insoluble residue of peloidal group microfacies. The Fig. 6.3a shows the X-ray Diffractograms of insoluble residue of fenestral laminate^d peloidal mudstone-wackestone microfacies (MF 22) in which the smectite (montmorillonite) predominate over other clay minerals and quartz. The microfacies-22 occurs as repeated thin-beds in bedded limestone and calcareous mudstone facies. The smectite enrichment over quartz indicates a shallow to deeper quiet marine environment of deposition for this microfacies development. The authigenic smectite rim cement as observed under the microscope is also a characteristic evidence of a deeper marine environment of this microfacies. The Fig. 6.3b represents the foraminiferal crinoidal peloidal packstone-grainstone microfacies (MF-23). In peloidal microfacies group the smectite is the most important clay mineral followed by

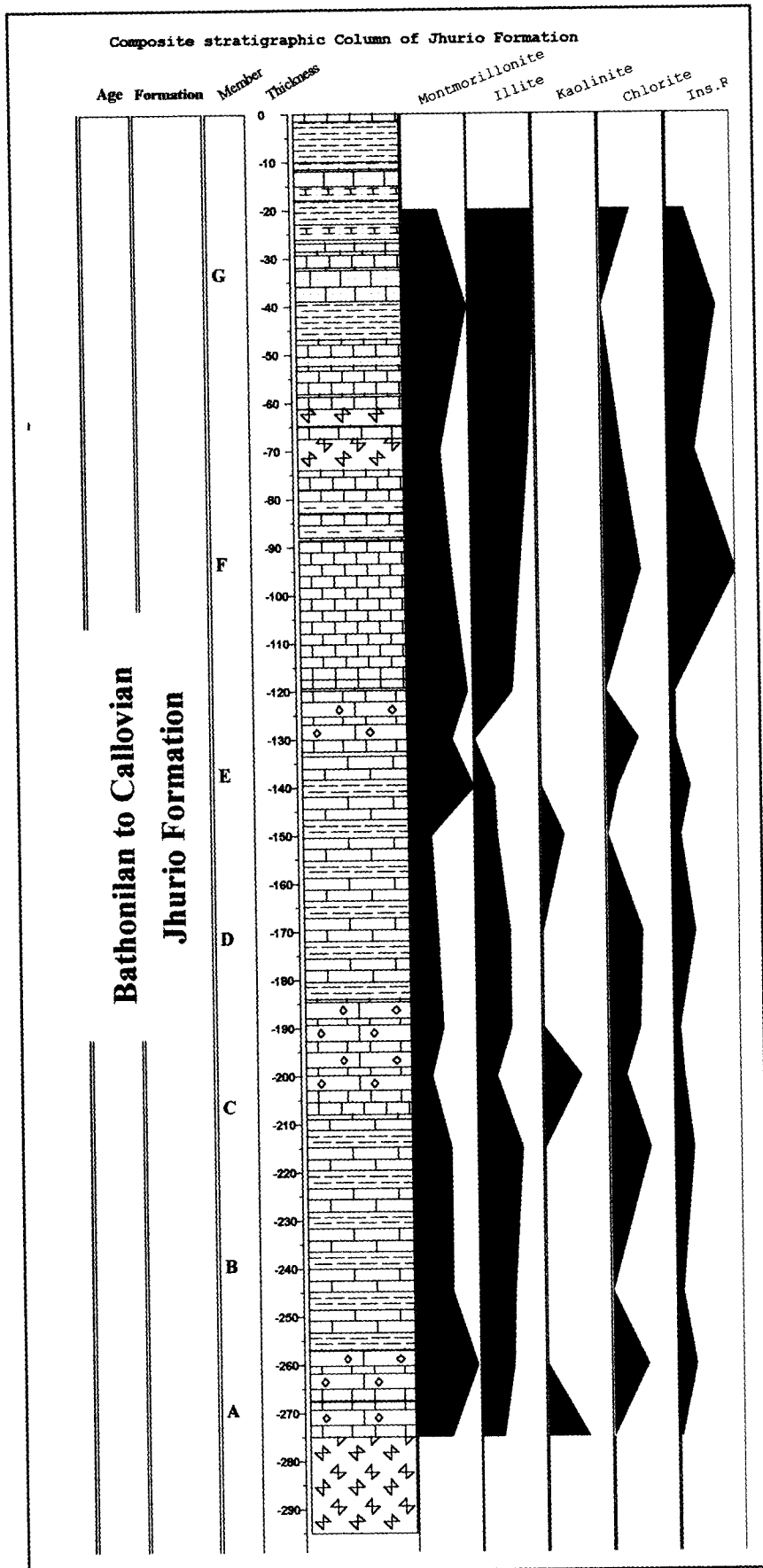


Fig. 6.2 Temporal distribution of Clay minerals of Jhurio Formation

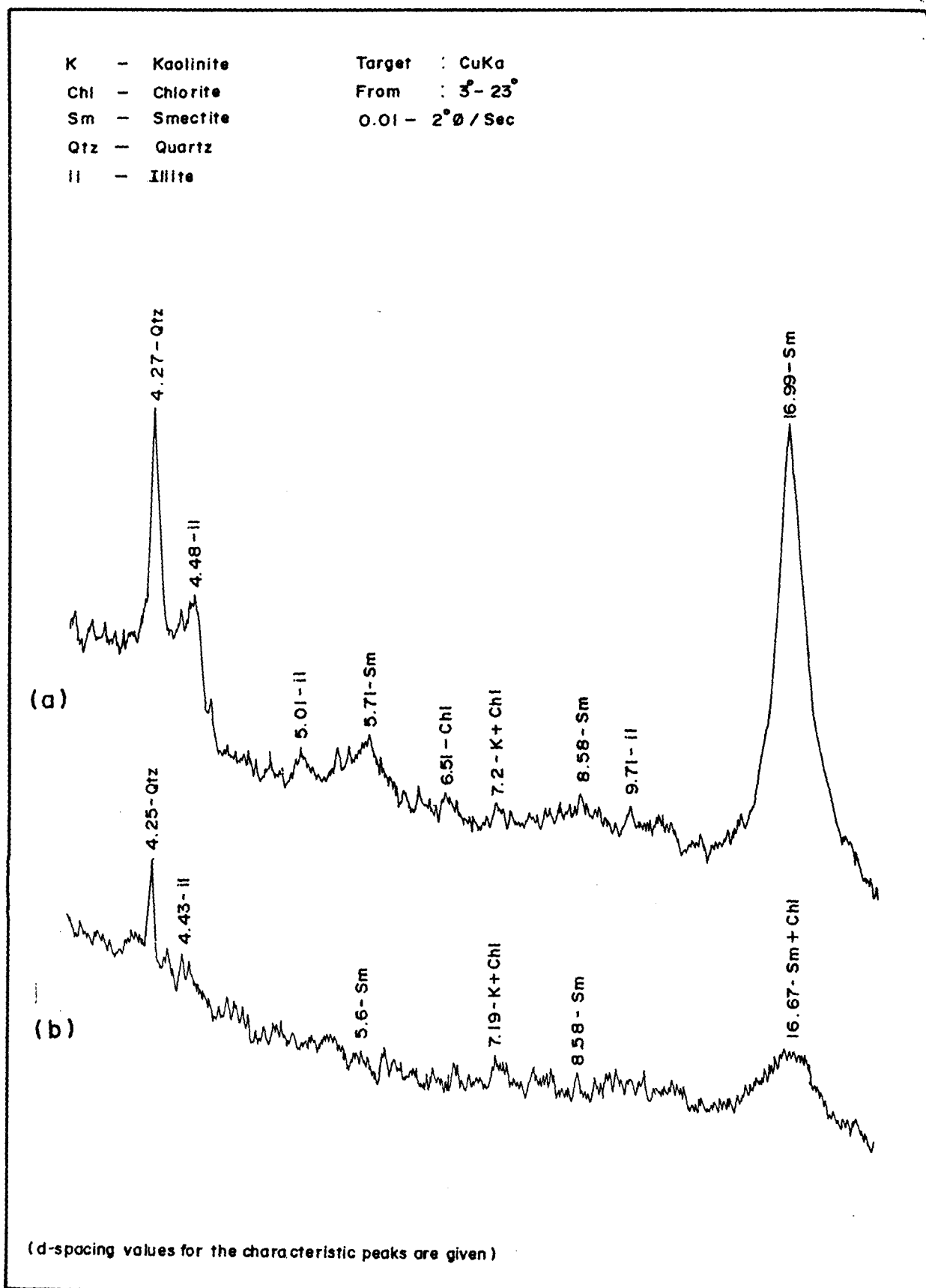


Fig. 6.3 X-ray Diffractograms of representative samples of IR of carbonate of Jhurio Formation, Kachchh Mainland

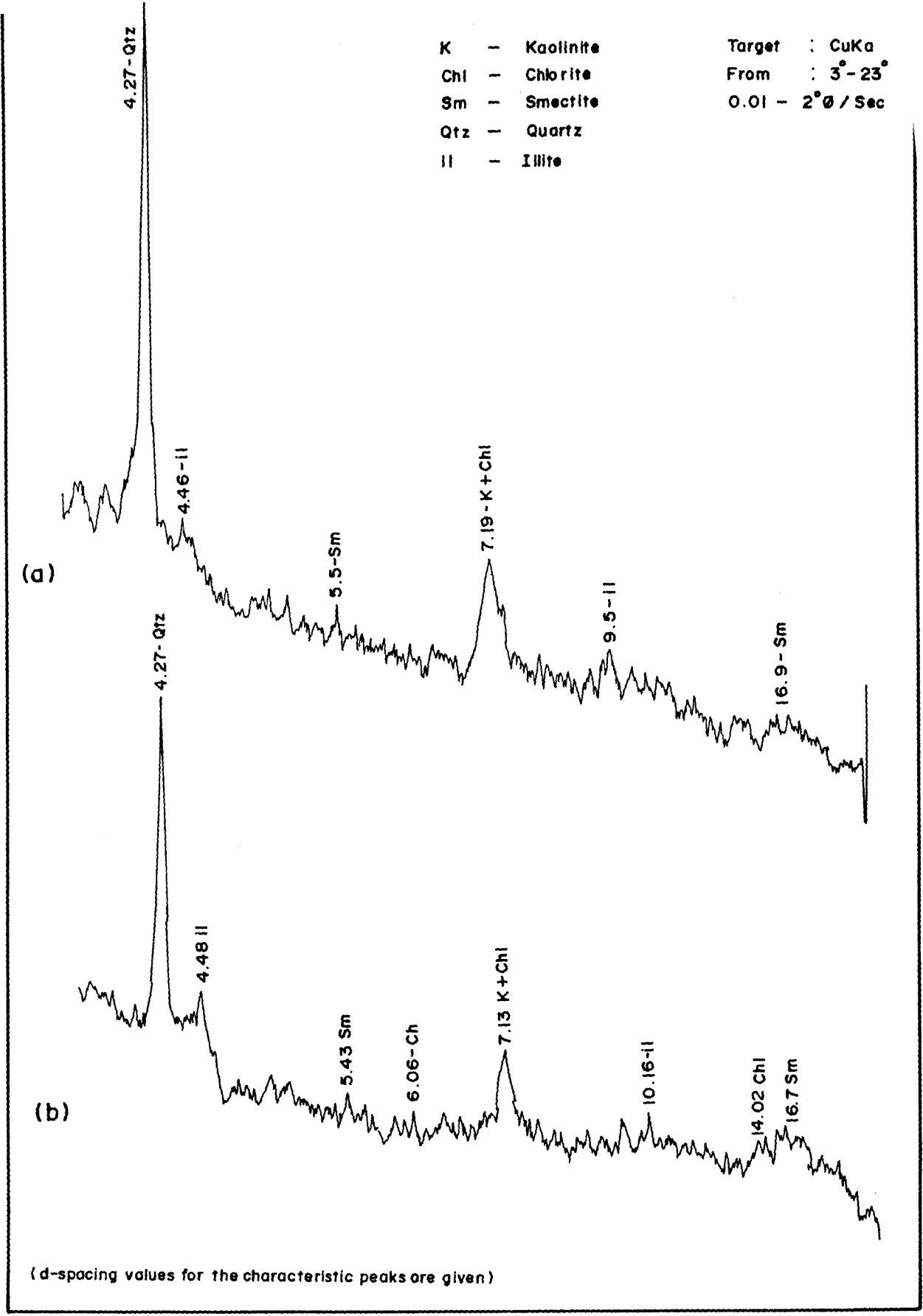


Fig.6.4 X-ray Diffractograms of representative samples of IR of carbonates of Jhurlo Formation, Kachchh Mainland

the abundance of illite. In some samples interlayering of smectite and chlorite are observed.

The Fig.6.4 represents the X-ray diffractograms of peritidal microfacies mainly bioclastic group. These microfacies indicate the abundance of quartz and Kaolinite interlayered with chlorite. The abundance of kaolinite is indication of the shallow water nearshore environment with influence of fresh water. The kaolinite associated with chlorite predominates over illite and smectite.

The main factors that control the clay mineral composition of carbonate rocks are the surface run-off and the wind. In the case of pericratonic basin both these factors are important. The supply of siliciclastics by surface run off occurs mainly to the attached platforms and basins separated from land by deeper water. The other parameters which may control the distribution of clay minerals in carbonates are climate and topography which together decide the drainage patterns. In fact, weathering and erosion prevailed in the nearby continental areas are responsible for the origin and presence of siliciclastic constituents in the carbonate facies. Kaolinite occurs nearshore environment due to the weathering in the hinterlands. Where as smectite occurs in peneplained terrain where drainage is poor and movement of pore waters is sluggish. The sediments formed in warm and humid climate are more kaolinitic in content. While Illite is observed in sediments originated during cold and drier periods. Therefore in the Middle Jurassic succession the evidence of cold and dry climate may be indicated during the deposition of lower and middle part of the Jhurio Formation. Where as the warm and dry climate may be prevailed during the deposition of upper part of the Jhurio Formation and Jumara Formation. The palaeogeography of Indian subcontinent during the initial fragmentation from the Gondwanaland and the climatic belt of that time may be indicative of the above.

6.2.3. Golden Oolitic Grainstone

The golden oolitic grainstones (MF-10 & 11) of Middle Jurassic succession of Kachchh Mainland are well exposed in the Jhura and Jumara domes. The Jhura dome exposes the oolitic grainstone facies of Jhurio Formation better than in any other locality. The ooids, ground mass and the mud intraclasts of the golden oolitic grainstones were analysed separately using the Philips X-ray Diffractometer in order to understand the mineralogy of the ooids as to whether these are oolitic ironstones as noticed in Switzerland and other parts of the world or oolitic calcareous ironstones as seen in Jurassic of England (Millot, 1988). The ooids were separated from the oolitic grainstones by soft hammering and picking up manually with the help of a hand-lens collected individual ooids. The idea of collecting the ooids (Millot, 1988) with the help of a magnet was completely unsuccessful. About 350-400 ooids were collected from different stratigraphical levels from the Jhurio Formation at Jhura dome. These ooids were washed and dried to avoid the impurities. Then, ooids were powdered and passed through 200 mesh. The collected powdered samples are put directly in X-ray diffractometer to identify the mineralogy. Apart from ooids the fine grained ground mass and the mud intraclasts were collected and powdered to 200 mesh size and the mineralogy of the same determined from the X-ray diffractogram.

From the XRD-data (Fig. 6.5 & 6.6) it is understood that the ooids, fine-grained ground mass and the mud intraclasts show the same mineralogical composition. The predominant mineral is low magnesian calcite and therefore the idea that the sideritic or chamositic oolites for this golden oolitic grainstone should be rejected. All the samples analysed (10 numbers from different stratigraphic levels) reveals the predominant peak is at 2.98 Å - 3.01 Å (relative intensity 100) and other peaks at 2.27 Å, 2.08 Å, 1.90 Å and 1.86 Å (Fig. 6.5 & 6.6). The Fig. 6.4a & b represents the x-ray

LMC - Low Mg Calcite
 Go - Goethite
 Stip - Stipnomelate
 Qtz - Quartz
 Sid - Siderite

Target : CuK α
 From : 3°-50°
 0.02 - 2°/Sec

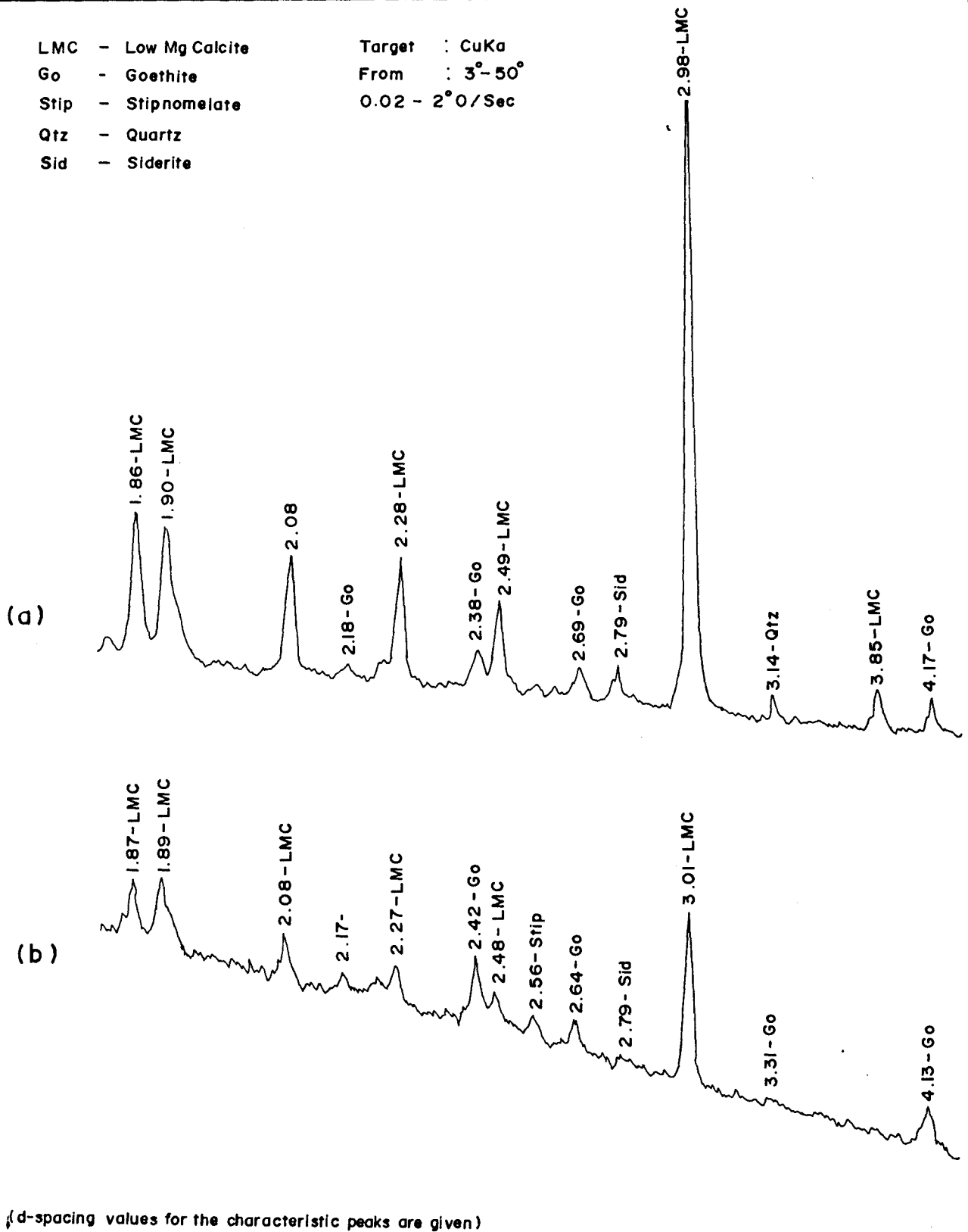
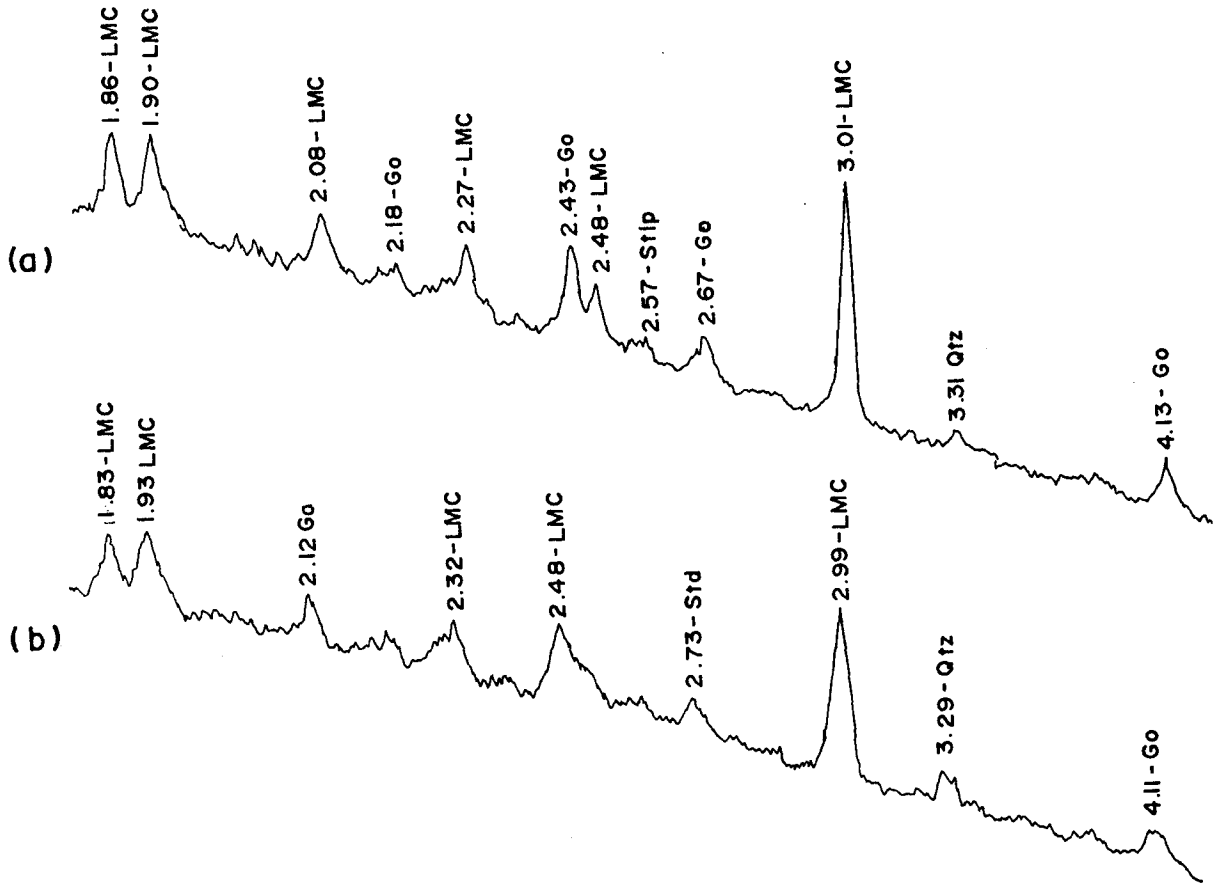


Fig. 6.5 X-ray Diffractograms of representative samples of oolitic grainstone facies of Jhurio Formation, Kachchh Mainland

LMC - Low Mg Calcite
 Go - Goethite
 Stip - Stipnomelate
 Qtz - Quartz
 Sid - Siderite

Target : CuK α
 From : 3°-50°
 0.02 - 2°/Sec



(d-spacing values for the characteristic peaks are given)

Fig. 6.6 X-ray Diffractograms of representative samples of oolitic grainstone facies of Jhurio Formation, Kachchh Mainland

diffractograms of calcareous iron ooids and Fig. 6.6a shows the X-ray diffractogram of representative sample of iron coated mud intraclast and the Fig.6.6b represents the X-ray diffractogram of representative sample of groundmass (cement material) of calcareous iron oolitic grainstones. The low magnesian mineralogy of the ooids, intraclasts and the ground mass has been well documented. Characteristic peaks are also seen at 4.13 Å, 2.67 Å, 2.43 Å and 2.18 Å. this represents the presence of goethite in the ooids and as well as in the ground mass. The presence of goethite in the ooids explain the golden yellow to golden yellowish brown coating over the ooids and over the mud intraclasts and the yellowish brown colour of the ground mass. The goethite coating over the calcareous ooids later oxidised to form the golden yellow colour to ooids and the mud intraclasts and also on the bioclasts. This oxidation process can be correlated with the regression of Tethys sea rhythmically, after the deposition of pelagic bedded limestone cyclically deposited with this oolitic grainstones, from the Kachchh Basin. The various other minerals present in minor amounts are quartz, illite, montmorillonite, chlorite and stipnomelane. From the XRD-data, along with the petrological observations, it is understood that the original mineralogy of the ooids was aragonite (also supported by the chemical data). The aragonitic ooids originated in the shallow agitated water were bound together by the aragonitic mud. These metastable aragonitic ooids later neomorphosed to low magnesian calcite and consequently the mineralogy of the ground mass also replaced to low magnesian calcite. The calcitic cement is formed due to neomorphism forming patches of coarser calcitic crystals to grade the oolitic wackestone in to oolitic grainstones. The origin of oolitic ironstones by the diagenetic replacement of originally calcareous ooids has been suggested by Sorby(1857). According to Kimberley (1979), ferruginisation occurred during a regression closely following the sedimentation of aragonitic oolite. Ferruginous

leachate, produced by the weathering of Delta topset muds, permeated the underlying oolite. Dissolution of aragonite and high magnesian calcite increased electrolyte concentrations, which aided by a related increase in pH induced the precipitation of iron minerals (Bradshaw et al., 1978). It is essential that surficial sediment containing some iron undergo weathering and erosion. To ferruginise an oolitic bed less than 1m thick, subaerial weathering and erosion of less than 30m of overlying marine mud would be sufficient.

The oolitic calcareous ironstones depict a high content iron which is reflected in their golden colour that results from the iron oxide coatings of the ooids. This morphological character of the unit has led to the nomenclature of this facies as "Golden Oolite". The Jhurio Formation dates back to Bathonian times as indicated by the ammonite faunal association of *Macrocephalites* (first occurrence) and *Sivajiceras congener* (Callomon, 1993; Khadkikar, 1996).

The source of iron observed in limestones throughout the world has been attributed conventionally to pedogenic breakdown of iron rich continental parent rocks and subsequent transportation to ocean waters through fluvial channels. However, contrasting palaeogeographic and palaeoclimatic conditions during Ordovician and Jurassic times appear to contradict the prevalent perspective on iron derivation (Khadkikar, 1996). Van Houten (1985) has observed that globally ironstones deposited during Ordovician times were formed in cold temperate climatic regimes while the younger Jurassic ironstones formed under tropical humid palaeoclimates. Also some researchers have suggested that superplume induced increased sea-floor spreading activity results in the formation of ironstones. Such ironstones mark peak global transgressions which are tectonically induced events. According to Khadkikar (1996) iron is contributed at the mid-oceanic ridges through hot spring fluids. Thus it seems

plausible that the Kachchh ironstones sequestered iron from Fe-rich ocean waters during phases of Event hydrothermal plumes. The older Bathonian Golden Oolite which extends in to the lower Callovian in Keera dome, shows greater enrichment relative to the younger Dhosa Oolite of Oxfordian age.

The occurrence of Fe oolitic limestones is not the norm in the Jurassic succession of Kachchh basin. The climate changed from tropical wet to temperate dry climate from Bathonian to Oxfordian. Thus iron may not be derived necessarily due to weathering of continental ferromagnesian rich rocks (Khadkikar, 1996). It is proposed that these horizons represent distinct short-lived episodes of magmatic activity at the mid-oceanic ridges. The golden oolites represent the first stage of actual rifting, resulting in the genesis of mid-oceanic ridge system between Greater India and Africa.

6.3. GEOCHEMISTRY

The distribution of major, minor and trace elements in sedimentary rocks are essentially controlled by the depositional facies (Veizer and Demovic, 1974), therefore, the knowledge of variation in the chemical composition of any succession of facies in time and space is important in order to reconstruct the depositional and diagenetic history. Carbonate sediments and rocks consist of two groups of elements: a) elements bound to a carbonate phase (Ca, Mg, Sr, Mn, sometimes Ba, etc.) and b) elements occurring in minerals of acid insoluble residues (e.g. Si, Al, Fe, B) (Flügel, 1982). The papers of Degens (1968), Ernst (1970), Ingerson (1961), Krejci-Graf (1964, 1966), and Starke (1968), describes that the "chemofacies" is valuable as an indicator of the formation and diagenesis of the sediments. Trace elements occurring in concentrations between 10^{-1} and 10^{-3} wt.% or less are either bound to the carbonate phase (and are then very dependent on the kind of mineralisation and the change during diagenesis) or to the non-carbonate phases (dependent on the process of

deposition on the grain size and mineralogy as well as the organic substances). According to Wedepohl (1970), the majority of the trace elements known in carbonate rocks are bound to the detrital silicate-oxidic fraction of the limestones. Mg, Sr, and Mn are linked in a specific way with the carbonate phase, depending on the similarity of the crystal chemistries of main components of more abundant carbonate minerals (Sr and Ca, Mg and Ca, Mn and Mg) and on the relatively high concentrations in ocean and pore waters. It is understandable that a major portion of the facies analyses are based on trace elements (see surveys in Friedman, 1969; Veizer, 1983). Up to now very few studies have been done on the correlation between limestone types (MF types) and geochemical parameters (e.g. Chester, 1965; Cerny, 1978) and many conjectured "correlations are not statistically correlated" (Flügel, 1982). Trace element distribution in carbonates can be used to differentiate reef from non-reef sediments, shallow-water from deep water limestones, and to know the sedimentation, diagenesis and palaeoecology (Flügel, 1982).

6.3.1. Analytical Methodology

The samples of Middle Jurassic succession have been analysed wholly or selectively for selected major, minor and trace elements to know their relative abundances and the distribution. Standard procedures of chemical analysis of rock samples have been followed for the determination of trace and rare element composition. Ca and Mg contents have been determined by EDTA titration method. The samples have been analysed for the trace and minor elements using AAS, XRF and ICP-AES at the laboratories of RSIC, IIT, Bombay; KDMIPE, ONGC, Dehradun and NIO, Goa. The selected rock samples were also analysed for Rare Earth Elements (REE) using ICP-MS at the National Geophysical Research Institute, Hyderabad following the procedures outlined in Balaram et al., (1996).

6.3.2. Results and Discussion

6.3.2.1. Jhurio Formation (Jhura Dome), Kachchh Mainland

The temporal distribution of major and trace elements in the carbonate rocks of Middle Jurassic succession of Kachchh Mainland (Jhurio Formation in its type section) suggest a shallow marine environment with fluctuating salinity due to the shifting of environment from shallow marine through slope to basinal facies and then shallow shelf to intertidal-supratidal environment. Each type of depositional environment has preserved a particular type of sedimentary unit. Thus each sedimentary unit has a peculiar type of chemical assemblages. Thus studying the temporal and spacial distribution of elements can differentiate the relationship between the microfacies units and the chemical composition particular to each type. This is extremely important in order to reconstruct the diagenetic sequence of this shallow water mixed carbonate-siliciclastic rocks.

The major elements analysed are Si, Al, Fe, Ca, Mg, Na, K, Ti, P and S. The trace elements include V, Cr, Co, Ni, Ga, Rb, Sr, Ba, and Zn. The Ca, and insoluble residue (IR) have been calculated by the titration method (EDTA), where as the other elements are analysed by XRF (ONGC, Dehra Dun).

The temporal distribution of elements in the Jhurio Formation in its type section at Jhura dome (Tables - 6.1 and Table - 6.3) shows the temporal (Member-wise) distribution of elements in Jhurio Formation. In the Jhurio Formation (Jhura Dome), Kachchh Mainland the distribution of Ca is high in the lower and middle and the percentage decreases towards the top. The reverse is the distribution of Si. The upper part of the Jhurio Formation is influenced by the high terrigenous input leading to a sandy limestone to calcareous sandstone and shale including gypsaceous shale facies. The high Si content and low Ca content supports this. The content of Ga also indicates

6.1. Temporal distribution of elements in the Jhurio Formation (Jhura Dome), Middle Jurassic, Kachchh Mainland.

e No.	Major element concentration in ppm											Trace element concentration in ppm									
	Si	Al	Fe	Ca	Mg	Na	K	Mn	Ti	P	S	V	Cr	Co	Ni	Ga	Rb	Sr	Ba	Zn	
1	57916	34665	16087	474339	45476	2745	4234	542	60	3012	1400	0	0	9	2	9	88	126	176	201	
2	334595	23445	0	114296	21713	1929	8551	77	659	349	500	164	0	7	19	11	98	310	281	187	
3	338849	31490	0	86347	25090	2077	11871	310	3357	349	600	72	54	7	24	13	95	332	462	198	
4	354929	14025	0	115797	13329	1409	166	155	659	306	400	109	20	8	19	9	90	153	112	178	
5	268359	128447	61062	8292	9530	3783	9381	232	9952	87	3400	0	78	28	35	20	118	32	501	371	
6	247558	43080	13429	177055	42762	2522	6475	775	3477	1091	700	0	79	13	56	13	97	242	317	288	
7	233675	35406	31685	192924	39867	2745	7056	697	3058	1222	900	95	51	22	28	13	77	128	329	126	
8	0	29373	13569	173481	25814	2819	830	232	60	960	1900	0	0	7	0	8	76	588	64	55	
9	0	27362	7064	614868	18516	3635	830	465	0	2750	4000	189	0	6	0	10	74	386	92	79	
10	24073	30378	11191	556969	33293	2893	1577	310	240	873	2000	0	0	7	0	9	66	394	46	54	
11	109382	38105	9512	374053	66883	3116	5977	310	659	873	2000	171	0	8	0	13	72	972	78	26	
12	0	31490	4476	624089	18577	2967	498	232	0	873	2800	189	0	6	0	9	71	434	69	40	
13	0	26991	8044	615654	22678	2893	498	310	0	786	1900	0	0	6	0	8	72	430	57	32	
14	0	28579	5316	610436	25935	2967	249	465	0	1353	3500	0	0	6	0	9	66	440	43	43	
15	13509	31543	124572	454253	27986	3561	2407	1007	360	3797	3100	173	0	30	0	10	59	81	135	15	
16	49783	29108	4826	524375	34318	3116	2490	232	180	829	1600	185	0	6	0	9	73	403	67	86	
17	84140	25033	47702	450322	20869	2819	0	310	240	1091	3100	0	0	17	0	8	65	258	86	92	
18	0	23816	3847	639242	10374	2819	0	155	60	655	2200	89	0	5	0	8	77	256	31	141	
19	80312	18358	45284	481523	23617	3185	0	255	60	655	2200	0	0	9	5	9	75	267	182	167	
20	748	29426	19235	597784	20808	3783	1743	310	60	1048	4500	187	0	8	3	9	78	479	74	52	
21	95078	21223	17136	455039	32630	3116	1826	465	180	1004	1600	182	0	9	4	9	79	431	246	195	
Mean	109186	33397	21145	397197	27622	2900	3174.3	373.6	1111	1141	2110	86	13	10.7	9.29	10.3	79	340	164	125	
SD	128730	22735	29061	212477	13259	583.96	3596	226	2318	928	1177	83.3	27	7.32	15.3	2.83	14	205	140	93.9	
Min	0	14025	0	8291.64	9529.6	1409.5	0	77.48	0	87.3	400	0	0	5	0	8	59	32	31	15	
Max	354929	128447	124572	639242	66888	3783.4	11871	1007	9952	3797	4500	189	79	30	56	20	118	972	501	371	

the same (more than 10 ppm; normal marine 4 - 8 ppm). The other evidences are the increase in the Cr, Ni, Rb, Ba, K, Ti, Al, and Zn and decrease in S and P. Where as the variations in the Fe, Na, Mn, Mg, and Sr are primarily due to the diagenetic processes. The Sr and Na are decreased during diagenesis, while Mn, Fe and Zn are increased. The correlation matrix of these elements is given in the Table-6.2. Fig 6.7 and 6.8 shows the temporal distribution (Member-wise) of elements and Fig. 6.9 show the temporal variation of selected elements in the Jhurio Formation.

6.3.2.1.1. Ca, Mg, Si and Al

The recent research works on understanding the relationship between Ca, Mg and insoluble residue (IR) indicate a direct relationship between Mg and insoluble residue (IR) contents and inverse relationship of Ca with Mg and IR. The positive correlation of Mg with Si (Table 6.2) is attributed to the selective leaching effect of Ca by the primary solution resulting in environment of Mg and IR (Chilingar et al., 1956). The significant positive correlation of Si with Mg further suggest that Si acts as a barrier (or membrane) preferentially concentrating Mg from the entrapped interstitial solutions which are squeezed out during syndiagenetic and late diagenetic stages of diagenesis. The negative correlation of Ca and Mg confirms the above concept. The Ca varies between 16.70 to 53.16%, where as Mg varies between 0.048 to 6.6% in carbonate sediments (Ca ranges from 0.83 - 12 % and Mg ranges from 0.95 - 26.0 % in the mixed siliciclastics), which indicate the broad mineralogy of these shallow marine to nearshore deposits. The insoluble residue content varies from 1 to 25% for the carbonate rocks (30 - 50% for the mixed siliciclastic rocks). The main factors that influence the Mg content are mineralogy, water and the biota and other factors such as salinity, water depth and size of individual organisms are secondary (Tucker and Wright, 1990). The prime factor which controls the amount of Mg in the present

Table - 6.2. Correlation matrix of the elements of Jhurio Formation (Jhura Dome), Kachchh Mainland.

	Si	Al	Fe	Ca	Mg	Na	K	Mn	Ti	P	S	V	Cr	Co	Ni	Ga	Rb	Sr	Ba	Zn	
Si	1																				
Al	0.252	1																			
Fe	-0.106	0.317	1																		
Ca	-0.871	-0.420	-0.066	1																	
Mg	-0.023	-0.11	-0.066	-0.019	1																
Na	-0.635	0.397	0.474	0.469	0.010	1															
K	0.724	0.507	0.009	-0.723	0.261	-0.198	1														
Mn	-0.111	0.017	0.577	0.041	0.392	0.271	0.096	1													
Ti	0.575	0.906	0.247	-0.666	-0.138	0.115	0.692	0.052	1												
P	-0.447	-0.16	0.495	0.365	0.237	0.376	-0.209	0.742	-0.313	1											
S	-0.649	0.237	0.346	0.556	-0.302	0.824	-0.414	0.066	-0.048	0.320	1										
V	-0.043	-0.25	-0.038	0.181	0.052	0.148	0.004	0.005	-0.268	0.164	0.120	1									
Cr	0.679	0.637	0.095	-0.705	-0.002	-0.137	0.699	0.241	0.873	-0.283	-0.297	-0.3	1								
Co	0.226	0.580	0.869	-0.381	-0.029	0.324	0.319	0.567	0.597	0.300	0.163	-0.09	0.473	1							
Ni	0.777	0.458	0.004	-0.745	0.032	-0.316	0.673	0.219	0.731	-0.306	-0.452	-0.23	0.928	0.366	1						
Ga	0.593	0.858	0.230	-0.656	0.090	0.147	0.796	0.114	0.937	-0.227	-0.056	-0.08	0.809	0.567	0.697	1					
Rb	0.749	0.616	-0.160	-0.739	-0.182	-0.265	0.695	-0.236	0.763	-0.427	-0.352	-0.17	0.717	0.161	0.753	0.711	1				
Sr	-0.345	-0.27	-0.450	0.273	0.468	0.119	-0.146	-0.298	-0.408	-0.196	0.119	0.264	-0.424	-0.57	-0.42	-0.22	-0.361	1			
Ba	0.762	0.580	0.175	-0.761	-0.020	-0.138	0.855	0.154	0.817	-0.234	-0.355	-0.140	0.823	0.477	0.783	0.806	0.787	-0.453	1		
Zn	0.688	0.563	0.003	-0.646	-0.160	-0.212	0.566	-0.055	0.738	-0.323	-0.363	-0.3	0.735	0.281	0.769	0.640	0.896	-0.546	0.8037	1	

Table - 6.3. Elemental distribution of Jhurio Formation in its type section at Jhura Dome, Kachchh Mainland.

Member	Elemental distribution in ppm																			
	Si	Al	Fe	Ca	Mg	Na	K	Mn	Ti	P	S	V	Cr	Co	Ni	Ga	Rb	Sr	Ba	Zn
G	262300	44400	17500	167000	28300	2490	6820	380	3030	920	1130	62.9	40.3	13	26.1	12.6	94.7	189	311.14	221.3
F	21900	30300	21000	505400	49000	3118	1710	400	170	1460	2530	101	0	9.1	0	9.4	69.9	458.7	72.33	47.8
E	84100	25000	47700	450300	20900	2820	0	310	248	1090	3100	0	0	17	0	8	65	258	86	92
D	0	23800	3847	639200	10400	2820	0	160	60	660	2200	89	0	5	0	8	77	256	31	141
C	80300	18400	45300	481500	23600	3190	1610	342	130	850	1800	0	0	9	5	9	75	267	182	167.2
B	748	29400	19200	597800	20800	3780	1740	310	60	1000	4500	187	0	8	3	9	78	479	74	52
A	95100	21200	17100	455800	32600	3120	1830	478	180	1000	1600	182	0	9	4	9	79	431	246	195
Mean	77778	27500	24521	471000	26514	3048	1959	340	554	997.1	2409	89	5.8	10	5.4	9.3	77	334	143.2	131
Std.Dev.	90830	8559	16029	152063	12098	404.4	2293	98.7	1094	246.4	1123	76	15	3.9	9.4	1.5	9.3	118	104.8	68.7
Min.	0	18400	43853	167000	10400	2490	0	160	60	660	1130	0	0	5	0	8	65	189	31	47.8
Max.	262300	44400	3847	639200	49000	3780	6820	478	3030	1460	4500	187	40	17	26	13	95	479	311.1	221

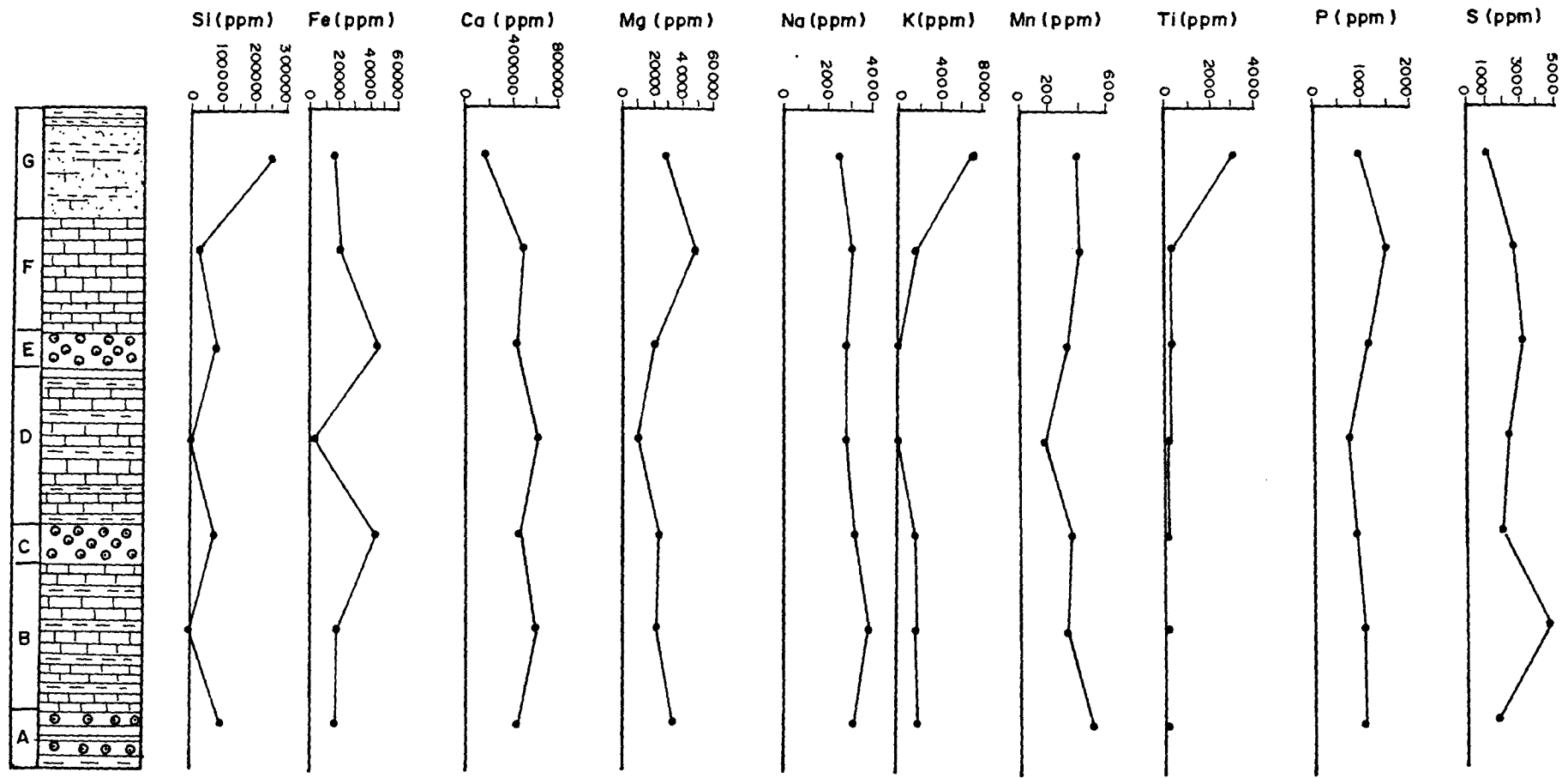


Fig. 6.7 Temporal distribution of elements in Jhurio Formation, Kachchh Mainland A- G : Members

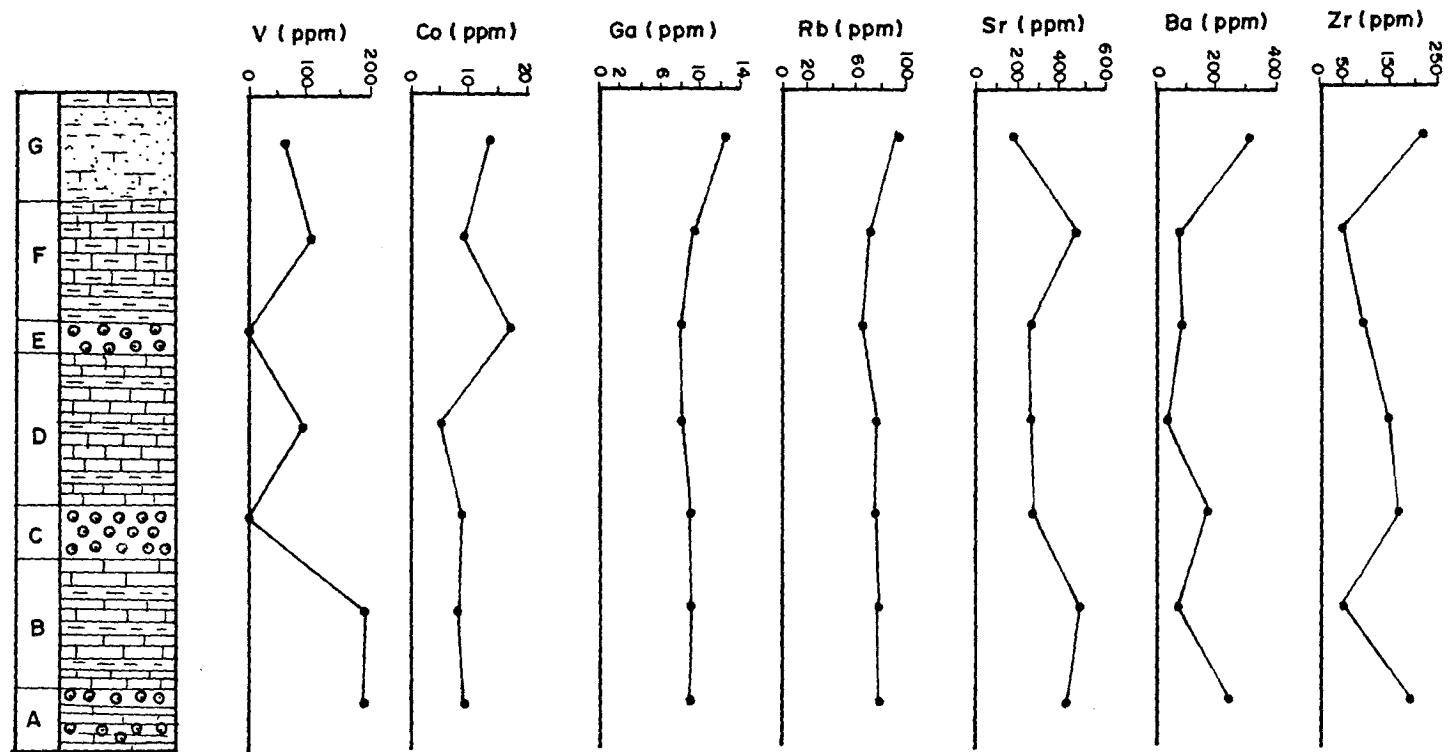


Fig.6.8 Temporal distribution of trace elements in Jhurio Formation, Kachchh Mainland
A-G : Members

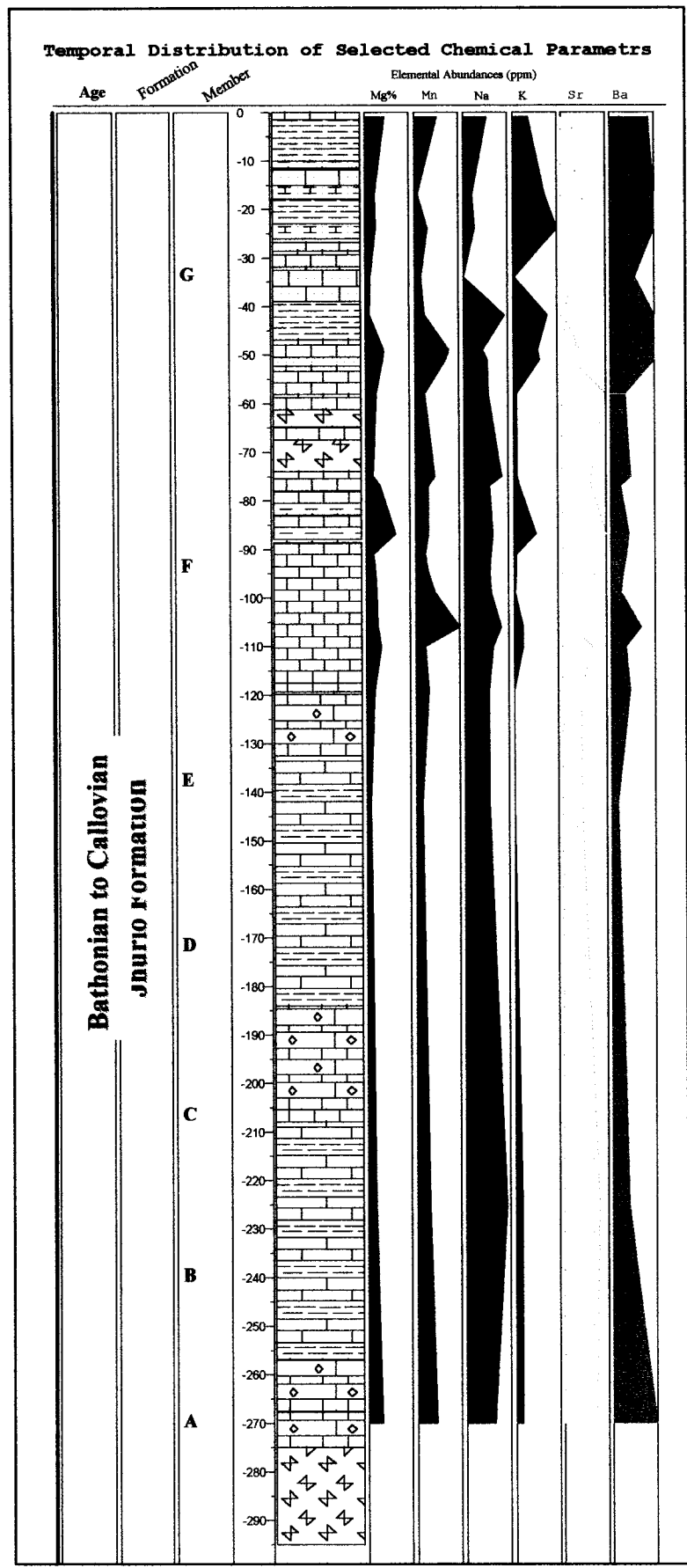


Fig. 6.9 Temporal variation of selected elements of Jhura Formation

samples is the shell mineralogy of organisms and their susceptibility to diagenetic modifications.

The quartz and clay minerals constitute the bulk of the IR in the carbonates of Jhurio Formation. The memberwise distribution (Table- 6.3, Fig. 6.7 & 6.8) shows that the Si content is maximum in the Member-G which is characterised by the mixed carbonate-siliciclastic-evaporite sedimentary facies. The average composition of Si in this is 262300 ppm (26.23%). Where as in the other lower members the Si content is less than 10000 ppm (10%). While Ca shows a strong reverse trend, that is the Member-G contains average Ca content 167000 ppm (16.7%) and the other lower members shows Ca content ranges from 450000 -640000 ppm (45-64%). This is characteristic evidence of facies migration towards the intertidal-supratidal area from an active shallow marine carbonate environment.

6.3.2.1.2. Fe and Mn

The first order control for the abundant Fe in limestones of all ages is provided by the iron oxide coatings of clays and various carbonate particles. The substitution of Fe for Ca and Mg play a secondary role with dolostones showing higher concentration of Fe than in limestones (Veizer, 1983). The carbonate rocks of Jhurio Formation has many iron coated grains including the ooids, bioclasts peloids and terrigenous grains. The ironstones of this formation contains much iron as coating of the calcareous ooids. The calcite and dolomite can accommodate appreciable ferrous ions in their structures; the ability of dolomite to do so is enhanced by more ready of Fe for Mg than Ca (Veizer, 1978). The Fe content ranges from 3847-124572 ppm (0.38 -12.46 %) in the carbonates (0 - 6.2 % for the mixed carbonate-siliciclastic-evaporite sediments). The mean is 21145 ppm (2.11%) and standard deviation is 29061 for the entire rock samples of Jhurio Formation (Jhura Dome). The memberwise distribution of elements (Table

6.3) shows that the Fe content is found to be maximum, in the Member-C and E which are dominated by the oolitic packstone-grainstone microfacies types. The average Fe content is 45300 ppm in the Member C and 47700 ppm in the Member-E. The high content of iron is due to the iron oxide coating over the grains such as calcareous ooids, peloids, bioclasts and intraclasts and also almost all the material available in the site of deposition. Where as in the peloidal mudstone-packstone-grainstone microfacies types the amount of Fe is below 20000 ppm. Also in the bioclastic-lithoclastic microfacies groups and in the mixed carbonate-siliciclastic-evaporite microfacies group, the Fe content is less than 22000 ppm. In the Fe shows low negative correlation with Si (-0.106) and positive correlation with Al (0.252) and significant negative correlation of Fe with Sr (-0.4635) indicates the increased content of Fe due to diagenesis, where the Sr was depleted during the diagenetic processes. The Mn content ranges from 155 - 1007 ppm (0.016-0.101%) for the carbonates (77 - 232ppm for the mixed carbonate-siliciclastic-evaporite rocks). The mean is 374 ppm and standard deviation is 226 (0.0374 % and standard deviation is 0.0226 %). The memberwise distribution of Mn shows (Table 6.3) that moderate content ranges from 160-478 ppm. The comparatively high amount of Mn is observed in the lag deposit (lithoclastic bioclastic rudstones) which might have been deposited as hard grounds. The Fe is positively correlated with Mn (0.577). Where as the Mn is negatively correlated with Sr (-0.296). This indicates that the Mn has increased during the post depositional changes, while the Sr has depleted. Thus Fe and Mn increased during the diagenetic alterations. Mn is mainly associated with carbonate fraction, while Fe associated with clay. This observation has also been made by many researchers regarding the Mesozoic rocks (see Bencini and Turi, 1974; Turi, et al., 1981). The low Mn content in the carbonates of Jhurio Formation is due to the presence of aragonite and low Mg calcite in the original

sediments. The evidence of original aragonitic mineralogy of the carbonate rocks has been observed by the petrographic study. The low Mn content (up to 1200 ppm.) also indicates a general shallow marine facies (Tucker and Wright, 1990) for the sediments of the Jhurio Formation.

6.3.2.1.3. Na and K

The alkali elements of limestones usually related to the non-carbonate fraction. Where as in the Jhurio Formation reverse trend is observed in Na content. The Na content ranges from 2522 to 3783 ppm (0.25% - 0.38%). The mean is 3032.3 ppm and the standard deviation is 349.92. Where as the K content ranges from 0 - 7056 ppm. The mean is 2293 ppm and standard deviation is 2366.7 ppm. The memberwise distribution shows (Table 6.3; Fig. 6.7 & 6.8) that Na is less abundant in the upper Member-G compared to the lower members. The K shows the characteristic abundance in the Member-G, while the K content is much less in the lower members.

The Na is negatively correlated with K (-0.196). Na also shows the negative correlation with Si (-0.635), Ni (-0.316), Rb (-0.265), etc. Where as positive correlation is observed with Ca (0.469), Fe (0.474), S (0.824), P (0.376) and low positive correlation with Sr (0.1636). Where as the K is positively correlated with Si (0.724), Al (0.507), Mn (0.5225), Ti (0.692), Cr (0.699), Co (0.3778), Ni (0.673), Ga (0.796), Rb (0.695), Ba (0.855) and Zn (0.566). Negative correlation is shown with Ca (-0.723), S (-0.414) and low negative correlation with Sr (-0.146). The significant positive correlation of Na with Ca and negative correlation with Si indicates a marine source of incorporation of Na in the carbonates of Jhurio Formation. Where as the presence of K is due to the terrigenous supply from the land. This is well documented by the low K content in the carbonate fraction and high content in the siliciclastic sediments. The main sources of potassium are the feldspars and clay minerals. Also K

is incorporated with coarse grained limestone fraction such as lithoclastic bioclastic rudstones (Microfacies 30). Where as both Na and K content is maximum in gypseous shale (Gypseous mudstone microfacies) which indicates the incorporation of both elements in the finer fraction (Table - 4.1). The high Na content is due to the hypersalinity of the depositional medium and evaporites are precipitated due to the intense evaporation. The negative correlation of Na with Mg (-0.2288) indicates that the Na is enriched with the dolomitisation process in some of the limestones (Table 6.2).

6.3.2.1.3. Strontium

Strontium as one of the most important minor elements in sedimentary carbonate rocks has been a subject of studies for a considerable period of time (Veizer and Demovic, 1974). The distribution of Sr content in the Mesozoic carbonate rocks can be used as a tool for facies analysis (Veizer and Demovic, 1974) and some geochemists has used it as a tool for the identification of sedimentary carbonate oil-basins. The different aspects of the subject of strontium distribution in carbonate rocks was reviewed by Graf (1960), Lowenstam (1961), Turekian (1964), Wolf et al., (1967), Flugel and Wedepohl (1967), Dodd (1967), Muller and Friedman (1968), Schroeder (1969), Wedepohl (1969), Kinsman (1969), Bathurst (1971), Katz (1972) and Veizer and Demovic (1974), Morrow and Mayers (1978) and Brand and Veizer (1983).

The Sr content in carbonates of Jhurio Formation (Table 6.1) shows the range of 81 - 972 ppm. The mean Sr content is 378 ppm. and the standard deviation is 213.32. The ancient limestones usually contain far less strontium than their modern analogues. Many limestones contain as little as a few hundred or even a few tens of parts per million strontium (Kinsman, 1969; Veizer and Demovic, 1974). The distribution and concentration of Sr in carbonate rocks is of interest because of the large differences between the strontium contents of modern carbonate sediments and their

ancient limestone analogues. Mineralogy is the primary factor controlling the strontium content of modern sediments. Most aragonite, skeletal or non-skeletal contains 8000 - 10,000 ppm strontium with the exception of molluscan aragonite, which contains 1000 - 4000 ppm. Generally high magnesium calcite ranges from 1000 - 3000 ppm strontium and most low-magnesian calcite from 1000 to 2000 ppm. Consequently the strontium content of majority of shallow water, predominantly aragonitic sediments is above 5000 ppm.

The low strontium content of ancient limestones can not be due to variations in the $m(\text{Sr})/m(\text{Ca})$ ratio of ancient sea waters from which these limestones were precipitated, for the $m(\text{Sr})/m(\text{Ca})$ ratio of sea water has remained remarkably constant through out the Phenerozoic Eon (Lowenstam, 1961). Instead, strontium is lost during the diagenesis so that ancient limestones have low strontium contents. In the carbonate samples of Jhurio Formation (Jhura Dome) the Sr ranges from 81 - 972 ppm. This variation has been attributed to, a number of factors: (1) primary mineralogical differences between facies, (2) facies-controlled porosity variations and (3) variations in the clay content (Morrow and Mayers (1978). The Sr concentration of sea water is more than that of fresh water and therefore, it reflects the nature of depositional basin water characteristics. (Veizer and Demovic, 1974)

There appears a positive correlation between calcite and Sr contents of the samples of Jhurio Formation from which the Sr concentration of calcite is deduced to 81 - 972 ppm which is in good agreement with $(1-2) \times 10^4$ ppm, as reported in literature (Turekian and Kulp, 1956; Milliman, 1974). According to Kinsman (1969) the calcite precipitated in equilibrium with sea water contains approximately 1375 ppm of Sr. During the conversion aragonite to calcite and calcite to dolomite through dissolution-reprecipitation and replacement processes respectively, Sr is lost. Also

Kinsman (1969) suggested that the value of Sr in calcite as a result of the passage of a large volume of fluid through the sediments. He found that the average Sr concentration in calcite to be 418 ppm. thereby indicating the process of diagenesis in an open system and in less saline environment. Thus it is interpreted that initially there was some finite amount of aragonite which is converted into calcite and subsequent dolomitisation, leading to decrease in the sodium contents.

6.3.2.2. Chemical Characteristics of Microfacies

The broad microfacies group of Jhurio Formation (Type section) include, the oolitic, peloidal, bioclastic, lithoclastic and mixed siliciclastic-carbonate-evaporite microfacies groups. The microfacies distribution and variation of Jhurio Formation in time and space can be not only be identified by the petrographic studies but also be documented by the geochemical distribution of elements. Thus each microfacies unit is characterized by a particular assemblage of elements. For the carbonate microfacies, the variation in water depth is the single most significant collective control on a wide range of environmental factors including hydrodynamic energy, water turbulence, light penetration, siliciclastic contamination and nutrient supply (Spence and Tucker, 1999).

The microfacies groups can be considered in a broad facies belt, according to which there can be three possible facies types in the Jhurio Formation (Jhura Dome)(see Chapter-VII). The first one is the subtidal facies that comprises the peloidal limestones with varying types of mudstone-wackestone types. The second is the peritidal facies which includes the oolitic packstone-grainstone and other bioclastic and lithoclastic microfacies facies types. The third one is represented by the intertidal-supratidal facies characterised by the mixed carbonate-siliciclastic-evaporite microfacies types.

The Factor analysis of all data shows five factors (Table 6.4) that account for most of the variation in the elemental distribution. Factor 1, shows positive relation with Si, Al, K, Ti, Cr, Co, Ni, Ga, Rb, Ba and Zn. This indicates the non-carbonate fraction. This Factor thus accounts for the provenance of non-carbonate fraction. It also controls most of the variance. Negative relation is seen with Ca, Sr and Na. The Factor 2 and 3 have related significance, which are diagenetic equilibration and dolomitisation respectively. Factor-² shows positive relation to Fe and Mn, which are strong and negative relation to Sr. This indicates the increase of Fe and Mn and decrease of Sr during the diagenetic stabilisation with fresh water. The Factor-4 shows the positive relation with Na, Al and S and negative relation with Si. Also reverse relationship shown between Ca and Mg. Factor 4 shows positive relation with Mg and Sr and Factor-5 shows strong positive relation with V.

6.3.2.2.1. Carbonate Microfacies

The carbonate microfacies is characterized by the subtidal facies (peloidal microfacies group, MF-20, 21, 22 & 23) and the peritidal facies (oolitic microfacies group, MF-10 & 11; bioclastic microfacies group, MF-40 & 41 and the lithoclastic microfacies group, MF-30).

6.3.2.2.1.1. Subtidal Facies (Peloidal Microfacies Group).

The peloidal group is characterised by the crinoidal-peloidal, algal-foraminiferal-peloidal and peloidal mudstone-wackestone and grainstone types (MF-20, 21, 22, & 23). The main biota thus includes crinoid oscicles, protoglobigerinids and other planktonic types.

The insoluble residue (IR) of peloidal microfacies group ranges from 2 to 12%. The main content of IR are quartz and clay minerals. The Ca content ranges from 35 to 65%. The high content of Ca is mainly contributed by the carbonate micritic mud in

Table - 6.4. Factor analysis of elements of Jhurio Formation.

Rotated Varimax Component Matrix						
	Factors					Communalities
	1	2	3	4	5	
Si	<u>0.7580</u>	-0.0922	<u>-0.5710</u>	-0.1194	0.1258	0.9391
Al	<u>0.7737</u>	0.0519	<u>0.5417</u>	-0.0864	-0.1734	0.9322
Fe	0.1143	<u>0.8097</u>	0.3233	-0.2178	0.0250	0.8212
Ca	<u>-0.8015</u>	0.0046	0.4022	0.0429	-0.0081	0.8061
Mg	0.0159	0.1875	-0.1425	<u>0.9326</u>	-0.0044	0.9254
Na	-0.0738	0.2807	<u>0.9106</u>	0.0834	0.0647	0.9245
K	<u>0.8534</u>	0.0319	-0.1831	0.2592	0.1741	0.8603
Mn	0.0315	<u>0.9039</u>	-0.0236	0.2867	-0.0689	0.9054
Ti	<u>0.9392</u>	0.0591	0.2272	-0.1325	-0.1583	0.9797
P	-0.3591	<u>0.7847</u>	0.1209	0.1305	0.0958	0.7854
S	-0.2677	0.1228	<u>0.8753</u>	-0.1792	0.0649	0.8891
V	-0.1343	0.0137	0.0459	0.0594	<u>0.9550</u>	0.9359
Cr	<u>0.8851</u>	0.1296	-0.1105	-0.0034	-0.2395	0.8697
Co	0.4858	<u>0.7426</u>	0.2335	-0.1819	-0.0083	0.8751
Ni	<u>0.8296</u>	0.0997	-0.3287	-0.0132	-0.1783	0.8382
Ga	<u>0.9453</u>	0.0820	0.2312	0.1000	0.0405	0.9654
Rb	<u>0.8596</u>	-0.2469	-0.1554	-0.2089	-0.0502	0.8702
Sr	-0.3184	<u>-0.5093</u>	0.2105	<u>0.6763</u>	0.2167	0.9093
Ba	<u>0.9104</u>	0.1434	-0.1653	-0.0728	0.0163	0.8823
Zn	<u>0.7964</u>	-0.0441	-0.1934	-0.2729	-0.2218	0.7972
Eigen Value	8.9923	3.8787	2.1002	1.6967	1.0441	
% Variance	42.8437	15.8041	14.8254	8.9563	6.1306	
Cumulat. %	42.8437	58.6478	73.4733	82.4295	88.5601	

the shallow marine to deep shelf slope depositional environment. The Mg content ranges from 1.03 to 6.69%. The Mg shows strong positive correlation with Sr (0.759), (Table 6.5). This indicates the depletion of Mg along with strontium during diagenesis. Also the limestones showing more than 2.5 % Mg content must be due to their partial dolomitisation. The weathering process also contributes slight increased content of Mg as shown by its slight positive correlation with Fe (0.173). The moderate to high content of Mn (Table 6.3) in this group of microfacies indicates shallow to deeper shelf slope depositional environment. The P and S has maximum content of 0.38 % (3797 ppm) and 0.45 % (4500 ppm) respectively which also indicates the deeper shelf environment, during which the conditions were near to the anoxic in the deeper levels. The Sr content ranges from 81-972 ppm. The high content of Sr is the indication of original aragonitic mineralogy of the peloidal microfacies. The low content (81 ppm) of Sr in these microfacies units indicates about the temporal diagenetic changes that affected these sediments. The low Ba and Zn content distinguish these microfacies units from the very shallow to nearshore sedimentary units. In general, the marine limestones contain low content BaO 10-30 ppm, as a rule, more rarely up to 200 ppm.

Strontium in diagenetic carbonates range from 20 ppm (Morrow and Mayers, 1978) to greater than 10,000 ppm. (Land, 1973). In ancient marine limestones, low Sr contents of 20-70 ppm are common in diagenetically altered components, including recrystallised allochems, micrite and pore filling cements (Banner, 1995). Several authors have noted that many groups of ancient limestones have a wide range or even a weakly bimodal distribution of strontium contents. In a literature survey, (Morrow and Mayers, 1978) found that reef complex limestones (i.e. reef and associated back reef limestones) range from less than 100 ppm up to 400 ppm strontium, whereas basinal (i.e., forereef) limestones range from 500 ppm to 3000 ppm.

Table - 6.5. Correlation coefficient of Subtidal facies of Jhurio Formation (Jhura Dome).

	Si	Al	Fe	Ca	Mg	Na	K	Mn	Ti	P	S	V	Co	Ni	Ga	Rb	Sr	Ba	Zn
Si	1																		
Al	0.200	1.000																	
Fe	-0.059	0.178	1.000																
Ca	-0.869	-0.420	-0.409	1															
Mg	0.840	0.648	0.017	-0.855	1.000														
Na	-0.108	0.136	0.456	-0.138	-0.061	1.000													
K	0.797	0.680	0.188	-0.890	0.932	0.200	1.000												
Mn	-0.025	0.092	0.908	-0.399	0.047	0.495	0.129	1.000											
Ti	0.754	0.640	0.349	-0.914	0.887	0.052	0.935	0.257	1.000										
P	-0.221	0.114	0.803	-0.188	-0.118	0.639	0.029	0.898	0.117	1.000									
S	-0.573	0.110	0.174	0.388	-0.390	0.728	-0.250	0.273	-0.354	0.465	1.000								
V	0.332	0.136	0.222	-0.370	0.134	0.610	0.398	0.152	0.242	0.285	0.195	1.000							
Co	0.010	0.212	0.997	-0.473	0.084	0.439	0.245	0.913	0.405	0.795	0.136	0.245	1.000						
Ni	0.338	-0.465	-0.021	-0.196	-0.027	0.340	0.042	0.024	-0.070	-0.160	0.092	0.347	-0.017	1.000					
Ga	0.624	0.752	0.166	-0.746	0.834	0.279	0.880	0.223	0.827	0.236	0.028	0.400	0.224	-0.130	1.000				
Rb	0.220	-0.470	-0.645	0.180	-0.136	0.021	-0.071	-0.656	-0.265	-0.572	-0.068	0.315	-0.650	0.576	-0.175	1.000			
Sr	0.616	0.535	-0.512	-0.409	0.759	-0.122	0.665	-0.445	0.493	-0.491	-0.160	0.092	-0.461	0.055	0.676	0.315	1.000		
Ba	0.545	-0.359	0.352	-0.549	0.169	0.289	0.214	0.471	0.206	0.287	-0.169	0.481	0.386	0.706	0.134	0.179	-0.087	1.000	
Zn	0.313	-0.802	-0.297	0.007	-0.222	-0.176	-0.225	-0.249	-0.206	-0.283	-0.341	0.185	-0.293	0.578	-0.341	0.665	-0.159	0.523	1.000

Veizer and Demovic(1973, 1974) also reported that the the strontium contents of Czechoslovakian Mesozoic limestones tended to occur in two groups: a low-strontium group with a mode of about 100-250 ppm and high-strontium group with a mode of 600-700 ppm. They found that light coloured algal bank, reefal and littoral biogenic limestones form the low-strontium group, whereas darker deep sea limestones and lagoonal, shallow water sediments deposited landward from the algal banks form the high strontium group. They suggested that this bimodality reflect the original mineralogical differences. In the peloidal group the Sr ranges from 250 - 972 ppm (excluded the ferruginous shale intercalation of peloidal mudstone which shows about 81 ppm). Thus the peloidal limestone group falls in the high strontium group and is characterised by the deep shelf slope peloidal mudstone-wackestone microfacies. The fossil assemblage indicates littoral to shallow neritic sedimentary environment with variable energy of its sedimentary environment characterised by the presence of micrite to sparite range of cements and pellet types.

According to the theoretical considerations of Brand and Veizer (1980) Sr, Na, and possibly Mg should decrease, while Fe and Mn should increase with increasing diagenetic equilibration. Sr shows significant correlation with Mn (-0.450). Mg shows positive correlation (though very weak), as indicated by Brand and Veizer (1980), with Mn (0.047), while Sr shows positive correlation with Mg (0.759). The factor analysis shows five factors (Table 6.7) accounts for most of the variation in the element distribution. Factor-1 shows positive relation with Si, Al, K, Ti, Cr, Co, Rb, Ba, and Zn. This indicates the non-carbonate fraction which accounts for laboratory leaching. Factor-2, diagenetic equilibration accounts similar significance as that of the first factor. The positive relation is observed with Fe and Mn and negative relation is observed with Sr. The Factor-3 shows the positive relation with In, Rb, Ba and Zn and negative

Table - 6.6. Correlation coefficient of Peritidal facies of Jhurio Formation (Jhura Dome).

	Si	Al	Fe	Ca	Mg	Na	K	Mn	Ti	P	S	V	Cr	Co	Ni	Ga	Rb	Sr	Ba	Zn	
Si	1.000																				
Al	0.626	1.000																			
Fe	-0.045	-0.748	1.000																		
Ca	-0.451	-0.627	0.578	1.000																	
Mg	0.539	0.845	-0.655	-0.280	1.000																
Na	-0.523	-0.942	0.658	0.587	-0.666	1.000															
K	0.809	0.878	-0.504	-0.539	0.898	-0.719	1.000														
Mn	0.871	0.880	-0.421	-0.440	0.870	-0.754	0.969	1.000													
Ti	0.959	0.772	-0.288	-0.667	0.612	-0.666	0.878	0.900	1.000												
P	-0.159	0.368	-0.418	0.333	0.654	-0.322	0.318	0.297	-0.138	1.000											
S	-0.657	-0.819	0.685	0.613	-0.873	0.584	-0.913	-0.843	-0.779	-0.246	1.000										
V	0.569	0.249	0.115	-0.409	0.308	-0.138	0.597	0.475	0.566	-0.068	-0.439	1.000									
Cr	0.933	0.784	-0.347	-0.672	0.593	-0.683	0.831	0.876	0.983	-0.174	-0.774	0.414	1.000								
Co	0.696	0.247	0.388	-0.221	0.142	-0.299	0.479	0.502	0.605	-0.154	-0.141	0.782	0.482	1.000							
Ni	0.902	0.757	-0.359	-0.609	0.580	-0.648	0.779	0.847	0.943	-0.180	-0.757	0.277	0.986	0.368	1.000						
Ga	0.959	0.717	-0.258	-0.585	0.668	-0.551	0.903	0.908	0.977	-0.083	-0.834	0.621	0.950	0.574	0.914	1.000					
Rb	0.453	0.783	-0.762	-0.337	0.830	-0.603	0.691	0.719	0.553	0.385	-0.827	-0.117	0.634	-0.234	0.701	0.581	1.000				
Sr	-0.571	-0.259	-0.244	-0.365	-0.564	0.155	-0.545	-0.623	-0.393	-0.467	0.305	-0.406	-0.314	-0.545	-0.296	-0.487	-0.241	1.000			
Ba	0.930	0.623	-0.174	-0.390	0.705	-0.413	0.880	0.893	0.901	0.017	-0.821	0.599	0.868	0.524	0.847	0.969	0.598	-0.636	1.000		
Zn	0.588	0.561	-0.329	0.003	0.675	-0.404	0.569	0.697	0.542	0.264	-0.607	-0.170	0.625	-0.061	0.720	0.588	0.856	-0.529	0.672	1.000	

Table - 6.7. Factor analysis of elements of Subtidal facies of Jhurio Formation (Jhura Dome).

Rotated Component Matrix						
	Factors					Communalities
	1	2	3	4	5	
Si	<u>0.8315</u>	-0.0967	0.4244	-0.3130	0.1018	0.9892
Al	<u>0.6830</u>	0.0780	<u>-0.6515</u>	0.2391	0.0024	0.9542
Fe	0.0886	<u>0.9634</u>	-0.0038	0.0777	0.0697	0.9470
Ca	<u>-0.8788</u>	-0.3501	-0.2509	0.1791	-0.0822	0.9967
Mg	<u>0.9789</u>	-0.0352	-0.0334	-0.1177	-0.1056	0.9855
Na	0.0763	0.3745	0.1784	<u>0.7918</u>	0.3647	0.9379
K	<u>0.9705</u>	0.0700	-0.0183	0.0153	0.1584	0.9724
Mn	0.0917	<u>0.9549</u>	0.1035	0.1885	-0.0673	0.9711
Ti	<u>0.9128</u>	0.2545	-0.0686	-0.1785	0.0691	0.9392
P	-0.0504	<u>0.8602</u>	-0.0890	0.3211	0.2110	0.8980
S	-0.2794	0.1379	-0.1250	<u>0.9167</u>	0.0528	0.9559
V	0.2793	0.1144	0.2683	0.2801	<u>0.8396</u>	0.9465
Co	0.1543	<u>0.9615</u>	0.0074	0.0556	0.0739	0.9569
Ni	0.0479	-0.0920	<u>0.9224</u>	0.2684	-0.0124	0.9337
Ga	<u>0.8953</u>	0.1003	-0.1766	0.2128	0.1832	0.9216
Rb	-0.0889	-0.7220	<u>0.5411</u>	0.0765	0.3397	0.9433
Sr	<u>0.7631</u>	<u>-0.5930</u>	-0.0543	0.1445	-0.0986	0.9674
Ba	0.2236	0.3781	<u>0.8345</u>	-0.0521	0.1588	0.9173
Zn	-0.2313	-0.2458	<u>0.7650</u>	-0.3755	0.2649	0.9104
Eigen Value	6.3654	4.9806	3.2711	2.2145	1.2125	
% Variance	33.5021	26.2139	17.2166	11.6553	6.3817	
Cumulat. %	33.5021	59.7160	76.9325	88.5879	94.9696	

relation with Al. The Factor-4 shows positive relation with Na and S. The Factor-5 shows the positive relation with V and Na.

The evidence for different geochemical partings for different original carbonate minerals has been summarised by Veizer (1977, 1983). Brand and Veizer (1980, 1981) carried out a particularly sophisticated study in which they recognised three different diagenetic trends on Sr-Mn plots, corresponding to original mineralogy to be determined as long as diagenetic alteration is in the lesser half of the samples. Statistically the degree of diagenesis is best demonstrated by the covariance of Sr and Mn. This relationship between Sr/Mn chemistry, furthermore relates to an increase in textural maturity of the carbonate matrix, in the peloidal group of microfacies, which changes from micrite to microspar to pseudospar. From this it is obvious that the chemical and textural variations of carbonate diagenesis in the meteoric environment.

The $Sr/Ca \cdot 1000$ ratio ranges from 0.17 to 2.6 with the mean value 0.81. The $Sr/Ca \cdot 1000$ - Mn relationship (Fig. 6.10, after Brand and Veizer, 1980, 81) show the different fields which are indicative of diagenetic trend of carbonate sediment from the original mineralogy to the final diagenetic product. The field 2 represents the samples showing textural characteristics of micrite to microsparite during the meteoric diagenetic equilibration. The Fig. 6.11 (after Brand and Veizer, 1980, 81) represents the different field level of original carbonate mineralogy, such aragonite (A), high Mg-calcite (HMC) and low Mg-calcite (LMC). Thus in the field 3 the samples of peloidal group shows higher textural maturity that is mostly microsparitised carbonate cement (from the original aragonitic micrite) modified in to pseudospar. Also this field is characterised by the crinoidal pelsparites and other pelsparites that exhibit the marine cementation and the second generation cement (as evidenced by the petrographic studies) follows it. Thus the samples of peloidal group fall in the field of aragonite (of

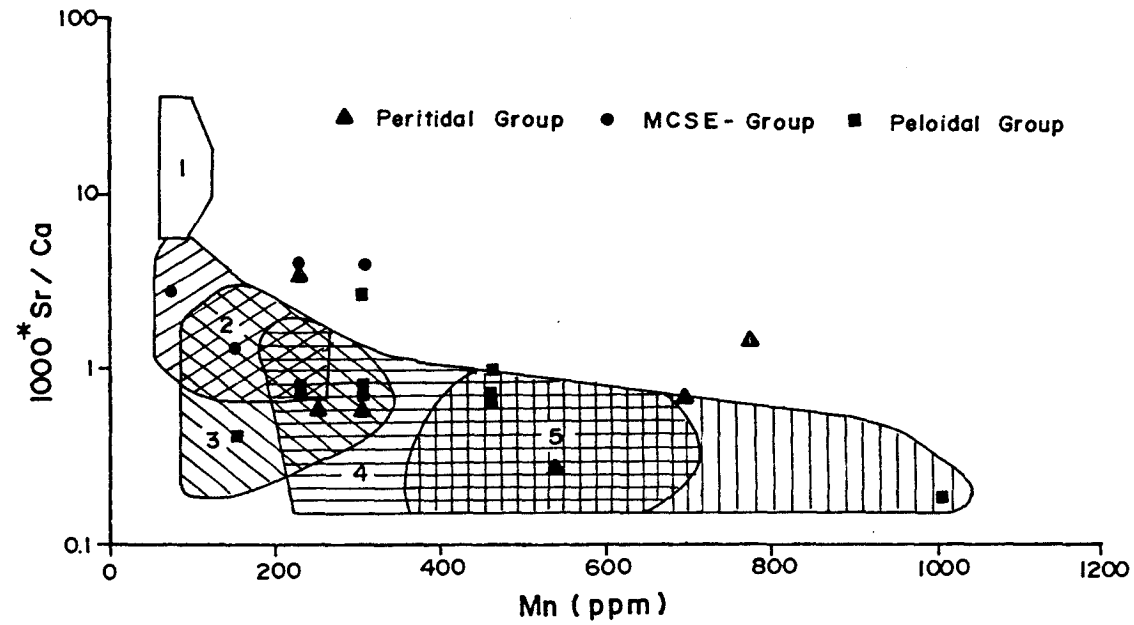


Fig. 6.10 Relationship between $1000^* \text{Sr} / \text{Ca}$ - Mn (ppm) in rocks of Jhurio Formation (Jhura Dome), Kachchh Mainland

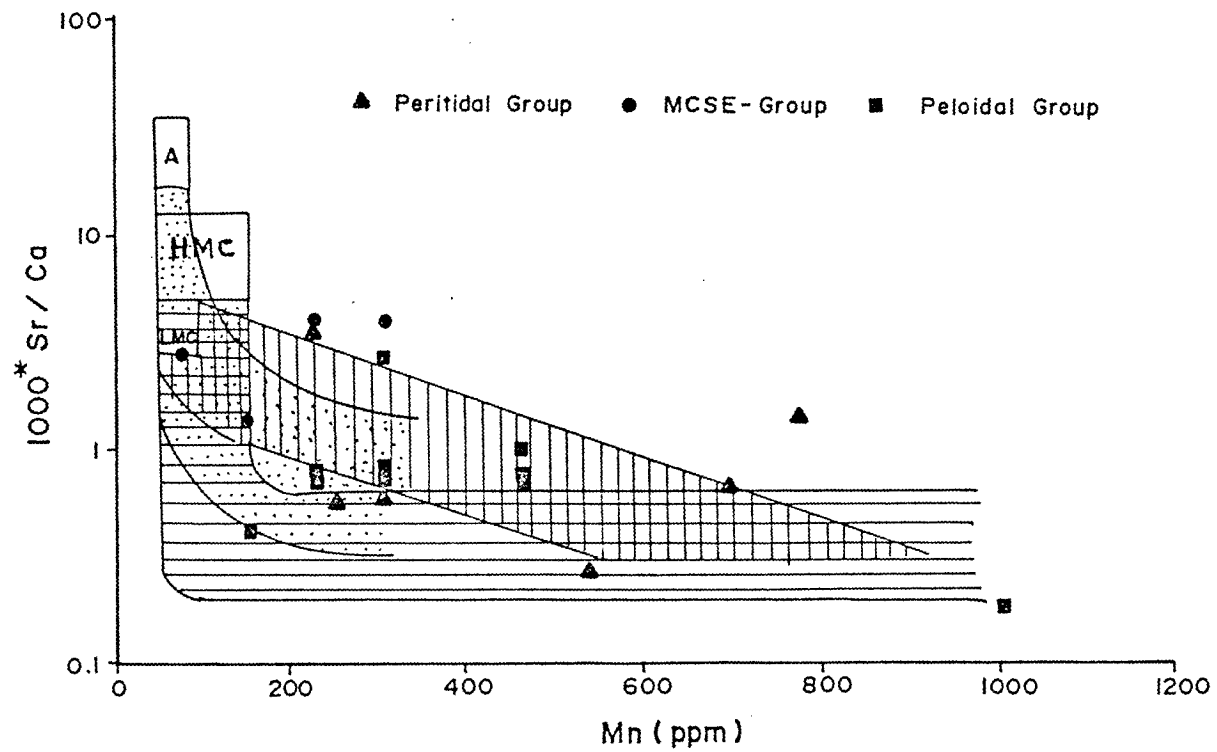


Fig. 6.11 Relationship between 1000^*Sr/Ca - Mn (ppm) in rocks of Jhurio Formation (Jhura Dome), Kachchh Mainland

Fig. 6.11) representing the original aragonitic mineralogy of the micrite mud which neomorphosed into microsparite and finally to pseudospar. (Field-2 and 3 of Fig. 6.10). The fields 4 and 5 show that the samples are of two diagenetic cementations, first generation marine cementation and the second generation fresh water diagenetic cementation and the field 5 the partial silicification of samples are observed. The Fig. 6.10 shows the fields 2 and 3 to 4 and 5 are indicative of diagenetic modifications of peloidal mudstones modified to the peloidal grainstone with coarse pseudosparite cements. The peloidal mudstone-wackestone of microsparite cement resulted from the diagenetic equilibration of the enclosed allochems and the cements with meteoric water.

6.3.2.2.1.2. Peritidal Facies

The peritidal facies include the microfacies groups such oolitic, bioclastic and lithoclastic types which are formed at marginal marine conditions. These microfacies groups which make also a part of the members A, C, E and top portion of G. The oolite group comprises oolitic grainstone to packstone microfacies and oolitic intraclastic bioclastic grainstone. These oolitic calcareous ironstones are characterized by high content of Fe, about 4.77 % (47702 ppm.) and also high Ca content, ranges from 35-45%. Whereas the Mg content is about 3 - 4.09%. The high content of Ca and low amount of IR (12%) indicates a shallow shoaling environment of deposition. The P and S contents also comparatively high, 1091 ppm. and 3100 ppm. respectively.

The Sr content is about 262.5 ppm. which is very low than the mean value. This indicates the depletion of Sr during the intensive diagenetic processes which is characterized by the dissolution of aragonite and reprecipitation as low magnesian calcite in the oolitic grainstone microfacies units. In bioclastic microfacies types the IR content is about 2 - 5 %. The Ca content range from 15 to 20 % and Mg ranges

from 2.5 - 4.0 %. The low content of Ca and high Mg content indicates the dolomitisation in the bioclastic grainstone microfacies in the mixed to fresh water phreatic diagenetic environment. The lithoclastic microfacies types indicate a nearshore environment of deposition. They must have deposited as lag deposit at the base of a transgressive facies. The high IR content, 20-30% and the low Ca content indicates the similar environment of deposition. The Fe and Mn content indicates the characteristic features of hard grounds in this particular microfacies which were developed during the highstand (maximum flooding) of the transgressive sea.

The peritidal facies group of samples shows strontium content ranging from 126 - 588 ppm with the mean value 268.17 ppm. Thus these carbonate rocks fall in the low strontium group. The Sr shows strong negative correlation with Mn (-0.623; Table 6.6). Mn shows strong positive correlation with Mg (0.87). The Mg that is more than 2.0 % (2.0 - 4.6 %) indicates the dolomitisation of these peritidal carbonates. The high Mg may also be contributed by the weathering processes. From the relationship between Sr, Mn, Mg and Na (positive correlation with Sr (0.155), it is understood that during the diagenetic equilibration with fresh water the Sr and Na has been depleted and Mn and Mg has been increased (Table 6.6).). The diagenetic stabilisation of these facies units with the fresh water can be interpreted from the Fig. 6.10 & 6.11. The original sediment might be of aragonite with HMC and LMC fossil assemblages. During diagenetic stabilisation with fresh water the sediment has neomorphosed into LMC showing two diagenetic phases. First, the marine diagenetic cementation observed in the samples of peritidal facies in the field-3 (Fig- 6. 10) and followed by the second generation fresh water coarse low Mg-cement, as observed in the oolitic grainstone microfacies, MF-10). This is also well observed in the samples of field-4.

6.3.2.2.2. Intertidal-supratidal facies

Calcareous sandstone microfacies is characterised by the little or no presence of Fe and low content of Mn (77 - 310 ppm). The Si ranges from 33 - 35% (Al ranges from 1.4 - 2.5%) and Ca ranges from 8 - 12%. Mg content ranges from 2 - 2.6% indicating dolomitisation (as evidenced by the petrographic studies). Na is low compared to high content of K (Na, 1805-2077ppm; K, 6863-11871 ppm). Both P and S have low contents (P, 300-350 ppm; S, 400-600 ppm). All these major element distribution has characteristic change from that of the shallow marine depositional environment. The trace elements such as Ba, Zn and Ga has high contents which indicate intertidal depositional facies. Where as the low Sr content is due to the diagenetic depletion during the burial diagenetic processes.

In the case of gypseous shale microfacies the Fe content is comparatively high with low Mn content. The high Na, K, Ba and Zn indicates restricted lagoonal hypersaline environment. The Sr content of these samples of intertidal-supratidal facies ranges from 32 - 332 ppm. The low Sr content is due to its precipitation from fresh water and hypersaline water in the intertidal-supratidal environment of deposition and diagenesis. The samples shows high $1000 \cdot \text{Sr}/\text{Ca}$ ratio and they shows original LMC cementation and depletion during the diagenetic stabilisation with fresh water (Fig. 6.10 & 6.11).

6.3.2.3. Middle Jurassic rocks of Kachchh Mainland

The temporal and spatial distribution of elements in the Middle Jurassic of Kachchh Mainland is well documented that the variation in the distribution is controlled by the facies and diagenetic modifications. The distribution of elements in the three exposures studied from the Middle Jurassic are given in the Tables 6.8a, 6.8b and 6.8c. The Table 6.8a shows the distribution of elements in the Habo dome. The Fe

Table - 6.8a Trace element distribution of Middle Jurassic succession of Habo Dome, Kachchh Mainland

		Fe	Mn	V	Cr	Co	Ni	Cu	Zn	Ga	Rb	Sr	Y	Zr	Nb	Cs	Hf	Ta	Ba	Pb	Bi	Th	U
Upper	\bar{x}	3515	430.3	65.1	72.6	8.4	51.4	86.5	480.5	13.1	56.9	212.5	18.5	111.7	16.1	2.1	6	1.5	230.3	20.9	108.7	15.3	2
	σ	1394	197.9	36.5	30.9	2	27.3	22.3	176.8	12.6	37.9	118.6	4	36.3	8.9	2.4	1.8	1	76.5	34.1	8.3	6.3	0.7
	Min.	1450	250	34	31.1	6.5	27.9	56.2	251	2.6	15.2	134.9	15	82.4	7.4	0	4.4	0.8	139.5	0.7	100	9.3	1.5
	Max.	4480	646	116.2	100.1	10.3	82.9	107.2	682.3	30.7	103.3	386.9	23.5	159.7	27.1	5.2	8.3	3	320.6	71.9	115.9	23.1	3.1
Middle	\bar{x}	3025	297.6	59.4	54.7	6.4	34.5	143.4	593.9	6.1	100	623.2	52.1	92.8	20.3	1	4.9	0.8	68.9	0.8	78.7	7.8	1.1
	σ	783.6	81.5	44.2	33.7	3.3	29	69.1	276.6	6.4	50.5	306.4	82.4	158.7	33.2	0.8	7	0.6	65.2	4.3	17.5	6.9	1
	Min.	1750	197	12.7	15.1	2.4	0	67	330.4	-0.2	20.8	136.9	8.8	3.3	0.6	0.1	0.3	0.1	7.1	3.6	57.2	1.6	0.4
	Max.	3890	402	114	90.1	11.5	79	224.2	912.7	13.8	144.2	885.1	199	372.8	79	1.7	17.2	1.3	163.3	5.2	95.8	18.3	2.8
Lower	\bar{x}	3305	526.8	96.4	79.2	7.4	41.3	33.2	184.5	15.4	75.7	197.2	19.5	209.4	32.6	3.9	10.3	1.6	285.8	4.6	94.3	15.1	2.7
	σ	1036	292.6	49.3	32.4	3.6	44.2	25.7	139.2	8.3	40.4	99.4	6.9	154.6	38.3	2.5	7	0.5	193.1	6.8	19.5	5.2	0.7
	Min.	2250	125	28.1	48.7	4	14.7	18.3	30.6	3.6	18.3	132.8	12.2	96.7	10	0.3	4.6	0.9	145.3	0.7	73.9	8.6	2.1
	Max.	4670	788	134.3	124.8	10.5	107.2	71.6	309.6	23	107.4	344.4	28.7	438	89.9	6.1	568	20.4	2	14.7	113.4	21.4	3.7

Table - 6.8b. Trace element distribution of Middle Jurassic succession of Jhura Dome, Kachchh Mainland

		Fe	Mn	V	Cr	Co	Ni	Cu	Zn	Ga	Rb	Sr	Y	Zr	Nb	Cs	Hf	Ta	Ba	Pb	Bi	Th	U
Upper	\bar{x}	1195	317.7	99.4	76.9	11.9	72.3	90.8	447.5	8	79.8	380.6	30.9	125.3	21.7	2	5.4	1	144.7	5.6	85.8	9.6	1.9
	σ	656.9	290.8	5.8	14.8	4.2	15.7	8.8	23.1	2.2	17.6	74.5	22.6	38.2	5.8	0.7	0.7	0.4	20.9	2.7	14.5	3	0.2
	Min.	1238	75	92.7	59.9	7.1	57.4	81.6	420.8	6.4	59.4	337	4.9	81.3	15	1.5	4.7	0.7	120.8	2.6	69.2	6.7	1.6
	Max.	2410	640	102.8	86.8	15	88.8	99.3	461.3	10.5	90.2	466.6	46.4	149.6	25.1	2.7	6	1.3	159.6	7.7	96	12.7	2.1
Middle	\bar{x}	591.5	214	99.3	81.3	5.3	38.3	72	331.6	10.2	66.2	461.9	39.6	109.3	21.9	1.4	3.8	1.1	173	2.7	95.4	9	1.5
	σ	30.4	18.4	11.7	28.6	1.9	30.2	14.6	1.6	1.4	2.1	99.3	2.7	19.3	9.7	0.3	0.4	0.5	108.8	1.7	12.4	1.8	0
	Min.	570	201	91	61	4	17	61.6	330.4	9.2	64.7	391.7	37.7	95.6	15	1.2	3.4	0.7	96.1	1.5	86.6	7.7	1.5
	Max.	613	227	107.5	101.5	6.6	59.7	82.3	332.7	11.2	67.7	532.2	41.5	122.9	28.8	1.6	4.1	1.4	250	3.9	104.2	10.3	1.5
Lower	\bar{x}	21145	373.62	85.95	13.43	10.7	9.29	63.87	125.1	10.3	79.33	340.1	32.8	58.6	29.8	1.3	2.5	2.9	164.2	1.5	77.3	8.7	1.8
	σ	29061	226	83.28	26.88	7.32	15.31	34.15	93.88	2.83	13.88	205.16	31.5	60.7	41.7	1.8	2.4	5	139.7	5.9	11.7	7	1.9
	Min.	0	77.46	0	0	5	0	8.8	15	8	59	32	6.1	4	1	0.2	0.3	0	31	-2.4	69.5	0.7	0.5
	Max.	1E+05	1007	189	79	30	56	99.3	371	20	118	972	41.5	122.9	28.8	1.6	4.1	1.4	501	3.9	104.2	10.3	1.5

Table - 6.8c. Trace element distribution of Middle Jurassic succession of Jumara dome, Kachchh Mainland

		Fe	Mn	V	Cr	Co	Ni	Cu	Zn	Ga	Rb	Sr	Y	Zr	Nb	Cs	Hf	Ta	Ba	Pb	Bi	Th	U
Upper	\bar{x}	1945	349.9	113.4	72	8.9	63.7	78.9	448.1	7.4	75.7	338.4	28.2	115.2	19.8	2.2	4	1.2	182.2	6	82.5	10.5	1.6
	σ	1003	181.6	31.5	38	8	26.2	15	100.6	1.3	5.9	92.9	21.8	4.1	6.5	0.3	1.4	0.1	34.4	3.9	15.7	0.9	0.5
	Min.	861	149.6	80.2	28.3	0.3	42.3	66.8	366.2	6.5	71	239.3	8.4	110.7	13.8	2	2.8	1.2	142.5	1.4	71.7	9.5	1.1
	Max.	2840	503.8	142.8	97	16.1	92.9	95.7	560.4	8.9	82.4	423.4	51.6	118.8	26.7	2.5	5.4	1.3	204.2	8.4	100.5	11.4	2.1
Middle	\bar{x}	3590	434.8	99.2	75.7	11.9	74.2	82.4	417.2	9.2	78.2	331.6	31.7	103.8	19.8	1.7	6.1	1.4	157	7.9	85.1	9.9	1.6
	σ	1546	268.5	18.2	15.6	3.3	17.9	10.7	51.5	1.3	15.7	30.1	26.7	33.4	1	0.3	1.8	0.5	16.3	3.1	4.7	1.9	0.3
	Min.	1317	48	87.7	60.1	7.9	47.4	71.6	381	7.9	56.4	289.2	-6.5	57	18.6	1.3	4.4	0.7	139.1	3.3	79.4	7.9	1.3
	Max.	4777	645.7	126.3	96.3	15.8	85.5	94.8	492.3	11	93.8	359.6	52.7	133.9	20.9	2	8.1	1.7	172.9	10	90.9	12.1	2
Lower	\bar{x}	2425	492.5	110.1	70.8	12.1	85.1	78.3	371.7	8.8	83.3	366.2	48.9	110.2	16.8	1.9	5.6	1.4	159.5	5.1	74.8	10.8	1.9
	σ	1430	60.6	15.9	4.5	5.4	30.5	9.5	114	1.5	7.6	82.1	31.7	14.6	4.7	4.7	0.5	0.5	50.9	2.1	2.2	3.3	0.3
	Min.	1109	438.9	95.1	67.9	6.8	50.5	68	262.7	7.9	74.9	274.2	25	93.8	11.5	1.4	5	0.9	101.1	2.9	72.3	7.1	1.6
	Max.	3947	558.2	126.8	76	17.6	108	86.8	490.2	10.5	89.6	432.1	84.8	121.9	20.3	2.6	6	1.8	194.6	7	76.7	13.1	2

and Mn ranges from 1450-4670 ppm and 125-788 ppm respectively. The Sr content is very low, ranges about 132.8-886.1 ppm. The Zn ranges from 30.6-912.7 ppm. While Sr shows the broad range which indicate the varied mineralogy of the mixed carbonate-siliciclastic-evaporite rock types of Habo Dome which was deposited ^{in a} shallow marine to near shore environment. The Ba ranges from 7.1-320.6 ppm. Ba is normally related to the non-carbonate facies in the sedimentary environment and the low Ba content (10-30ppm) related to shallow marine facies where as the high Ba content related to the clastic fraction especially to the finer ones. In the Habo Dome the lower part is characterised by the limestones of Jhurio Formation which high Fe and Mn content compared to the middle and upper part which is basically comprised of clastic facies mainly sandstones and shales with few limestones. While Sr shows low range about 132.8 - 344.4 ppm. This may be due to the partial dolomitisation of peloidal limestones as evidenced from the petrographic studies.

The Jhura Dome is characterised by the limestone dominated lower Jhurio Formation and the clastic dominated Jumara Formation in the middle and upper. The distribution of elements of Jhurio Formation is given in the Table-6.1 and 6.3 and the Fig. 6.7 & 6.8. The distribution shows the high content of Fe and Mn is related to the oolitic grainstone facies (Member-C and E and also in A). During the diagenesis Sr content has reduced to the range 81-972ppm. This indicates a broad mineralogy of this typical mixed carbonate-siliciclastic-evaporite facies. During the diagenesis Fe and Mn increased considerably while Sr depleted drastically. Whereas the middle and upper part of the Jhura Dome characterised by the Jumara Formation shows low to moderate content of Fe and Mn (Table- 6.8b) compared to the rocks of Jhurio Formation. The Zn shows high content which ranges from 330-462 ppm in the Jumara samples while Jhurio

samples shows wide range, about 15-371 ppm. The Fe, Mn and Zn has increased during the diagenetic stabilisation while Sr has depleted during diagenesis.

The distribution of elements in the Jumara dome is given in the Table-6.8c. The lower and middle part is characterised by Jhurio Formation with thick shale beds and thin bedded limestones. The limestones are mainly bioclastic coarse grained and mudstone types. The upper part is characterized by the Jumara Formation that is characterised by the thick bedded shales, sandstones (Ridge sandstone), thin bedded limestones (especially Dhosa Oolite Member). The Jhurio Formation is characterised by the high content of Fe and Mn ranges from 1109.3 - 4776.9 ppm and 48- 645.7 ppm respectively. Sr shows low to moderate content ranges from 274.2-432.1 ppm. The iron oolites and the ferruginous shales contribute the high Fe and Mn. Also during diagenetic equilibration with the meteoric water the Fe and Mn content has increased. The Sr while shows that the depletion was considerable during the diagenesis. The Jumara Formation is characterised by the high content of Fe and Mn and is contributed by the calcareous iron oolitic grainstones and ferruginous shales.

The other trace elements analyzed include V, Cr, Co, Cu, Ga, Rb, Y, Zr, Nb, Cs, Ba, Hf, Ta, Bi, Th, U and REE which have been used in the interpretation of origin and provenance. The distribution of these elements and their interrelationships are shown in Fig. 6.12 a , b & c and 6.13. In general, the elements with low water rock coefficients and low residence time values including Zr, Hf, Ga, Y, Th, Nb, Be and REE are strongly excluded from natural waters and remain in the oceans for time less than average ocean mixing times. Consequently, it is likely that these elements are transferred quantitatively into clastic sedimentary rocks and hence give best information regarding source rock composition. Therefore, their distribution in the sedimentary rocks is most useful.

180

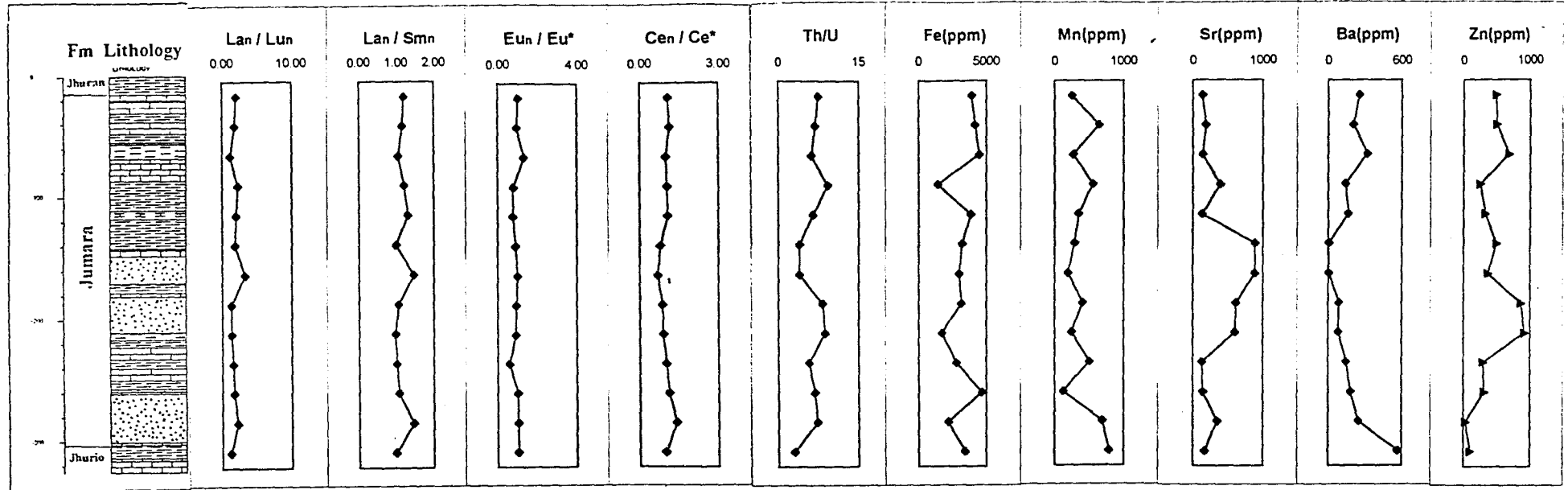
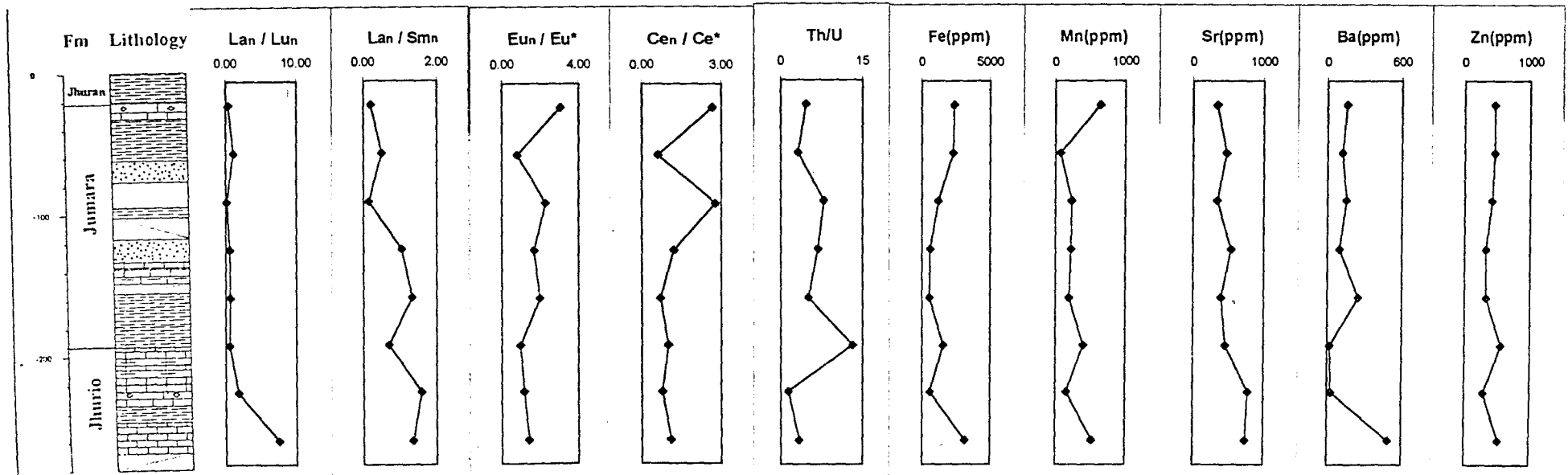


Fig. 6.12a Vertical variation of chemical parameters, Habo section.



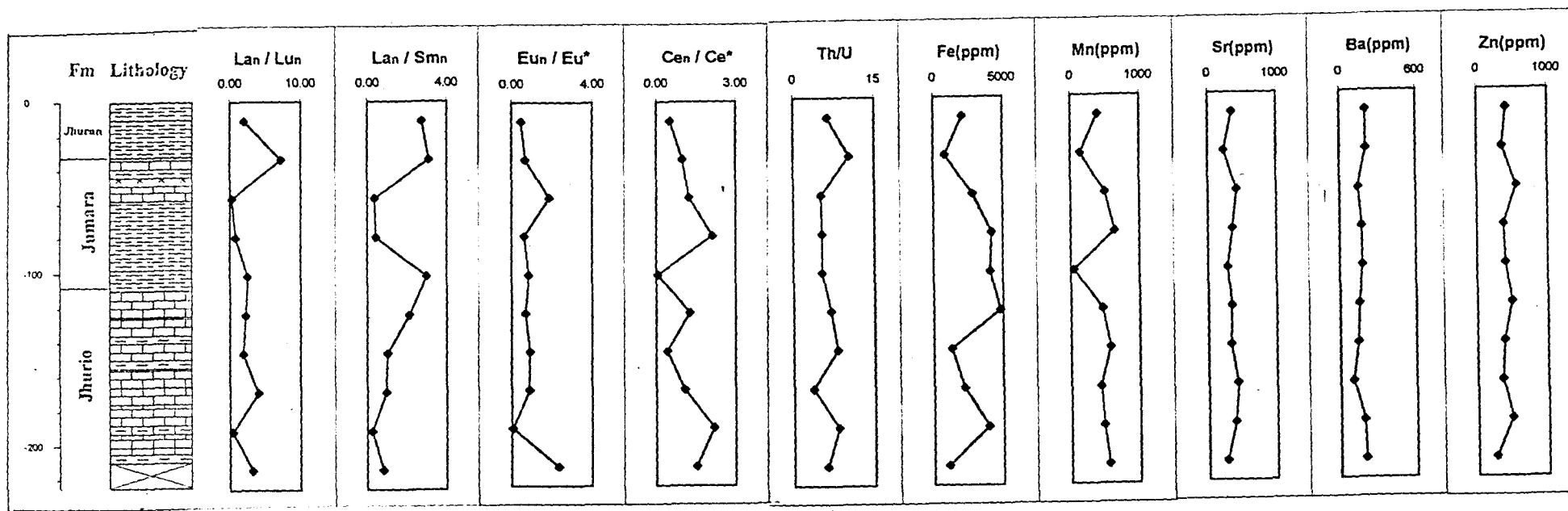


Fig. 6.11 Vertical variation of chemical parameters, Jumara section.

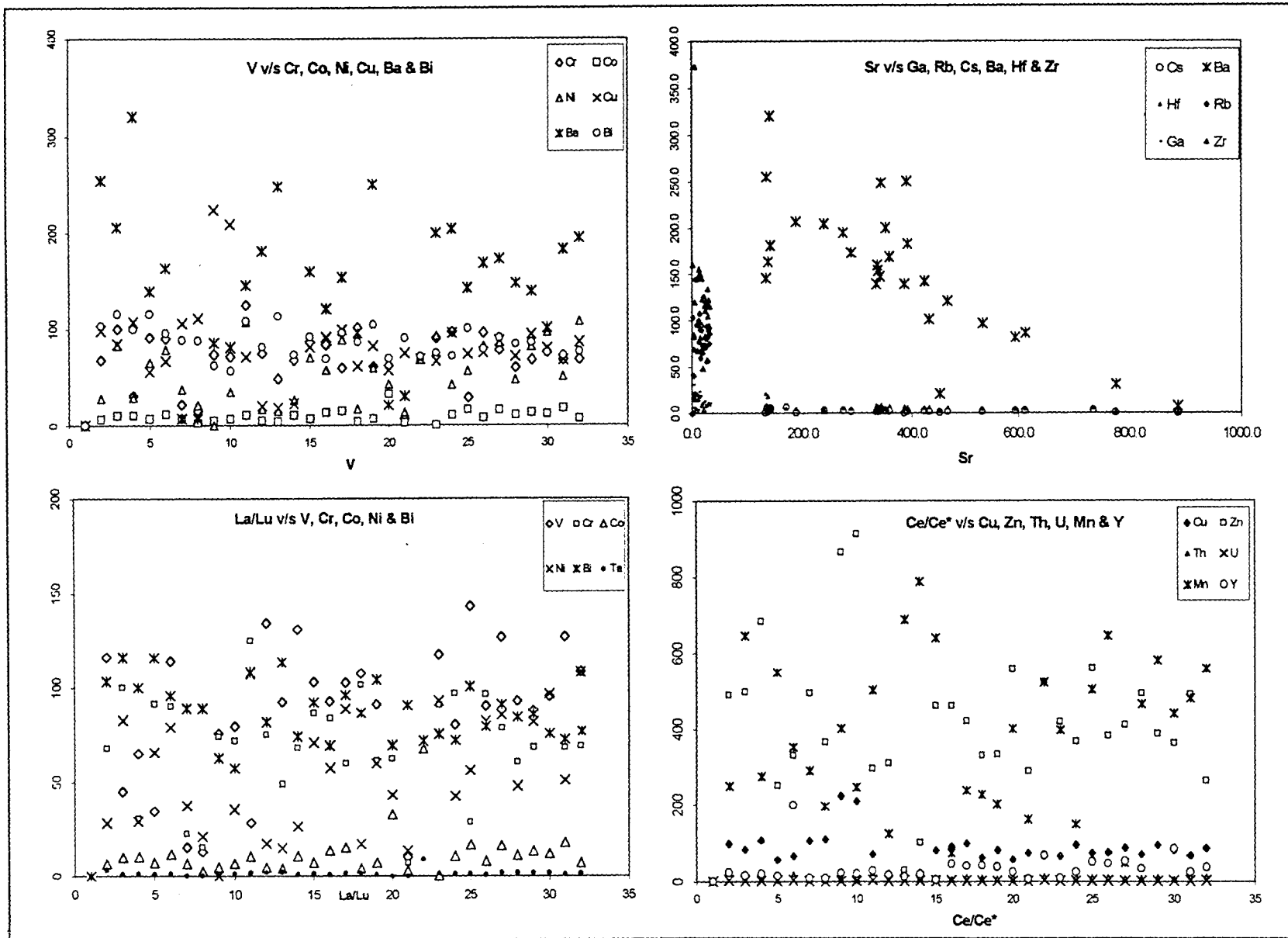


Fig. 6.13. Scatter Plots of Chemical Data for Middle Jurassic samples of Kachchh Mainland

6.4. Rare Earth Elements (REE)

The rare earth elements (REE) are a group of 15 elements from La to Lu that exhibit generally similar chemical behavior. Owing to their electronic configurations, these elements form ions that are nearly all trivalent, with smoothly decreasing ionic radii. Notable exceptions are stabilisation of Ce⁴⁺ and Eu²⁺ under appropriate oxidizing and reducing conditions, respectively.

Goldschmidt (1954) was the first to suggest that the constant distribution of REE in sedimentary processes and therefore, the REE pattern of sedimentary rocks reflect the continental crustal abundances. The generally higher prevalence in nature of even atomic numbers is manifest by ratios of up to an order of magnitude between neighbouring pairs of elements. Consequently, comparisons among the REE are facilitated by normalizing analytical values to an appropriate reference, such as Chondrite, but for sedimentary rocks the preferred reference is the North American Shale Composite (NASC) a representative of the average upper crust (Gromet et al., 1984, Condie, 1991). With respect to such a reference certain fractionation effects may enhance the light REE (LREE) or the heavy REE (HREE), and those may be quantified by the ratio of normalized $La_n/Lu_n > 1$ ($La/Lu > 9.63$) or $La_n/Lu_n < 1$ respectively. Curvature in an REE plot may document an enhancement of the middle REE (MREE) with respect to both LREE and HREE. The resulting "hat-shaped" REE plot may be quantified by a ratio such as $2GD_n / (La_n/Lu_n) > 1$.

6.4.1. REE distribution in the Middle Jurassic succession of Kachchh Mainland

In the present study the REE have been analyzed with an objective of understanding their distribution in order to interpret the provenance and sedimentary processes. The total concentration of REE in the present samples varies from 44.93 to 255.3 with a mean content of 151.88 (Table 6.9a, b & c) and is almost similar to the crustal average of 151.10 (after Mason and Moore, 1982).

The Chondrite normalized REE patterns (Fig. 6.14) of these rock samples are very similar to each other, (i) being enriched in the LREE relative to the HREE - show a greater degree of rare earth element fractionation when compared to source rock, as indicated in their $(La/Yb)_N$ mean ratio of 12.58, (ii) fractionated LREE and flat HREE and (iii) a negative europium anomaly. The difference in the relative degrees of fractionation among LREE and HREE is reflected in their high La_N/Sm_N ratios (5.60 to 2.44; mean - 4.09) but relatively lower Gd_N/Yb_N mean ratio of 2.28. This kind of fractionation is characteristic of post-Archaean sediments (McLennan and Taylor, 1991).

Shale normalized REE abundance of the samples gives a relatively flat pattern (Fig. 6.15) with approximately 0.2 times NASC. The low concentration of REE in the present samples when compared to NASC (ΣREE of NASC is 173.2) is due to their sandy nature, devoid of much clay minerals and rock fragments that contain high REE among the eroded materials. Although, their REE concentration is low, the variability in terms of bulk rare earth elements and LREE/HREE ratio for all the samples is low. This kind of similarity among sediment samples could be attributed to the homogenization due to erosion and transportation (Goldschmidt, 1954). The LREE enrichment as compared to the HREE is attributed to the weathering and recycling of the provenance rocks. No substantial change in the elemental concentration is seen in

Table-6.7a Rare earth element distribution of Middle Jurassic Sequence of Habo Hill, Kachchh Mainland

		La	Ce	Pr	Nd	Sm	Eu	Gd	Tb	Dy	Ho	Er	Tm	Yb	Lu	SREE	LREE	Eu _{an}	Ce _{an}
Upper	\bar{X}	37.0	78.5	8.5	29.4	5.7	1.3	5.8	0.8	4.9	1.2	2.5	0.5	2.3	0.3	1.82	1.15	1.03	1.06
	σ	14.5	29.8	3.0	10.4	2.0	0.4	1.4	0.3	0.9	0.3	0.6	0.1	0.6	0.1	0.48	0.07	0.22	0.06
	Min.	23.9	52.2	5.7	20.2	3.7	0.9	4.4	0.5	4.1	0.9	2.0	0.4	1.9	0.2	1.17	1.05	0.79	1.00
	Max.	53.8	114.2	12.0	41.6	8.0	1.8	7.5	1.1	6.0	1.6	3.4	0.7	3.1	0.4	2.29	1.20	1.33	1.13
Middle	\bar{X}	25.8	46.6	5.6	21.2	4.2	0.9	4.7	0.6	4.0	1.0	2.3	0.5	1.9	0.2	1.98	1.16	0.90	0.86
	σ	9.2	20.3	2.0	7.2	1.7	0.4	1.9	0.2	1.4	0.4	0.9	0.2	0.9	0.1	0.82	0.22	0.08	0.14
	Min.	11.1	15.2	2.3	8.7	1.4	0.4	2.0	0.3	1.8	0.4	0.9	0.1	0.4	0.1	1.31	0.96	0.77	0.69
	Max.	33.6	71.6	7.6	26.5	6.1	1.4	7.2	0.9	5.5	1.4	3.5	0.6	2.7	0.3	3.33	1.47	0.99	1.07
Lower	\bar{X}	39.6	88.4	9.0	30.8	6.4	1.2	5.8	0.8	4.5	1.1	2.7	0.5	2.7	0.4	1.73	1.13	0.93	1.13
	σ	7.8	18.6	1.8	5.0	1.7	0.3	1.8	0.1	1.0	0.3	0.7	0.1	0.7	0.1	0.41	0.22	0.21	0.18
	Min.	29.4	61.7	6.6	26.0	4.6	1.0	4.1	0.6	3.3	0.9	1.8	0.4	1.9	0.3	1.30	0.99	0.61	0.99
	Max.	45.8	102.2	10.6	36.2	8.1	1.7	7.9	0.9	5.7	1.5	3.5	0.7	3.3	0.4	2.26	1.46	1.06	1.39

SREE-La_N/Lu_N; LREE-La_N/Sm_N; Eu_{an}-Eu anomaly(Eu_N/Eu_N); Ce_{an}-Ce anomaly(Ce_N/Ce_N); \bar{X} -Mean; σ - Std.Deviation.

Table-6.7b Rare earth element distribution of Middle Jurassic Sequence of Jhura Hill, Kachchh Mainland

		La	Ce	Pr	Nd	Sm	Eu	Gd	Tb	Dy	Ho	Er	Tm	Yb	Lu	SREE	LREE	Eu _{an}	Ce _{an}
Upper	\bar{X}	32.6	68.6	6.8	25.5	4.9	1.4	5.0	0.6	3.8	0.8	1.9	0.3	1.5	0.2	0.53	0.28	2.05	2.01
	σ	37.4	81.0	7.7	27.1	4.6	1.5	4.1	0.4	2.4	0.6	1.3	0.2	1.4	0.2	0.51	0.18	1.14	1.22
	Min.	7.5	11.2	1.2	5.5	0.8	0.2	0.9	0.2	1.0	0.2	0.6	0.1	0.4	0.1	0.14	0.15	0.81	0.61
	Max.	75.6	161.3	15.6	56.4	9.9	3.1	9.0	0.9	5.4	1.4	3.2	0.6	3.1	0.4	1.14	0.49	3.05	2.77
Middle	\bar{X}	18.3	43.2	7.4	20.8	2.8	1.7	6.3	0.5	4.8	1.1	2.9	0.4	2.8	0.4	0.63	1.19	1.83	0.95
	σ	2.5	24.4	1.7	6.1	0.9	0.4	3.0	0.0	0.1	0.1	0.4	0.2	0.2	0.1	0.07	0.20	0.22	0.35
	Min.	16.5	26.0	6.2	16.5	2.2	1.4	4.2	0.5	4.7	1.1	2.6	0.3	2.6	0.4	0.59	1.04	1.67	0.70
	Max.	20.0	60.4	8.5	25.1	3.4	1.9	8.4	0.5	4.8	1.2	3.2	0.5	2.9	0.5	0.69	1.33	1.98	1.20
Lower	\bar{X}	9.1	48.7	5.1	30.5	4.5	1.3	3.4	0.6	5.5	1.3	1.7	0.5	2.0	0.2	3.34	1.21	1.19	0.96
	σ	10.8	20.6	3.7	7.3	3.0	0.5	3.0	0.2	0.5	0.7	0.2	0.1	0.9	0.1	3.71	0.46	0.23	0.17
	Min.	1.6	36.3	1.5	22.1	1.9	0.9	0.7	0.4	4.9	0.7	1.5	0.5	1.4	0.2	0.58	0.69	0.97	0.78
	Max.	21.4	72.5	8.9	34.8	7.8	1.8	6.6	0.8	5.8	2.1	1.9	0.6	3.1	0.3	7.56	1.58	1.42	1.10

SREE-La_N/Lu_N; LREE-La_N/Sm_N; Eu_{an}-Eu anomaly(Eu_N/Eu_N); Ce_{an}-Ce anomaly(Ce_N/Ce_N); \bar{X} -Mean; σ - Std.Deviation.

Table-6.7c Rare earth element distribution of Middle Jurassic Sequence of Jumara Hill, Kachchh Mainland

		La	Ce	Pr	Nd	Sm	Eu	Gd	Tb	Dy	Ho	Er	Tm	Yb	Lu	SREE	LREE	Eu _{an}	Ce _{an}
Upper	\bar{X}	40.4	40.3	8.3	23.4	3.1	0.9	5.5	0.8	3.8	1.1	2.7	0.6	2.5	0.3	3.18	2.06	1.00	0.92
	σ	31.7	14.3	2.3	25.4	0.9	0.5	1.9	0.2	0.4	0.3	0.1	0.3	0.2	0.1	3.66	1.48	0.75	0.36
	Min.	4.2	25.3	6.9	8.5	2.1	0.4	3.5	0.7	3.4	0.8	2.5	0.3	2.3	0.1	0.24	0.36	0.47	0.53
	Max.	63.1	53.9	10.9	52.7	3.7	1.5	7.3	1.0	4.1	1.4	2.8	0.8	2.7	0.4	7.28	3.08	1.86	1.24
Middle	\bar{X}	37.8	64.2	9.0	37.7	5.2	0.8	4.9	0.8	3.6	1.2	2.2	0.5	1.9	0.3	1.87	1.64	0.77	0.97
	σ	19.3	52.2	5.8	9.0	3.2	0.3	2.0	0.3	1.3	0.2	1.1	0.1	0.9	0.1	0.74	1.13	0.14	0.93
	Min.	14.6	7.0	4.9	26.5	2.5	0.5	3.2	0.4	2.6	0.9	1.2	0.4	1.1	0.2	0.81	0.45	0.62	0.06
	Max.	55.3	122.8	17.2	45.5	9.6	1.2	7.7	1.1	5.4	1.4	3.8	0.6	2.8	0.4	2.52	2.98	0.92	2.14
Lower	\bar{X}	25.7	71.6	11.0	19.1	7.1	1.0	3.7	0.5	3.6	1.1	2.8	0.4	2.1	0.2	2.55	0.67	1.09	1.60
	σ	13.3	8.8	4.0	5.7	1.0	0.8	1.7	0.2	1.2	0.3	0.6	0.1	0.4	0.2	1.91	0.37	1.15	0.56
	Min.	11.3	61.8	7.4	13.9	6.1	0.1	1.7	0.3	2.9	0.9	2.4	0.4	1.8	0.1	0.4	0.25	0.1	1.07
	Max.	37.5	78.8	15.2	25.3	8.2	1.7	5.0	0.7	5.0	1.4	3.5	0.5	2.6	0.4	4.02	0.95	2.3	2.19

SREE-La_N/Lu_N; LREE-La_N/Sm_N; Eu_{an}-Eu anomaly(Eu_N/Eu_N); Ce_{an}-Ce anomaly(Ce_N/Ce_N); \bar{X} -Mean; σ - Std.Deviation.

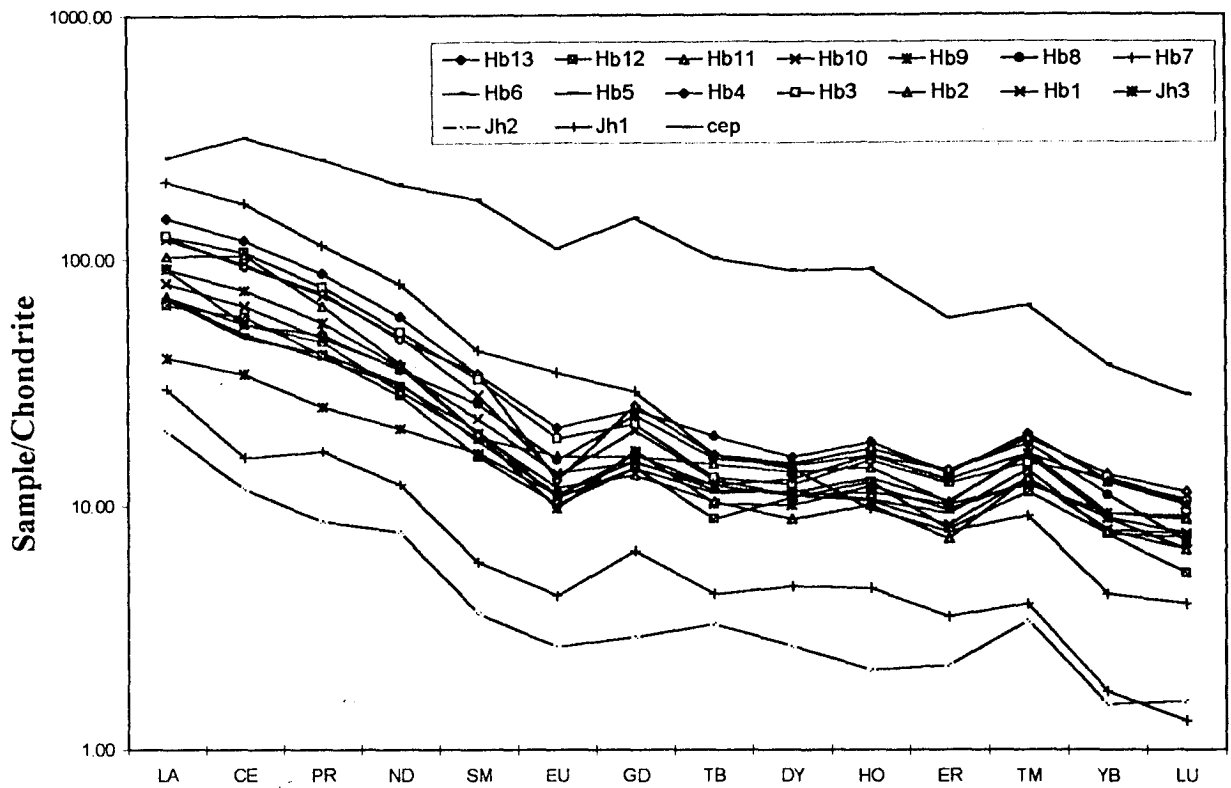


Fig. 6.14 Chondrite Normalized REE plot for Jurassic samples of Kachchh

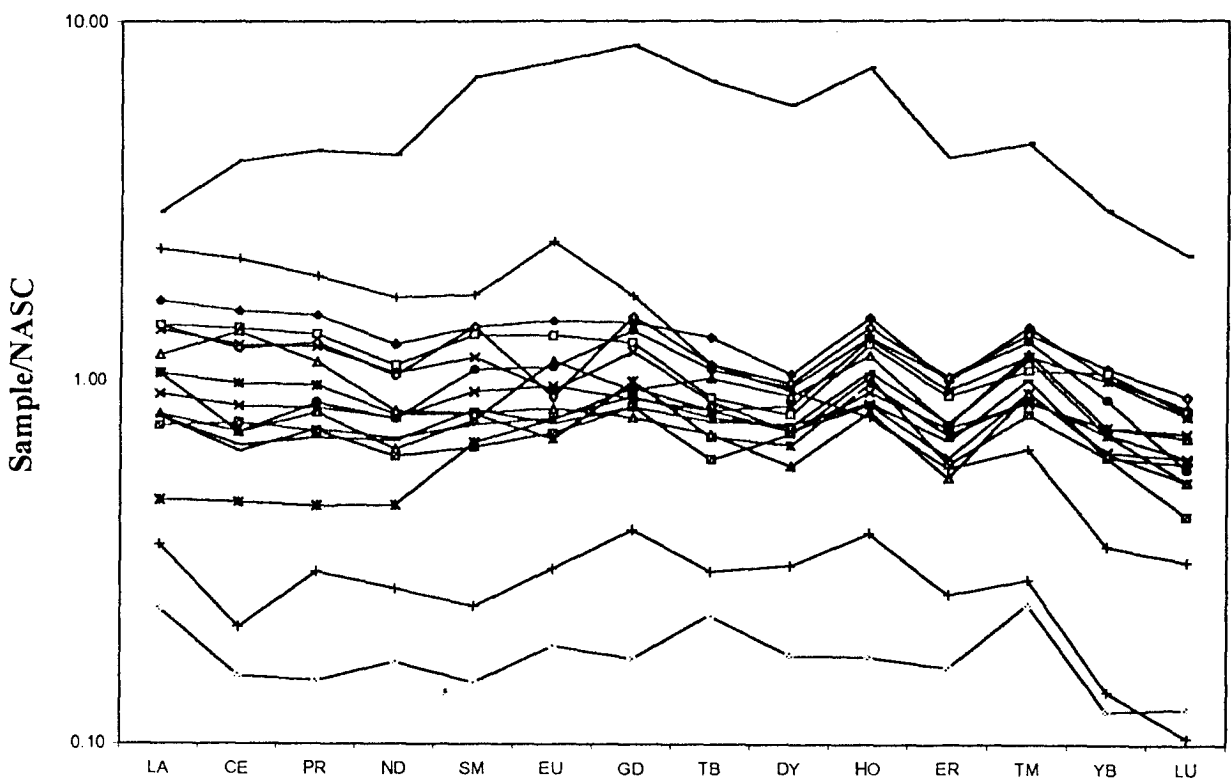


Fig. 6.15 Shale Normalized REE plot for Jurassic samples of Kachchh

samples from different locations of Kachchh Mainland which undergone varying degrees of transport, implying that the REE is not mobile during transportation and reflect a relatively stable tectonic under which they have been evolved.

6.4.2. REE Anomalies

The most distinctive deviations from regular behavior of the REE are "anomalous" levels of Ce and Eu. Understanding the origin of the depletion in Eu and Ce, relative to the other normalized REE in clastic sedimentary rocks is fundamental to most interpretations of crustal composition and evolution. The deviation of Ce and Eu may be quantified as ratio to Ce and Eu respectively by interpolating neighbouring REE $\{Ce_{an} = Ce_n / [(La_n)(Nd_n)]^{1/2}$ and $Eu_{an} = Eu_n / [(Sm_n)(Gd_n)]^{1/2}\}$.

6.4.3. Eu anomaly

Almost all the post-Archaean sedimentary rocks (except volcanogenic sediments) are characterised by Eu depletion (Taylor and McLennan, 1985). The negative Eu anomaly in some of these rocks indicates preferential removal of feldspar due to weathering (Nesbitt et al., 1966). The samples have a relatively higher mean value (0.81) Eu/Eu^* compare to NASC representing the typical post-Archaean submature sediments derived from differentiated upper continental crustal provenance. Though the rare earth elements are known to be immobile in weathering, Eu has slightly higher mobility than other REE (Albarede and Semhi, 1995).

6.4.4. Ce anomaly

The possibility that Ce anomaly could be used as a possible indicator of redox conditions in natural water masses and their associated sediments, and that such sediments were preserved as reliable indicator of palaeoredox in ancient oceans, attracted a good deal of attention in recent years (Wright et al., 1988). The prominent

feature observed in REE distribution in present day waters and palaeoseas is a negative Ce anomaly. If an oxic-suboxic boundary is encountered in a basin, the Ce anomaly reduces sharply to zero as Ce is re-mobilized (Sholkovitz et al., 1992). In general, strongly negative to zero Ce_{an} anomalies, and more rarely a weakly positive Ce_{an} are prominent features of REE distribution in a wide variety of modern and ancient sedimentary environments. In the present samples the value of Ce anomaly varies from 0.83 to 1.67 indicating toxic state of depositional basin.

CHAPTER VII

SEDIMENTATION HISTORY AND PALAEOENVIRONMENT

7.1. GENERAL

The Kachchh sedimentary basin developed on the western margin of the Indian plate comprises of a thick succession of sediments deposited during Bathonian to Pleistocene. The Mesozoic succession deposited during Bathonian to Lower Cretaceous, consisting of a thickness of about 3000m. is exposed in six highland areas scattered over the plains of the RANN of Kachchh in Gujarat, Western India. The rock units recognized in these widely separated areas are grouped in to three lithostratigraphic provinces that are known as Kachchh Mainland, Pachham Island and Eastern Kachchh. The lithostratigraphic successions of three provinces represent the vertical profiles of environments respectively at the depocentre and at northern and eastern margins of the basin (Biswas, 1981). The Jurassic sedimentary record comprises of a siliciclastic succession with intervening horizons of carbonates. The siliciclastic sediments consists mainly of fine-grained sandstone, siltstone and shales (calcareous and gypseous).

Kachchh graben is the earliest rift basin which opened up during the beginning of the rifting of Indian plate from the Gondwanaland in Late Triassic (Biswas, 1982). Major part of the Mesozoic sedimentation took place during the early-rift-phase of the evolution of India's Western continental margin. The rifting was terminated in the Late Cretaceous as evidenced by the Jurassic-Cretaceous basin fill culminating with Late Cretaceous regressive cycle. The rifting took place in different stages by a series of parallel longitudinal faulting along primordial tectonic trends (Biswas, 1987) starting from the north. In Late Triassic, a narrow graben opened up in the north between Nagar Parker fault and Island Belt fault which was filled up by granite

cobble fanglomerates and arkoses in rift valley stage. Later the graben opened up between Island Belt and Mainland, which was filled by continental to paralic valley fill clastics. The first marine transgression started with extension of the graben up to Kathiawar Uplift by activation of North Kathiawar fault during rift-drift transition of Indian plate movement. The graben was inundated forming a gulf. By Argovian time, proto-oceanic stage was reached with complete inundation of the embayed basin. The rifting failed by Early Cretaceous when the basin got filled up by clastics of prograding delta as the sea regressed (Biswas, 1982). The two mega cycles - Early Mesozoic transgression and the Late Mesozoic regression, therefore register two major tectonic phases. Early Rift Phase and its termination by failing of rifting process.

7.2. DEPOSITIONAL HISTORY : SEQUENCE STRATIGRAPHIC APPROACH

The earlier studies on the palaeoenvironmental reconstruction, mostly, on the Mesozoic stratigraphic units were qualitative and based on the geological and palaeontological approach, such as gross lithology and palaeoecology of fossil fauna/flora (Ghosh, 1969, Mitra et al., 1979). The subsequent studies of Jaikrishna et al. (1983) and Howard and Singh (1985) on interpretation of the depositional environments were based on the trace fossils with some supporting evidences from gross lithology. Very little emphasis was given in the past for an integrated study to substantiate their conclusions with detailed sedimentologic observations. The first comprehensive study of the basin framework, depositional processes and the evolution based on the detailed study of the gross facies and quantitative assessment of the basin is given by Biswas (1981). His interpretation on the palaeoenvironmental reconstruction was based on the observed material-process response models of Krumbein and Sloss (1963). The vertical environment profiles of lithologic successions indicate two distinct megacycles of Kachchh (Biswas, 1982): a transgressive followed by a regressive cycle with several

transgressive-regressive sub-cycles corresponds to the fluctuations of sea levels in an unstable basin. From this point of view and that of Jaikrishna, et al., (1983) and Howard and Singh(1985), a new approach, sequence stratigraphic technique, has been adopted in the present study in order to understand and elaborate the detailed sedimentation history of mixed carbonate-siliciclastic-evaporite rock successions of Kachchh Mainland during Middle Jurassic. Using the combined data on the carbonate petrography, clastic sedimentology, clay mineral and geochemical analysis, facies migration and development with respect to change in sea level across the Kachchh basin has been predicted.

Sequence stratigraphy integrates time and relative sea-level changes to track the migration of facies. Carbonate platforms are similar to siliciclastic shelves to the extent that they are constructed and modified by depositional and erosional processes acting under the controls exerted by eustasy, tectonic subsidence, sedimentation rate and climate (Vail, 1987; Sarg, 1988). Sequence stratigraphic models are routinely applied to interpret ancient carbonate platforms using stratal architecture and distribution of key stratal bounding surfaces and facies description within depositional units, with in the context of changing accommodation space during third order sea-level cycles. Even though standard microfacies (SMF) types do not take in to account gradual changes in the marine environment resulting from variations in water depth during the cycle of relative sea-level change, individual system tracts can be described using standard microfacies models (Spence and Tucker, 1999). Key stratal surfaces represent depositional hiatuses formed during major episodes of subaerial exposure or maximum marine flooding at the exposures of sea-level cycles (Vail,et al., 1984; Galloway 1989; Vail et al., 1991). Successions are divided up in to sequences ("Depositional Sequence", Vail,1984) and their constituent system tracts that

characterize the different phases of deposition during third-order relative sea-level cycles (1-10My.). While two or three sequences which are genetically related to each other build up to form a Megasequence, (equivalent to Supergroup of Sloss, 1963) formed during the second order sea level transgressive or regressive cycle. However, there has been little consideration of the way that microfacies within these stratigraphic units vary in response to the effects of gradual environmental shifts caused by the relative sea-level changes.

Variation in water depth is the single most significant collective control on the wide range of environmental factors including hydrodynamic energy, water turbulence, light penetration, siliciclastic contamination and nutrient supply. Carbonate microfacies are most widely interpreted using standard microfacies models (e.g. Wilson 1975; Flugel 1982). However, the rate at which environmental changes occurred, especially, fluctuations in relative sea-level, were thought to have been much slower than we know now them to have been (Spence and Tucker, 1999). Carbonate sub-environments represented by individual microfacies assemblages are defined relative to fixed palaeogeographic positions within the platform and static palaeobathymetries. However, against a background of dynamic relative sea-level changes neither palaeogeographic position nor palaeobathymetry remain constant. The spatial arrangement and composition of microfacies within a carbonate platform will be affected by changes in the type of carbonate generated by the carbonate factory and carbonate factory size, related in large part to the position of sea-level and the nature of any change. Thus, different microfacies can exist at similar locations and depths on a platform at different times within a cycle of relative sea-level change.

The vertical profiles of Jhurio Formation in Jhura Dome section (Fig.3.3; Fig.7.1) reveals the development of parasequences and parasequence sets that are stacked

characteristically in a carbonate dominated third order sequence. The petrographic, mineralogic and also the geochemical evidences have been utilized to support the field evidences of distribution of facies and the cyclicity in their depositional pattern. Thus sedimentary processes such as regression or transgression can be inferred from such evidences. The identification and detailed description of facies distribution which have passed through the Middle Jurassic since its deposition have been incorporated to understand the parasequences, parasequence sets, their stacking pattern to predict the system tract model and thereby establishing the palaeogeography and basin set-up of Kachchh basin during the Middle Jurassic. The distribution of facies and diagenetic sequence is well accounted by the response of sedimentary deposits due to the change in global sea-level. The microfacies identification and description in the vertical stratigraphic order has revealed the type of parasequence sets and their stacking pattern. The Middle Jurassic facies distribution in the temporal and spatial scale documents the stacking of three different third order sequences with many parasequence sets which are mainly build up by shallowing upward parasequences. The three sequences are stacked in to a megasequence developed during the second order transgressive cycle started during the Middle Bathonian.

7.2.1. Megasequence and Third Order Sequences

According to Biswas (1981) two distinct sedimentary sequences are observed in the Kachchh Mainland in a broad lithofacies context: 1) shales and carbonates, deposited in sub-littoral environment where rate of sedimentation being slow (Jhurio and Jumara Formations) and 2) mainly clastics representing deltaic deposits, rate of sedimentation being rapid (Jhuran and Bhuj Formations). The first sedimentary sequence of Biswas (1981) mentioned above is identified as a Megasequence developed during the second order transgressive cycle of Tethys over the Kachchh Basin. The lower

boundary of this megasequence is not exposed in the Kachchh Mainland and the upper boundary is characterized by the unconformity developed on the upper surface of Dhosa Oolite. This megasequence are divided into three depositional sequences that are stacked in to lower retrogradational to upper progradational pattern. The Jhurio Formation with a thickness of 278 m. is the lower most formation in the Mesozoic sequence of Kachchh Mainland well exposed in Jhura dome. The exposed lower part of the formation composed primarily of bedded limestones with intercalations of calcareous shale and oolitic ironstones (golden oolitic limestones), and siliciclastic deposits with laminations of evaporites at the top and has been identified as a third order sequence, named, Sequence-I. The siliciclastic deposits capping the calcareous shale and thin bedded limestone towards the top was deposited in a transgressive environment. The lower boundary of the this third order sequence (Sequence-I) is not exposed and the upper boundary is an erosional surface and ferruginous hard ground surface developed on the upper surface of the fossiliferous sandstone. The Sequence - I and its parasequences are studied and described in detail. The Sequence-II, starts from the base of calcareous shale (of Jhurio Formation) up to the upper boundary defined by erosional surfaces and hard ground features seen on the Ridge Sandstone. The Sequence-III starts from the top of Ridge Sandstone up to its upper boundary defined by the upper surface of Dhosa Oolite developed during the peak of the major transgression, which is the upper limit of Jumara Formation. The Sequence-II and Sequence-III are identified as depositional sequences developed during third order sea-level cycle. Both these sequences make the Jumara Formation (of Biswas, 1977) in Kachchh Mainland. Due to the limitation of time and availability of good exposures, the parasequences of Sequence-II and -III are not identified and described in details. The present study focuses

attention mainly on the development of parasequences of Sequence-I and its diagenetic properties in a fourth to fifth order sea-level changes.

The Sequence-I was deposited under a transgressive-regressive sea-levels of Tethys during the fragmentation of Gondwanaland. The carbonates, oolitic grainstones, and calcareous shale facies deposited during the major transgressive sea-level and the top portion has deposited during the regressive sea-level.

7.2.2. Fourth and Fifth Order Sequences or Parasequences of Sequence-I

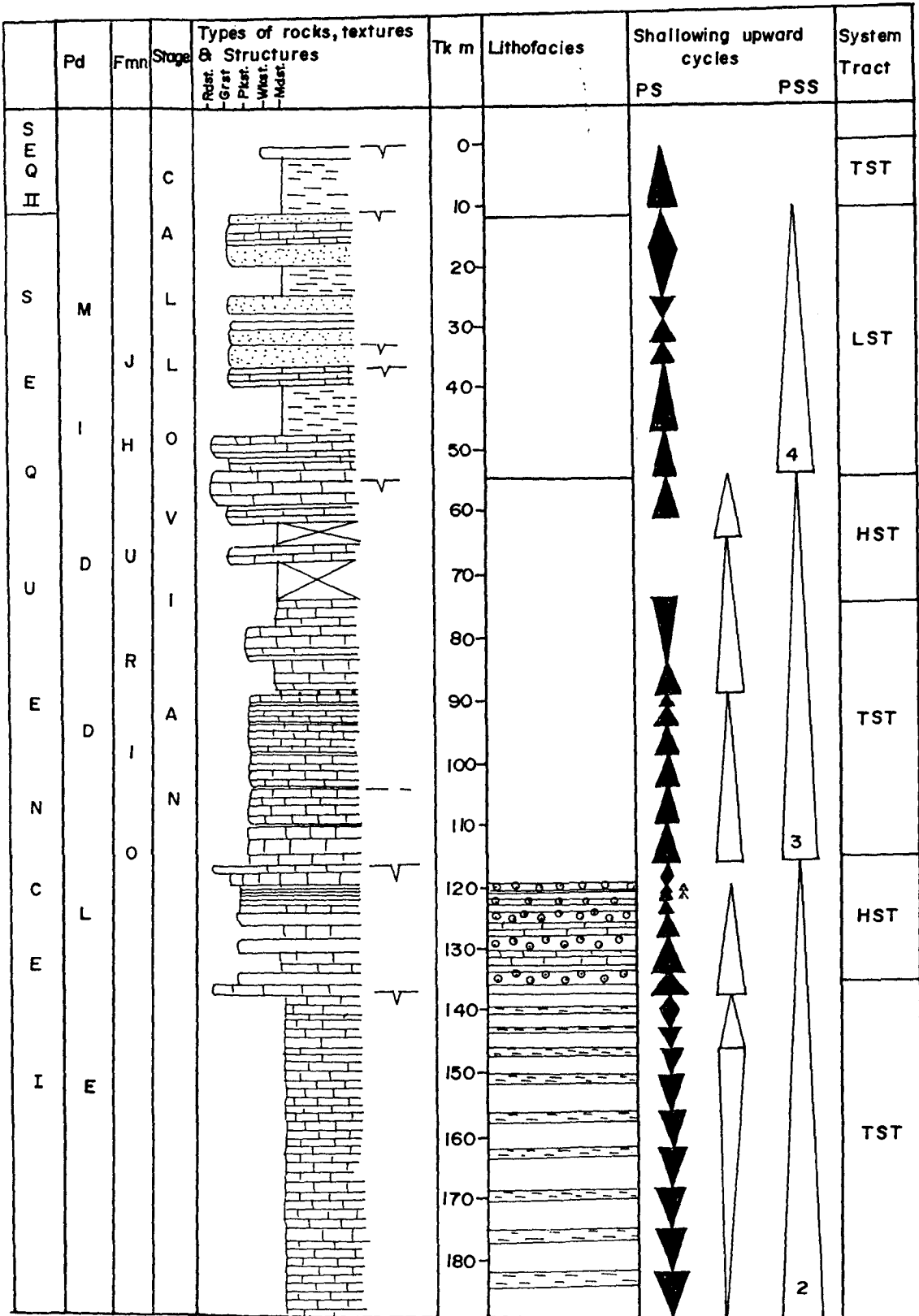
With in many third order carbonate sequences there are commonly metre-scale shallowing upward units, termed parasequences resulting from the fourth/fifth order relative sea-level changes on a shorter time-frame (10,000 - 100 000 years mostly). Usually sequences consist of many tens or even hundreds of metre-scale parasequences and in some instances they are bundled into packets of four to six. Eventhough the facies with in parasequences vary in different formations, they nearly show shallowing upward trends. Parasequences are generally the result of transgressive-regressive events, with most of the sediment deposited during the still stand/regressive interval. Most carbonate parasequences have an upper surface recording emergence, but the length of time represented here is generally relatively short (a few thousand years perhaps), especially compared to many sequence boundaries. Parasequences commonly display systematic changes in thickness and facies through a sequence.

The third order sequence, Sequence-I (Jhurio Formation), was deposited during Middle Jurassic Period (Bathonian to Callovian Age). Shallowing upward parasequences deposited during fourth-order (0.1 - 1 My) to fifth order (0.01 - 0.1My.) relative sea-level cycles are the fundamental building blocks of sequence stratigraphy.

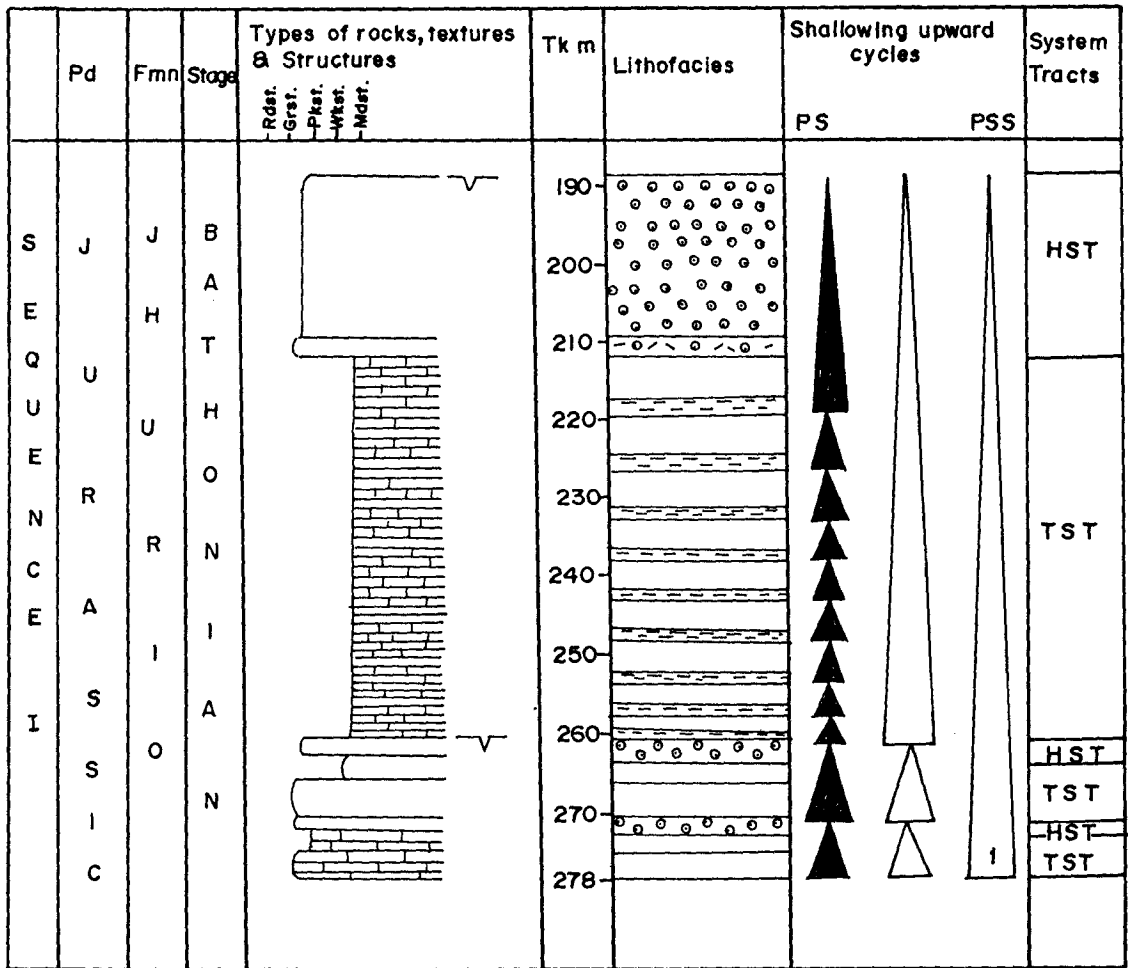
The fourth and fifth order sequences can be identified as different parasequences can be divided in to four parasequences sets. The parasequences are identified by the lower maximum flooding surface and upper subaerial exposure surface or break in sedimentation such as hard ground surface, etc. The parasequence sets are identified by the rhythmic deposition of a set of similar cycles which are bounded at the base by maximum flooding surfaces and the top by subaerial exposure surfaces. The cyclic sedimentation in the Sequence-I is of hemicyclic type (ABABAB; Wilson, 1975).

Fig.7.1 shows the parasequences, and parasequence sets in temporal scale. The sequence was deposited over the Precambrian basement in the Kachchh basin during the Bathonian to Callovian Age, due to the transgression of the Tethys sea. The types of parasequences identified are given in the Fig. 7.2. Different parasequences are stacked in to four parasequence sets numbered as PSS-1, -2, -3, and -4. The Microfacies distribution shown in the Fig. 4.2 also given for the proper understanding of the cyclic units. The parasequence set-1 (PSS-1) comprises 3 parasequences. Subtidal bedded lime mudstone (MF-20, -20, & -23,) passing up in to oolitic packstone-grainstone (MF-10) deposited in a shallow shelf to deep shelf slope environment to high energy shallow marine shoal environment. The three parasequences are characterized by the similar cycle pattern. Initially the sedimentation was slow and then subtidal facies dominated over the marginal marine grainstones in the PSS-1. The parasequence was deposited during the initial transgression of the sea. The thin bedded grainstones are indications of the still stand of the sea during which the water depth was low due to carbonate build up within the shelf region. This parasequence set is formed during the initial transgression of the Tethys sea. The subtidal microfacies is characterized by the presence of pelagic fauna such as planktonic foraminifers and pelagic bivalves, and peloids which are indicative high water depth. The upper part of the subtidal facies

Fig. 7.1



71.



Pd : Period ; Fmn : Formation ; Tk : Thickness

PS : Parasequence ; PSS : Parasequence set.



Limestone



Sandstone



Oolitic limestone



Oolitic Intraclastic limestone



Calcareous shale



Ooids



Intraclasts



Subaerial exposure surface



Shallowing upward parasequence



Deepening upward parasequence

Trend of Facies

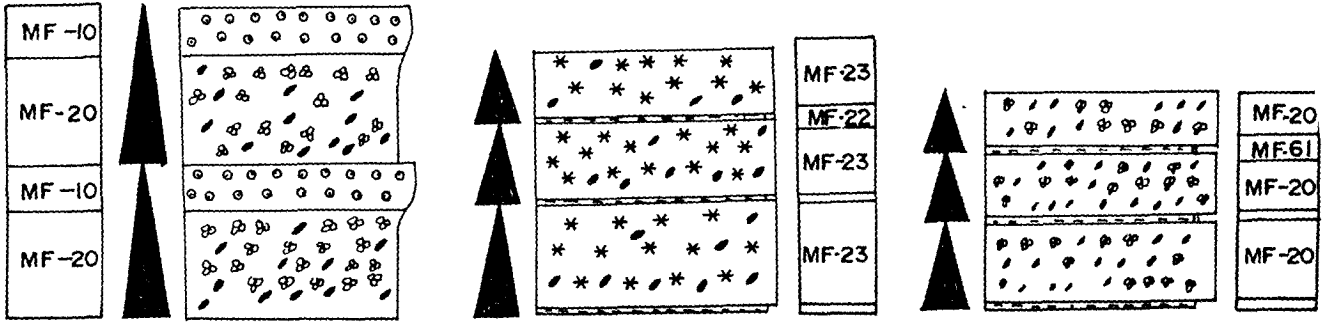
TST Transgressive system tract

HST Highstand system tract

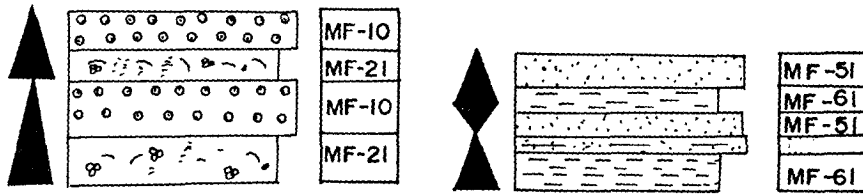
LST Lowstand system tract

Fig. 7.1 Facies distribution and shallowing upward cycles stacked in a system tract model of sequence -I (Jhurio Formation) Kachchh Mainland

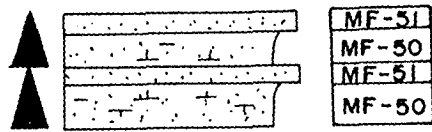
1. Subtidal cycles



2. Peritidal cycles



3. Intertidal - supratidal cycles



- | | | | |
|----|----------------------|---|-------------------------|
| ⊙⊙ | Ooids | ▨ | Sandstone |
| ⊕ | Peloids | ▩ | Calcareous sandstone |
| ⊗ | Foraminifers (small) | ▲ | Shallowing upward cycle |
| ** | Crinoids | ▼ | Deepening upward cycle |
| ⌘ | Algae | | |

Fig.7.2 Types of shallowing and deepening upward cycles [Parasequences] in Jhurio formation

shows the characteristic association of benthic foraminifers and larger peloids. The subtidal facies of PSS-1 is capped by the thick bedded oolitic packstone-grainstone facies(MF-10), which are indicative of near shore shoaling and subaerial exposure.

The PSS-2 comprises alternations of pelagic limestone (foraminiferal packstone-grainstone microfacies: MF-20) and hemipelagic mudstone (MF-61) which were deposited during the transgressive sea soon after a stillstand. The PSS-2, also imitates the rhythmicity of PSS-1 and its characteristic fossil assemblages are mainly planktonic foraminifers and pelagic bivalves at the bottom and its association with peloids and benthic foraminifers and crinoidal types towards the top. The PSS-2 is capped by the thin parasequences (five) of bioclastic peloidal mudstone(MF-21)/oolitic packstone-grainstone microfacies (MF-10, -11) which were deposited during the stillstands of the sea.

The PSS-3 was deposited during transgressive system tract. The parasequence set comprises parasequences with lower thin bedded algal foraminiferal peloidal mudstone-wackestone fenestral laminated microfacies passing in to crinoidal peloidal packstone-grainstone. The lower thin bedded (5 to 15cms. thick) wackestone-mudstone could be deposited in a basinal marine environment as it is indicated by the smectite rich laminations and rim cementation. Where as the overlying thick bedded packstone-grainstone microfacies deposited in the outer shelf slope. The parasequence is formed by the transgressive system tract representing the fourth and fifth order cycle pattern.

The PSS-4 represents a low stand system tract during which the sea-level has fallen across the Kachchh basin either due to the gradual or sudden upliftment of the basin or due to the effect of climate which has brought to the high input of siliciclastic sediments through the nearby proxies in to the carbonate factory and there by interrupting the carbonate production. The gypseous shale, calcareous sandstones and

sandy limestones are the main facies elements formed during this low stand system tract. The gypsum laminations in the shale facies indicates a hot and arid climatic condition when the sea level has fallen and the sandy limestone and calcareous sandstone and pure sandstones were deposited in this intertidal-supratidal facies. The regressive features in the different microfacies are the dolomitisation, corrosion by the ferruginous matrix, worn out and corroded bioclasts, cementation by the evaporites and the replacement of the carbonate grains by evaporite minerals.

7.2.2.1. Terrigenous clastic input

The most important factor in the sequence development of Jhurio Formation is the high terrigenous clastic input towards the upper part of the Sequence-I. The terrigenous clastic input separates the depositional conditions into two environments. The lower shallow marine subtidal and the upper intertidal-supratidal depositional conditions. In the general sequence stratigraphic model for mixed systems, the input of clastic is generally considered typical of low stand of relative sea-level and fluvial, deltaic and coastal plain environments are characteristic. Whereas the thick shale beds must have formed in a moderate to deep water on a shelf basin. The main terrigenous constituents are the quartz and clay minerals. The insoluble residue studies indicate that quartz is the most abundant mineral constituent in almost all the microfacies studied in the vertical section of Jhurio Formation. Whereas the smectite is noticed in the fenestral laminated algal foraminiferal wackestone-mudstone microfacies. This is a characteristic microfacies indicator of basinal depositional environment. Except in the Member-G in all other members the IR content is less than 15% while in the Member-G the IR content above 30-60%. Mostly these may have been major influxes of siliciclastics during development of a carbonate platform (Spence and Tucker, 1999). This is usually in association with the formation of a type 1 sequence boundary on a

rimmed shelf when coarse clastics may be introduced and bypass the platform to constitute lowstand fans (Spence and Tucker, 1999). During deposition of carbonates generally, fine-grained siliciclastics are deposited in the basin as hemipelagic muds and these may form thick units, especially if there is an axial supply.

7.2.2.2. Parasequence types and its boundaries

Thin repeated units, on a scale of 1-10m, are usually referred to as cycles (or cyclothems or rhythms), or in sequence stratigraphy terminology, parasequences. They were deposited over time spans of a few tens of thousands to hundreds of thousands of years. Parasequences are building blocks of sequences which are generally on the scale of many tens to hundreds of meters in thickness, deposited over a time span of 0.5 - 3 million years (Tucker and Wright, 1990). The parasequences identified in the Sequence-I are three types depending upon the condition of deposition. These are subtidal cycles, peritidal cycles and intertidal-supratidal cycles. The subtidal cycles are given in the Fig.7.2. The main types of subtidal cycles are, one, calcareous shale passing up in to bedded lime mudstone (peloidal packstone-grainstone), second is lime mudstone (peloidal packstone) passing up in to oolitic packstone-grainstone (MF-10) and the third type is the thin bedded fenestrate laminated algal foraminiferal peloidal mudstone-mudstone (MF-22) passing up in to thick bedded foraminiferal crinoidal packstone-packstone-grainstone (MF-23) facies. These subtidal parasequence shows few repeated cycles and generally the stacking pattern is a shallowing upward of the facies. During the beginning of the deposition of facies the environment was shallow shelf marine in the case of the second type and in the case of first and third the environment was deep basinal which pass in to the very shallow shoaling environment. Thus in all these parasequences the trend of system tracts are shallowing upward facies. Intertidal transgression is there by followed by a still

stand and soon after the peak of high stand^{and} the surface either exposed subaerially or lithified in the shallow oxidising conditions.

Subtidal parasequences, in most cases were not subaerially exposed, but shows evidence of shallowing and pause in deposition in the form of intense bioturbation or hard ground with encrusting and boring organisms. The base of cycle is usually a flooding surface. The cycle boundaries are identified considering the coarsening upward grainsize patterns (shallowing upward trend) and also the repetition of cycles and their microfaeces characteristics.

The peritidal cycles include, two parasequences types, the first one shallow shelf marine bioclastic peloidal wackestone-mudstone (MF-21) which passing in to oolitic packstone-grainstone (MF-10) and the second one the gypseous shale (mudstone) passing in to the sandy bioclastic grainstones. The cycles are developed in a marginal marine condition. Therefore, the identification of cycle boundary is comparatively easy and well documented. The cycle boundary in the first case can usually be identified as coarsening upward trend which indicates a shallowing upward cycle development. In the case of second type also the coarsening upward trend gives shallowing upward direction of facies.

Development of lag deposits (MF-30) at the boundary is the evidence of maximum flooding surface in the intertidal-supratidal conditions. The intertidal-supratidal cycles include sandy limestone passing over to calcareous sandstone and also calcareous limestone passing over to ferruginous sandstones and sandstone passing to conglomerates. These intertidal-supratidal cycles are represented by very few cycles or mostly presence of single cycle in the Jhurio Formation.

7.2.2.3. Parasequence Stacking Pattern and System Tract Model.

The four parasequence sets are stacked into a retrogradational pattern at the lower and progrades at the upper part of the Sequence-I of Jurassic of Kachchh developed during the third order relative sea-level. In this mixed carbonate-siliciclastic sequences, carbonate sedimentation usually lagged behind the transgression across platform tops. If siliciclastic input is great, transgressive shelf deposits may consist of carbonate sequences overlain by condensed marine shales and a progradational highstand fluvial deltaic strata. This is a suitable model for the Jurassic of Kachchh, as according to Biswas (1981) two distinct sedimentary sequences are observed in the Kachchh Mainland in a broad lithofacies context: 1) shales and carbonates, deposited in sub-littoral environment where rate of sedimentation being slow (Jhurio and Jumara Formations) and 2) mainly clastics representing deltaic deposits, rate of sedimentation being rapid (Jhuran and Bhuj Formations). The retrogradational-aggradational stacking pattern is observed in the parasequence sets, PSS-1, -2, -3 and -4. These retrogradationally stacked parasequences were deposited during the transgressive system tracts. In the fourth order relative sea-level changes over a mixed siliciclastic-carbonate basin each parasequence set is formed during transgressive phases is characterized by the development of aggradational parasequences developed in a third order sea-level rise.

Platform interior transgressive system tracts comprise stacked parasequences of shallowing upward facies. In these shallowing upward trend of facies lag conglomerates with bored, worn, encrusted or mineral-stained clasts derived from underlying material are common and these may be succeeded by freshwater pond or marine facies (Enos and Perkins, 1979). Transgressive parasequences, in the case of Sequence -I, are cyclic and they shallow upward in to intertidal supratidal environments with muddy or grainy

caps. Similar to siliciclastic examples (Van Wagoner et al., 1990), carbonate parasequences are bounded by marine-flooding surfaces or their correlative surfaces.

These flooding surfaces may form the upper boundary to subtidal, intertidal and supratidal portions of sequences. The lag deposits form the base of the parasequence sets in the Sequence-I, Kachchh Mainland. These lag deposits are characterized by the conglomeratic lithoclastic limestones with corroded and worn out bioclasts and lithoclasts. Condensed deposits may occur atop platforms during maximum transgression (Loutit et al., 1988, Wendt, 1988). These sediments are thin when compared to the very low sedimentation rates or non-deposition, long subaerial exposure, erosion and reworking.

An interesting and effective mechanism for the development of carbonate platform during the transgression of sea is explained in Kendall and Schlager (1981). A relative rise of sea-level over a carbonate platform will lead to sediment starvation and platform drowning. Start up of the carbonate factory lags behind initial transgression. Once water depth is great enough for adequate circulation, sedimentation production catches up with sea-level rise to aggradational or progradational shallowing upward successions of organic build ups, grain-shoals and tidal flats along shelf edges and shoreline. Progradation may eventually stall as a result of building out in to a deeper shelf during a continued rise of sea-level subsequent flooding and catch up sedimentation follow and when repeated the result is a transgressive systems tract made up of an aggrading or retrogradational parasequence set is more likely to occur when the sea level is reached. The carbonate build up in the three parasequence sets in Sequence-I, Kachchh Mainland can be explained based on the above mechanism.

During the deposition of Parasequence Set-1 (PSS-1) the basin was initially very shallow with a deposition of thin bedded subtidal cycles in a shallow shoaling and

lagoonal environment. The thin-bedded limestone with interbeds of calcareous shale of subtidal facies is thus overlain by the oolitic grainstone facies (MF-10, 11). This cyclic sedimentation started during the initial transgression of Tethys. Then the water depth increased slowly due to the rise in eustatic sea-level. The condensed sections of pelagic bedded limestone/hemipelagic calcareous mudstone deposited during this transgressive system tract (TST). This led to formation of Member-B in the Jhurio Formation (see, Biswas, 1977). Since the transgression continued with a rate which was much more than the rate of sedimentation, very thin condensed sections were deposited during a large span of time. The sedimentation in Kachchh Basin started during the Bathonian Age. From the Jurassic global regressive-transgressive trends (Vail et al., 1984; McGhee & Bayer in Bayer & Seilacher, 1985), it may be understood that the sedimentation rate was very low (<1 cm/Kyr.) during the Bathonian Age. This has been well documented by the thin parasequences of bedded limestone/calcareous mudstone deposited during the transgressive system tract. The thinness is due to the low sedimentation and the deposition was well below the euphotic zone which is evidenced by the lack of micritic envelopes and calcareous algae.

The carbonate factory was active till the carbonate build up reached near the sea level. This occurred during the catch up phase when the accumulation exceeded the rate of sea level rise. During this period circulation was enough for adequate sedimentation and production often catch up with sea level rise to form aggradational shallowing upward cycles. Thus in a third order sea level rise, fourth to fifth order sea level taken a highstand system tract. Accordingly oolitic packstone- grainstone microfacies, regressive facies, were deposited over the transgressive deposits. The water depth became shallow and due to aggradation of the sea floor and progradation of shoals and shallow mounds. The condensed oolitic grainstone facies mark a stillstand at the peak

of transgression. The energy conditions were high in the shallowing sea level over the transgressive deposits which lead to the oolitisation of bioclasts, peloids and intraclasts. Thick oolitic deposits were formed which show a gradation in the ooids deposited in this highstand system tract and thus indicates a larger time span of this highstand condition and the rate of sedimentation equaling with the rate of subsidence. Oolitisation continued till the subsidence rate increased than that of the rate of sedimentation. Thus the water depth over the basin increased due to eustatic sea level rise.

Thus the transgressive facies was deposited in the PSS-2 during the TST when the platform drowning occurred due to subsidence of the basin and subsequent global sea level rise (Member-D). The transgressive system tract followed with the deepening up of the trend of facies till the carbonate build up catch the sea level. Thus oolitisation followed in the highstand system tract forming peritidal cycles deposited in a subtidal lagoonal condition to the shallow shoaling environment. Thus at the top of PSS-2 five parasequences were formed during this highstand system tract (Member-E, Fig.7.1). The rate of sedimentation was very slow and it kept pace with the rate of subsidence due to which very thin deposits of oolitic grainstone/bedded limestone deposited.

The subaerial exposure and the development of maximum flooding surface on the top of it terminated the highstand system tract. Thus characteristic lag deposits comprises are worn bioclasts and ferruginous coatings over the bioclasts. The transgressive system tract during which crinoidal limestone/lime mudstone with fenestral laminae are deposited in a shallowing upward facies follows this. This is followed by the thin oolitic grainstone and bioclastic grainstone at the top and finally lead to the subaerial exposure during the highstand system tract and formation of lag deposits. This

highstand system tract is followed by a lowstand system tract (LST) during which mixed carbonate-clastic-evaporite facies belt (Member-G) were formed in an intertidal-supratidal environment. The evaporites were formed within the shale bed forming thin laminations separating the thin fine-grained sandstone beds from the shale. This thin lamination of evaporite indicates an arid evaporitic condition towards the end of the formation of Sequence-I in lowstand system tract. The upper boundary of the Sequence-I is thus demarcated by the erosional and hardground surface seen over the ferruginous sandstone. Thus the parasequences developed during this third order fall, might be late HST or early LST, shows thinning upward trend and intertidal facies are observed as dominated over the subtidal facies.

7.3. DEPOSITIONAL MODEL FOR MIDDLE JURASSIC

The stacking pattern of parasequence in the parasequence sets of Sequence-I of Middle Jurassic of Kachchh basin reveals the system tract model for the fourth-fifth order sea level of Tethys. The stacking pattern of facies of Sequence-II and III reveals the third order sea-level fluctuations during the Middle Jurassic. In the earlier works it is explained that the transgressive megacycle starts with the initial transgression of sea over Kachchh graben in (?) Bajocian (see Jaikrishna, 1983) or even before that, that is Aalenian (Dubey & Chatterjee, 1997) and continued cyclically till Oxfordian. While from the sedimentological expressions the transgressive deposits are recorded from the early or Middle Bathonian (see Biswas, 1981,1987). During this cycle the Jhurio and Jumara Formations were deposited near the depocentre of the basin (Mainland).

Middle Jurassic succession of Kachchh Mainland is represented by the upper part of the Jhurio Formation and the entire Jumara Formation and exposed in the E-W trending eroded domal structures (Jumara, Jhura and Habo domes from west to east). The temporal and spatial study of these facies assemblages on different aspects such as

petrography, geochemistry and mineralogy has given detailed understanding of the microfacies types, its distribution and depositional environment, and also the variation in the depositional environment with respect to the change in global sea level.

The microfacies types and its vertical and spatial variation is understood from the petrographic studies (Fig. 4.2). The microfacies types are indicative of palaeobathymetry and palaeoecology of the depositional environment. Other frame works such as oolite and peloids are also used as facies indicators. Thus subtidal microfacies types of carbonate parasequences and sets of Middle Jurassic of Kachchh Mainland are characterized by the well preserved and early diagenetised peloids and true faecal pellets and the planktonic fossil assemblages and pelagic fossil grains, such as smaller foraminifers, pelagic bivalves with benthic foraminifers and crinoidal echinoidal assemblages towards the shallowing up of the subtidal facies. The abundant oolites, coarse intraclasts and the large bioclasts of brachiopods and molluscs, etc. are the characteristics of the peritidal facies. Intertidal facies are well documented by the thick bedded shale passing in to thick bedded sandstones with thin evaporite as observed in the upper part of the Sequence-I and in the Sequence II and III. The microfacies analysis thus indicates a major transgressive third order sea level till the end of the deposition of PSS-3 in the Sequence-I with several periodic stillstands of the sea during which the fourth-fifth order transgressive-regressive subcycles are formed. The PSS-4 represents a fourth order sea-level fall with the build up of thick clastic wedges with thinner carbonate facies.

The clastic textural study suggests a mixed depositional condition of fluctuating coastal beach-shallow marine environment. The clastic sediment deposition was abundant during the uppermost part of the Sequence I and most part of the Sequence-II and Sequence-III. The Ridge Sandstone deposited during the third order sea level fall

culminating the deposition of Sequence-II is the characteristic regressive facies deposited in the Kachchh Mainland. The average grain size of these rocks resembles that of near shore, beach shallow marine sands. In general the clastic grains are moderate to well sorted, negative to positively skewed and mesokurtic in nature. Standard deviation values according to Friedman (1962) fits into the category of moderately sorted to well sorted sand; and are similar to those of the beach sands. Friedman (1961) and Folk (1968) have suggested that, the beach sediments owing to the influence of swifter currents are better-sorted (low values). The near symmetrically skewed values of the sands probably indicate beach-shallow marine high energy condition, and displays the variations in the grain size and sorting of these clastics from east to west. Although the general grain textural characteristics suggest a beach-shallow marine depositional environment, the oscillating nature of the depositional environment can be clearly shown by the vertical variation in the size and sorting values.

The grain size data plotted on various standard bivariate and multivariate discriminatory plots (Figs.5.2a-d, 5.3 and 5.4) suggest a beach to shallow marine environment of deposition of these rocks. The clustering of the sample data points (dashed area on the CM plot in Fig. 5.4) resembles the pattern of Passega (1957) given for sediments. The original form and abrasion history during transportation control the sphericity, roundness and surface texture of the clastic sediments. The near spherical and subangular to subrounded nature of these clastic sediments indicate considerable reworking and transportation before their final deposition.

The Middle Jurassic succession of Kachchh Mainland shows a clay mineral association, which includes the lower montmorillonite-chlorite-illite assemblage, the middle kaolinite-illite assemblage and the top illite chlorite assemblage. The insoluble residue(IR) analysis of carbonate of Jhurio Formation indicates the abundance of quartz

over the clay minerals. The clay mineral assemblage in the IR is basically montmorillonite, illite, chlorite and Kaolinite. Kaolinite and chlorite are present as interlayered in the carbonate rocks. The subtidal facies with outer shelf faunal assemblages show montmorillonite-illite-chlorite assemblage, while inner near shelf facies show montmorillonite-illite-Kaolinite+chlorite assemblages. The peritidal facies, oolitic grainstones are important facies indicators with their low content of clay mineral assemblages. The montmorillonite-chlorite-kaolinite clay mineral assemblage occurs in less than 1% of the total insoluble residue content, which indicates the high energy conditions in shallow shoaling environment which lead to the washing away of the finer fractions. However, the iron oxide coating of original aragonite ooids occurred in a chemically active environment.

The association of different types of clay minerals within the Middle Jurassic succession is indicative of the oscillating nature the depositional environments from typical shallow marine to lagoonal environment having continuously affected by the flow of fresh water. The postdepositional changes in different facies assemblages have resulted the complexity in the clay mineral association. Marine diagenesis results in a mixture of illite and montmorillonite, where as the kaolinite is formed under continental and near shore acidic environments. In deep burial diagenesis kaolinite and montmorillonite gradually change to chlorite under an environment rich in Fe and Mg and to illite with K rich environment. The kaolinite mineral could have been formed by the alteration of feldspars transported by minor currents in to near-shore environment, where there was a continuous supply of fresh water. The occurrence of kaolinite also suggests a fairly intense chemical weathering of the source area and acidic condition of the depositional basin.

The geochemical analysis also support the migration of facies from a shallow to deep shelf marine, with the deposition of retrogradational parasequence sets, to intertidal near shore-beach environment characterized by the deposition of progradational parasequence sets through peritidal shoaling environment with the deposition of aggradational oolitic grainstone/peloidal wackestone parasequence sets. The high content of Si in the upper part of the Sequence I and Sequence II shows the LST clastic wedges. The high content of K and Na within fine grained and clastic facies types indicate the weathering and erosion on the hinterland areas. The Na and S are high in some of the subtidal facies especially those parasequences which make up the lower part of the shallowing upward cycle, indicate the restricted deep lagoonal environment with anoxic conditions. The rare earth elements also indicate the paleoceanographic and palaeoclimatic condition characteristic of a shallow marine shelf basin.

The combined lithofacies distribution (Fig.3.3) the petrographic, textural, geochemical and mineralogical studies together with the analysis of temporal microfacies distribution (Fig.4.2) the stacking pattern of parasequence sets and sequences (Fig.7.1) and a system tract model can be a suitable depositional model for the Middle Jurassic of Kachchh Mainland. This depositional model can be explained basically with the consideration of various frame work elements, relations of different biota to their ecology and the compositional maturity of the framework elements, etc. Vertical stratigraphic columns have been utilized for the graphic representation of the submarine topography at a given time and the carbonate production rates could be understood with temporal and spatial changes. Temporal changes in the relations between submarine relief and sea level are neither directly related to transgressions and regressions (Heckel, 1980), nor do they represent the effects of any tectonism. Thus a depositional model has been proposed transposing the stratigraphic sections in to

horizontal sections by the application of Walther's Law of Facies Correlation (see, Middleton, 1973). The Fig. 7.3. explains the different facies development and migration which can be correlated with the system tract model (Fig.7.1). Since Water depth is the single most factor that controls the depositional facies the transgressive facies are developed under a rising sea level curve. While the Highstand is represented by a lowering curve (does not mean the falling sea level) represents the decreased water depth due to catch up of the carbonate build up with the still standing/slow rising sea level. While low stand system tracts are characterized by the development of thick coarser clastic capping the marine mudstone facies.

The depositional model (Fig.7.3) shows that Sequence I deposition is initiated during Middle Bathonian and culminated during the early Callovian with different parasequences stacked in it. The three sequences were developed during the three major transgressive-regressive third order sea level changes, which was characterized by various minor transgressive-regressive phases of fourth to fifth order sea level change which lead to the deposition of different parasequences which are stacked in a shallowing upward trend mainly, in different system tracts characterized by the microfacies distribution (Fig. 7.1 and Fig.7.2 & Fig. 4.2).

The base of Sequence-II is characterized by the thick calcareous shale deposited during the transgressive system tract. While, Late Callovian regression is indicated by a thick sequence of sandstone and conglomerate in the middle part of Sequence II (Jumara Formation) (Biswas, 1987). The upper boundary of the Sequence-II thus is characterized by the deposition of this thick sandstone sequence, the Ridge Sandstone. The Ridge Sandstone' was deposited during the third order sea level fall due to the major regressive phase of Tethys from the Kachchh basin. The oolitic grainstone and the Ridge Sandstone were deposited during the highstand system tract

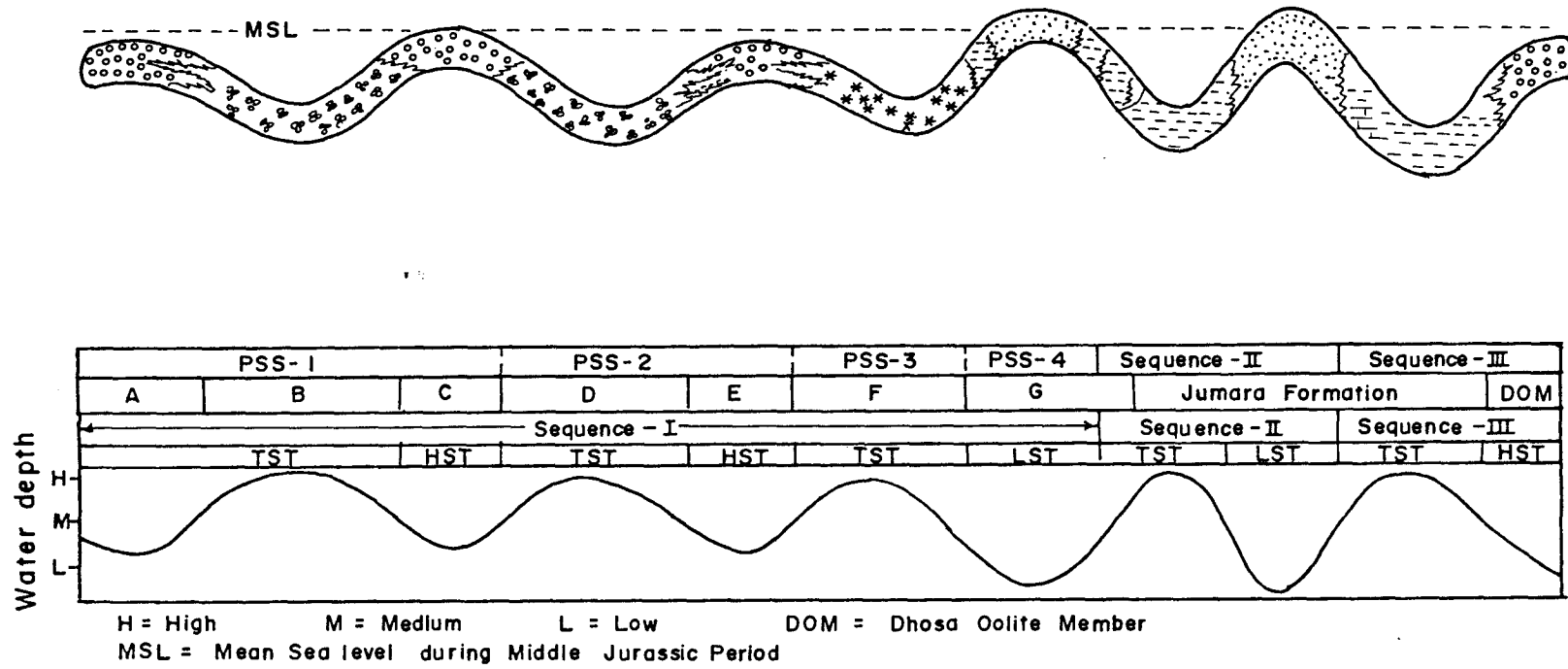


Fig. 7.3 Facies Depositional model of Middle Jurassic Megasequence of Kachchh Mainland

followed by the lowstand of the third order sea level. The shale deposits of Sequence-III were deposited during the further transgression and which has reached its peak of transgression during Oxfordian and oolitic grainstone facies, Dhosa Oolite, were formed during this highstand system tract. This regression is marked by the deposition of silty oolitic limestone beds of the Dhosa Oolite Member in the Mainland (Biswas, 1987). Thus the deposition of Sequence-III was culminated during the end of Oxfordian time which is characterized by the characteristic unconformity surface developed over the Dhosa oolite Member separating the transgressive Megasequence of Kachchh Mainland from the Upper regressive Megasequence (Jhuran and Bhuj Formation).

7.4. DIAGENETIC MODEL: PARASEQUENCE AND SEQUENCE SCALE

The diagenesis of carbonate sediments has been a major topic of research for many decades, with the fundamental observations being made by Sorby way back in the mid-19th century. Thus there is an extensive literature on carbonate diagenesis, and this has been reviewed in Moore (1989), McIlreath and Morrow (1990), Tucker and Bathurst (1990), Tucker and Wright (1990) and Tucker (1991a). The similar way that the facies models were developed in the 1970s, there has been little attempt made to produce diagenetic models which are useful for understanding and predicting the paths of carbonate diagenesis and also for the prediction of porosity which is one of the main factors in hydrocarbon reservoir potential.

With the development and widespread application of sequence stratigraphy in the last decade, it is possible to integrate carbonate diagenesis into pattern of relative sea-level change, which are the underlying control on the formation of sequences and their system tracts (Wright, 1990). Two other factors of great importance to the type of diagenesis affecting a limestone are the prevailing climate and the carbonate sediment mineralogy. Carbonate mineralogy has a major influence on diagenetic

potential and is controlled by sea water chemistry, environmental conditions and the skeletal evolution/extinction. Climate, sea water chemistry, carbonate sediment mineralogy and even the nature of sequences themselves and the patterns of relative sea-level change, have all varied through geological time and thus carbonate diagenesis has also varied through time. From the sequence stratigraphic approach it is understood that the change in sea-level is important not only for the developing facies, but also for already deposited facies units which are greatly modified by the post-depositional changes with respect to change in relative sea level across the basin.

Transgressive parts of a parasequence would be expected to show marine diagenetic textures, whereas regressive part would show the effects of surface related diagenesis, such as palaeokarstic surfaces, laminated crusts, leached bioclasts and other framework elements such as ooids, etc., if the climate was humid and meteoric diagenesis was operative or supratidal/evaporative dolomite crusts, pisoids and botryoids, and displacive gypsum, if the climate is arid (Wright, 1990). These features are well documented in the parasequences of Sequence-I and in the Sequence-II and Sequence III. A diagenetic model is developed for the Middle Jurassic mixed carbonate-siliciclastic-evaporite sequences from the depositional model of the same.

In Sequence-I the parasequences are stacked in to retrogradational type with aggradational type of parasequences sandwiched in the former and later build up in to progradational type in the upper part of the Sequence-I and in the Sequence II and III. The retrogradationally stacked subtidal parasequences in the Sequence-I show evidences of marine diagenesis such as abundant micrite mud and fringe cementation over the grains. Where the parasequences are arranged in to retrogradational type early marine and/or meteoric diagenesis will be followed by shallow to moderate burial in marine pore water.

The peloidal mudstone-packstone-grainstone (MF-20)/calcareous mudstone (MF-61) subtidal parasequences exhibit the evidences of early marine diagenesis such well preserved faecal pellets and micritised peloids and bioclasts with micrite rims (Plate 4.2-1&2) This has followed by the shallow to moderate burial diagenesis with the preservation of syntaxial cementation and partial dolomitisation (Plate 4.1-4) The syntaxial cementation and partial dolomitisation of peloidal grainstones are due to the effective circulation of marine pore water within the thick calcareous mud rich deposits.

In the peritidal facies, the aggradational oolitic packstone-grainstone facies capping the transgressive facies types showing aggradational stacking pattern. Where the parasequences/sequences arranged in to aggradational parasequence/ sequence set, then the early diagenetic processes (marine and/ or meteoric) will be followed by burial diagenetic processes, with the former determining the path of the latter. In the vertical stack of carbonate platform in the initial transgression of Tethys over Kachchh basin, TST aquicludes of lime mudstones (Peloidal packstone-grainstone/calcareous mudstone microfacies) are capped by the confined aquifers such as porous oolitic packstones-grainstones. Thus meteoric water reaches the sedimentary package through the porous grainstones from the hinterland areas. Thus meteoric diagenesis followed the marine diagenesis and evidences are seen in the oolitic grainstones and oolitic intraclastic bioclastic grainstone with leached oolites and bioclasts (Plate 4.3-2; 4.6-1) So during the intense fresh water diagenesis of capped grainstones fresh water percolated to the underlying thick lime mudstones (peloidal mudstone-packstone-grainstone microfacies). The syneresis cracks produced are filled with the coarse fresh water diagenetic calcites (peloidal packstone-grainstone microfacies, Plate-). Since the high stand oolitic grainstone facies followed by the next lime mudstone/grainstone

facies, karst topography developed at the sequence boundaries are occluded by the next TST sediments from succeeding parasequences/parasequence sets.

The diagenetic model of Megasequence can be predicted with the depositional model (Fig.7.3) characterized by the marine diagenetic cementation during the deposition of subtidal cycles during TST followed by the fresh water diagenesis of subtidal facies during the deposition of oolitic grainstone facies during HST. The burial diagenetic process started in the oolitic grainstone and the underlying subtidal facies, when the next subtidal facies deposited during the next phase of TST (Fig. 7.3). This repeats in the diagenesis of sediments of retrogradational succession. While during LST (Fig.7.1 & 7.3) the upper PSS-4 deposited (Fig.7.1) over the HST grainstone, thick clastic facies deposited over (LFA-3). This bring the fresh water access to the lower subtidal and peritidal facies and thus diagenetic stabilization of component grains of both the TST facies and HST oolitic grainstones and bioclastic grainstone microfacies (MF-10,-11 & MF-40). Also the facies units have undergone a mixed marine water-freshwater diagenetic realm occurred prior to the above phase due to the approach of ground water towards the marine basin due to sea level fall (LST)(Fig.7.3) This diagenetic model thus explains the diagenetic changes in the mudstone/Ridge Sandstone cycle and the mudstone/oolitic grainstone (Dhosa Oolite Member) of Sequence -II and Sequence-III (Jumara Formation), forming a explaining a complete diagenetic model from the depositional model (Fig. 7.3) for the Megasequence of Middle Jurassic of Kachchh Mainland.

SUMMARY AND CONCLUSIONS

The sedimentary basin of Kachchh is well known for extensive development of Middle Jurassic Sequence representing variable field characters and petrographic, mineralogical and geochemical composition and accordingly has created a greater interest in their study.

The present study on the Middle Jurassic Jhurio Formation of Kachchh Mainland is an attempt to provide additional information on the sedimentology and microfacies characteristics to decipher the stratigraphic and sedimentary configuration of different rock types exposed therein. The study involves a detailed field and laboratory study of the sedimentary terrain lying to the southwest of Aravallis: identification of stratigraphic units; textural analysis of coarse clastics; mineralogy of finer sediments; microfacies study of carbonate rocks; distribution of trace and rare earth elements; statistical interpretation of geochemical data and finally an attempt towards the reconstruction of palaeoenvironmental and sedimentation history with a sequence stratigraphic approach. The analytical data discussed in earlier chapters is further summarized for a meaningful understanding of the stratigraphy, depositional characteristics and sedimentation history of the Middle Jurassic succession of Kachchh Mainland, western India.

Middle Jurassic succession of Kachchh Mainland is represented by the upper part of the Jhurio Formation and the entire Jumara Formation and is exposed in the E-W trending eroded domal structures (Jumara, Jhurio and Habo from west to east). The upper part of the Jhurio Formation is represented mainly by limestone with shales with interbedded oolitic limestone beds. The limestones are jointed and bioturbated and the golden oolitic interbeds are often conglomeratic in nature. The overlying Jumara Formation is well exposed in all the

three domal structures and is represented mainly by lower carbonate and fine clastic association, middle coarse clastic association with minor shale and limestone and the upper fine-clastic and carbonate lithological associations. The shales at some levels are gypsiferous clays comprising also of other evaporitic minerals.

The lithofacies of the Jhurio Formation have been broadly grouped into three Lithofacies associations (LFA 1 to 3) representing the earlier classified seven members (Member A to G in ascending order) of Biswas (1977). These include the Golden oolitic limestone – Grey limestone lithofacies (LFA – 1; Member A-C), the Pelagic limestone – hemipelagic mudstone lithofacies (LFA – 2; Member B-F)) and the limestone - calcareous sandstone – gypseous shale lithofacies (LFA – 3; Member G) and indicate a fluctuating sea level of the depositional environments.

The overall skeletal and non-skeletal assemblage of the carbonates consisting of abundant molluscs, brachiopods, algae and other skeletal fragments of echinoids, corals and foraminifera, oolites, pellets and intraclasts suggests a shallow marine, high energy environment of deposition probably subtidal and intertidal zones. The carbonate petrographic types (dominating wackestone-packstone followed by mudstone and grainstone types) with variable allochem particles correspond to the standard microfacies SMF-5, 9, 11, 14, 15 and 16 of Wilson (1975) characterizing the facies belts of 6,7,8 & 9.

The study has documented the distribution of two broad microfacies groups, the carbonate and the mixed carbonate-siliciclastic-evaporite facies developed in a subtidal to peritidal depositional and intertidal–supratidal depositional realms and embracing five microfacies assemblages viz., peloidal, oolitic, bioclastic, bio-lithoclastic and mixed carbonate-siliciclastic-evaporite assemblages. These microfacies assemblages indicate marine transgressive features of the depositional environment followed by the later regression during

Middle Jurassic. The microfacies assemblages also exhibit the preservation of four important diagenetic environments, such as marine phreatic, fresh water phreatic, burial and fresh water vadose subsequent to the deposition of the sediments resulted in a variety of cement textures.

The clastic sediment influx was more abundant during the deposition of uppermost part of the Sequence. The sedimentary structures, variation in clastic texture and the grain size data plots (Figs.5.2a-d, 5.3 and 5.4) suggest a beach to shallow marine environment of deposition of these rocks. The clustering of the sample data points (dashed area on the CM plot in Fig. 5.4) resembles the pattern of Passega (1957) given for sediments.

Petrographically, the coarse clastics correspond to Quartz arenite and Feldspathic arenite types with little mud suggesting greater winnowing action of the depositional medium. The mineralogical composition and provenance study in association with their textural characteristic suggest that their derivation from crystalline igneous and metamorphic source (possibly from north and east) after considerable recycling (Fig.4.6 b-c).

The clay mineral association includes the lower montmorillonite-chlorite-illite assemblage, the middle kaolinite-illite assemblage, and the top illite-kaolinite-chlorite assemblage. The association of different types of clay minerals within the Middle Jurassic sequence is indicative of the oscillating nature of the depositional environments.

The geochemical observation of selected chemical parameters suggest in general a normal marine to less saline depositional environment of the with minor hypersaline condition of the depositional area.

The three main types of parasequences, the building blocks of a depositional sequence, are recognized resulting in development of the Jhurio Formation, which are Subtidal, Peritidal and Intertidal-supratidal parasequence types and exhibits a general shallowing upward trend of environment. The pelagic fauna characterizes transgressive part of the parasequence and

facies unit and other features associated with the high water depth. The near-shore fauna and the facies unit characterize the regressive part of the parasequence. Genetically related parasequences are stacked in to Parasequence sets (PSS) which are numbered as 1, 2, 3 and 4 (Fig. 7.1& 7.2). These parasequences are stacked in to a retrogradational stacking pattern at the lower in which oolitic grainstones are stacked as aggradational type and prograded at the upper part of the Jhurio Formation. The Jhurio Formation, is thus named as Sequence-I which is developed during the third order sea level change. The Sequence-II is marked on top by the upper surface of the Ridge Sandstone and the Sequence -III was developed during the peak of transgression followed by the high stand and regression. This is documented by the regressive oolitic grainstones (Dhosa Oolitic limestone). These three sequences are stacked in to a retrogradational to progradational stacking pattern forming a Megasequence (Fig.7.3) developed during Middle Bathonian to Oxfordian during a major second order transgressive-regressive phase. .

The diagenetic model of the Megasequence of Middle Jurassic of Kachchh Mainland explained with the depositional model (Fig. 7.3). The transgressive parasequence/sequence are characterized by the early marine cementation during TST and the regressive part is shown by the coarse sparite cementation during dissolution-reprecipitation during the fresh water diagenesis during the HST and LST. The respective evidences are documented from the facies units, which can be fitted with the depositional model (Fig. 7.1, 2 & 3).

CONCLUSIONS

1. Three Lithofacies associations (LFA 1 to 3) recognized in the Jhurio succession include the Golden oolitic limestone – Grey limestone lithofacies (LFA – 1), the Pelagic limestone – hemipelagic mudstone lithofacies (LFA – 2)) and the limestone - calcareous sandstone –

gypseous shale lithofacies (LFA – 3) indicate a fluctuating sea level of the depositional environments.

2. Sedimentary depositional structural and textural study supports for a fluctuating beach to shallow marine environment.
3. The petrographic observations reveal the presence of a variety of carbonate microfacies assemblages representing the three important microfacies groups viz., Subtidal, Peritidal and Intertidal –supratidal facies indicating a fluctuating sea level during Middle Jurassic.
4. The vertical distribution of the carbonate microfacies and the results of the geochemical and clay mineralogical study further substantiate above conclusions.
5. The cyclicity of sedimentation recognized from the above data which upon application of sequence stratigraphic techniques facilitated the identification of three types of parasequences (Subtidal, Peritidal and Intertidal-supratidal cycles) that form the parasequences sets which are stacked in to the retrogradational stacking pattern (subtidal peloidal microfacies) sandwiched with the aggradational peritidal facies (Oolitic grainstone microfacies) and progrades in to the intertidal –supratidal facies (Sandy mudstone-sandstone microfacies) in the Sequence-I.
6. A diagenetic model has been proposed using the relationship of sea-level changes and the diagenetic signatures.

SCOPE FOR FURTHER STUDY

The present study conducted on the outcropping sequence of rocks in Kachchh mainland reveal a variable nature of rock-types and lithological associations on account of their varying environments of deposition. It is generally believed that most of the hydrocarbons are formed in dark coloured, fine grained, marine sediments originally rich in organic matter, which are likely, to get accommodated in clastic-carbonate associations

(Landes, 1951; Levenson, 1956). Any well developed sedimentary sequence particularly, of the shallow marine to shelf facies is thus worthy of being explored.

The Middle Jurassic sequence of Kachchh Mainland comprise both clastic and carbonate facies followed by mainly sandstone and shales of Upper Jurassic. The entire sequence is characterized by a major transgressive cycle followed by a regression. The sedimentary thickness greatly increases towards west. The variable nature of carbonate rocks in association with coarse clastics and abundant organic material including calcareous algae etc. are considered favourable for inducing conditions for generation and preservation of hydrocarbons. The complex associations of clastic-carbonate sediments within the succession, having abundant organic constituents, variable porosity characters and environments of deposition, favour the conditions of hydrocarbon generation and entrapment. The gradation of carbonate facies suggests the possibility of development of biohermal build up, further down basin. The dark colored shales of Jhurio and the unexposed older formations might form source rocks in the deeper basinal parts of the west. The degree of maturation of the organic content would obviously be attained in the deeper part of the basin due to increased overburden of the sedimentary column. The bedded and the massive sandstones overlying these shales are good and readily available reservoirs.

The present study made on the exposed sequence does not provide any definite indication about the occurrence of hydrocarbons in the area, however, further study in conjunction with the subsurface data will certainly give a better account of the hydrocarbon generation and accumulation potentiality of the basin.

oooOOOooo

BIBLIOGRAPHY

- Abbate, E., Ficarelli, G., Pirini Radrizzani, C., Salvietti, A., Torre, D. and Turi, A. 1974. Jurassic sequence from the Somali Coast of the Gulf of Aden. *Riv. Ital. Palaeont.*, 80: 409-478.
- Adams, A. E., McKenzie, W. S. and Guilford, C. 1984. Atlas of Sedimentary rocks under the microscope; Wiley; New York: 104p.
- Agarwal, S.K. (1957). Kutch Mesozoic: A study of the Jurassic of Kutch with special reference to the Jhura Dome, *Jour. Pal. Soc. India*. V. 2., pp. 119-130.
- Agarwal, S. K. 1975. Kachchh Mesozoic: Some problems and Recent contributions. *Recent Researches in Geology*, 397-414.
- Agarwal, S.K. and Kacker, A.K. (1978). Succession and fossil molluscs of Jurassic rocks near Mouwana Eastern Bela Island, District Kutchh Gujarat, *Recent Res. Geol. V. 4.(Chiplonkar Vol)* pp. 482-492.
- Agarwal, S. K and Kachhara, R. P. 1979. Habo beds near Ler (Kutch) : Pt-2 Succession and fossil molluscs of the beds on the East of Ler *Recent Researches in geology*, 3: 495-503.
- Agrawal, S.K. and Kacker, A.K. 1975. Biostratigraphy of Bathonian-Callovian Beds of Mouwana Dome, Eastern Bela Island, District Kutch (Gujarat). *Recent Researches in Geology*, 6: 631-649.
- Agrawal, S.K. and Kacker, A.K. 1978. Succession and fossil molluscs of the Jurassic rocks near Mouwana, Eastern Bela Island, District Kutch (Gujarat). *Recent researches in Geology*, 4: 482 - 492.
- Agrawal, S.K. and Singh, C.S.P. 1961. Kutch Mesozoic : On the occurrence of Foraminifers in the Jurassic of Kutch (Gujarat, W. India). *The Jour. of Scientific Research, B.H.U*, XI(2): 313 - 331.
- Agrawal, S.K. 1956. Contribution a l'etude stratigraphique et paleontologique du Jurassique du Kutch (Inde). *Ann. centre et document. Paeontol., Paris*, 19: 188.
- Agrawal, S.K. 1956. On the so-called "Macrocephalus" Beds of Kutch. *Current Science*, 25: 84.
- Alberede, F. and Semhi, K. 1995. Patterns of elemental transport in the bed load of the Meurhe River (NE France). *Chem. Geol.*, 122: 129-145.
- Allen, P (1969). Lower cretaceous surce lands and the North Atlantic, *nature*, V. 222., pp. 657-658.
- Arkell, W.J. (1933). *The Jurassic system in Great Britain*. Oxford Univ. Press.
- Arkell, W.J (1956). *Jurassic geology of the world*. Oliver and Boyd., Edinburgh.
- Balagopal, A. 1972. Classification of Patcham and Chari Limestones in Jhura and Habo Domes, Kutch, Gujarat State with a Note on Golden Oolites. *Geol. Society of India*, 44. 81-87.
- Balagopal, A. T. and Shrivastava, A. K. 1973. Petrography and classification of the arenites of the Chari Series in the Jurassic rocks of central Kutch, Gujarat, India, *Sed. Geol.*, 10: 215-224.
- Balaram, V., Ramesh, S. L. and Anjaiah, K. V. 1996. New trace element and REE data in thirteen GSF reference samples by ICP-MS. *Geostandards Newsletter*, 20: 71-78.
- Banner, J.L., (1995). Application of the trace element and isotope geochemistry of strontium to studies of

- carbonate diagenesis, sedimentology, v.42, pp.805-824.
- Bardhan, S. and Datta, K. 1987. Biostratigraphy of Jurassic Chari Formation : A study in Keera Dome, Kutch, Gujarat. *Jour. Geol. Soc. India*, 39 (2): 121 – 131.
- Bardhan, S., Dutta, K., Khan, D. and Bhaumik, D. 1988. Tullitidae genus *Bullatimorphites* from upper Bathonian Patcham Formation, Kutch, India. *Newsl. Stratigr.*, 20 (1): 21 – 27.
- Barnad, P. D. W. (1973). Mesozoic floras. In. N. F. Hughes (Ed.). *Organisms and Continents through time*. Palaeon. Spec. paper No.12, p.175-185.
- Bathurst, R.G.C. (1966). Boring algae, micrite envelopes and lithification of molluscan biosprites. *Geol. Jour.* V. 5, pp. 15-32.
- Bathurst, R.G.C. (1971). *Carbonate sediments and their diagenesis*: Elsevier, 2nd ed. Amsterdam, p. 620.
- Bathurst, R. G. C., and L. S. Land. 1986. Carbonate depositional environments. Part 5: Diagenesis. *Colorado School of Mines Quarterly*, 81: 1 -41.
- Beales (1958). Ancient sediments of Bahaman type. *Bull. Am. Ass. Petrol. Geol.* V. 42, pp. 1845-1880.
- Belussov, V.V. (1962). *Basic problems of Geotectonics*: London, McGraw Hill Book Co Inc., p. 816.
- Bencini, A and Turi, A. 1974. Mn distribution in the Mesozoic carbonate rocks from Lima Valley, Northern Apennines. *Sedimentary Petrology*, 44 (3): 774 – 782.
- Bhalla, S.N., Abbas, S.M., Talib, A. and Ahmad. 1994. Petrography and Depositional Environment of Jurassic Sediments, Habo Hills, Central Kutch. *Indian Jour. of Earth Sciences*, 12 (3): 142 –147.
- Bhalla, S. N., Abbas, S.M., Talib, A and Ahmed, A.H.M. 1994. Petrography and Depositional environment of Jurassic Sediments of Habo Hills, Central Kutch, *Ind. Jour. of Earth Sc.*, 21/3: 142-147.
- Bhalla, S.N. and Abbas, S.M. 1978. Jurassic foraminifera from Kutch, India, *Micropal.*, 24 (2). 160 – 209.
- Bhalla, S.N. and Abbas, S.M. 1984. Depositional environment of the Jurassic rocks of Habo Hills, Kutch, India.
- Bhalla, S.N. 1977. Stratigraphic nomenclature of the Jurassic sequence of Kutch. *Bull. Ind. Geol. Assoc.* 10 (2): 71-72.
- Bhalla, S.N. and Abbas, S.M. 1975c. Additional foraminifera from the Jurassic rocks of Kutch. *Jour. Geol. Soc. India*, 16 (2): 225 – 226.
- Bhalla, S.N. and Abbas, S.M. 1976. The age and Palaeogeographical significance of Jurassic foraminifera of Kutch, India, - In first Int. Sym. on Benthonic foraminifera of continental margins, Canada. *Maritime sed. Spec. Pub.* 1(b): 537 – 544.
- Bhalla, S.N. and Talib, A. 1980. Foraminifera from Jurassic rocks of Badi, Central Kutch. *Bull. Ind. Geol. Assoc.*, 13(2): 99 – 121.
- Bhalla, S.N. and Lal, M. 1985. A note on Jurassic foraminifera from Kaiya Hill, Kutch. *Bull. Ind. Geol. Assoc.*, 18(1): 23–24.
- Bhalla, S.N. and Gauri, K.N. 1987. A preliminary communication on Jurassic foraminifera from Jumara Hills,

- Kutch. Bull. Ind. Geol. Assoc., 20 (2): 171 – 174.
- Bhushan, S.K. 1990. Sedimentary Basins of Western Rajasthan. Jour. Ind. Ass. Sedimentol., 9: 103 – 106.
- Biswas, S. K. 1970. Geologic and Tectonic maps of Kutch. Bull. ONGC, 7 (2): 115-123.
- Biswas, S. K. 1981. Basin framework, Palaeoenvironment and Depositional History of the Mesozoic Sediments of Kutch Basin, Western India. Quart. Jour. Geol. Min. Met. Soc. India, 53: 56-85.
- Biswas, S. K. 1982. Rift basins in Western margin of India and their Hydrocarbon Prospects with special reference to Kutch Basin. Bull. Am. Assoc. Petrol. Geol., 66(10): 1497-1513.
- Biswas, S. K. 1987. Stratigraphy and Sedimentary Evolution of the Mesozoic Basin of Kutch, Western India: In Tendon, S. K and others : Sedimentary Basins of India, Chapter – 6: 74-103.
- Biswas, S. K. 1987. Regional tectonic framework, structure and evolution of the western marginal basins of India. Tectonophysics, 135: 307-327.
- Biswas, S. K. 1977. Mesozoic Rock-Stratigraphy of Kutch, Gujarat, Quart. Jour. Geol. Min. Metal. Soc. Ind., 49 (3 & 4): 1-52.
- Biswas, S. K. 1974. Landscape of Kutch - A morphotectonic analysis, Ind. Jour. Earth Sc., 1 (2): 177-190.
- Biswas, S. K. 1971. Note on the Geology of Kutch, , Quart. Jour. Geol. Min. Met. Soc. Ind., 43: 223-234.
- Biswas, S. K. and Deshpande, S. V. 1968. The Basement of the Mesozoic sediments of Kutch, Western India. Quart. Jour. Geol. Min. Met. Soc. Ind., 40: 1-7.
- Biswas, S.K. and Deshpande, S.V. 1973. Mode of Eruption of Deccan Trap Lavas with special reference to Kutch. Jour. Geol. Soc. India. 14 (2): 134 – 141.
- Biswas, S.K. and Deshpande, S.V. 1970. Geological and Tectonic Maps of Kutch, Western India. Bull. Oil & Nat. Gas Comm., 7 (2): 115 - 116
- Biswas, S. K. 1978. On the status of the Bhuj and Umia Series of Kutch, W. India. Proc. 7th Indian Colloquium on Micropalaeontology
- Biswas, S. K. 1980. Structure of Kutch-Kathiawar Region, Western India. Proc. 3rd. Ind. Geol. Cong., Poona,; 225-272.
- Blandford, W.T. 1867. On the Geology of a portion of Kutch. Mem. Geol. Sur. India, 6: 1
- Bose, P.K., Shome, S., Bardhan, S. and Ghosh, G. 1986. Facies mosaic in the Ghuner Member (Jurassic) of the Bhuj Formation, Western Kutch, India. Sed. Geol., 46: 293 – 309.
- Bosellini, a. and Broglio-Lorgia, C.B., (1971). Calcari Grim. Di Rotzo (Giurassico Inferiore, Al topiano d' Asiago). Ann. Univ. Ferrara Series , 9., pp. 1-61.
- Bradshaw et al (1979). Origin of iron oolites – Discussion. Jour. Sed. Petrol., V.50, pp. 295-304.
- Brand, V. and Veizer, J (1980). Chemical diagenesis of a multicomponent carbonate system – I: Trace elements. Jour. Sed. Petrol., V. 50., pp. 1219-1236.
- Brand, U. and Veizer, J. (1981). Chemical diagenesis of a multicomponent carbonate system-2: Stable

- Isotopes, *J. Sed. Petrol.*, V. 51., pp. 987-997.
- Brand, U. and Veizer, J., (1983). Origin of Coated Grains: Trace element constraints, in T.M. Peryt (ed.), *Coated Grains*, p.655, Springer and Verlag, Berlin Heidelberg.
- Brown, P.R. 1964. Petrography and Origin of some upper Jurassic beds from Dorset, England. *Jour. Sed. Petrol.*, 34 (2): 254-269.
- Bruckmann, R. 1904. Die foraminiferendes litauisch - Jurischen Jura. *Physikokon ges. Königsberg t Pr. Schrift*, 45p.
- Bruckschen, P., Neuser, R.D. and Richter, D, K. 1992. Cement stratigraphy in Triassic and Jurassic limestones of the Weserbergland (Northwestern Germany). *Sed. Geol.*, 81: 195-214.
- Buatois, L.A. and Mangano, M.G. 1994. Lithofacies and depositional processes from a Carboniferous Lake, Sierra de Narvaez, north west Argentina. *Sed. Geol.*, 93: 25 – 49.
- Burgess, C. J. and Lee, C. W. 1978. The development of a lower carbonate tidal flat, Central high atlas, Morocco.1; Sedimentary history. *Jour. Sed. Petrol.*, 48 (3): 777- 794.
- Busch, D. A. 1974. Stratigraphic traps in sandstone – Exploration Techniques : Mem.21, Amer. Assoc. Petrol. Geol., Tulsa, Oklahoma.
- Callomon, J. H. 1993. On *Perisphinctes congener*, Waagen, 1875, and the age of the Palcham Limestone in the Middle Jurassic of Jumara, Kutch, India. *Geologische Blätter fuer NO Bayern*, 43 (1-3): 227 – 246.
- Cariou, E. and Jaikrishna, 1988. The Tethyan *reineckeiinae* of Kachchh and Jaisalmer (West India), systematic, biostratigraphic implications. *Southern Abduck; aus Palaeontographica beitrage*, 203: 149 –170.
- Cariou, E. 1984. Biostratigraphic subdivision of the Callovian stage in the Subtethyan Province of Ammonites, Correlations with the Sub-Boreal zonal scheme. *Int. Symp. Jurassic Strati.*, 2: 315 – 326.
- Carozzi, A.V. (1958). Micro-mechanisms of sedimentation in the continental environment., *J. Sed. Petrol.* m V. 28/2, Pp. 133- 150
- Carozzi, A.V., Bouroullec, J., Delloffre, R., and Rumeau, J.L., (1989). Carbonate rock depositional models-A microfacies approach. Prentice Hall Advanced Reference Series. Prentice Hall, Englewood cliffs, New Jersey 07632, p.604.
- Carozzi, A.V. (1971). Geochemical data on back reef carbonates. Traverse group (Givetian) of the Northern part of the Southern Peninsula of Michigan Bull. Centre. Rech. Pam. SNPA 5/2, pp. 213-222.
- Carver, R. E. (Ed.). 1971. *Procedures in Sedimentary Petrology*, 653p, John Wiley, New York.
- Carter, A. M. (1998). Two models : Global sea level changes and sequence stratigraphic architectures. *Sed. Geol.*, V.122., Pp. 23-36.
- Cashyap, S.M. Dev, P. and Tewari, R. C. 1983. Ichnofossils from Bhuj Formation (Cretaceous) as palaeoenvironmental parameters. *Current Science*, 52: 73 – 74.

- Cerny, (1978). Geochemie "anisisher" sedimentgesteine in den Nordkarawankern, carintma – II, V. 88. Pp. 55-70.
- Chester, A (1965). Geochemical criteria for differentiating reef from Mn-reef facies in carbonate rocks. Bull. Amer. Ass. Petrol. Geol. V. 49, pp. 258-276.
- Chilingar, G.V. (1956). Relationship between Ca/Mg ration and geological age. Bull. Am. Ass. Petrol. Geol. V. 40., pp. 2256-2266.
- Chilingar, G. V., Bissel, Fairbridge, R. W. (eds). (1967). Carbonate rocks. Dev. Sedimentol., V.9A, 9711p.
- Cloud, P.E (1962) . Environment of Calcium Carbonate deposition west of Andres Island, Bahamas. Prof. Pap. US Geol. Surv. 350, p. 138.
- Condie, K. C. 1991. Another look at rare earth elements in shales. Geochim. Cosmochim. Acta, 55, 2527-2531.
- Cox,L.R. 1952. The Jurassic lamellibranch fauna of Cutch (Kachh). Pal. Indica,GSI, Ser.9, 3(4): 1-128.
- Cox,L.R. 1940. The Jurassic Lamellibranch of Kutch (Cutch), Pal. Indica. 9(3): 157.
- Curray, J. R. 1956. The analysis of two-dimensional data. Jour. Geol., 64: 117-131.
- Dahanayake, K. 1977. Classification of oncoids from the upper Jurassic Carbonates of the French Jhura. Sed. Geol., 18: 337-353.
- Cuvillier, G. V. (1952.). La notion de microfacies et ses applications, VIII Congre. Naz Methane Petrolio, sect.1, pp.1-7.
- Datta,K., Bhaumik,D., Jana, S.K. and Bardhan,S. 1996. Age, Ontogeny and Dimorphism of Macrocephalites triangularis Spath - The Oldest Macrocephalitid Ammonite from Kutch ,India. Jour. Geol. Soc. Ind. 47: 447 – 458.
- Dave, A. 1996. Dhosaian Stage (Oxfordian) in Kutch, India. Indian Jour. Geol. 68 (2): 100 – 111.
- Dave, A. and Chatterjee,T.K. 1996. Integrated Foraminiferal and Ammonia Biostratigraphy of Jurassic Sediments in Jaisalmer Basin, Rajasthan. Jour. Geol. Soc. Ind., 47: 477 –490.
- Davies, D.K. (1969). Shelf sedimentation : An example from the Jurassic of Britain. Jour. Sedim. Petrol. V. 39., pp. 1344-1370.
- Davies, P.J., (1971). Calcite precipitation and recrystallisation fabrics – their significance in Jurassic limestones of Europe., J. Geol. Soc. Austra., V. 18., pp. 279-292.
- Davies, P. J. 1972. Trace element distribution in reef and sub reef rocks of Jurassic age in Britain and Switzerland. Jour. Sed. Petrol., 42(1) ; 183-194.
- Davis, J. C. 1973. Statistics and Data analysis in Geology, John Wiley & sons publ., New York, 550p.
- Davis, J. C. and Conley C. D. 1977. Relationship between variability in grain size and area of samples on a carbonate sand beach. Jour. Sed. Petrol., 47/1: 251-256.
- Dawson, W.C., and Carozzi, A.V., (1986). Anatomy of a phylloid algal build up, Raytown Limestone, Iola Formation, Pennsylvanian, South east Kansas, U.S.A., Sed. Geol. v.47, pp.221-261.

- Degens, E.T. (1968). *Geochemise de sedimente* P. 282. Stuttgart: Enke
- Deshpande, S. V. and Merh, S. 1980. Mesozoic Sedimentary Model of Wagad Hills, Kutch, Western India. *Jour. of Geol. Society of India*, 21: 75-83.
- Dessai, G., Shringarpure, D. M. and Merh, S.S. 1975. Western Wagad Mesozoic Sediments and their Depositional Environments. *Proc. Sym. on Sediment, Sedimentation & Sedimentary environments*, 313-322.
- De Wet, C. B. 1987. Deposition and diagenesis in an extensional basin: the Corallian Formation (Jurassic) near Oxford, England. Un. J. D. Marshall (Ed.). *Diagenesis of Sedimentary Sequences*. *Geol. Soc. Spec. Publ.*, 3: 863-877.
- De Wet, C. B. (1998). Deciphering the sedimentological expression of tectonics, eustacy, and climate : A basin wise study of the Corallian Formation, S. England. *Jour. Sed. Petrol.*, V.68, No.4, pp.653-657.
- Dhahanayake, K. 1977. Classification of oncoids from the upper Jurassic Carbonates of the French Jhura. *Sed. Geol.*, 18: 337 – 353.
- Dickson, W.R. (1985). Interpreting provenance relations from detrital modes in sandstones; pp. 333-361 in Inffa, G.G., ed., *Provenance of Arenites*; Reidel; p. 408.
- Dickinson, K. A. 1969. Upper Jurassic carbonate rocks in northeastern Texas and adjoining parts of Arkansas and Louisiana. *Trans. Gulf Coast Ass. Geol. Soc.*, 19: 175-188.
- Dodd, J.R (1967). Magnesium and strontium in calcereous skeletons: a review *Journ. Palaeontology*. V. 41, pp. 1313-1329.
- Dravis, J.J. 1989. Deep-burial microporosity in upper Jurassic Haynesville oolitic grainstones, East Texas . *Sed. Geol.*, 63: 325 – 341.
- Dubey, N and Chatterjee, B. K. (1997). Sandstones of Kachchh Basin. The provenance and basinal evolution. *Ind. Jour. Petrol. Geol.*, V. 6, No.1, pp.55-68.
- Dunham, R. J. 1962. Classification of carbonate rocks according to depositional texture. In W. E. Ham (Ed). *Classification of carbonate rocks*, *Mem. Amer. Assoc. Petrol. Geol.*, 1: 108-121.
- Embry, A.F., 1993. Transgressive-Regressive (T-R) sequence analysis of the Svedrup Basin, Canadian Arctic Archipelago. *Can. J. Earth Sci.*, 30: 301-320.
- Emery, D. and Dickson, J.A.D. 1989. A syndepositional meteoric lens in the Middle Jurassic Lincolnshire limestone, England, U.K. *Sed. Geol.*, 65 (3/4): 273 – 284.
- Embry, A.F., (1993). Transgressive –regressive (T-R) sequence analysis of the Jurassic succession of the Svedrup Basin Canadian Arctic Archipelago., *Can. J. Earth Sci.* V. 30., pp. 301-320.
- Enos, and Perkins, (1979). Evolution of Florida Bay from island stratigraphy: *Geol. Soc. Am. Bull.*, V. 90, pp. 59-83.
- Ernst, W. (1970). Geochemical facies analysis: methods *Geochim. Geophys.* V. 11, p. 152.
- Espitalie, J. and Sigal, J. 1963. Contribution a L'etude des foraminiferes du Jurassique superieur Et due

- neocomienn du Bassin de Majunga (Madagascar). *Annales, Geologique de Madagascar*, 32: 1 – 87.
- Evamy, B.D., and Shearman, D.J., (1969). Early stages in development of overgrowths on eolinsderm fragments in limestones, *Sedimentology*, V. 12., pp. 317-322.
- Fairbridge, R. W. (1954) . Stratigraphic correlation by Microfacies, *Am. J. Sci.*, v. 252 , pp. 683- 694.
- Feizmia, S., and Carozzi, A.V. (1987). Tidal and deltaic controls on carbonate platforms: Glen Dean Formation (Upper Mississippian) of Illinois Basin, U.S.A., *Sed. Geol.* V. 54., pp. 201-243.
- Flügel, E. 1982. *Microfacies Analysis of Limestones*, 633p, Springer-Verlag, Berlin.
- Flügel, H.W. and Wedepohl, K.H. (1967). Die Verteilung des Strontiums in oberjurassischem Karbonatgesteinen der Nordli Petrology, V. 14, pp. 229-249.
- Folk, R. L. 1954. The distinction between grain size and mineral composition in sedimentary rocks. *Jour. Geol.*, V.62: 344-359.
- Folk, R. L. 1959. Practical petrographic classification of limestones. *Bull. Amer. Assoc. Petrol. Geol.*, V. 43, pp. 1-38.
- Folk, R. L. 1962. Sorting in some carbonate beaches of Mexico. *Trans. New York Acad. Sci.* (2)V. 25, No.2, pp.222-224.
- Folk, R. L. 1965. Some aspects of recrystallization in ancient limestones. In L. C. Pray and R. C. Murray (eds). *Dolomitization and Limestone Diagenesis*, Spec. Publ. Soc. Econ. Paleont. Miner., V.13, pp. 14-48.
- Folk, R. L. 1966. A review of grain size parameters. *Sedimentol.*, V. 6, pp. 73-93.
- Folk, R. L. *Petrology of Sedimentary rocks*. Hemphill's, Austin, Texas.
- Folk, R. L. and Land, L. S. 1975. Mg/Ca ratio and salinity : two controls over crystallization of dolomite. *Bull. Amer. Assoc. Petrol. Geol.*, V. 59, pp. 60-68.
- Folk, R. L. and Ward, W. C. 1957. Brazos River bar : a study in the significance of grain size parameters. *Jour. Sed. Petrol.*, 27: 3-26.
- Friedman, G.M., (1959). Identification of carbonates minerals carbonate minerals by staining methods. *J. Sedim. Petro.* V. 29., pp. 87-97.
- Friedman, G. M. 1961. Distinction between dune, beach and river sands from their textural characteristics. *Jour. Sed. Petrol.*, 31: 514-529.
- Friedman, G.M. 1964. Early diagenesis & lithification in carbonate sediments. *Jour. Sed. Petro.*, 34(4): 777-813.
- Friedman, G. M. 1967. Dynamic process and statistical parameters compared for size frequency distribution of beach and river sands. *Jour. Sed. Petrol.*, 37: 327-354.
- Friedman, G. M. (Ed.). 1969 *Depositional Sedimentary environments in carbonate rocks*, 209p, Spec. Publ. Soc. Econ. Paleont. Miner., 14, Tulsa.
- Fursich, F. T, Oschmann, W., Jaitley. and A. K and Singh. 1991. Faunal response to transgressive-regressive cycles: example from the Jurassic of western India, *Palaeogeog. Palaeocli. Palaeoecol.*, 85: 149-159.

- Fursich, F.T., and Oschmann, W. (1993). Shell beds as the tools in basin analysis: The Jurassic of Kachchh, Western India, *Jour. Geol. Soc. London.*, V. 150, pp. 169-185.
- Fursich, F. T., Oschmann, W., Singh, I. B and Jaitly, A. 1992. Hardgrounds, reworked concretion levels and condensed horizons in the Jurassic of western India; their significance for basin analysis, *Jour. Geol. Soc. of London*, 149: 313-331.
- Fursich, F. T., Pandey, D. K. and Oschmann, W. 1994. Contribution to the Jurassic of Kachchh, W. India-II. Bathonian stratigraphy & depositional environment of Sathara Dome, Pachchham, Beringeria, 12: 95 – 25.
- Gad, M.A., Call, J.A., and Le Riche, H.H., (1969). Geochemistry of the Whitebian (upper Lias) sediments of the YorkShire Coast. *Proc. Yorks., Geol. Soc.*, V. 37., pp. 105-136.
- Galloway, W.E. (1989). Genetic stratigraphic signatures in basin analysis 1: architecture and genesis of flooding surface bounded depositional units: *Am. Ass. Petrol. Geol. Bull.*, V. 73, pp. 125-142.
- Garcia, J. P. and Dromart G. 1997. The validity of two biostratigraphic approaches in sequence stratigraphic correlations : brachiopod zones and marker-beds in the Jurassic. *Sed. Geol.*, 114: 55-79.
- Garcia, J. P., Philippe, M. and Gaumet, F. 1998. Fossil wood in Middle-Upper Jurassic marine sedimentary cycles of France: relations with climate, sea-level dynamics, and carbonate-platform environments. *Palaeoeco. Palaeocli. Palaeoeco.*, V. 141, pp. 199 - 214.
- Geel, J. (2000). Recognition of stratigraphic sequences in carbonate platform and slope deposits : empirical models based on microfacies analysis of Palaeogene deposits of SW Spain. *Palaeoogeog. Palaeocli. Palaeoecol.*, V. 155, pp.211-238.
- Ghosh, D.N. 1965. Depositional environment in the development of Patcham-Chari sequence at Kutch. *Proc. 56th. Ind. Sci. Cong.*, pt.III, 205.
- Ghosh, D.N. 1969. biostratigraphic classification of Patcham - Chari sequence at the Jumara section, Kutch (abstract). *Proc. 56th sess. Indian Sc. cong. Assoc.* 3: 214.
- Gibling, M.R. and Stuart, C.J. 1988. Carbonate slide deposits in the Middle Jurassic of Portugal. *Sed. Geol.*, 57: 59 – 73.
- Gignoux, M. 1950. *Stratigraphic Geology* (English translation from the 4th French edition, 1950), W.H. Freeman and Company, Sans Fransisco.
- Ginsburg, R. N.. 1956. Environmental relationships of grain size and constituent particles on some South Florida Carbonate sediments. *Bull. Amer. Assoc. Petrol. Geol.*, 40: 2384-2427.
- Ginsburg, R.N. (1957). Early diagenesis and lithification of shallow water carbonate sediments in South Florida. In: *Regional Aspects of carbonate deposition* (Ed. By R.J. LeBlanc and J.C. Breeding) Field trip Guide, p. 72.
- Goldschmidt, V. M. 1954. *Geochemistry*. Oxford University Press, Oxford, 730p.

- Graf, D. L., (1960), Geochemistry of carbonate sediments and sedimentary carbonates , 1-4; Illinois State Geol. Surv Circ. V. 297, 298, 301, 308, p. 250.
- Grant, C.W. 1837. Memoir to illustrate a geological map of Kutch. Trans. Geol. Surv. India, ser.2, 5(2): 289 - 326
- Green, G.W., and Donovan, D.J. (1969). The Great Oolite of the Bath area, Bull. Geol. Surv. G.B. No. 30., pp. 1-63.
- Gregory, J.W. 1900. Jurassic fauna of Cutch : The corals. Pal. Indica, Geol. Surv. India, ser.9, 2 (2): 12-196.
- Gregory, J.W. 1893. Jurassic fauna of Cutch : The echinoidea, Pal. Indica, Geol. Surv. India, ser.9, 2 (1): 1-11
- Gromet, L. P., Dymek, R. F., Haskin, L. A. and Korolev, R. L. 1984. The "North American Shale Composite": Its compilation, major and trace element characteristics. Geochim. Cosmochim. Acta, 48 : 2469-2482.
- Guha, D.K. 1976. On some Mesozoic ostracoda from subcrops of Banni, Rann of Kutch, India. Proc. VI Ind. Colloq. Micropal. Strat., 84 - 90.
- Hallam, A. 1969. A pyritized limestone hardground in the Lower Jurassic of Dorset (England). Sedimentology, 12 (3/4): 231 - 240.
- Hallam, A. (1970). Gyrochorate and other trace fossils in the Forest marble (Bathonian) of Dorset, England. In: T.P. Crimes and J.C. Harper (Editors), Trace Fossils, Seel House Press, Liverpool, pp. 89-100.
- Hallam, A., and Bradshaw, M.J. (1979). Bituminous shales and oolitic ironstones as indicators of transgressions and regressions: Jour. Geol. Soc. (London) 136., pp. 157-164.
- Hallam, A., and Sellwood, B.W. (1968). Origin of Fuller's Earth in the Mesozoic of Southern England, Nature, V. 220., pp. 1193-1195.
- Hallam, (1972 a). Diversity and density characteristics of Pliesbachian Toarcian Nolluscan and brachiopod faunas of the North Atlantic Lethia, V. 5., pp. 389-412.
- Hallam, A. (1975). Coral patch reefs in the Bajocian (Middle Jurassic) of Lorraine. Geol. Mag.
- Hallam, A., Hancock, J.M. and La Breque. 1985. The chronology of the Geological record. Jurassic to Palaeogenes Pt.1. Jurassic and Cretaceous geochronology and Jurassic to Palaeogene Magnetostratigraphy. The Geol. Soc. Memoir, No.10: 118 -133.
- Hantzschel, W., and Reineck, H.E. (1968). Fazies-Untersuchungen in Hettangium von Helmstedt (Niedersachsen). Mitt. Geol. Staatsinst. Hamburg., V. 37., pp. 5-39.
- Harland, W.B., Cox, A.V. and Pickton, C. 1982. A Geological time scale. Cambridge. University Press, 128p.
- Harland, W.B., Armstrong, R.L., Cox, A.V., Craig, L.E. and Smith. 1989. A Geological time scale. Cambridge University Press, 263.
- Harman, H. H. 1976. Modern factor analysis, : University of Chicago Press, Chicago, 474p.
- Harris, W. H. and Mathews, R. K. 1968. Subaerial diagenesis of carbonate sediments : efficiency of the solution. Science, N.Y., 160: 72-79.
- Haq, B.U., Hardenbol, J. and Vail, P.R. 1987. Chronology of fluctuating sea levels since the Triassic. Science.

235: 1156 - 1167.

- Heckel, P.H., (1980). Palaeogeography of Eustatic model for deposition of Midcontinent, Upper Pennsylvanian Cyclothems, in Fouch, J.D. and Magathan, E.R., eds., *Booky Mtu, section., Soc. Econ. Paleontologists Minerealogists, West. Central U.S. Paleogeography Symposium I, Paleozoic Paleogeography of West-Central United States*, pp. 197-215.
- Heckel, P.H., (1983). Diagenetic model for carbonate rocks in midcontinent Pennsylvanian Eustatic Cyclothems, *J. Sedim. Petrol.* V. 53., No.3., pp. 733-759.
- Heinze, M. 1991. Evolution benthonischer Faunengemeinschaften im subborealen Jura des Pariser Beckens and in der athiopischen Faunaenprovinc des Beckens voa Kachchh (Indien) - ein verleich. *Beringeria*, 4: 3 - 126.
- Holder, H., (1964). *Jur . In the series : F.Lotze (editor). Hand buch der stratigraphischen Geologie*, Enke, Stuttgart.
- Holser, W.T (1997). Evaluation of the application of rare earth elements to paleonography, palaeoeco, palaeoclim. *Palaeoecol.*, V. 132, pp. 309-323.
- Horwitz and Potter (1971) *Introductory Petrography of fossils*, p.302, Springer-Verlag, Berlin.
- Howard, J.D. and Singh, I.B. 1985. Trace fossils in the Mesozoic sediments of Kachchh, Western India. *Palaeogeog. Palaeocli. Palaeoecol.*, 52: 99 - 122.
- Hudson, J.D. (1964). The petology of the sandstones of the Great Esturine series and the Jurassic palaeogeography of Scotland. *Proc. Geol. Ass. London.*, V. 75., pp. 499-528.
- Hudson, J. D. (1970). Algal limestones with pseudomorphs after gypsum from the Middle Jurassic of Scotland. *Lethaia*, V.3, p.11-40.
- Hudson, J.D., and Palframan, D.F. B., (1969). The ecology and preservation of the Oxford clay fauna at Woodhan, Buckinghamshire *Quart. J. Geol. Sox. London*, V. 124., pp. 387-418.
- Hutchison, C.S (1971). *Laboratory Handbook of petrographic Techniques*. Wiley-Interscience, New-York.
- Imlay, R.W., (1967 a) Twin Creek Limestones (Jurassic) in the Western Interior of the United States. *U.S. Geol. Surv. Prof. Paper* 540.
- Imlay, R.W., (1967 b). The Mesozoic pelecypods *Otapiria Marnick* and *Lupherella Imlay*, new genesis, in the United States, *U.S. Geol. Surv. Prof. Paper* 573-B.
- Ingerson, E. (1961). Problems of the sedimentary carbonate rocks, *Geochim. Coschim, Acta*, V. 26, pp. 815-847.
- Ismail, M.H.B. and M'Rabet, A. 1990. Evaporite, carbonate and siliciclastic transitions in the Jurassic sequence of southeastern Tunisia. *Sed. Geol.*, 66: 65 - 82.
- Jai Krishna and Westermann, G. E. G. 1987. Faunal associations of the Middle Jurassic ammonite genus *Macrocephalites* in Kachchh, western India, *Canadian Jour. of earth Sciences*, 24: 1570-1582.

- Jai Krishna and Cariou, E. 1986. The Callovian of Western India : New data on the Biostratigraphy, Biogeography of the Ammonites and Correlations with Western Tethys (Submediterranean Province). *Newsl. Stratigr.*, 17 (1): 1 – 8.
- Jai Krishna. 1984. Current status of the Jurassic in Kachchh, Western India. *International Symposium on Jurassic Stratigraphy*, 3: 731 - 742
- Jai Krishna, Cariou, E. and Enay, R. 1988. Succession of Macrocephalinitinae assemblages as revealed at Keera Dome in Kachchh, Western India. *Proc. 2nd International Symposium on Jurassic*, 383 - 394.
- Jai Krishna, Singh, I. B., Howard, J. D and others 1983. Implications of new data on Mesozoic rocks of Kachchh, western India, *Nature*, 305, No.5937: 790-792.
- Jaikrishna and Pathak, D. B. 1991. Ammonia Biochronology of the Upper Jurassic Kimmeridgian Stage in Kachchh, India, *Jour. of Palaeontological Society*, 36: 1-13.
- Jaikrishna, Pathak, D.B., and Pandey, B., (1999). Development of Oxfordian (Early Upper Jurassic) in the most proximally exposed part of the Kachchh Basin at Wagad outside the Kachchh mainland, *Jour. Geol. Soc. India*, V. 52., pp. 513-522.
- Jaitly, A.K. and Singh, C.S.P. 1983. Discovery of Late Bajocian *Leptosphinctes* BUCKMAN (Jurassic Ammonitina) from Kachchh, Western India - *Neues Jahrbuch fuer Geologie und Palaeontologie, Monatshefte N. Jour. Geol. Paleont.*, 91 – 96.
- Jaitly, A.K., Fursich, F.T. and Heinze, M. 1995. Contributions to the Jurassic of Kachchh, western India. IV. The bivalve fauna Part I. Subclass Palaeotaxodonta, Pteriomorphia and Isofilibranchia. *Beringeria*, 6: 147-257.
- Jain, S. 1997. On the Earliest Occurrence of Genus *Phlycticeras* Hyatt in Kachchh, Western India. In *Short Communications, Jour. Geol. Society of India*, 49: 75 – 80.
- James, N. P., and P. W. Choquette. 1983. Diagenesis #6. Limestones: The sea floor diagenetic environment. *Geoscience Canada* 10:162-179.
- James, N. P., and P. W. Choquette. 1984. Diagenesis #9. Limestones: The meteoric diagenetic environment. *Geoscience Canada* 11:161-194.
- Jenkyns-Hugh, C., Geczy-Barnabas and Marshal- James, D. 1991. Jurassic manganese carbonates of Central Europe and the early Toracian anoxic event. *Jour. of Geology*, 99 (2): 137 – 149.
- Kalantari, A. 1969. Foraminifera from the Middle Jurassic to Cretaceous succession of Koppet-Dagh Region (NE Iran), National Oil Co., Publ. No.3.
- Kalia, P. and Chowdhury, S. 1983. Foraminiferal biostratigraphy, biogeography and environment of the Callovian Sequence, Rajasthan, western India. *Micropalaeontology*, 29 (2): 223 – 254.
- Kanjilal, S. and Singh, C.S.P. 1973. A new Nuculanid Genus from the Callovian of Kutch (Gujarat), India. *Proc. malac. Soc. London*, 40: 469 – 471.
- Kanjilal, S. 1975. A study on the fauna and stratigraphy of the Jurassic rocks of Habo Hill, District Kutch ,

- (Gujarat), W. India. Unpublished Ph.D Thesis. B.H.U.
- Kanjilal, S. 1978. Geology and Stratigraphy of the Jurassic rocks of Habo hill, District Kutch(Gujarat). Proc. Indian National Science Academy - Part - A, 44: 1-15.
- Kanjilal, S. 1978. A new species of *Kheraiceras* SPATH (Ammonoidea) from the Lower Callovian of the Habo Hill, Kutch. Jour. Palaeontol., 52 (2): 495 – 496.
- Kanjilal, S. 1978. Ammonoids from the Basal Katrol rocks around the Habo hill, Kutch. Recent Researches in Geology, 7: 255 – 261.
- Kanjilal, S. 1980. Upper Jurassic Phyllocerate and Haplocerate Ammonoids from the Habo Hill, District Kutch (Gujarat), W. India. Recent researches in Geology, 5. Part. I, 300 – 309.
- Kanjilal, S. and Singh, B.N. 1986. On *Unipeltoceras jeanet*, Jurassic Peltocerate ammonite from Kutch, Gujarat. Quart. Jour. Geol. Min. Met. Soc. India, 58: 29 – 34.
- Kanjilal, S. 1990. Middle Callovian (Jurassic) *Acesta Adams* and *Adams* and *Plagiostoma* J. Sowerby (*Limidae*: *Bivalvia*) from the Habo Hill, District Kachchh, Gujarat : their taxonomy and palaeoecology. Ind. Jour. Geol. 66 (1): 45 – 55.
- Katz, et al (1972). Strontium behavior in the aragonite–calcite transformation an experimental study at 40-98°C. Geochim. Coschim. Acta, V. 36., pp. 481-486.
- Kayal (1998). Geology and stratigraphy of the Jurassic rocks of Habo Hill, District Kuchchh (Gujarat), Proc. Ind. Nat. Sci. Acade. V. 44 A., pp. 1-15.
- Kayal, A., and Bardhwn, S., (1998). *Epistrenoceras Benz* (Ammonoidea) from the Middle Jurassic of Kutch (Western India): a new record and its chronostratigraphic implication, Can. J. Earth. Sci. V. 35., pp. 931-935.
- Kendall. C.G.St.c and Schlager (1981). Carbonates and relative changes in sea level : Marine geology. V. 44., pp. 181-212.
- Kent, D.V. and Gradstein, G. M. 1985. A Jurassic and Cretaceous geochronology. Geol. Soc. Amer. Bull., 96: 1419 – 1427.
- Khadikar, A. S. 1996. Breakup of Gondwanaland and the Jurassic record of the Kachchh Basin, Gujarat, Western India. Current Science, 70 (12): 1093-1096.
- Khadikar, A.S. and Phansalkar, V.G. 1995. Diagnostic bivariate plot for the differentiation of species of the Genus *stenosaurus*. Jour. Geol. Soc. India. 46: 675 – 677.
- Khosla, S.C., and Jakhar, S.R., (1999). A note on the Ostracode Fauna from the Jurassic Beds of Jumara Dome, Kachchh, J. Geol. Soc. India., V. 54., pp. 43-49.
- Kimberley. (1979). Origin of iron oolitic formations – reply. Jour. Sed. Petrol., V.50, pp.295-304.
- Kinsman, D.J.J and Holland, H.D. (1969). The co-precipitation of cations with CaCO₃ – IV. The Co-precipitation of Sr+2 with aragonite between 16 and 96°C: Ceochim. Cosmochim. Acta, V. 33, pp. 1-18.
- Khosla, S.C., Jakhar, S.R. and Mohammed, M.H. (1997). Ostracodes from the Jurassic beds of Habo

- Hills, Kachchh, Gujarat, India. *Micropalaeontology*, 43 (1): 1 – 40.
- Kichin, F.L. 1900. The Brachiopods of Kutch, Pal. Indica, ser. 9, 3, pt. 1.
- Kinsman, D. J. J. 1969. Interpretation of Sr concentration in carbonate minerals and rocks. *Jour. Sed. Petrol.*, 39/2: 486-502.
- Klovan, J. E. 1966. The use of factor analysis in determining depositional environments from grain size distributions. *Jour. Sed. petrol.*, 36: 115-125.
- Knox, R.W., (1973). The Eller Beck formation (Bajocian) of the Ravenscar Group of N.E Yorkshire, *Geol. Mag.* 110., pp. 511-534.
- Koshal, V.N. 1975. Palynozonation of Mesozoic subsurface sediments in Banni, Kutch, Gujarat, W. India. *Quart. Jour. Geol. Min. Met. Soc. India*: 47 (2): 79 – 82.
- Krejci-Graf, K (1964). Geochemical diagnosis of facies. *Proc. Yorkshire Geol. Soc.* V. 34., pp. 469-521.
- Krejci-Graf, K. (1966). Geochemische Faziesdiagnostik. *Freiberger Forschungsteft C 224*, p. 80
- Krishna, J. 1984. Current status of the Jurassic stratigraphy in Kachchh, Western India. *Int. Symp. on Jurassic stratigraphy, Copenhagen* . 3: 731 – 742.
- Krishnan, M.S. 1968. *Geology of India and Burma*. Heggimbotham.
- Krumbein, W.C., (1934). Size frequency distributions of sediments: *Jour. Sed. Petrogr.* V. 4., pp. 65-77.
- Krumbein, W., and Sloss, L.L. (1963). *Stratigraphy and sedimentation* . P. 660. San Francisco-London: W.H. Freeman Co.
- Land, L.S. (1973), Holocene meteoric dolomitisation of pleistocene limestones, N. Jamaica. *Sedimentology*, V. 20, pp. 411- 424.
- Land, L. S. 1985. The origin of massive dolomite. *J. Geol. Educ.* 33:112-125.
- Loucks, R.G. and R. Sarag, J.F. (1993). Carbonate sequence stratigraphy ; Recent developments and applications. *Am. Ass. Petrol. Geol. Memoir*-57.
- Loutit, T.S., Hardenbol, J. Vail, P.R., Baum, G.R. (1978). Condensed sections: The key to age determination and correlation of continental margin sequences, in C.K. Wilgus, B.S. Hastings, C.G. St and J.C. Van Wagoner, eds., *Sea level changes: An integrated Approach: SEPM Special Publication No. 42*, pp. 183-213.
- Lowenstam, H. A., (1961), *Mineralogy*, O^{18} / O^{16} ratios and strontium and magnesium contents of recent and fossil brachiopods and their bearing on the history of the oceans: *Jour. Geology*, V. 69, pp. 241-260.
- Lubimova, P.S., Guha, D.K. and Mohan, M. 1960. Ostracoda of Jurassic and Tertiary deposits from Kutch and Rajasthan (Jaisalmer), India. *Bull. Geol. Min. Met. Soc. India*, 22 (2): 1 – 60.
- Maliva, R.G. and Dickson, J.A.D. 1992. The mechanism of skeletal aragonite neomorphism : evidence from neomorphosed Mollusks from the upper Purbeck Formation (Late Jurassic - Early Cretaceous), Southern England. *Sed. Geol.*, 76 (3/4): 221 – 232.

- Mallik, et al (1999). Modern and historic seismicity of Kachchh Peninsula, Western India, *Journ. Geol. Soc. India*, V. 54., pp. 545-550.
- Marshal, J.D., (1981). Zoned calcites in Jurassic ammonite chambers: trace elements, isotopes and neomorphic origin. *Sedimentology*, V. 28., pp. 867-887.
- Marshal, J.F. (1983 a). Submarine cementation in a high energy platform reef: One Tree Reef, Southern Great Barrier Reef, *J. Sedim. Petrol.* V. 53, pp. 1113-1149.
- Marshal, J.D. and Ashton, M., (1980). Isotopic and trace element evidence for submarine lithification of handground in the Jurassic of eastern England *sedimentology*, V. 27., pp. 271-289.
- Mason, B. and Moore, C. B. 1982. *Principles of Geochemistry (4th Edition)*. John Wiley and Sons Inc. New York, p. 46-47
- Mason, C. C. Folk, R. L. 1958. Differentiation of beach, dune, and aeolian flat environments by grain size analysis, Mustang Island, Texas. *Jour. Sed. Petrol.*, 28: 211-216.
- Mathur, U.B., Pant, S.C., Mehra, S. and Mathur, A.K. 1985. Discovery of dinosaurian remains in Middle Jurassic of Jaisalmer, Rajasthan, Western India. *Bull. Ind. Geol. Assoc.*, 18 (2): 59 – 65.
- Mathur, Y.K. 1972. Plant fossils from the Kuar Bet, Pachham Island, Kutch. *Current Science*, 41(13): 488-489.
- Mathur, Y.K., Soodan, K.S., Mathur, K. and Bhatia, M. 1970. Microfossil evidences on the presence of Upper cretaceous and Paleogene sediments in Kutch, *ONGC Bull.*, 7 (2): 109 – 114.
- Mathur, Y.K., Soodan, K.S., Mathur, K. and Bhatia, M. 1971. New geological horizons in Kutch. *ONGC Bull.*, 8 (11&12).
- Mathur, L.P., and Evans, P., (1964). *Oil in India Brochure* published by the International Geological Congress 2nd Session. India., pp. 85.
- McKee, E.D and Gutschick, R.C. (1969). History of Redwall Limestone of Northern Arizona. *Mem. Geol. KSoc. Am.* V. 14., p. 726.
- McGhee, G.R. and Bauger, U. (1985). The local signature of sea level changes in U. Bayer and A. seilacher (eds), *Sedimentary and evolutionary cycles*, V. 1/1, p. 465.
- McIlreath and Morrow (1990). *Diagenesis Geoscience. Can. Rep. Ser.* 4.
- McLane, M., (1995). *Sedimentology*, p.423, Oxford University Press, Inc. New York.
- McLennan, S. M. and Taylor, S. R. 1991. Sedimentary rocks and crustal evolution revisited: Tectonic setting and secular trend. *Jour. Geol.*, 99: 1-21.
- Michalzik, D. and Schumann, D. 1994. Lithofacies relations and palaeoecology of a late Jurassic to Early Cretaceous fan delta to Shelf depositional system in the Sierra Madre Oriental of north-east Mexico. *Sedimentology*, 41: 463-477.
- Middleton G.V. (1973). Johannes Walther's Law of correlation of facies, *Bull. Geol. Soc. Am.* V. 84, pp. 979-988.

- Milliman, J.D. (1974). Marine carbonates, p. 375. Springer –Verlag, New York.
- Millot, G., (1988). Green Marine Clays, Springer-Verlag.
- Minoura-Koji, Nakaya-Shu, and Takemura-Atsushi. 1991. Origin of Manganese carbonates in Jurassic red shale, central Japan, *Sedimentology*, 38 (1): 137 – 152.
- Mitchum, R.M. Vail, Jr. P.R. and Thompson, S (1977). Seismic stratigraphy and global changes of sea level part 2: The depositional sequence as a Basic Unit for stratigraphic Analysis.
- Mitra, K.C. and Ghosh, D.N. 1964. A note on the Chari series around Jhura Dome, Kutch. *Science & Culture*, 30: 192 - 194
- Mitra, K.C. and Ghosh, D.N. 1965. A note on the chari Series around Jhura Dome, Kutch, Gujarat with special reference to rock stratigraphy and Biostratigraphy of Keera Dome. *Bull. Ind. Geol. Assoc.*, 12: 129 - 143.
- Moiola, R. J. and Weiser, D. (1968). Textural parameters: an evaluation. *Jour. Sed. Petrol.*, V.38: 45-53.
- Moore, C.H., (1989). Carbonate diagenesis and porosity, Elsevier: Amsterdam.
- Morrow and Mayers, (1978). Simulation of limestone diagenesis- a model based on strontium depletion, *Can. J. Earth Sci.*, v.15, pp.376-396.
- Morse, J. W., and F. W. Mackenzie. 1990. *Geochemistry of Sedimentary Carbonates*. New York: Elsevier.
- Muller, G. and Friedman, G.M. (Editors) (1968). Recent developments in carbonate sedimentology in Central Europe, Springer-Verlag, Berlin, p. 255.
- Muto, T and Steel, R. J. (1997). Principles of regression and transgression in the nature of the interplay between accommodation and sediment supply. *Jour. Sed. Res.*, V.67, No.6, pp. 994-1000.
- Nandi, A.K. and Desai (1997). Petrographic and Geochemical evidences of diagenesis within the middle Jurassic carbonates of Kutch, India., *ln. J. Petrol. Geol.* V. 6., No. 2., pp. 40-59.
- Neale, J.W. and Singh, P. (1986). Jurassic Ostracoda from the Banni well No. 2, Kutch, India. *Rev. Esp. De Micropal.*, 17 (3): 347 – 372.
- Nesbit, H.W., Young, G.M., McLennan, S.M. and Keays, R.R. (1996). Effects of chemical weathering and sorting on the petrogenesis of siliciclastic sediments, with implications for provenance studies. *Jour. Geol.*, 14: 525-542.
- Niti Mandal and Singh (1994). The Jurassic Foraminifera from the patcham chair formations of Jhurio Hill (Jhura Dome) Kachchh, Western India., *J. Geol. Soc. India.*, V. 44., pp. 675-680. Niti Mandal and Singh (1994). The Jurassic Foraminifera from the patcham chair formations of Jhurio Hill (Jhura Dome) Kachchh, Western India., *J. Geol. Soc. India.*, V. 44., pp. 675-680.
- Odin (1988) Green marine clays from the oolitic ironstone facies: habit, mineralogy, environment in Millot (ed.) *Green Marine Clays*, p. Springer-Verlag.
- Omara, S, Bishara, W. W. and Nasr, M. 1974. Grain size parameters and palaeoenvironments of the Nubia

- Sandstone. *Jour. Sed. Petro.*, V.44: 136-144.
- Oschmann, W. 1990. Environmental clues in the Late Jurassic north west European epeiric basin : interaction with atmospheric and hydrospheric circulations. *Sed. Geol.*, 69 (3/4): 313 – 323.
- Osman and Mahender (1997). Stratigraphy and sedimentology of the middle Jurassic (Call Oxfordian) sequences of Habo Hill, Kutch (Gujarat)., *J. Ind. Ass. Sed.* V.16, No.1., p.103-110.
- Pal, A.K. and Gangopadhyaya, S. 1970. Two species of *Acicularia* from Jurassic of Kutch. *Jour. Geol. Soc. India*, 11 (3): 278-282.
- Pandey, J. 1983. Biostratigraphical and palaeoecological studies of the Bathonian- Callovian rocks of Khavda-Sadhara area, Pachchham "Island", (Kachchh, Gujarat). Unpublished Ph.D. Thesis, B.H.U., 576p.
- Pandey, D. K. and Callomon, J. H. 1994. On the occurrence of Callovian ammonite *Parapatoceras tuberculatum* (Baugier & Sauze 1843) in Kachchh, western India, *Palaont. Z.*, 88 (1/2): 63-69.
- Pandey D.K., and Calloman, J.H., (1995). Contribution to the Jurassic of Kachchh Western India. III. The middle Bathonian ammonite families *Clydonceratidae* and *Perisphinetidae* from Pachchham Island, Beringeria, V. 16., pp. 125-145.
- Pandey, J. and Dave, A. 1992. Jurassic/ Cretaceous Boundary and Benthic Foraminifera in Kutch , India . *Studies in Benthic Foraminifera, Benthos '90*: 403 – 420.
- Pandey, J. and Dave, A. 1993. Studies in Mesozoic foraminifera and Chronostratigraphy of Western Kutch, Gujarat. *Palaeontographica Indica* Number-1. ONGC, 220p.
- Pandey, D.K. and Fursich, F.T. 1998. Distribution and succession of Jurassic Rocks in Gora Dongar, Pachchham "Island" Kachchh, India. *Jour. Geol. Soc. India*, 51: 331 –344.
- Pandey, D.K. and Westermann, G.E.G. 1988. First record of Bathonian *Bullatimorphites* (Jurassic, Ammonitina) from Kachchh, India. *Jour. Palaeontology*, 62: 148 – 150.
- Pandey, D.K. and Agarwal, S.K. 1984a. On two new species of the Middle Jurassic ammonite genus *Clydoniceras* Blake from Kachchh, W. India - *Neues Jahrbuch fuer Geologie und Palaeontologie*, pp.321-326.
- Pandey, D.K. and Agarwal, S.K. 1984b. Bathonian-Callovian molluscs of Gora Dongar, Pachchham "Island" (District Kachchh, Gujarat). *Quart. Jour. Geol. Min. Met. Soc. India*, 56: 176 – 196.
- Pandey, D.K., Singh, C.S.P. and Agrawal, S.K. 1984. A note on new fossil finds from Gora Dongar, Pachchham "Island", District Kachchh, (Gujarat). *The Jour. Scientific Research, B.H.U.*, 34: 299 – 310.
- Pascoe, E.H. 1959. *A Manual of India and Burma*. Govt. of India Publ., *Geol. Surv. India*, 2: 485 - 1349.
- Passega, R. 1957. Texture as characteristic of clastic deposition. *Bull. Am. Ass. Petrol. Geol.*, 41: 1952-1984.
- Passega, R. 1964. Grain size representation by CM pattern as geological tool. *Jour. Sed. Petrol.*, 34: 830-847.
- Peryt, T.M., (1983 a). *Coated Grains*, p.655, Springer-Verlag.
- Pettijohn (1984). *Sedimentary Rocks*. Harper & Row Publ. Inc., USA, p.628.
- Phansalkar, V.G., Khadkikar, A.S. and Sudha, G. 1992. Sedimentary Characters of the Late Jurassic.- Early

- Cretaceous Clastics near Bhuj and their Environmental Implications. *Jour. Ind. Ass. Sedimentol.*, 11: 47 – 53.
- Pilkey, O. H., Morton, R. W. and Lutenuer. 1967. The carbonate fraction of beach and dune sands. *Sedimentology*, 8: 311-327.
- Poddar, M.C. 1964. Mesozoic of Western India - their geology and oil possibilities , *Int. Geol. Cong. India*, 22 sers. Rept. Proc. Sec. 1, *Geology of Petroleum*, 126 – 143.
- Poddar, M.C. 1959. Stratigraphy and oil possibilities in Kutch, Western India. *Proc. Sym., on the Dev. of Petroleum Resource of* , 146 – 148.
- Powers, R. W. 1962. Arabian U. Jurassic carbonate reservoir rocks. *Mem. Am. Ass. Petrol. Geol.*, 1: 122-199
- Pratap Singh (1977). Late Jurassic Nanoplankton from the Jurassic sequence in the subsurface of the Banni Rann Kutch, *J. Palaeontol. Soc. India.*, V. 20., pp. 331-332.
- Pray, L. C., and R. C. Murray. 1965. Dolomitization and Limestone Diagenesis. *SEPM Special Publication* 13.
- Prince and Sellwood (1994)
- Pugh, M.E. (1968), Algae from the Lower Purbeck Limestones of Dorset, *Proc. Geol. Ass. London*. V. 79., pp. 513-523.
- Purdy, E.G. (1963 a). Recent calcium carbonate facies of the Great Bahama Bank. 1. Petrography and reaction group. *J. Geol.* V. 71, pp. 334-355.
- Purdy, E.G. (1963 b). Recent carbonate facies of the Great Bahama Bank. II. Sedimentary facies. Pp. 472-497
- Purser, B.H. 1969. Syn-sedimentary marine lithification of Middle Jurassic limestones in the Paris Basin. *Sedimentology*, 12 (3/4): 205 – 230.
- Purser, b.H. (1978). Early diagenesis and preservation of porosity in Jurassic limestones, *J. Petrol. Geol.* V. 01., pp. 83-94.
- Rai, J.N. 1972. Palaeontological and stratigraphical studies of the Jurassic rocks of Western Bela Island , Kutch, Gujarat, Unpublished Ph. D. Thesis, B.H.U.
- Rajnath. 1942. The Jurassic rocks of Kutch , their bearing on some problems of Indian geology. *Press. Addr. Proc. 29th Ind. Sci. Cong.*, Pt. II, 93 – 106.
- Rajnath. 1932. A contribution to stratigraphy of Kutch. *Quart. Jour. Geol. Min. Met. Soc. India*, 4: 161 - 174
- Rajnath. 1938a Paleontological study of belemnites from the Jurassic rocks of Cutch, (abstract). *Proc. 25th Ind. Sci. Cong. Assoc.*, 3: 115.
- Rajnath. 1938b. Coral from the Jurassic rocks of Cutch, (abstract). *Proc. 25th . Ind. Sci. Cong. Assoc.* 3: 115.
- Rajnath. 1934a. Stratigraphy of the Jumara area, Cutch,(abstract) *Proc. 21st Ind. Sci. Cong. Assoc.*, 3: 346.
- Rajnath. 1934b. Revision of Jurassic Brachiopod fauna of Cutch (abs). *Proc. 21st Ind. Sci. Cong. Assoc.*, 3: 381.
- Rajnath. 1932. A contribution to the stratigraphy of the Kutch. *Quart. Jour. Geol. Min. Met. Soc. India*, V.4, No.4,

pp. 161 - 174

- Rao, P.V. 1964. Geology and mineral resources of India. Int. Geol. Cong. India, 22nd Sess., 1-43.
- Ravanas, R., and Bondevik, K. 1997. Architecture and controls on Bathonian-Kimmeridgian shallow-marine synrift wedges of the Oseberg-Brage area, northern North Sea. Basin Research, 9: 197-226.
- Riley, N. A. 1942. Projection sphericity. Jour. SED. petrol., 11: 94-97.
- Roy, S.K. 1967. Pteridophytic remains from Kutch and Kathiawar, India. the Palaeobotanist, 16 (2): 108 - 114.
- Sahni, M.R. and Prasad, K.N. 1957. On a new species of *Astarte* from Umia beds Ghuneri, Cutch, W. India and remarks on the age of the *Trigonia* beds. Rec. Geol. Surv. India, 84: 282-306.
- Sahu, B. K. 1983. Multigroup discrimination of depositional environments using grain size distributions. Ind. Jour. Earth. Sc., 10/1: 20-29.
- Sandberg, P.A., (1983). An oscillating trend in Phanerozoic non-skeletal carbonate mineralogy, Nature, V. 305., pp. 19-22.
- Sathyanarayana, K., Dasgupta, D.K., Dave, A. and Das, K.K., (1999). Record of skeletal remains of dinosaurs from the early Middle Jurassic of Kaur Belt, Kutch, Gujrat, Curr. Sci. V. 77., pp. 639-641.
- Tucker, M.E. and Bathurst, R.G.C. (Eds.,) (1990). Carbonate diagenesis. Int. Ass. Sediment .Rep. Ser. 1.
- Sarg, J.F. (1988). Carbonate sequence stratigraphy in C.K. Wilgus, B.S. Hastings, C.G. St. C. Kendall, , H.W. Posamentier, C.A. Ross and J.C. Van Wagoner, eds., Sea level changes: An integrated Approach: SEPM Special Publication No. 42, pp. 155-181.
- Sastri, V. V. and Datta, A. K. 1969. Tectonic setting and Meso-Cenozoic palaeogeography of western part of the Indian Subcontinent. Proc. Symposium on the Development of Petroleum, 1-14.
- Scofin, T. P. (ed). 1987. An Introduction to Carbonate sediments and Rocks, 274p, Blackie, Glasgow and Chapman and Hall, New York.
- Scholle, P. A. 1978. A Color Illustrated Guide to Carbonate Rock Constituents. Amer. Assoc. Petrol. Geol. Memoir 27.
- Schneidermann, N., and P. M. Harris. 1985. Carbonate Cements. SEPM Special Publication 36.
- Sellwood, B.W., (1970). The relation of trace fossils to small sedimentary cycles in the British Lias, In: J.P. Grimes and J.C. Harper (editors), Trace fossils, Seel House Press, Liverpool., pp. 489-584.
- Sellwood, B.W., (1971). The genesis of some sideritic beds in the Yorkshire Lias (England) Jour. Sedim. Petrol. V. 41., pp. 854-858.
- Sellwood, B.W., (1972 a). Tidal flat sedimentation in the Lower Jurassic of Bornham Denmark. Palaeogeogr. Palaeoclimat. Palaeoecol. V. 11., pp. 93-106.
- Sellwood, B.W., (1972 b). Regional environmental changes across a Lower Jurassic stage boundary in Britain, Palaeontology, V. 15., pp. 125-157.
- Sellwood, B.W., and Mckerrow, U.S., (1974). Depositional environments in the lower part of the Great Oolite

Group of Oxfordshire and North Gloucestershire.

- Sellwood, B.W., Shepherd, T.J., Evans, M. R. and James, B. 1989. Origin of Late cements in oolitic reservoir facies: a fluid inclusion and isotopic study (Mid-Jurassic, Southern England). *Sed. Geol.*, 61: 223 – 237.
- Shearman et al. (1970). Genesis and Diagenesis of oolites: *Proc. Geol. Assoc.*, Vol. 81, p. 561-575.
- Shinn, E.A., and Robin, D.M. (1983). Mechanical and chemical compaction in fine grained shallow- water limestones. *J. Sedim. Petrol.* V. 53. Pp. 595-618.
- Sholkovitz, E. R., Shaw, T. J. and Schneider, D. L. 1992. The geochemistry of rare earth elements in the seasonally anoxic water column and porewaters of Chesapeake Bay. *Geochim. Cosmochim. Acta*, 56 : 3389-3402.
- Schroeder, J.H. (1969). Experimental dissolution of calcium, magnesium and strontium from recent biogenic carbonates; a model of diagenesis: *Jour. Sed. Petrology*, V. 39, pp. 1057-1073.
- Schroll, E. (1967). Über den Wert geochemischer Analysen bei stratigraphischen and lithologischem untersuchung von Sedimentgesteinen and Beispiel agsge wahlter profile der postalpien Trias *Geol. Sbornik*, V. 18/2, pp. 315-330.
- Schroll, E (1976). *Analytische Geochemie 2, Grundlagen and Anwendung*, pp. 374.
- Shukla, U. K and Singh, I. B. 1990. Markov Chain analysis and recognition of Transgressive events in the Bhuj Sandstone (Late Jurassic - Early Cretaceous), Kachchh, *Contrib. to Sem. and Workshop, IGCP216*: 52-53.
- Shukla, U. K. and Singh, I. B. 1991. Significance of Trace Fossils in the Bhuj Sandstone (Lower Cretaceous), Bhuj Area, Kachchh, *Jour. of Palaeontological Society*, 36: 121-126.
- Shukla, U. K. and Singh, I. B. 1993. First record of marine macroinvertebrate from Bhuj Sandstone (Lower Cretaceous) of eastern Kachchh, *Current Science*, 65 (2): 171-173.
- Shukla, U. K. and Singh, I. B. 1990. Facies analysis of Bhuj sandstone (Lower Cretaceous) Bhuj Area, Kachchh, *Jour. of Palaeontological Society of India*, 35: 189-196.
- Singh, I. B. 1989. Dhosa Oolite - A transgressive Condensation Horizon of Oxfordian Age in Kachchh, Western India, *Jour. Geol. Society of India*, 34: 152-160.
- Singh, N.N. and Tripathi, H.C. 1969. A note on the stratigraphy of Kanthkote (E.Kutch), (abstract). *Proc. 56th Sess. Ind. Sci. Cong. Assoc.*, 3: 217.
- Singh, C.S.P., Jaitly, A.K. and Pandey, D.K. 1982. First report of some Bajocian - Bathonian (Middle Jurassic ammonoids) and the age of Oldest sediments from Kachchh, India. *Newsletters on Stratigraphy*, 11: 37 –40.
- Singh, C.S.P. and Rai, J.N. 1980. Bathonian - Callovian fauna of Western Bela Island (Kutch), Bivalvia families *Cardiidae*, *Neomidontidae*, *Corbulidae*. *Jour. Palaeontol. Soc. India*. 23-24: 17 –80.
- Singh, C.S.P. and Kanjilal, S. 1974. Some fossil Mussels from the Jurassic rocks of Habo Hill in Kutch, Gujarat, Western India. *Indian Jour. Earth Sciences*, 1 (1): 113 – 125.
- Singh, C.S.P., Pandey, D.K. and Jaitly, A.K. 1983. Discovery of *Clydoniceras BLAKE* and *Gracilispinctes*

- BUCKMAN (Bathonian- Middle Jurassic ammonites) in W.India, *Jour. Palaeontology*, 57: 821 – 824.
- Singh, H.P. and Srivastava, S.K. and Roy, S.L. 1963. Studies on the Upper Gondwana of Cutch-1 Micro and Macrospores. *The Palaeobotanist*. 12 (3): 282 – 306.
- Singh, P. 1977a. Late Jurassic Epistomina from the subsurface of Banni Deep well-2, Kutch. *Proc. IV Indian Colloq. Micropal. Strat.*, 30 – 35.
- Singh, P. 1977b. The Jurassic nannoplankton from the Jurassic sequence of the Rann, Kutch. *Jour. Pal. Soc. India*, 20: 331 – 332.
- Singh, P. 1979. Biostratigraphic zonation in the Jurassic sequence in the subsurface Banni Rann, Kutch. *Bull. Ind. Geol. Assoc.*, 12 (1): 111 – 128.
- Sloss, L.L. (1963). Sequences in cratonic interior of North America. *Geol. Soc. Am. Bull.* V. 74., pp. 93-114.
- Smith, A.G. Briden, J.C. and Drewry, G.E., (1973). Phanerozoic world maps, *Spec. Papers in Palaeont.* No. 12., pp. 1-39.
- Smithson, (1942). The middle Jurassic rocks of Yorkshire: a petrological and palaeogeographical study, *Quart. J. Geol. Soc. London*. 98., pp. 27-59.
- Solohub, J. T. and Klován, J. E. 1970. Evaluation of grain size parameters in lacustrine environments. *Jour. Sed. Petrol.*, 40: 81-101.
- Soodan, K.S. 1975. Revision of fossil Holothuroidea family Priscopedatidea Frizzelt and Exline and some new genera from Kutch, India. *Geophytology, India*. 5 (2): 213 - 224.
- Soodan, K.S. 1977a. Fossils Holothuroidea from Kutch, India. *Proc. IV Ind. Coll. Micropal. Strat.*, 101 – 103.
- Sorby, H.C., (1957). On the origin of the Cleveland Hill ironstone: *Proc. Yorks. Geol. Polytech. Soc.*, v.3, pp.457-461.
- Sorby, H.C. (1858). On the Microscopical Structure of crystals, Indication the origin of the minerals and rocks: *Geol. Soc. London. Quart. Jour.* V. 14, p. 453-500.
- Sorby, H.C. (1851) On the microscopical structure of the calcareous grit of the Yorkshire Coast. *Quart. J. Geol. Soc. London* 7, pp. 1-6
- Soreghan, G. S. (1997). Walther's law, climate change and Upper palaeozoic cyclostratigraphy in the ancestral rocky mountains. *Jour. Sed. Petrol.*, V.67, No.6, PP.1001-1004.
- Spath, L.F. 1924. On the Blake collection of Ammonites from Kachh, India. *Pal. Indica, Geol. Sur. India, New series* 9, (1): 1 -29.
- Spath, L.F. 1933. Revision of the Jurassic Cephalopod fauna of Kutch (Cutch). *Palaeontologia Indica (Geological Survey of India), New Series* 9, Mem. pts. I-VI, 945p.
- Spath, L.F. 1933. Revision of the Jurassic Cephalopod fauna of Kachh (Cutch). *Pal. Indica, geol. Sur. India, New series*, 9(2): 1 – 945.
- Spence, G.H. and Tucker, M.E. (1999). Modelling carbonate Microfacies in the context of high frequency

- dynamic relative sea level and environmental algae. *J. Sed. Res.* V. 69, No. 4, pp. 947-961.
- Sreepat Jain (1997). On the occurrence of Genus *Phlycticeras* Hyatt in Kachchh, Western India, *J. Geol. Soc. India*, V. 49., pp. 75-80.
- Steineke, M. Bramkamp, R. A., and Sanders, N. J. 1958. Stratigraphic relations of Arabian Jurassic oil. In : L. G. Weeks (ED.): *Habitat of Oil, A symposium, Am. Ass. Petrol. Geol.*, 1294-1329.
- Stoliczka. 1867. Determination of Jurassic fossils from Cutch, *Mem. Geol. Sur. India*, 4 (1).
- Strke, R. (1968). Mineralogisch-geochemische methoden der Faziesdiagnostik *Ber. Dtsch. Ges. Geol. Wiss. B; Min-4, Lagerstättenerforsch*, V. 13., pp. 219-226.
- Subbolina, N.N., Dutta, A.K. and Srivastava, B.N. 1960. Foraminifera from the Upper Jurassic deposits of Rajasthan (Jaisalmer) and Kutch, India. *Bull. Geol. Min. Met. Soc. India*. 23: 1 – 48.
- Sun, S.Q., and Wright, V.P. 1989. Peloidal fabrics in upper Jurassic reefal limestones, Weald Basin, southern England. *Sed. Geol.*, 65: 165 – 181.
- Sykes. 1834. Notice Respecting some fossils, collected in Kutch by Walter Smee of Bombay Army. *Trans. Geol. Soc. London*, 2 (5): 715 – 718.
- Talbot, M.R., (1971). Calcite cements in the Corallian Beds (Upper Oxfordian) of southern England. *J. Sedim. Petrol.* V. 41., pp. 261-273.
- Talbot, M.P., (1973). Mahor sedimentary cycle in the Corallian Beds. *Palaeogeogr. Palaeoclimatol. Palaeocol.*, v. 14., pp. 293-317.
- Talbot, M.B. 1974. Ironstones in the Upper Oxfordian of southern England. *Sedimentology*, 21: 433 – 450.
- Taylor, S. R. and McLennan, S. M. 1985. *The continental Crust: Its composition and Evolution*. Blackwell Scientific Publications, 312p.
- Tewari, B. S. and Kashyap, S. M. 1969. Some Sedimentary structures from the Bhuj series, Middle Cretaceous of Kutch, *Research Bull. of the Punjab University*, 21: 157-159
- Tewari, B.S. 1948. The geology of Habo hills, Cutch state, (abs). *Proc. 35th Sess. Ind. Sci. Cong. Assoc.*, 2: 148.
- Tucker, M. E. 1981. *Sedimentary Petrology*, ELBS, Blackwell Scientific Publications, Oxford, 252p
- Tucker, M. E. (Ed.). 1988. *Techniques in Sedimentology*, 394p., Blackwell Scientific Publications, Oxford.
- Tucker, M. E. and Paul Wright, V. 1990. *Carbonate Sedimentology*, 485p, Blackwell scientific Publications, Oxford, London.
- Tucker, M.E. (1991 a). *Sedimentary petology: an introduction to the origin of sedimentary rocks*. Blackwell Scientific publications: Oxford.
- Turekian, K.K. (1964). The marine geochemistry of strontium : *Geochim. Cosmochim. Acta*, V. 28, pp. 1479-1496.
- Turekian, K. K. and Kulp, J. L. 1956. The geochemistry of strontium. *Geochim. Cosmoch. Acta*, 10: 245-296.

- Turi, A., Bencini, A. and Gonnelli, I. 1980. Mn and Fe distribution in the Jurassic sequence of Bihendula, Northern Somalia. *Boll. Soc. Geol. It.*, 99: 23-34
- Turi, A., Bencini, A. and Gonnelli, I. 1981. Mn and Fe distribution in the Jurassic sequence of Bihendula, Northern Somalia. *Boll. Soc. Geol. Italy*, 99: 23-34.
- Vail, P.R. (1987). Seismic Stratigraphy interpretation using sequence stratigraphy, Part- I, Seismic interpretation procedures in Bally, A.W. Ed., *Atlas of Seismic stratigraphy*, V. 01, Am. Ass. Petrol. Geol. Studies in Geology, No. 27, pp. 1-10.
- Vail, P.R. Hardenbol, J., and Todd, R.G. (1984). Jurassic fossils chronostratigraphy and sea level changes from seismic stratigraphy and biostratigraphy. GCPSSSEPM foundation Third Annual Res. Conference. Proc.
- Vail, P.R., Andmard, F., Bowen, S.A., Eisner, P.N., and Perez-Cruz, C. 1991 Part-II, Larger cycles and sequences the stratigraphic signatures of tectonic, eustasy and sedimentology an overview, in Einsele, G. Ricken, W., and seilacher, A, eds. *Cycles and events in stratigraphy*: Berlin, Springer-Verlag, pp. 167-659.
- Van Hinte, H.E. 1976. A Jurassic Time Scale. *Am. Assoc. Petrol. Geol.*, 60 (4): 489 - 497
- Van Houten, F.B. (1985). *Geology*, V. 13, pp. 722- 724.
- Van Wagoner, J.C. , Posamentier, H.W., Mitchum, R. M. Jr., et al (1988). An overview of the fundamentals of sequence stratigraphy and key definitions. In: *Sea level changes an intergrated approach* (Eds). C.K. Wilgus, B.S. Hastings, H.Posamentier et al). *Soc. Econ. Paleont. Miner Spec. Publ. V. 42.*, pp. 39-45.
- Van Wagoner, J.C., Mitchum, R.M. Campin, K.M. and Rahmanian, V.D. (1990). Silici-clastic sequence stratigraphy in well logs, cores, and outcrops: concepts for Higher-Resolution correlation of Time and Facies: *AAPG Methods in Exploration series*, No. 7, pp. 55
- Venkatachala, B.S. 1974. Palynological zonation of the Mesozoic and Tertiary subsurface sediments in the Cauvery Basin . *Aspects and Appraisal of Indian Palaeobotany*, 476 -495
- Veizer, J., and Demovic (1973)
- Veizer, J., (1983). Chemical diagenesis of carbonates: theory and application of trace element techniques. In : *stable isotope in sedimentology geology*, pp. 3-1 to 3-100. *Soc. Econ. Paleont. Miner. Short Course 10.*
- Veizer, J. 1983. Trace elements and isotopes in carbonate minerals. *Soc. Amer. Rev. in Mineral.*, 11: 265-299.
- Veizer, J., and Demovic, R., (1974) Strontium as a tool in facies analysis : *Jour. Sed. Petrology* , V.44, P. 93-115.
- Veizer, J., Lemieux, J., Jones, B., Gibling, M. R. and Savelle, J. 1978. Palaeosalinity and dolomitization of Lower Palaeozoic Carbonate Sequence, Somerset and Prince of Wales Islands, Arctic Canada. *Can. Jour. Earth Sci.*, 15: 1448-1461.
- Visher, G.S. (1965). Use of vertical profile in Environmental reconstruction. *Am. Assoc. Petrol. Geol.*, V.49, No.1, pp. 41 – 61.

- Vrendenberg, E.W. (1910). A summary of Geology of India, 2nd Edition.
- Waagen,W. 1871. Abstract of result of examination of the Ammonite fauna of Cutch , with remarks on their distribution among the beds and probable age. Rec. Geol. Surv. India. 4 (4).
- Waagen,W. 1875. Jurassic fauna of Cutch. Pal. Indica, Geol. Sur. India., ser. 9. 1
- Wagner, P. D. and Mathews, R. K. 1982. Porosity preservation in the Upper Smackover (Jurassic) carbonate grainstone, Walker Creek field, Arkansas: response of palaeophreatic lenses to burial processes. Jour. Sed. Petrol., 52: 13-18.
- Wedephol, K.H. (1969). Primary and diagenetic strontium-Gehalte von karbonatgesteinen: Geol. Ges. Deutsch. Demoker. Rep. Gesamtgel, Geol. Wiss., V. 14, pp. 17-23.
- Wedephol, K.H. (1970). Geochemische Daten Von Sedimentaren karbonaten and Karbonatgesteinen in ihrem faziellen and petrogenetischem aussagewert. Verh. Geol. Bundesanst. 1970/4, pp. 692-705.
- Wendt, J., (1988). Condensed carbonate sedimentation in the Late Devonian of the eastern Anti-Atlas (Morocco): Ecologiae Geologica Helvetica, V. 81., pp. 155-173.
- Westermann,G.E.G. and Callomon,J.H. 1988. The Macrocephalitinae and associated Bathonian and Early Callovian (Jurassic) ammonoids of the Sula Islands. New-Palaeontographica A. 203: 1 -90
- Wilkinson, B.H., Owen, R.B. and Carroll, A.R. (1985). Submarine hydrothermal weathering, global eustasy and carbonate polymorphism in phanerozoic marine oolites. Jour. Seim. Petrol. V. 55., pp. 171-183.
- Wilson, A.D., (1964). The sampling of silicate rock powders for chemical analysis, Analyst (London), V. 89., pp.18-30.
- Wilson, (1975). Carbonate facies in Geologic History. Springer-Verlag, Berlin, New York, 471p.
- Wolf, et al (1967). Elemental composition of carbonate skeletons, minerals and sediments: In Chilinga, G.V. H.J Bissel and R.W. Fairbridge (eds). Carbonate Rocks B: Elsevier, Amsterdam, pp. 23-149.
- Wright, et al., (1988). Palaeokarsts and palaeosols as indicators of paleoclimate and porosity evolution: a case study from the carboniferous of south Wales. In: pleokarst (Ed. By N.P. James and P.W. Choquette) pp. 329-341., Springer-Verlag, New-York.
- Wright V. P., (1993) Sedimentology Review/1 p.142, Blackwell scientific publications. 200p.
- Wright, J., Schrader and H., Holser, W. T. 1987. Palaeoredox variations in ancient oceans recorded by rare earth elements in fossil apatite. Geochim. Cosmochim. Acta, 51 : 631-644.
- Wright- Clark, J. and Holser, W. T. 1981. Rare earth elements in conodont apatite as a measure of redox conditions in ancient seas. Geol. Soc. Am. Abstr., 13 : 586.
- Wynne,A.B. 1875. Memoir on the Geology of Kutch to accompany a map compiled by A.B. Wynne and F.Fedden during the sessions 1867-68 and 1868- 69. Mem. Geol. Surv. India, 9: 1 – 289.

Zempolich-William, G. 1993. The drowning succession in Jurassic carbonates of the Venetian Alps, Italy ; a record of supercontinent breakup, gradual eustatic rise, and eutrophication of shallow water environments. Mem. Am. Ass. Petrol., 57: 63 – 105.

oooOOOooo

Temporal Variation of Microfacies Types

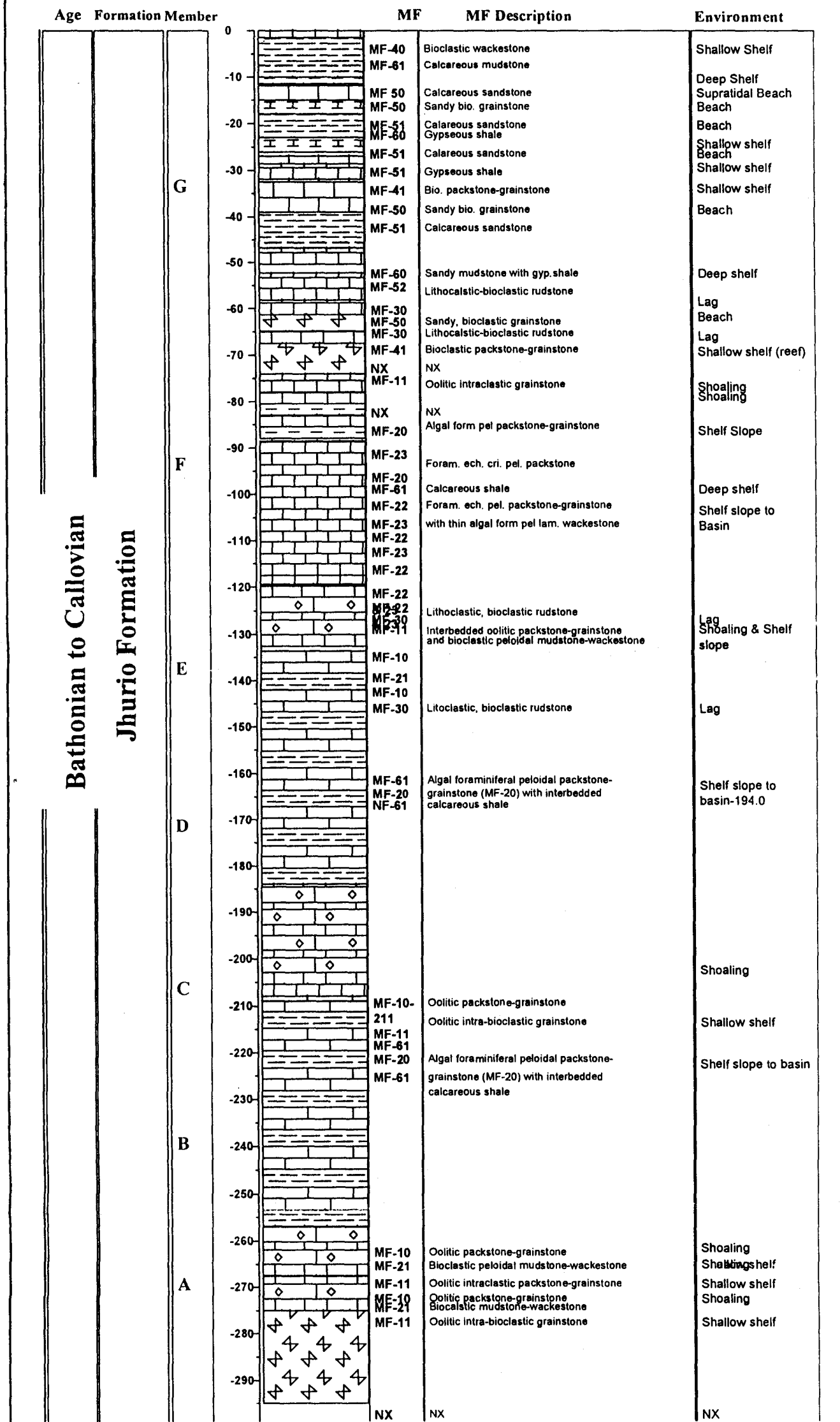


Fig.4.2 Temporal distribution of Carbonate Microfacies of Jhurio Formation.